

CIE5060-09 MSc Thesis

Tidal Wave Energy Converter

FEASIBILITY STUDY FOR AN INNOVATIVE TIDAL ENERGY SOLUTION



antea[®]group


TU Delft

Mark de Kloet

Final report CIE5060-09 Master Thesis
Delft, 24 June 2015

Written by Mark de Kloet
Student number: 1363336
E-mail: Mark_de_Kloet@msn.com

This research has been performed to fulfil the requirements of the Master of Science degree in Civil Engineering as set forth by Delft University of Technology, Faculty of Civil Engineering and Geosciences, Section of Hydraulic Engineering.

Graduation Committee

Prof.dr.ir. S.N. Jonkman
Prof. dr. ir. J.K. Vrijling
Ir. A. van der Toorn
Dr. P.J. Vardon
Ir. K. Sektani

TU Delft, section Hydraulic Engineering
TU Delft, section Hydraulic Engineering
TU Delft, section Hydraulic Engineering
TU Delft, section Geoscience & Engineering
Antea Group Nederland

Cover art by Robert Voogt, Sphere Industries

Preface

After a period of hard work in various settings I am proud to present this report in which I have done a feasibility study regarding the harvesting of energy from the vertical motion of pontoons in the tide, which I have called the Tidal Wave Energy Converter principle. I performed this study as graduation thesis for the Master of Science track in Hydraulic Engineering at Delft University of Technology, faculty of Civil Engineering and Geosciences in cooperation with Antea Group Nederland.

I chose the subject of this research for my thesis due to a combination of interests in waterpower engineering and innovation. Waterpower has been a passion of mine ever since visiting the large hydropower plants of Brazil in the Itaipú Dam on the Paraguayan border and the Simplício hydroelectric complex just North of Rio de Janeiro. These projects inspired me to pursue waterpower engineering and through the waterpower engineering course in the Hydraulic Engineering MSc track my understanding of the broad spectrum that is waterpower increase to the point where I wanted to get the subject of my thesis from this field.

After having discussed my interests with waterpower engineering tutor Ad van der Toorn I decided to take up the subject of energy from pontoons in tidal waves, which was a question initially broached to him by Peter Ligthart. After making a preliminary calculation (included in Appendix R of this report) Antea Group decided to provide me with an internship where I could develop this principle at their office in Almere with the support of experts from their company.

The report has been split up in five sections each handling a distinct part of the research. Section 1 handles an overall introduction into the problem at hand with some historical background of energy production and an introduction in what the field of hydroelectric energy entails. Section 2 focusses on a method to easily predict the tidal motion at a certain location in the world using satellite laser altimetry data for ocean tides and transposing this onto near shore locations with an adjustment script. Furthermore it applies this method to the Dutch hydrologic system.

Section 3 provides the framework in which the research will be done with the boundary conditions and reference projects that will be used to gain inspiration from for the design process. To conclude this section the program of requirements is set up which defines what characteristics the design needs to adhere to. In section 4 the determination of the components of the device is considered using Multi Criteria Decision Analysis tools and cost related motivations to decide what the best means is of filling out the different components of the device. In the final section, section 5, the devised design criteria from the previous sections are combined and applied to a real life location with a high tidal energy potential in the Bay of Fundy in Canada to determine the feasibility conditions and answer the main question of the report.

As a final part of this preface I would like to express a word of thanks to several individuals without whom I would not have been able to complete my degree as a whole and this thesis in specific. Firstly I'd like to thank Ad van der Toorn, my mentor during this thesis and the one responsible for getting me the subject of the thesis. Kodo Sektani and George Bitter from Antea Group who despite their busy schedules have found the time and enthusiasm to not only help me with my thesis but also give me an insight in the daily operations of the company. The colleagues from Antea who I have been able to consult with practical engineering questions I could not find an answer to myself (Jan Peter Kluiwstra, Peter Minnesma, Robert de Vries, Harmen van Meekeren, Edwin Velthuis and Klaas Pascha).

I would like to thank the members of my graduation committee. Han Vrijling for taking the time to be in the committee despite already having retired and for helping to inspire my passion for waterpower back in 2010. Phil Vardon for his attention to detail and time spent judging my work and thinking along with the progress. And lastly Bas Jonkman who despite not having been fully involved in the process still showed an interest in my work and kept an eye on the speedy conclusion of my graduation. Bert Everts, who unfortunately did not have the time to take place in the committee but still helped whenever needed both during the course of my thesis as well as during my study as a whole.

A big thanks too to my friends and family who have kept me sane through the course of my education and thesis especially during the rough patches when things did not go as I'd have liked them to. To Robert Voogt of Sphere Industries who made the 3D concept art. And last but not least, and certainly most deserving of all, my parents Jan and Evelien de Kloet who have not only supported me morally throughout my education but have also provided the financial means needed to bring it to its conclusion.

I wish everyone who came this far in the preface and intends to continue into the rest of the document a good reading experience and hope it will bring you the information that you are looking for.

Mark de Kloet
Delft, 24 June 2015

List of used symbols

| Symbol | Meaning | Unit |
|--------------------|--|----------------------------------|
| A | Amplitude | m |
| a | Column diameter | m |
| A _a | Cross sectional area | m ² |
| A _b | Cross sectional area | m ² |
| A _s | Flow area | m ² |
| A _s | Reinforcement steel cross sectional area | m ² |
| B | storage area | m ² |
| B | Width at location x | m |
| b | contraction coefficient | - |
| b | Convergeance length of the stream width | m |
| B | Footing width | m |
| B ₀ | Initial width | m |
| b ^a | Width | m |
| c | Wave celerity | m s ⁻¹ |
| c | Cohesion | Pa |
| c ₀ | Tidal average wave celerity | m s ⁻¹ |
| c _u | Undrained shear strength of clay | Pa |
| d _b | Diameter of bar | m |
| D _i | Inner pile diameter | m |
| D _o | Outer pile diameter | m |
| DR | Displacement ratio | - |
| E _s | Young's modulus of steel | N m ⁻² |
| F | Diurnality ratio | - |
| f | Friction factor | - |
| F | Force | N |
| f _c | Outside skin friction in compression | N m ⁻¹ |
| F _g | Gravitational force | N |
| f _{k,rep} | Unit skin friction | N m ⁻¹ |
| F _{max} | Maximum force | N |
| F _r | Bearing capacity | N |
| F _{wall} | Force on wall | N |
| g | Gravitational acceleration | m s ⁻² |
| H | Energy head | m |
| h | Water level | m |
| h | depth | m |
| h | Height of the block | m |
| h | Average stream depth | m |
| i | Load direction factors | - |
| I _{zz} | Moment of inertia | m ⁴ |
| K | Manning's roughness coefficient | m ^{1/3} s ⁻¹ |
| K ₁ | Lunisolar diurnal tidal constituent | m |
| K ₂ | Lunisolar semidiurnal tidal constituent | m |

| | | |
|---------------|---|--------------|
| L | Bay length | m |
| l | centre-to-centre distance | m |
| L | Footing length | m |
| l | Span length | m |
| L_a | Anchor length | m |
| l_b | Bond length | m |
| l_{buc} | Buckling length | m |
| l_d | Development length | m |
| M_2 | Semidiurnal lunar tidal constituent | m |
| M_4 | Shallow water lunar overtide tidal constituent | m |
| M_f | Fortnightly lunar tidal constituent | m |
| M_m | Monthly lunar tidal constituent | m |
| M_z | Bending moment around z axis | N m |
| N | Load coefficients | - |
| N_2 | Larger lunar elliptic semidiurnal tidal constituent | m |
| N_s | Tensile force | N |
| O_1 | Lunar diurnal tidal constituent | m |
| P | Power | W |
| p | Pressure | BAR |
| P_1 | Solar diurnal tidal constituent | m |
| p_a | Atmospheric pressure | Pa |
| p_r | Unit bearing capacity | Pa |
| Q | Discharge | $m^3 s^{-1}$ |
| q | Side load | $N m^{-2}$ |
| q | Distributed load | $N m^{-1}$ |
| Q_1 | Larger lunar elliptic diurnal tidal constituent | m |
| q_c | Cone resistance | Pa |
| Q_{eb} | End bearing capacity | N |
| $q_{eb,clay}$ | End bearing capacity in clay | $N m^{-2}$ |
| $q_{eb,sand}$ | End bearing capacity in sand | $N m^{-2}$ |
| Q_{fr} | Skin friction capacity | N |
| Q_r | River discharge | $m^3 s^{-1}$ |
| Q_r | Bearing capacity | N |
| R^* | Effective pile radius | - |
| R_i | Inner radius | m |
| r_s | Storage width ratio | - |
| R_u | Outer radius | m |
| s | Pile shape factor | - |
| s | Footing shape factors | - |
| S_2 | Semidiurnal solar tidal constituent | m |
| S_z^a | Static moment | m^3 |
| T | Tide period | s |
| T | Tensile force | N |
| $t_{turbine}$ | spin-up time of turbine | s |
| t_{wall} | Wall thickness | m |

| | | |
|-----------------|---------------------------------------|--------------|
| u | Fluid velocity | $m\ s^{-1}$ |
| V_z | Shear force in z direction | N |
| x | Inland location | m |
| Z | Location height | m |
| Z | water level | m |
| Z | Internal lever arm | m |
| z_c | Distance from center of cross section | m |
| z_{max} | Maximum distance from center | m |
| α_c | Friction factor | - |
| α_p | Penetration type factor | - |
| β | Foot factor | - |
| γ | Shape number | - |
| γ_c | Critical shape number | - |
| γ_m | Material safety factor | - |
| γ' | Effective soil weight | $N\ m^{-3}$ |
| δ | Damping number | - |
| ε | Phase lag | - |
| ζ | Depth tidal amplitude ratio | - |
| η | Coefficient for losses | - |
| η | Tidal amplitude | m |
| η | efficiency | - |
| λ | Celerity number | - |
| λ_{rel} | Relative slenderness | - |
| μ | contraction coefficient | - |
| μ_m | Velocity number | - |
| ρ | Fluid density | $kg\ m^{-3}$ |
| σ_g | Soil stress | $N\ m^{-2}$ |
| σ_{max} | Maximum stress | $N\ m^{-2}$ |
| σ_s | Yield strnngth of steel | $N\ m^{-2}$ |
| σ_{uc} | Compressive strength of grout | Pa |
| σ_v' | Vertical effective soil stress | $N\ m^{-2}$ |
| σ_y | Yield stress of bar | Pa |
| τ_1 | Tensile strength of concrete | $N\ m^{-2}$ |
| τ_a | Maximum bond stress | $N\ m^{-2}$ |
| τ_d | Shear stress | $N\ m^{-2}$ |
| ϕ | Phase shift | ° |
| χ | Friction number | - |
| ψ | Safety factor | - |
| ω | Angular velocity | °/hr |
| ω | reinforcement percentage | % |
| ω_{buc} | Buckling factor | - |

Index

| | |
|--|-----|
| Preface | 3 |
| List of used symbols | 5 |
| Index..... | 9 |
| Summary | 11 |
| Section 1 – Introduction..... | 17 |
| 1 Introduction..... | 19 |
| 2 Historical background of energy production..... | 21 |
| 3 Brief introduction into hydroelectric energy | 25 |
| 4 Problem definition..... | 27 |
| 5 Limitations of the research..... | 31 |
| Section 2 – General scope of tidal energy..... | 33 |
| 6 Introduction to general scope of tidal energy..... | 35 |
| 7 Global estimation tool for tidal amplitudes | 37 |
| 8 The applicability of tidal energy in the Dutch hydrologic system | 43 |
| 9 Electric network..... | 53 |
| 10 Conclusions on tidal energy scope | 57 |
| Section 3 – Development framework | 59 |
| 11 Introduction of development framework | 61 |
| 12 Reference Projects | 63 |
| 13 Possible host structures for the Tidal Wave Energy Converter..... | 77 |
| 14 Generalized boundary conditions | 85 |
| 15 Program of Requirements | 89 |
| Section 4 – Engineering aspects..... | 91 |
| 16 Introduction of engineering aspects | 93 |
| 17 Environmental scenarios | 95 |
| 18 Limit states | 99 |
| 19 Method of energy conversion | 101 |
| 20 Operational characteristics | 105 |
| 21 Type and dimensions of foundation..... | 111 |
| 22 Adjustments to the host structure | 129 |
| 23 Piston and rod dimensions | 133 |
| 24 Possibilities for energy storage | 139 |
| 25 Design criteria..... | 141 |
| Section 5 – Final design and conclusions | 145 |
| 26 Introduction to final design and conclusions | 147 |
| 27 Location analysis..... | 149 |
| 28 Specific design: Bay of Fundy | 153 |
| 29 Financial considerations | 159 |
| 30 Conclusions and recommendations | 161 |
| Reflection | 165 |
| Bibliography | 167 |
| Appendices | 171 |

Summary

In modern society the call for cleaner and more renewable sources for energy is becoming increasingly loud and persistent. Governments are implementing targets for percentages of the total energy production that need to consist of renewable energy and are granting subsidies to projects that fit this bill. Solar and wind energy have managed to reap the rewards of these policies due their small scale application possibilities, but despite the Earth's surface being 71% covered with water marine power, the energy harvested from the ocean, has as of yet not managed to catch up. There are, however, numerous innovative ideas which are trying to become Columbus' egg in terms of marine energy in the fields of wave energy, osmosis energy (the energy potential when water bodies of different salinities mix) and tidal energy.

One of these innovative concepts is the "Kieuwbalg" principle of Peter Ligthart which uses the vertical motion of pontoons in the tide to pressurize a bellows type water container and harvests the energy through turbines. This concept has been expanded on to include any type of pressurized chamber and pressure to electricity conversion mechanism and renamed the Tidal Wave Energy Converter. A representation of this concept has been illustrated in Figure 1 where the blue arrows indicate the direction of movement of the water level and the green arrows the direction of motion of the pontoon. It can be observed that if the pontoon is in motion energy can be harvested, if it is not no energy harvesting occurs (indicated with the light bulbs).

The principle revolves around the relative motion of pontoons compared to the tide. By holding the pontoon in one place a pressure differential can be created by either the force of gravity or the force of buoyancy. By releasing the pontoon again and leading the pressurized fluid flowing in or out of the container through a conversion device, electricity can be harvested from the tidal wave.

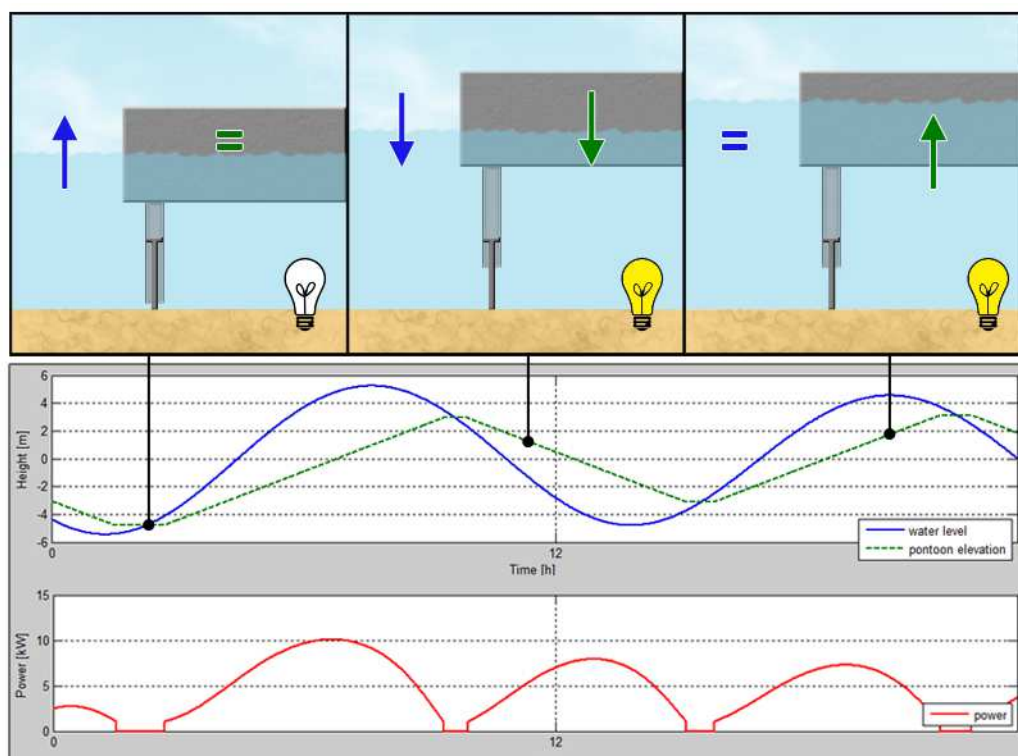


Figure 1 - The Tidal Wave Energy Converter concept

The main question that needs to be answered is whether this concept is feasible to continue to develop or not, and if so what technical and environmental conditions apply to that. To attain an answer to that question research has to be done in terms of the tidal propagation worldwide, the common types of soil composition and the general bathymetry in such areas. From there the influence of these characteristics on the design of the Tidal Wave Energy Converter can be analysed.

From a multi criteria decisions analysis it has been decided that the best means of harvesting the energy from the pressurized fluid is by means of hydraulic motors. The main benefit of these devices over the use of turbines is that the possibilities for pressure build up and release regulation are better. Furthermore the required container for the fluid is far smaller than for turbines if a reasonable spread in production is to be attained (for smaller containers the produced energy is similar, but spread out over a shorter time and therefore not practically of use).

For the foundation four types have been considered, steel pipe piles, precast concrete piles, anchors and shallow foundations, which have been researched for applications in soils of sand, rock and clay. The conclusion of this research is that, due to the significant price of steel as a construction material, anchors and piles are the preferred method of foundation. Piles herein are used primarily for compressive forces, as it is difficult to install a system of tension piles under water, anchors are primarily for tensile forces.

To test the feasibility of the device a “highest probability” location is determined on the basis that if it does not work there, it will not work anywhere. A location analysis based on the magnitude of the tide, its return period and the bottom characteristics resulted in the choice for the Bay of Fundy in Canada (Figure 2). This location has a high, relatively constant tide with a bi-daily return period and is of medium depth with a bedrock soil profile. In this research a floating bridge, a bridge which uses the buoyant force of the water under its pontoons as foundation, is considered to be constructed between Nova Scotia on one side and New Brunswick on the other, where the Tidal Wave Energy Converter will be used underneath the pontoons of this bridge. This means the pontoons themselves do not fall within the scope of the research and only the pistons, the foundation and how to connect the device to the pontoon are.



Figure 2 - Final design location, Bay of Fundy, Canada

The design for this specific location has been made such that it is anchored to the bedrock sea floor with rock anchors to handle the tensile forces of the operational device. These anchors are attached to the structure with chains at a height such that the angle of the anchors does not become too steep and the motion of the piston is not hindered. For compressive forces the system rests on the ocean floor in an excavated hole so that horizontal slipping is countered. The section below the attachment point of the chains is hollow and slides over the solid rod leading upward to the piston. These components are connected by bolts specifically designed to fail in case of severe loading, but at a lower load than the rest of the structure. This mechanism ensures that in case of failure the costs of repair are limited. Furthermore this method creates a means of artificially lowering the maximum design load of the entire structure, thereby also limiting the costs. A representation of the designed device at the chosen location is given in Figure 3.

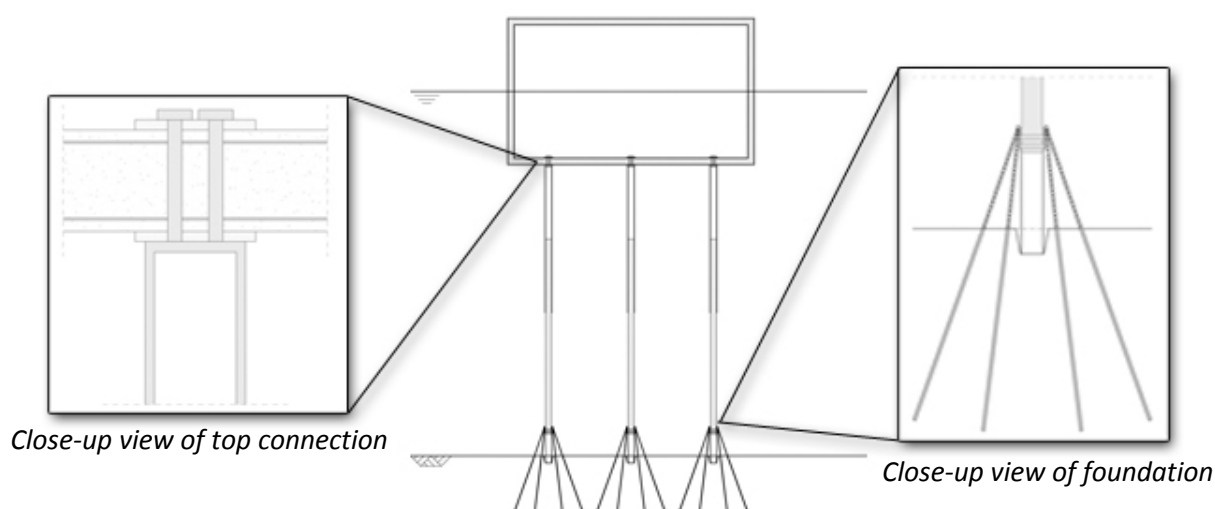


Figure 3 - Tidal Wave Energy Converter design

With the technical design made the costs of the structure can be calculated as well as the costs for maintenance. Compared with the electrical revenue over the 10 year lifespan that is considered for the device this leads to a certain cost per kWh for the production of electricity with the Tidal Wave Energy Converter. The results of the cost calculation and the electric revenue as well as the cost per kWh are given in Table 1.

| | |
|------------------------------------|-----------------|
| Lifetime costs | €3,387,488.17 |
| Lifetime electrical revenue | 228,758.0 [kWh] |
| Price per kWh | €14,81 |

Table 1 - Costs and revenue of the Tidal Wave Energy Converter

To determine based on the price per kWh if it is a feasible concept it needs to be compared to the production costs of other types of electricity. Figure 4 gives a graph of how the price per unit of produced electricity relates to that of other sources. It can easily be seen that the order magnitude for this concept is so high that it is highly unfeasible to be applied at locations where any other sort of energy source is available. Only if the construction price of some of the main components drastically drops, the production price of alternatives increases or the majority of the device's components is already paid for by the host structure is there a small possibility this is workable.

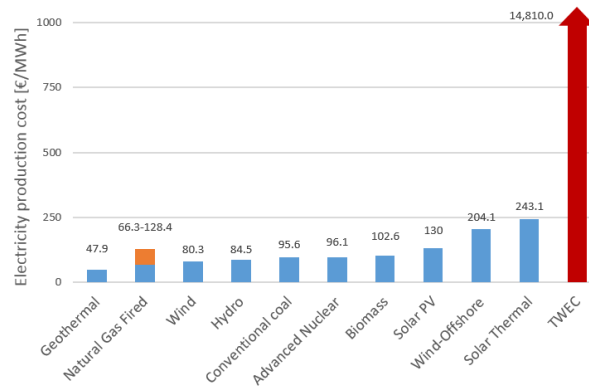


Figure 4 - Production costs per MWh of various energy sources after (US Energy Information Administration, 2014)

Section 1 – Introduction

| | | |
|-----|--|----|
| 1 | Introduction..... | 19 |
| 2 | Historical background of energy production..... | 21 |
| 2.1 | Non-renewable energy sources | 21 |
| 2.2 | Renewable energy sources..... | 22 |
| 3 | Brief introduction into hydroelectric energy | 25 |
| 3.1 | Conventional hydropower..... | 25 |
| 3.2 | Marine energy | 26 |
| 4 | Problem definition..... | 27 |
| 5 | Limitations of the research..... | 31 |



1 Introduction

Energy consumption is an ever relevant issue that modern society has to face. Virtually no house in the developed world is devoid of some sort of electronic device and the demand for more electricity is increasing on a daily basis. Over the past decades this increase in the global consumption pattern has been compensated by burning more and more fossil fuels, but with an increasing awareness of the environmental consequences and the realization that the fossil fuel reserves are limited a movement has come into existence that seeks for solutions that are both renewable and environmentally friendly.

One of these solutions is the so called Tidal Wave Energy Converter, or TWEC. This concept utilizes the vertical motion of floating bodies in basins subject to a tidal motion to generate electricity. The principle revolves around the tide bringing the body to the extreme high tide or low tide elevation, after which it is locked in the maximum extruded position. The tide then moves to the opposite extreme point, while the body stays in the same position, building up a pressure difference between the fluid inside and outside the device based on either the force of gravity or buoyancy. Once the energy head difference is sufficient the valves are opened and the pressurized fluid is led through a conversion device, harvesting the stored energy.

The purpose of this report is to determine whether or not the Tidal Wave Energy Converter concept is feasible to continue developing. In order to be able to make a recommendation on this a framework will have to be sketched containing all the relevant variables needed to draw a conclusion. The framework will consist of several sets of boundary conditions of significantly different locations to test the workings of the apparatus in different circumstances. The components that will be considered are the tidal motion, the local water depth, the properties of possible superstructures and the water's chemical composition.

Apart from the feasibility study of the Tidal Wave Energy Converter principle itself this report will also seek to answer questions regarding the overall potential of tidal energy within the Netherlands, with special attention to the application of the TWEC. As well as seek to develop a method of easily estimating the tidal range in a certain area based on a limited amount of available information.

The rest of the report will be structured in a funnel shape starting with a broad introduction into the field of energy production, waterpower and the definition of the problem the report aims to solve (Section 1 - Introduction). After that the questions regarding the tidal motion and tidal power potential will be considered starting with tidal predictions, then the potential of tidal energy in the Netherlands and finally how tidal energy fits into the Dutch electric network (Section 2 – General scope of tidal energy). From here on the actual design of the TWEC will be discussed with consecutively the current state of the art, the boundary conditions and the requirements (Section 3 – Development framework), the shape, set-up and material and operational properties of the device (Section 4 – Engineering aspects) and finally a highest probability design and the financial consequences of installing and operating the device (Section 5 – Final design and conclusions). This last section will also include the conclusions on feasibility and recommendations on how to progress from this report onwards.

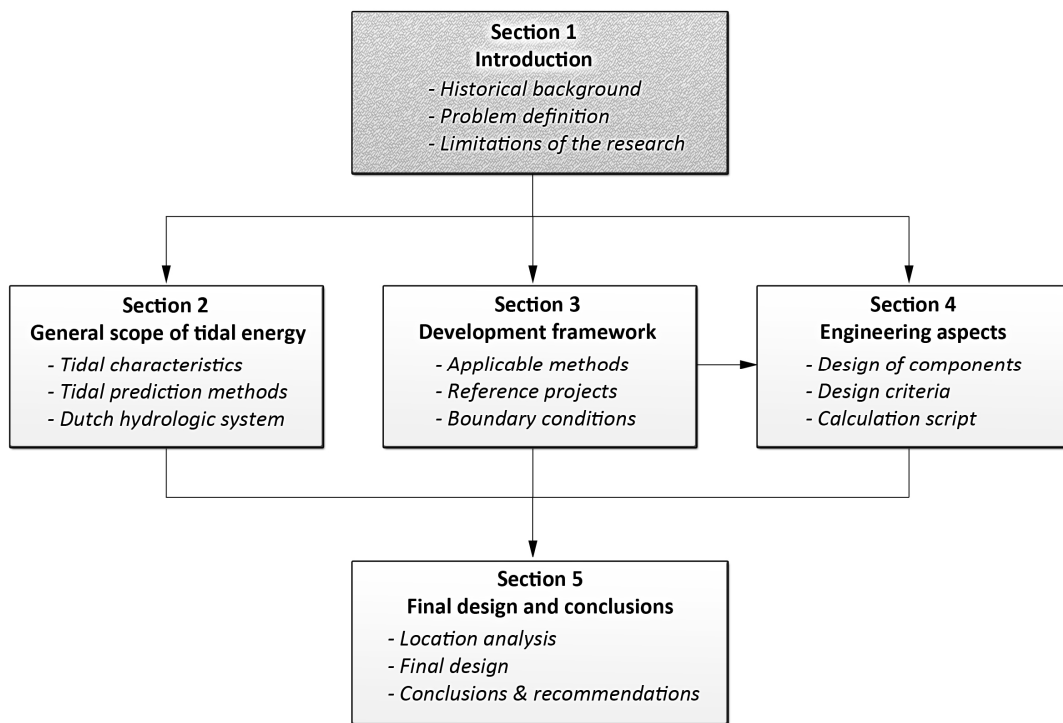


Figure 5 - Structure of the report

2 Historical background of energy production

Ever since the second industrial revolution got a grip on society in the late 19th century, the use of electricity as a tool for improving welfare has taken a gigantic leap. Especially the invention of the electric motor by Michael Faraday in 1821 meant that the abstract phenomena of electricity transformed from being a scientific curiosity to having practical applications in everyday life. This pivotal period in modern day history saw electrification, “the most important engineering achievement of the 20th century” (as named by the United States National Academy of Engineering), slowly grab a hold of society. First through factories, where mass production and the assembly line were direct results, and as a response to the Great Depression in the 1930’s houses too started being electrified throughout the Western society.

In the century since the large scale electrification of modern day households kicked in, a lot has changed. On average a Dutch household uses 3,471 kWh of electricity a year (Enerdata, 2013), where the variety in global consumption ranges from 570 kWh/year in Nigeria to 11,879 kWh/year in Canada. The dependency on electricity is large and with African and Asian countries still on their way to catch up with Western Europe and North America the demand is only expected to explode even further. Figure 6 shows the global energy consumption is growing rapidly and the growth rate has been more or less constant since the 1960s, showing no signs of slowing down.

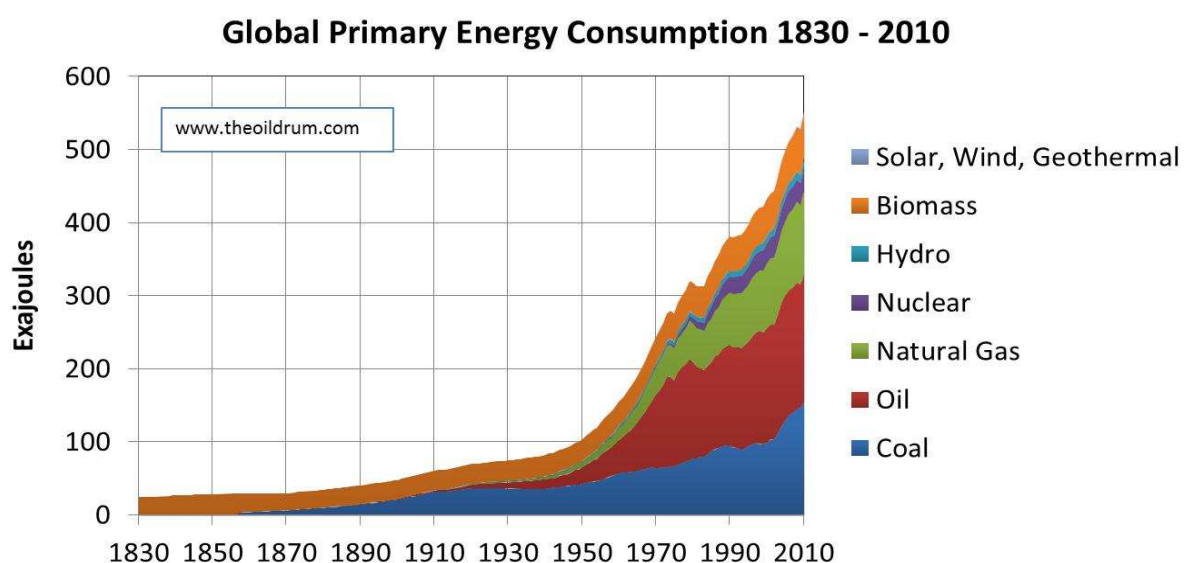


Figure 6 - Global Primary Energy Consumption 1830 – 2010 (The Oil Drum, 2012)

It can be observed from Figure 6 that there is a variety of classifications in the sources of consumed energy. From the seven that are mentioned a split can be made into two major classifications with energy sources of roughly the same characteristics in terms of sustainability, non-renewable- and renewable energy.

2.1 Non-renewable energy sources

The group of non-renewable energy sources is characterized by its property that it does not get replenished by nature in a short timeframe. This means that the amount of available resources is finite and will, at some point in the future, be depleted. Of the energy sources in this category, Nuclear energy, Natural Gas, Oil and Coal, the latter three are so called fossil fuels. They are produced by nature over millions of years and converted into energy through combustion, a process

where the carbon based fossil fuels (C_nH_m) reacts with oxygen (O_2) turning it into a combination of water (H_2O) and carbon dioxide (CO_2).

In a world that is more and more captivated by the influence of humanity on the environment, the role of the carbon footprint has been of increasing importance. Converting fossil fuels into electricity results in significant production of CO_2 as a by-product and although nowadays many filtering techniques are applied to factories' emissions large amounts still spill into the earth's atmosphere. Research shows the influence of CO_2 on the climate is severe and that the contribution of mankind on the increase of CO_2 emissions is significant (Houghton, et al., 2001).

Aside from the influence of greenhouse gas emissions on the global climate, another aspect that plays a role is that fossil fuels are not infinite. Given the required time for refilling the reserves that are currently being tapped into, it is to be expected that the current demand of 86.4% of the global energy consumption cannot be satisfied indefinitely. And although new ways of extracting even the last amounts of fossil fuel from the soil are being developed (e.g.: shale gas) the costs of these expeditions will at some point exceed what customers are willing to pay for that type of electricity. To illustrate the finite nature of non-renewable energy sources a quote from former Minister of Petroleum of Saudi Arabia is fitting:

"The Stone Age came to an end not for a lack of stones and the oil age will end, but not for a lack of oil."

Ahmed Zaki Yamani (Minister of Petroleum, Saudi Arabia).

Ahmed Zaki Yamani hereby illustrates that it will not be the depletion of the reserves that will trigger a shift towards alternative energy sources, but that at some point financial, practical or other motivations will cause fossil fuels to lose their appeal.

2.2 Renewable energy sources

Ideally an energy source would be continuously available and infinite in stock, so that it can be used indefinitely and on-demand. Because such energy sources are as of yet unavailable the next best thing is what nature provides and replenishes in a short timeframe. These are so called renewable energy sources because, as mentioned, they get renewed by nature after they have been tapped into. The main energy sources in this category are biomass, biofuel, solar, wind, geothermal and hydroelectric energy. Apart from the first two energy sources mentioned these are also free of greenhouse gas emissions, which means they belong in the category of so called "Green Energy" sources.

Albeit these energy sources are in essence infinite in their lifespan, they are not without flaws. The availability often fluctuates over time and construction of plants often has a severe influence on the environment in terms of flora, fauna and local population. Besides that the aesthetics of the structures often too find resistance with inhabitants of the area.

Figure 7 illustrates that the market share of renewable energy in the current energy network is limited to 19%. This is already a small portion which is even inflated by a 68% share of traditional biomass (e.g.: the burning of wood). The total market share of green energy is about 4%, which is only a tiny portion of the whole. So with all the known issues that carbon dioxide emissions are causing to the environment, we still rely on a 96% share of pollutant energy sources to fuel a rapidly increasing consumption pattern.

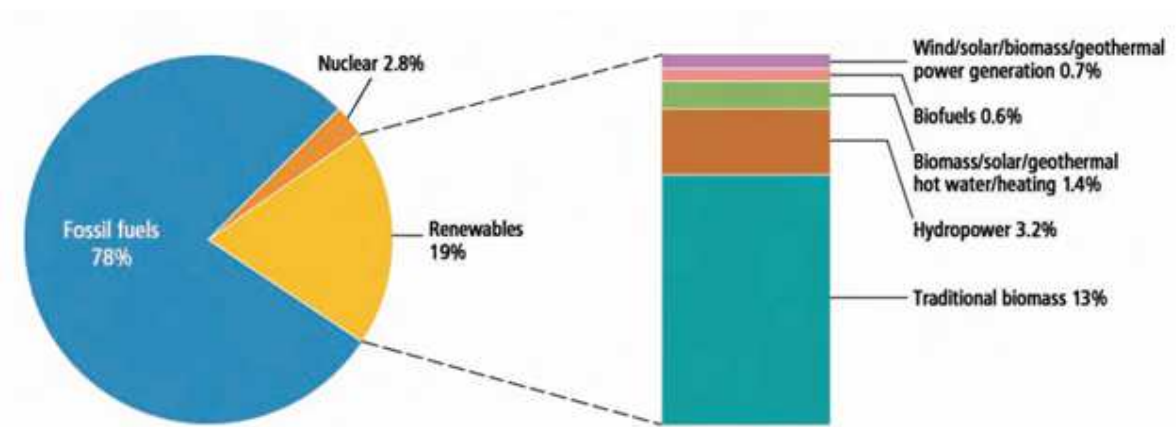


Figure 7 - Market share of renewable energy sources globally (Renewable Energy Policy Network for the 21st Century, 2010).

3 Brief introduction into hydroelectric energy

The energy potential of hydropower is considerable. Figure 7 shows that out of the current green energy production this type of natural resource is responsible for a whopping 80% of the production. This should not really come as a surprise when around 71% of the earth's surface is covered by oceans, but what is curious about it is that virtually none of the production originates from this area. For the sake of generalization the distinction can be made between conventional hydropower and marine energy.

3.1 Conventional hydropower

Conventional hydropower is the main contributor to all the hydroelectric energy that is being produced around the world and besides that also the most eye-catching source. It is carried by massive reservoir plant projects capable of covering for the electricity demand of an entire nation. One of the more known projects in this category is the Itaipu Dam on the border of Brazil and Paraguay which, with its installed capacity of 14 Gigawatts is responsible for a 72.5% market share of Paraguay's energy consumption and nearly 25% of Brazil's (Itaipu Binacional, 2013).

However, other than the well-known reservoir plants there are several other, less productive but equally impressive, types of land-based hydroelectric plants. Mountainous countries such as Austria have constructed so called High Head Plants with penstocks of over 1000 meters. In rivers with a large water level gradient such as the Columbia River or the River Meuse there are possibilities to install Run of River plants, which utilizes the flow of the river to generate electricity. These plants exist both with and without the capability of flow regulating water storage (or "pondage"); plants without this feature are highly dependent on seasonal fluctuations and produce irregular amounts of energy, whereas plants with a pondage can produce a more constant output. Lastly there are tidal basins which border on the field of marine energy. An example of a large plant exists in La Rance, France and has an installed capacity of 240 Megawatts (Wyre Tidal Energy, 2014). This type of plant utilizes the oscillating motion of large tidal waves to create a water level difference between high and low water level. A special type of tidal barrage that is currently being developed is the Dynamic Tidal Power principle (DTP). Here the barrage is a large dam stretching into the ocean, perpendicular to the propagation direction of the tidal wave, which the wave has to flow around. The time it takes for the wave to propagate creates a water level difference between one end of the dam and the other due to the fact that the crest of the wave is on one side and the trough on the other.

| | Order magnitude head |
|------------------------------|----------------------|
| High head power plant | 1,000 [m] |
| Reservoir plant | 100 [m] |
| Run-of-River plant | 15 - 30 [m] |
| Tidal basin | 5 - 15 [m] |

Table 2 - Minimal operational boundary conditions of various hydropower plants

Table 2 illustrates the approximate operation range of the different types of plants previously discussed. It goes without saying that in flat countries like the Netherlands it is virtually impossible to create the required flow conditions for the high head and reservoir plants. Moreover with a tidal range of approximately 2 meters and river heads of respectively 10 and 45 meters over the rivers Rhine and Meuse (EWA, 2008), the latter housing several run of river plants, the possibilities in the other fields are limited as well.

3.2 Marine energy

Marine energy is the collective name of all energy originating in the ocean, so technically the aforementioned tidal basins also fit into this category. With 71% of the world being covered by ocean and most of the potential still being untapped there is a lot of innovation taking place to try and utilize the potential of this energy source. Estimates of its power potential go as high as 6000 GW of potential energy stored in the ocean (International Energy Agency, 2010) which albeit being impossible to fully extract is still a vast reservoir of largely untapped energy resources.

One of the more active fields of development is the field of Wave Energy Converters (WECs). Devices in a varying range of sizes that harvest the energy from the oscillating motion of swell and wind waves. Although various names and classifications have been given over the years the distinction comes down to two basic types: buoyancy based devices and oscillating water surface based devices. In the former type (Figure 8a) there is a large variety of buoys and other (partially) floating structures that use the oscillating water surface on which they are floating to move part of the structure relative to a fixed point to drive a generator.

The types that utilize the oscillating water surface include overtopping devices and devices that transfer the energy to an air column before extracting it. The former type lets the wave run up a slope from where it overtops to a reservoir with a head relative to the mean water level of the surrounding ocean (Figure 8b). The water is then led through a turbine as it flows back into the ocean so energy can be extracted. The latter has a pressure chamber enclosing the ocean surface connected to the outside air through a wind turbine. The oscillating water pushes air out of the chamber as the water goes up and sucks it into the chamber as the water goes down, thereby putting the turbine in motion and powering a generator (Figure 8c).

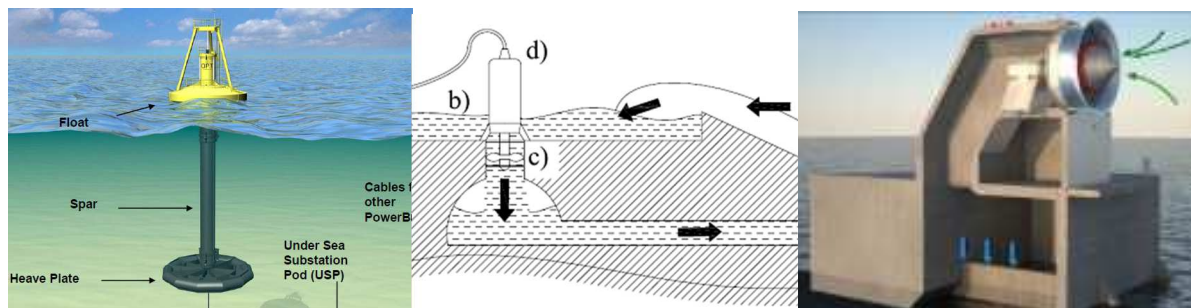


Figure 8 - (a) buoy type device (PowerBuoy) (b) overtopping type device (Wave Dragon)
(c) air chamber device (Oceanlinx)

Another field of innovation is that of the Tidal Energy Converter (TEC). These devices, also referred to as tidal stream energy or tidal current energy, use the velocity of the water as it flows around the world along with the propagating tidal wave. Large underwater mills similar to windmills are installed in areas where the water velocity is high. This is usually in places where the local bathymetry creates a funnel effect to accelerate the water. The flowing water rotates the blades of the mill which in turn drive a generator.

Lastly another interesting method of marine energy is the use of osmosis. Rivers flowing into the ocean cause many meeting places of salt and fresh water all over the world. The mixing process of these two substances is a potential source of energy as well. Chambers are created in which the salt and fresh water are stored side by side separated by a membrane that is only permeable to fresh water. The natural attraction of the two fluids causes the fresh water to flow into the salt water container and cause an overpressure there which can be used to power a turbine.

4 Problem definition

Before the actual engineering part of the research can be done it has to be determined what questions actually need to be answered by this report. A good definition of the problem has to be set up to narrow down the scope of the investigation and make sure the results are obtained in a systematic way that yields the desired results in an efficient manner. This chapter aims to define that scope and to clearly define what this report aims to answer by its conclusion.

It can be concluded from the previously discussed current state of affairs that the increasing demand for electricity is unlikely to be sustained indefinitely by a dwindling supply of fossil fuels and that a large part of the answer may lie in hydroelectricity and the oceans in specific. An innovation in this field that is in the very early stages of development is the Tidal Wave Energy Converter (TWEC) based on the “Kieuwbalg” idea of Peter Ligthart. This principle seeks to increase efficiency when harvesting from small tidal ranges by amplifying the gravitational or buoyant forces of large floating objects in water such as pontoons.

The guiding principle in how this method will be advantageous can be found in the physics behind hydroelectric energy. Equation 1 shows the relation between the generated power in Watts and a fluid’s pressure and velocity. Given that both defining parameters, head and discharge, are not in abundance in many hydrological systems worldwide it is essential that either one is somehow amplified in order for the process to yield sufficient results.

$$P = \eta \cdot \rho \cdot g \cdot Q \cdot H$$

P = power [W]

η = coefficient for losses [-]

ρ = fluid density [kg/m^3]

g = gravitational acceleration [m/s^2]

Q = discharge [m^3/s]

H = energy head [m]

Equation 1 – Hydraulic power

The discharge is a set variable given by local boundary conditions. You cannot add more discharge without either diverting a river into the considered system (implausible) or by pumping extra water into it, which defeats the purpose of energy production as it would cost more energy than it yields. The logical step therefore is to increase the head. This principle is also used in reservoir plants where a dam holds back the river so that the water level builds up and the head is increased. In a country where the overall slope of the countryside is 1 meter in 15 kilometres, however, the required basin would practically flood most of Western Europe.

Equation 2 gives the relation between the energy head and the components of velocity head and pressure head. The velocity is directly related to the flow area and the discharge, reducing the flow area, however, means the power output also reduces as the power diminishes quadratically with the

diameter ($P/P_2 = (D/D_2)^2$ (van Duivendijk)). The only option for increasing the energy head is therefore to amplify the pressure head and therefore the pressure itself.

$$H = z + \underbrace{\left(\frac{p}{\rho \cdot g} \right)}_{\text{pressure head}} + \underbrace{\left(\frac{u^2}{2 \cdot g} \right)}_{\text{velocity head}}$$

H = Energy head [m]

z = location height [m]

u = fluid velocity [m/s]

Equation 2 – Energy head

The presence of a discharge in the system implies that the system is open ended, after all there has to be an inflowing discharge and an out flowing discharge (which are of equal magnitude) for the system to maintain itself. Given that water flows to the area with the lowest energy head applying an additional pressure to the water in this situation would be impossible, as before any pressure could build up the water would flow to an area where the energy head is lower. In order to successfully apply pressure to a water body it is therefore required that it is stationary.

To increase the pressure in a body of fluid is one thing, but to make sure the source of the energy is renewable by nature is another. Somehow nature will have to apply a force to the water body in such a way that after extracting energy from this force, it reloads again. The only natural phenomena occurring in the water system that has this oscillating character are waves. As mentioned before there are some innovations under development that apply this principle to swell and wind waves.

The TWEC, however, seeks to use the motion of tidal waves as a means of generating electricity in a similar fashion. Tidal waves are much larger than swell waves with periods of 12 hours and amplitudes of up to 10 meters in some areas on the globe. One of the benefits of harvesting “wave energy” from tidal waves is that many floating structures are already situated in tidal waves all over the world. Efficiently harvesting this energy would mean a tremendous boost to green energy production.

The principle is as follows. A pontoon or other type of buoyant object floats on an arbitrary, tide influenced water body. As the floating body reaches an extreme extrusion relative to the mean water level (maximum high or low water level) valves are closed and the pontoon is locked in position. As the tide moves towards the opposite extreme extrusion a pressure is built up in a chamber due to the forces of gravity or buoyancy that are exerted on the pontoon. As the water level reaches its opposite maximum height the valves are opened and water will flow in or out of the chamber due to the pressure gradient created between the atmosphere and the fluid in the chamber. Figure 9 illustrates the process where the dotted blue line indicates the equilibrium water level, the black line cutting through the pontoon being the water level in that specific situation and the arrows indicate the direction of the forces on the system.

The added benefit of the delay in the actual harvesting of the energy in the pressure chamber is that it leaves room for the possibility of keeping it stored until a moment when the energy is actually needed. Due to the irregularities in the production patterns of many renewable energy sources, it is

often produced when it is not needed and not available when there is high demand. There is an increasing demand for energy storage to go along with the rise of renewable energy production. Adding that functionality to the device would boost its application range greatly.

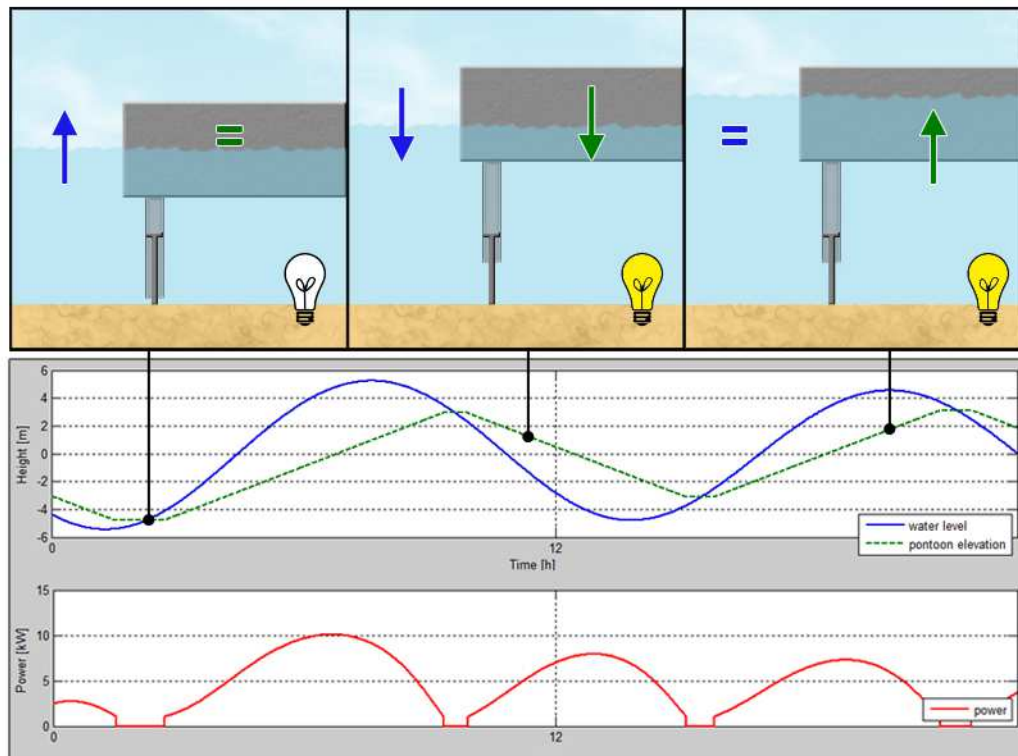


Figure 9 - Schematization of the Tidal Wave Energy Converter principle

The scope of the research is, however, not limited to the development of just the TWEC. There are a lot of unknowns in the field of tidal energy that need to be addressed before a definitive conclusion on feasibility can be derived. Firstly a simple model or rule-of-thumb equation needs to be developed for tidal predictions around the world. Currently it is difficult to get estimates on the tidal range in a certain area unless you place a measuring buoy or station at the desired location and measure the tide for a certain amount of time. Often this time is not available and results need to be presented sooner. In case of the TWEC often times its application location is not one that is intensively monitored and a simple approximation would be desirable to determine whether it is wise to carry on with the development at the location.

Furthermore it is important to know what the application possibilities of the device are within the Dutch hydrologic system. Therefore an analysis will be made of the potential for tidal energy within the Netherlands as a whole with special attention to the specific application of the TWEC. It is, after all, most interesting for countries with relatively little possibilities for harvesting hydroelectric energy to apply this new method. If it works there it is very likely to be feasible on a larger scale in countries with more tidal energy potential.

All in all the report aims to answer the following main question based on scientifically sound argumentation:

How, if at all, can the Tidal Wave Energy Converter be made a financially and technically feasible means of harvesting energy from (relatively small) tidal motions?

5 Limitations of the research

Because not every aspect of the development of the Tidal Wave Energy Converter can be taken into account in the limited amount of time available for this research there are some aspects that remain outside the scope of the research. To provide clarity on what can and cannot be found in this report and what is included in its conclusions the limitations of the research will be discussed in this chapter.

Exempt from consideration in this research are:

- **Detailed analysis of the application area's boundary conditions.**
It is deemed unnecessary to have detailed information on only some locations when its application area is much larger, fictional standard locations will be derived from existing high potential locations. The locations will be determined based on strongly differing boundary conditions (soil composition, water depth, tidal range) and the potential of existing or developing projects that could serve as a catalyst.
- **Detailed constructive design of the foundation.**
For cost estimation purposes the foundation will be schematized globally with identification of what foundation can be used, but the finer details will not be considered. In essence this means that the designed foundation will be based on of-the-shelf solutions with characteristics provided by the manufacturer without an in-situ analysis of local conditions.
- **Detailed analysis of how the network will process the generated electricity.**
Recommendations will be made regarding the matching of production patterns with consumption and the possibilities for using the TWEC as an energy storage buffer, but a detailed description of how the electricity from the TWEC gets to its destination will not be given. The energy grid will be deemed capable of handling the TWEC's production.
- **Production process of components of the TWEC.**
The dimensions and materials of the components will be determined but not what processes should be used to actually make these. The design process will mostly attempt to use off the shelf products to construct the device meaning the production methods are irrelevant to whoever builds the device itself. For specifically designed components it is assumed the industry will know how to produce them as long as the dimensions and used materials are given.
- **The detailed effects of corrosion and other material degradation catalysts.**
Potential hazards will be identified but not the severity of the influence the effects have on the product. It is important for the estimation of maintenance costs to have an idea of what processes affect the device and to take appropriate protective countermeasures, but determining the exact timeframes of material degradation is too detailed for this study.
- **The used energy conversion mechanism will be chosen from existing technology.**
There is a lot of innovation still to be done regarding low head hydro energy conversion mechanisms which is an entire study in itself. Because this research regards a different study which only uses the technology it is deemed sufficient to consider existing technology and chose an of the shelf solution rather than designing a completely new energy conversion mechanism. If necessary potential new technology can always be applied to the device at a later date.

Section 2 – General scope of tidal energy

| | | |
|-----|--|----|
| 6 | Introduction to general scope of tidal energy..... | 35 |
| 7 | Global estimation tool for tidal amplitudes | 37 |
| 7.1 | Global Inverse Tide Model..... | 37 |
| 7.2 | Near shore tidal amplitude adjustment script | 38 |
| 8 | The applicability of tidal energy in the Dutch hydrologic system | 43 |
| 8.1 | Estuaries | 43 |
| 8.2 | Open basins | 46 |
| 8.3 | Closed basins | 47 |
| 8.4 | Waddenzee..... | 51 |
| 9 | Electric network..... | 53 |
| 9.1 | Consumption patterns..... | 53 |
| 9.2 | Production patterns | 53 |
| 9.3 | Bridging the gap | 55 |
| 10 | Conclusions on tidal energy scope | 57 |



6 Introduction to general scope of tidal energy

Having defined the problem definition and background of the problem, the next step is to look into the general framework in which the Tidal Wave Energy Converter will be required to operate. This section will aim to provide that framework by looking at the hydrologic situation on a global scale and the state of affairs in the electric network the device will be connected to.

Regarding the hydrologic system the aim is to create a tool with which easy estimates can be made regarding the tidal motion in a certain arbitrary area in the world. The basis of this tool should be the ocean tide as much information on this is available from radar altimetry projects such as TOPEX/Poseidon. From the ocean tide data gathered by these projects the tidal constituents can be obtained which in turn shall be scaled accordingly depending on the near-shore conditions. A distinction in this is made between estuaries and basins. More information on the developed method can be found in Chapter 0. The created model will subsequently be put into practice by applying it to several locations of interest along the Dutch coastline where possibilities may occur for generating tidal power, which is expanded on in Chapter 8.

Finally the state of the Electric network will be evaluated in chapter 9 with special attention to how tidal power as a whole and the Tidal Wave Energy Converter in specific fit into it. Basis of the analysis will be the means in which electricity is currently generated, how these means of generating electricity affect the production and how the consumption pattern and production pattern relate to each other.

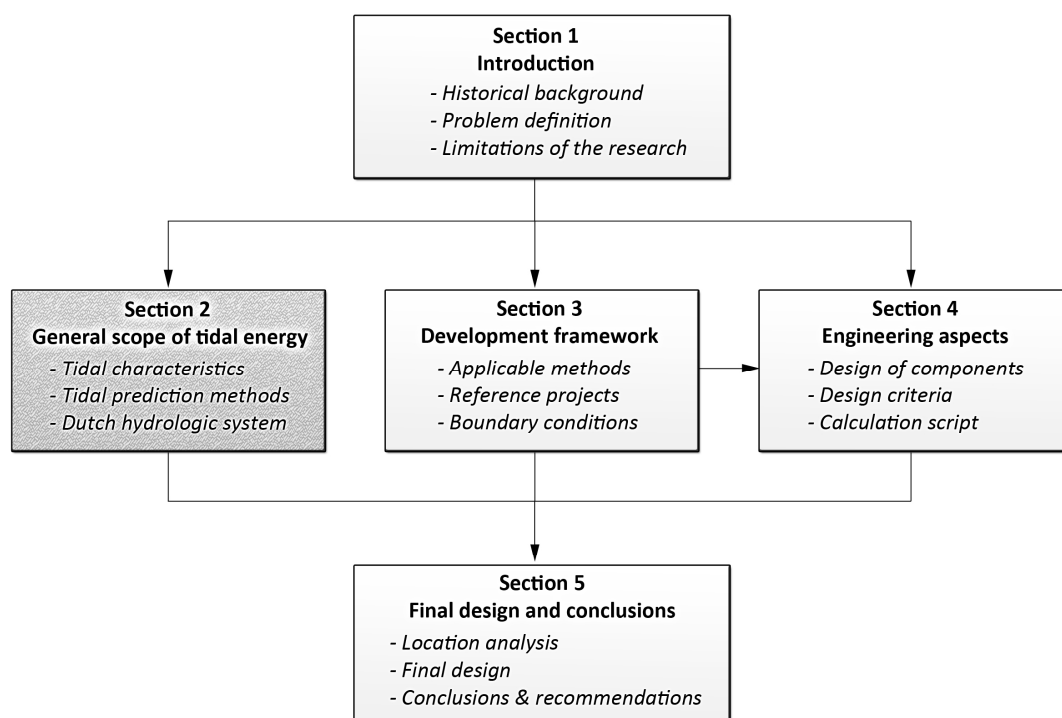


Figure 10 - Structure of the report

7 Global estimation tool for tidal amplitudes

Because the Tidal Wave Energy Converter has a large potential application area it is interesting to develop a tool that can be used to estimate the tidal potential in a certain area in a relatively early stage of the feasibility study. To avoid having to do prolonged in-situ measurements, for which often the time and the resources are not available, a method has been developed that allows for rough tidal predictions all over the world based on the ocean tide and a schematisation of the coastal system.

The method that has been developed consists of two main components:

- Global Inverse Tide Model (Erofeeva, 2002)
- Near shore tidal amplitude adjustment script

7.1 Global Inverse Tide Model

The Global Inverse Tide Model is a model that analyses and predicts the ocean tides on a global scale. It is a medium resolution tidal model with a grid size of 0.25° by 0.25° based on satellite radar altimetry from the TOPEX/Poseidon program. Based on its dataset the tidal constituents can be obtained of the monthly M_M tide, the fortnightly M_F tide, the diurnal K_1 , O_1 , P_1 and Q_1 tides, the semi-diurnal M_2 , S_2 , N_2 and K_2 tides and the higher order M_4 tide for any desired location in the ocean (explanation on these tides in Appendix A).

Figure 11 shows the Graphic User Interface (GUI) of the Tidal Model Driver (TMD) with a plot of the M_2 tidal heat map displayed. The TMD is a MatLab toolbox that can be used to easily access the data in the model and display it in a user friendly format. The GUI has the option of displaying heat maps of tidal amplitude and phase shift of the previously mentioned tidal constituents and can make tidal predictions of any desired combination of constituents and timeframe. Furthermore it has data on the tidal velocities, transport and ellipse based on the specific constituents, which is of lesser interest to this research.

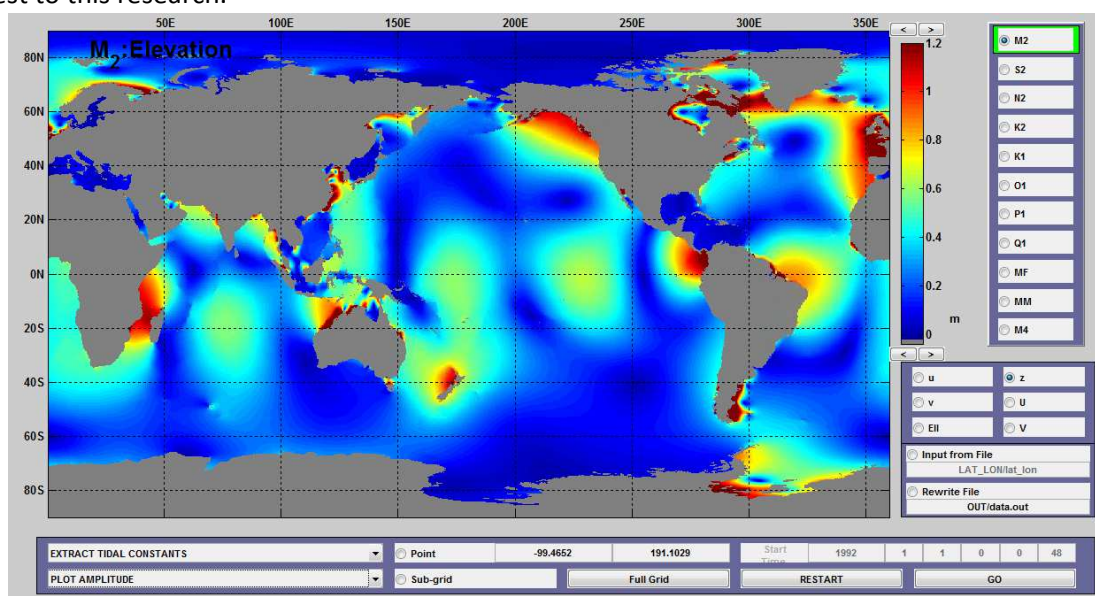


Figure 11 - Global Inverse Tide Model plot for M_2 amplitude

7.2 Near shore tidal amplitude adjustment script

The previously described tidal model has a finite amount of data and is, given its medium resolution base, limited to the tidal motion on the open sea and ocean. To translate this to conditions in various environments in the near shore area a second step is required to adjust the tidal amplitude to the different conditions. To model this, two different types of near shore areas are identified and analysed: Bays and Estuaries.

7.2.1 Tidal motion in (semi) open basins

For the tidal propagation in basins a distinction can be made between two different types of basins, long and short. Short basins are characterised by being relatively short compared to the wave length of the tidal wave. This means a simplification can be made in that the water level along the basin moves uniformly in vertical direction according to Equation 3. The water is forced into the basin due to the water level differential between the water outside the basin and the water inside the basin forcing the water to rise and fall. In these short basins the tidal amplitude will always be smaller or equal to the tidal forcing on the outside because no resonance will occur. The size of the flow area determines how much the tide is damped inside the basin.

$$B \cdot \frac{\partial h}{\partial t} = \mu \cdot A_s \cdot \sqrt{2 \cdot g \cdot (|h_{bay} - h_{sea}|)} + Q_r$$

B = storage area $[m^2]$
 μ = contraction coefficient $[-]$
 A_s = flow area $[m^2]$
 Q_r = river discharge $[m^3/s]$
 h = water level $[m]$

Equation 3 – Storage equation

The second type of basin that may occur is a basin with an Eigen period equal to the period of a major tidal constituent. Equation 4 indicates the mathematical formula to derive the length of such a system. In these basins the tidal wave is reflected at the end of the basin in such a way that the reflected wave is in phase with the incoming wave, creating a standing resonant wave with amplified amplitude. An example of such a basin is the Bay of Fundy in Canada which is approximately 300 km long (Cleveland, 2013) and 75 meters deep (Pelletier & McCullen, 1972) causing a second order resonant harmonic to occur.

$$L = \frac{1}{2 \cdot k} \cdot T \cdot \sqrt{g \cdot h}$$

L = bay length; $k = 1, 2, 3, \dots$; T = tide period

Equation 4 – Merian formula

The first occurring phenomenon is modelled in a MatLab script which can be found in Appendix B, an example of a result of this method is given in Figure 12. The displayed situation involves a basin with a relatively small flow opening compared to the storage surface ($A_s/B = 0.02\%$). This causes the average tidal amplitude to be damped as the capacity of the flow opening is insufficient to facilitate the water level in the bay to rise as quickly as the outside tide. The script also accounts for the effect

that an elevated bottom level at the entrance may have when acting like a weir in shallow waters. For large basins deviations from the mean amplitude may occur in the areas closest to the ocean and furthest from the ocean.

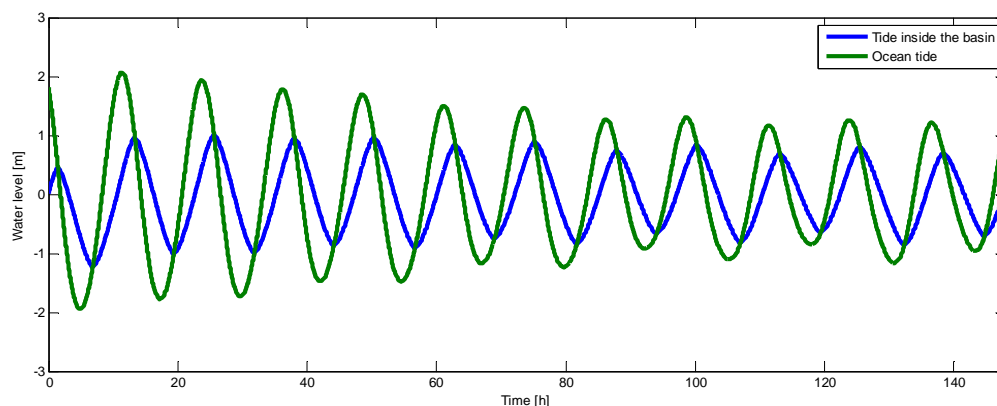


Figure 12 - Damped tidal excitation in bay

The second phenomenon in which the tidal amplitude is magnified through resonance occurs mainly on large continental shelves (e.g.: the Patagonian shelf on the Argentine coast) and large bays (e.g.: the Bay of Fundy). These locations are deemed to be of sufficient magnitude to be accurately available in the Global Inverse Tide Model.

7.2.2 Tidal motion in estuaries

Estuaries are naturally formed coastal zones in the area where a river flows into the ocean. The interaction between the salt ocean water and the fresh river water causes the water in these environments to be brackish and subject to the tidal motion, ocean waves as well as the discharge of the local river. It has been observed that the water depth in an estuary is mainly influenced by the sediment transport coming from the river and that the horizontal shape is created by the incoming tidal wave (Savenije, 2014). The incoming tidal wave has a certain amount of wave energy at the mouth of the estuary creating a certain width. As the wave propagates upstream friction causes the amount of energy stored in the wave to diminish. The wave energy per unit width remains the same, causing the width to diminish upstream in accordance with the dissipation of energy.

This process occurs ideally in the so-called “ideal estuary”, where the process of sedimentation and erosion causes the banks of the estuary to take an exponential form as given in Equation 5. In these ideal estuaries there is a balance between friction forces and convergence of the banks, causing the energy per unit width to remain constant and therefore no damping or amplification to take place. Such estuaries could form on long coastal plains with a gentle topography and relatively fine sediment, giving nature free reign to form the banks in an ideal way. In reality, however, they are more of a scientific curiosity and do not naturally exist.

$$B(x) = B_0 \cdot e^{-\frac{x}{b}}$$

B = width at location x

B_0 = initial width

x = inland location

b = contraction coefficient

Equation 5 – Contraction of estuaries

It follows from the previously discussed characteristics of the ideal estuary that amplification and damping occur when the balance between convergence and friction is disturbed. When the estuary converges more rapidly than the ideal situation, the tide will be amplified; when it converges slower, the tide will be damped. The easiest way to qualitatively determine whether the tide in an estuary will be damped or amplified is by comparing the wave celerity at the mouth to the wave celerity in the estuary. If the wave travels slower inside the estuary than outside, more water will be pushed in than the flow can handle causing the water to back up and increase in amplitude. The opposite applies when the wave can travel faster inside the estuary and the tide will be damped. This phenomenon can be explained through Bernoulli's principle of energy head, as is illustrated in Figure 13 where c is the wave celerity and z the water height relative to the bottom. Friction is neglected for the sake of visualising the principle.

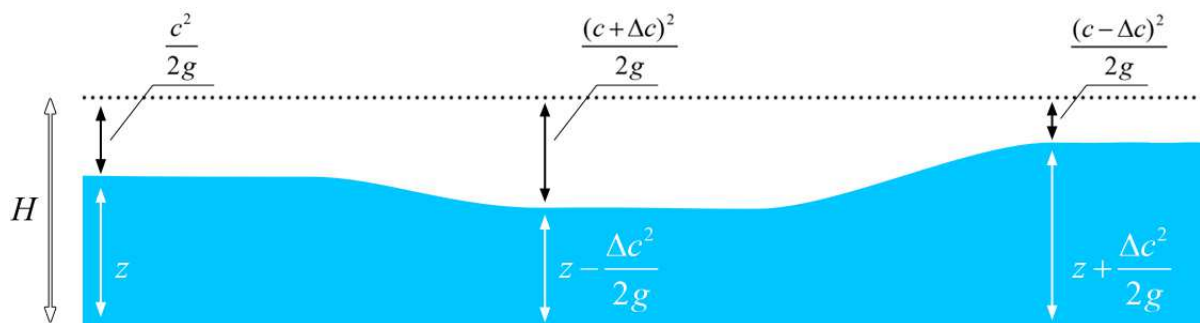


Figure 13 - The effect of wave celerity on the water level

Studies have been done in the past to quantify the amplification of tides in estuaries. The results of these studies can be used to again write a MatLab script to quantify the behaviour of the tide in estuaries. The chosen method of analysing the propagation of the tidal amplitude upstream is that of (Savenije, et al., 2008). This method, just as most other available methods, has been developed and gauged with the (Western) Scheldt estuary and calculates the tidal damping/amplification based on the input variables of bathymetry, storage/width ratio, convergence length, tidal forcing and friction coefficient (explanation in Appendix B) which can be estimated relatively easily. Figure 14 shows the result of the calculation done for the (Western) Scheldt estuary with the created MatLab script. The maximum value for the tidal amplification and the distance upstream where this maximum occurs can easily be read from this graph.

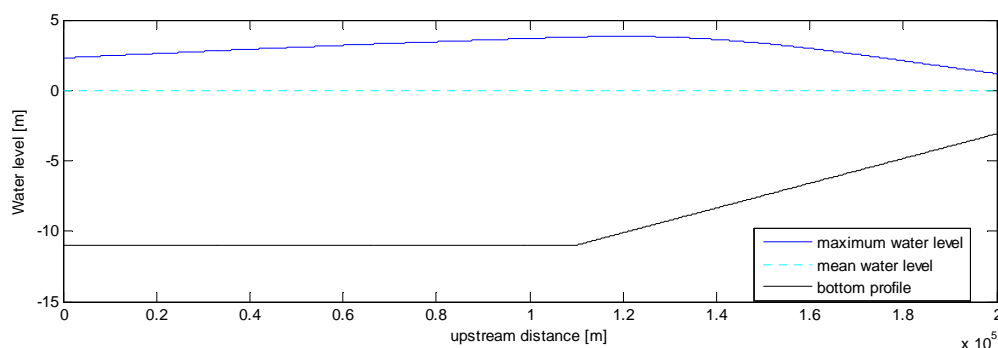


Figure 14 - Modelled tidal propagation in the Scheldt estuary

The river discharge has not been taken into account in this calculation. It follows from (Horrevoets, et al., 2004) that the influence of the river's discharge on the location and amplitude of

the maximum tide is negligible. Furthermore it should be noted that the used method of (Savenije, et al., 2008) gives a slight overestimation of the tidal range. Because for practical applications it is more desirable to have a lower limit rather than an upper limit this should be taken into account. The revised equations of (Cai, et al., 2012) would serve as a better tool to use for this application, as it's both more accurate as well as that it underestimates the tide slightly. This method, however, has not been included in this research. Because the method is only applicable to a single tidal constituent and not yet to the full tidal spectrum it is deemed a sufficient countermeasure for the overestimation of the tide to only use the dominant tidal constituent. The other constituents then serve as a buffer to counter the error in the method of (Savenije, et al., 2008).

8 The applicability of tidal energy in the Dutch hydrologic system

Having created a system for easily determining the tidal amplitude at any given location in 7.1 it is interesting to look into the application of this system on the Dutch hydrologic system. To do that first an understanding is required of what tide influenced areas exist in the Netherlands and how they should be classified for the calculation method. In Figure 15 a map of the Netherlands is presented on which the considered grid of the Global Inverse Tide Model is drawn as well as indications of what areas of interest should be looked into. The tidal characteristics of these locations are given in Appendix C. All heights and depths mentioned are relative to the Normaal Amsterdam's Peil (NAP) reference level.



Figure 15 - Map of the Netherlands with model grid and areas of interest

8.1 Estuaries

Estuaries are the result of a river flowing into a tide influenced ocean. Funnel shaped morphological structures are created by the interaction of tide, waves and river discharge with the land. What is often referred to as a Delta in the Netherlands is actually a complex system of estuaries of three major rivers (the Scheldt, the Meuse and the Rhine) which has been domesticated and

dammed shut by colonisation of Zeeland and the Delta Works. Two actual estuaries still exist in the Dutch coastal system, being the Western Scheldt (Scheldt estuary) and the Eems (Ems Estuary). Furthermore the Nieuwe Waterweg in the Port of Rotterdam can be considered a special case of estuary for this research.

8.1.1 Western Scheldt

The Western Scheldt is the Southernmost and fully open branch of the Scheldt estuary. It serves as the seaward approach channel for the Antwerp port and is therefore subject to severe human interference in terms of depth, in the lower reaches of the estuary it is constant, and as of 110km upstream it slowly shallows. Furthermore the colonisation of Zeeland combined with the flood protection measures of the Delta works mean the shape of the estuary has also been altered from its original shape. These alterations mean that the estuary has a relatively large water depth and short convergence length compared to the tidal forcing it is subject to. The increased water depth causes the wave celerity in the estuary to increase, which would imply damping, the shortened convergence length, however, causes the opposite effect in that the decrease of width is quicker than the decrease in energy through friction, causing amplification. The calculation as described in 7.2.2 yields the figure as presented in Figure 16 and the numerical output as given here.

► Input variables:

- Average water depth: 11 [m]
(decreases to 2.6 metres between 110km and 200k upstream)
- Convergence length: 27,000 [m]
- Dominant tidal amplitude (M_2): 1.5315 [m]
- Friction coefficient: 38 [$\text{m}^{0.33} \text{s}^{-1}$]
- Storage-width ratio: 1.4 [-]
- Estuary length: 200,000 [m]

► Output:

- Maximum tidal amplitude: 3.3086 [m] (216%)
- Maximum tidal range: 6.6172 [m]
- Upstream distance to maximum: 127 [km]

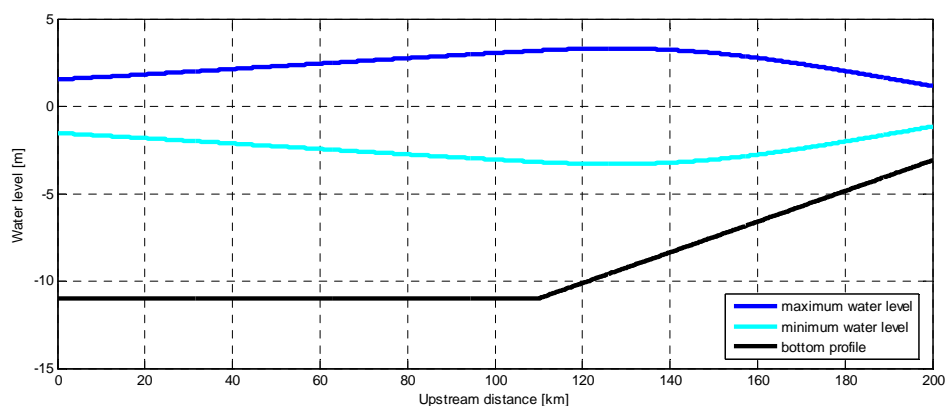


Figure 16 - Tidal response upstream in the Western Scheldt

8.1.2 Nieuwe Waterweg

The Nieuwe Waterweg is the approach channel for the older parts of the Port of Rotterdam (the new areas such as the Maasvlakte use the adjacent Calandkanaal). It is a manmade waterway that was dug in the late 19th century. This means it is not an estuary by nature, but in its behaviour it can be modelled as one. In this case the convergence length of the estuary is infinite, as the banks of the waterway remain parallel to each other. Figure 17 shows that the tidal amplitude remains the same as it propagates inland along the first 20 kilometres of the channel, after which it splits into a South-eastern branch called the Oude Maas and a North-eastern branch called the Nieuwe Maas. The balance in this case comes from the balance of friction with the convergence of the bottom profile, which due to a lack of better information has been modelled as a straight line going from the maximum depth at the channel entrance to 20 metres at the point of the split. In reality this decrease in depth happens in steps rather than a gradual decline. Furthermore the distance is not that large, meaning the amplification does not have much room to develop.

► Input variables:

- Average water depth: 23 [m]
(decreases to 16 meters around 20 kilometres upstream)
- Convergence length: ∞ [m]
- Dominant tidal amplitude (M_2): 0.8927 [m]
- Friction coefficient: 38 [$m^{0.33} s^{-1}$]

► Output:

- Maximum tidal amplitude: 0.8927 [m] (100%)
- Maximum tidal range: 1.7854 [m]

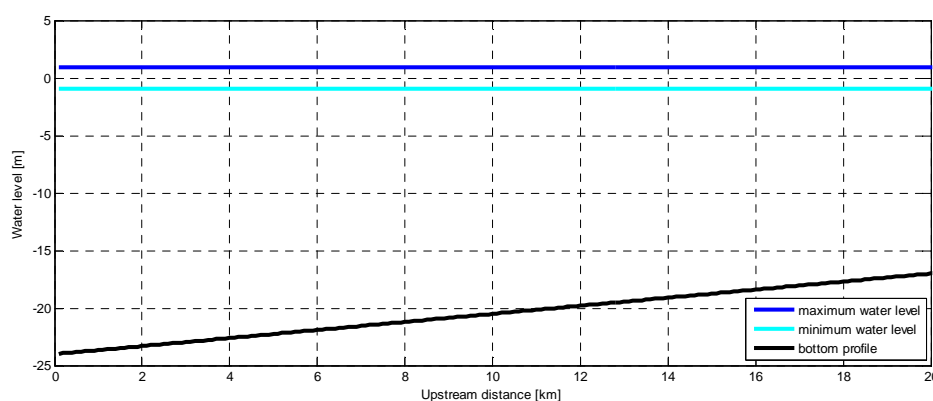


Figure 17 - Tidal response upstream in the Nieuwe Waterweg

8.1.3 Eems – Dollard

The Eems-Dollard estuary is one of a relatively complicated shape. It starts out as a usual estuary of the Ems River into the Wadden Sea (the Eems), but suddenly bulges out into a large basin at the Dollard. Because the Dollard is relatively shallow (order of 2.5 meters depth) and the Eems and Ems are significantly deeper this can be viewed as a flood plain rather than an actual part of the estuary. The water depth in the Eems estuary fluctuates significantly and has been approximated by a series of strait lines between significant locations. It can be observed from Figure 18 that the tidal amplitude amplifies slightly close to the ocean side of the estuary and damps out again further along

the estuary. It can be expected that the Dollard basin will respond accordingly with the tidal amplitude between 25km and 35 km upstream, where the Dollard connects to the Eems.

► Input variables:

- Water depth: 13 [m]
 - Convergence length: 30,000 [m]
 - Dominant tidal amplitude (M_2): 1.35 [m]
 - Friction coefficient: 38 [$m^{0.33} s^{-1}$]
 - Estuary length: 70,000 [m]
- (data from (Schuttelaars, et al., 2011))

► Output:

- Maximum tidal amplitude: 1.5308 [m] (113%)
- Maximum tidal range: 3.0616 [m]
- Upstream distance to maximum: 23 [km]

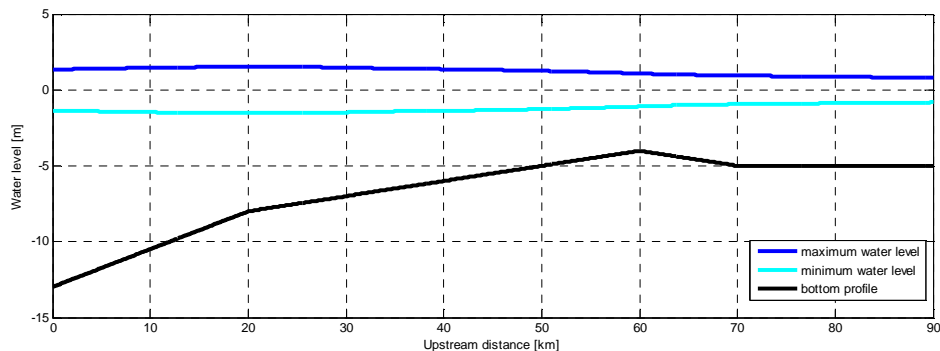


Figure 18 - Tidal response upstream in the Eems

8.2 Open basins

Open basins are basins that are in direct contact with the ocean. The external forcing of the tide causes the water level inside the basin to react in some way and oscillate at the same angular velocity of the tidal forcing. Depending on the length of the connection channel there may be a phase shift between the oscillations of the basin and the ocean, furthermore the tidal range inside the basin may be damped depending on the flow capacity of the opening and the size of the storage surface of the basin. An example of such a basin along the Dutch coast is the Eastern Scheldt.

8.2.1 Eastern Scheldt

The Eastern Scheldt is the Northern branch of the Scheldt estuary. Like the Western Scheldt branch it has been subject to the influence of man on its coastlines and therefore does not follow the natural estuary shape anymore. Moreover, the Delta Works have taken away the characteristics of the branch as an estuary. It is no longer connected to the river and only has some upstream influence of pumping stations, which is negligible to its tidal motion. The ocean side of the Eastern Scheldt is partially dammed by the Eastern Scheldt storm surge barrier which blocks five of the nine kilometres of the opening and is approximately 20 meters deep above the barrier's foundation layer. Four kilometres of the opening are connected to the ocean to allow for a tidal range and the accompanying salt water intrusion to remain for ecological reasons. Figure 19 shows that the relative magnitude of the inflow area is small compared to the storage area and the ocean tide is damped over the average storage area of the Eastern Scheldt. Because it is a large reservoir the actual situation will differ in that the tide will not rise simultaneously over the surface area of the basin,

causing the tidal range to be higher at the ocean side (approximately equal to the ocean tidal range) and lower at the river side. The two values can be seen as an upper and lower bound for the actual tide.

► Input variables:

| | | |
|----------------------------------|--|--------------------|
| ○ Tidal amplitude(s): | $M_M, M_F, K_1, O_1, P_1, Q_1, M_2, S_2, N_2, K_2$ and M_4 | |
| ○ Average ocean tidal amplitude: | 1.3424 | [m] |
| ○ Storage surface: | 350 | [km ²] |
| ○ Inlet area: | 36,000 | [m ²] |
| ○ Average water depth: | 20 | [m] |
| ○ Threshold depth: | 20 | [m] |

► Output:

| | | |
|----------------------------------|--------|-----|
| ○ Average ocean tidal amplitude: | 1.3424 | [m] |
| ○ Average ocean tidal range: | 2.6848 | [m] |
| ○ Average basin tidal amplitude: | 0.5726 | [m] |
| ○ Average basin tidal range: | 1.1452 | [m] |

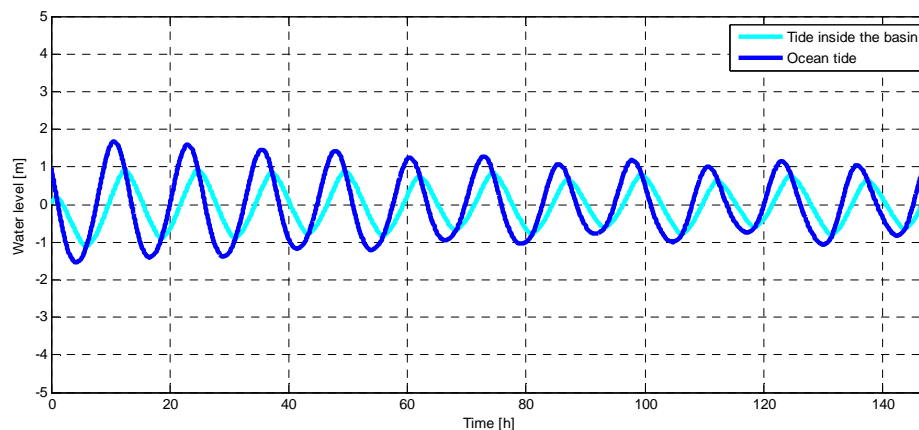


Figure 19 - Tidal response inside the Eastern Scheldt

8.3 Closed basins

Closed basins are characterised by their lack of open connection to the ocean. Examples of such basins in the Netherlands are the Grevelingen, Haringvliet, IJsselmeer and Lauwersmeer. Most of these have been dammed in at some point in the past to protect the land behind it. With the realisation that these closures have caused unforeseen environmental impacts, however, there are ideas to open some of these basins back up to re-establish a brackish environment with ebb and flood for the local marine life to thrive in. Creating such a flow would mean there is a possibility for generating electricity from the newly instated water flow. The important characteristics in these systems are the water level in the basin and the tidal fluctuation on the outside (based on the $M_M, M_F, K_1, O_1, P_1, Q_1, M_2, S_2, N_2, K_2$ and M_4 constituents obtained from the Global Inverse Tidal Model). The difference between the two is the head over which energy can be generated. The storage area of the basins is also important as it determines the sensitivity of the basin to water fluctuations. Smaller basins will rise/fall more rapidly than bigger basins, meaning they have less water to spill before running out of head difference (and therefore less energy potential) and the inside basin will be subject to faster changes which could be undesirable for the users and inhabitants of the basin.

8.3.1 Grevelingen

The Grevelingen is a former estuary branch of the River Rhine that has been completely cut off from natural influences on its tidal motion. In the East it is cut off by the Grevelingen Dam and in the West it is cut off by the Brouwersdam. The water level is kept artificially low at -0.2 meters to facilitate the local ecology as well as to keep the bordering municipalities from suffering water hazards. Because there are many calls to re-open the Brouwersdam (partially) and let the tidal motion re-introduce the brackish tidal environment into the Grevelingen it has for a long time been a subject of discussion to install a tidal power facility alongside the potential new opening.

► Input variables:

- Storage surface: 140 [km²]
- Average water level: -0.2 [m]

► Output:

- Maximum water level difference: 1.7828 [m]

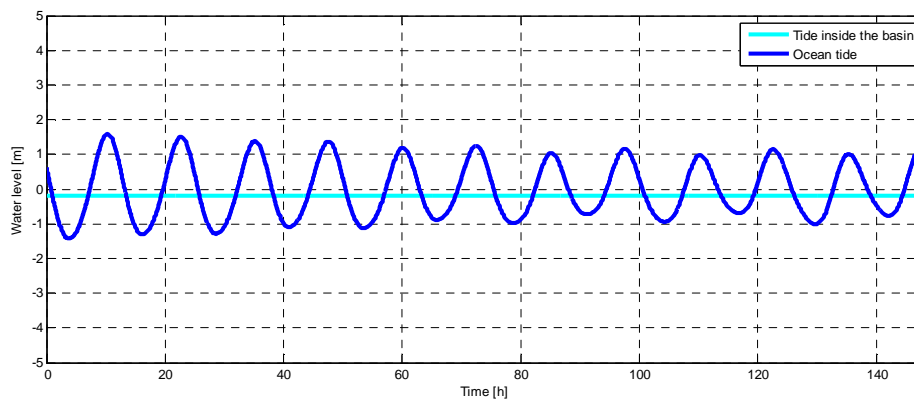


Figure 20 - Tide outside the Grevelingen and basin water level

8.3.2 Haringvliet

The Haringvliet is a former estuary branch that has lost its direct connection to the North Sea due to the construction of the Delta Works. It is still connected to the sea through the Nieuwe Waterweg, but the tide is damped with such significance over the long route it takes to reach the Haringvliet (an order 0.3 meters remains) that the water level is considered constant at the average level of 0.5 metres. Figure 11 illustrates the tidal motion outside the Haringvliet and plots it in a figure with the inside water level. This gives an indication of the water level difference between the basin and the sea outside and indicates its maximum value is around 1.8 meters.

► Input variables:

- Storage surface: 60 [km²]
- Average water level: 0.5 [m]

► Output:

- Maximum water level difference: 1.8184 [m]

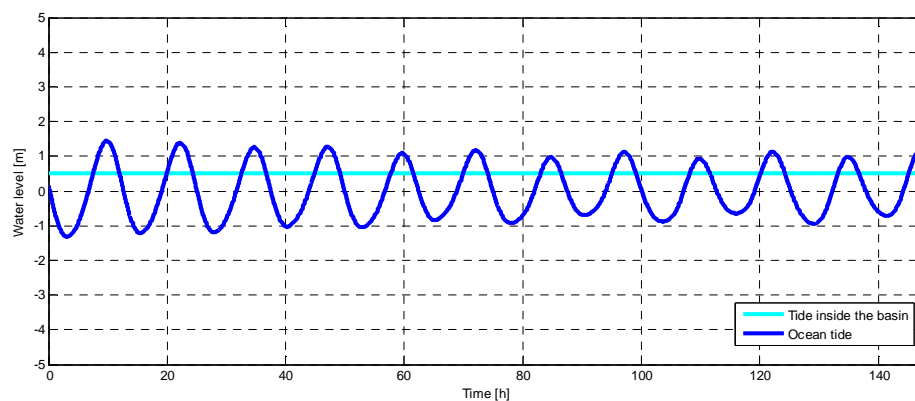


Figure 21 - Tide outside the Haringvliet and basin water level

8.3.3 Lauwersmeer

The Lauwersmeer is a former sea that has been dammed in cut off from the sea in the late 1960s. It mainly serves a purpose as ecologic habitat and recreational area where small vessels can enter through the marinas on its shores and the locks connecting it to the sea. It has a relatively large head difference between the outside water level and the level inside the basin due to its artificially low water level of -0.94 meters. The potential is, however, limited due to its relatively low surface area.

► Input variables:

- Storage surface: 20 [km²]
- Water level: -0.93 [m]

► Output:

- Maximum water level difference: 2.173 [m]

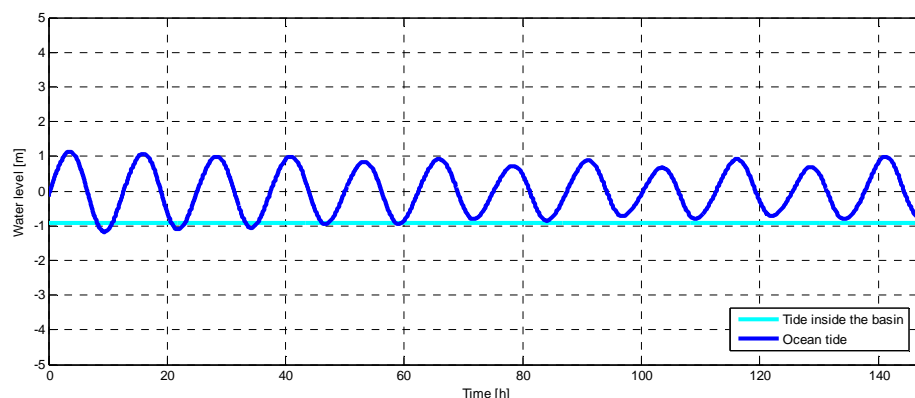


Figure 22 - Tide outside the Lauwersmeer and basin water level

8.3.4 IJsselmeer

The IJsselmeer is an artificial lake in the Netherlands which was created in 1932 when the 32 kilometres long Afsluitdijk dam was created between the provinces of North Holland and Friesland. Originally it was much larger than its current size, but the creation of the Houtribdijk (1976) between Enkhuizen and Lelystad as well as the artificial island of Flevoland (1986) severely diminished its size. The lake serves as a fresh water reserve for drinking water and agricultural purposes and is widely used for marine recreational activities.

The IJsselmeer is not directly connected to the ocean in any way as its border with the Waddenzee has been shut by the aforementioned Afsluitdijk. This means the tidal motion in the lake is negligible. There have, however, been plans to increase the water level in the basin by 1.5 meters to counter the effects of global warming and to increase the fresh water storage capacities of the lake. This would mean that a significant water level difference would be created between the inside of the lake and the Waddenzee on the other side of the dam. The outside fluctuation of the water level added to this mean differential would create some potential for tidal energy generation. As is explained in 0, the water level on the outside of the Afsluitdijk cannot be estimated with the tools considered in this report.

‣ Input variables:

- | | | |
|--------------------|-------|--------------------|
| ○ Storage surface: | 1,100 | [km ²] |
| ○ Water level: | -0.40 | [m] |

8.4 Waddenzee

The Waddenzee (or Wadden Sea) is a complicated hybrid between the open ocean and a basin. It is a relatively shallow system of which large portions of the bottom emerge from the water during low tide and is sheltered by the series of islands that separate it from the North Sea. Due to the bathymetry of the sea and its protective islands large tidal velocities occur between the islands when the tidal wave approaches and departs. These flows leave large tidal deltas on the bottom of the sea, which makes it easy to recognise where the large flow velocities occur and where they meet to push the tide up. Figure 23 is a satellite image that clearly shows the tidal deltas between the islands and the relatively shallow areas where the water loses its velocity and the sediment settles again.



Figure 23 - Waddenzee with clear tidal deltas

There are models available that map the tidal situation in the Waddenzee, for instance (Ridderinkhof, 1988), as the developed system does not suffice for approximating it. These models, or alternatively a tide calendar, should be consulted in favour of the model in 7.1.

9 Electric network

Before engaging on a quest to solve the energy problem it is important to know what exactly the problem is, because it is more complicated than just “we need more electricity”. There are certain gaps in the market where, for whatever reason, consumption and production do not agree with each other. To assess where to look for the solution one must look into the patterns that occur in both consumption and production of energy. Naturally it would be too idealistic to expect the Tidal Wave Energy Converter to cover the complete problem, but even without delving into the exact numbers of the deficit an area can be defined where its revenue can be of service.

9.1 Consumption patterns

The electricity consumption differs depending on location, season and time of day. During cold weather people will want to use heaters to make their houses warm, whereas with moderate temperatures they will not. On the other side, with hot temperatures they might want to use air conditioning. When it is dark consumers will turn their lights on, which is unnecessary during the day. This leads to certain patterns of usage depending on the local climate and season.

Across the world very different climates exist with different consumption patterns. Figure 24 shows the consumption patterns of the general areas with Great Britain (a) and another Australian province New South Wales (b).

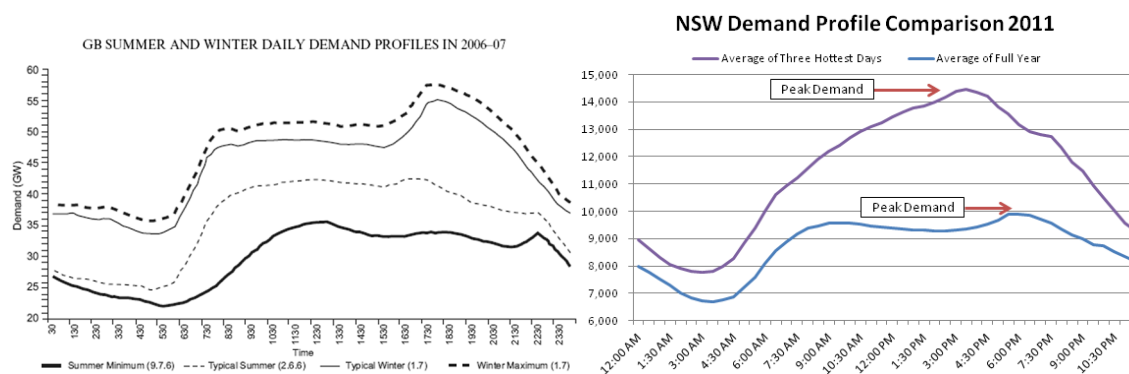


Figure 24 - Average daily consumption patterns for (a) Great Britain and (b) New South Wales, Australia

The first figure shows that the winter is a high demand season due to low temperatures and a need for heating houses whereas the summer has a relatively low demand due to the moderate climate. The second figure shows that the demand in Australia is significantly higher during the warmer periods of the year due to air conditioning requirements. It should be noted that some countries, like the Netherlands, use gas for heating without converting it into electricity in a plant. This means the energy required for heating houses is not included in the electricity consumption.

9.2 Production patterns

To fully understand the patterns in the production of electricity it is important to understand the characteristics of the various energy sources. Different energy sources operate in different fashion and the application of energy sources to the grid is not uniform for all sources. The most relevant factor in this is the start-up time, the time needed to start using the power plant from idle position. This time will determine the capability of the plant to compensate for peak demands. A summary of the start-up times of the various types of plants is given in Table 3, after which a short explanation is presented on what influences the start-up time of the various types of plants and whether or not they are suitable to serve as peak power energy providers.

| Plant type | Start-up time [s] |
|----------------------|-------------------|
| Nuclear | 19800 |
| Combustion (solid) | 19800 |
| Combustion (gas) | 120 |
| Wind, wave, solar | 0 |
| Hydroelectric, tidal | 15 |

Table 3 - Start-up time of different types of plants (Imambaks, 2013)

9.2.1 Combustion Energy

Combustion energy comes in the forms of fossil fuels and biofuels. Both forms of resources come in the three conventional states of matter: solid, fluid and gas. For fossil fuels this expresses itself in the more common wordings of coal (solid), petroleum (fluid) and natural gas. Biofuels come in the forms of for example peat (solid), bioethanol (liquid) and methane (gas), but also other products are applied. The important factor that separates these stages of matter in terms of power plants is the required activation energy, less dense materials such as gasses generally require a much lower amount of energy to be inserted into it before they ignite than denser materials like solids. Figure 25 illustrates the principle of activation energy.

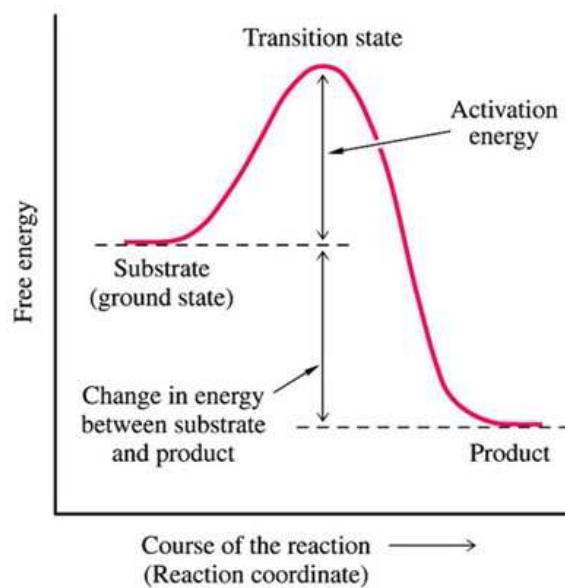


Figure 25 - Activation energy (Campbell University, 2015)

Combined with the longer time needed for denser materials to ignite, they also require a longer time to cool down again. Where gasses burn up rapidly and therefore a discontinuation of the supply discharge pretty much instantly stops the combustion process, solid materials stay ignited for a longer period of time and keep smouldering for long periods of time. This, however, does not have an influence on the capability of responding to peak demands, but rather on the amount of material going to waste after no further energy production is required.

9.2.2 Nuclear energy

The principle of nuclear reactors is much the same as that of combustion engines. A process of nuclear fission generates heat, driving a fluid or gas through turbines. For a nuclear reactor to be operational, a steady rate of nuclear fission in its source material is required. Starting up this steady state reaction takes some time, the length of which depends on the rate of purification of the source

material. The most used material is Uranium-235 due to its relatively large natural occurrence, but even that occurrence is limited and enrichment of Uranium-236 atoms is required. The percentage of Uranium-235 in the mixture determines the start up speed of the reaction and is usually in the order of multiple minutes.

9.2.3 Hydroelectric energy

Hydroelectric energy in the considered sense involves mainly the types of plants that have some sort of reservoir. So Reservoir plants, Run-of-river plants and High head plants. This reservoir ensures that potential energy can be built up when the power plant is not operational and that this energy can be released into the turbines with the small interference of opening the valves. This means the determining factor in start-up time is the time required for the falling water, through the penstock and into the turbines. This means the time to put the turbines in action is in the order of $\sqrt{L/9.81} + t_{\text{turbine}}$, with L the length of the penstock below the valve and t_{turbine} the time required to put the turbine in motion. Another advantage in this is that no activation energy is required to start up the process of harvesting energy.

9.2.4 Wind, wave, solar energy

The renewable energy sources of wind, waves and solar energy can mostly be activated nearly instantaneously. The only limiting factor is the start-up time of the turbines, which only plays a role for wind energy and wave energy and is a relatively short time. The problem with this type of energy, however, is its availability. The sun is not available at night, wave density varies and so does the wind. It is therefore not automatic that when electricity is required there is actually a source available for these types of energy generation. Actually the increasing popularity of these types of renewable energy are one of the main reasons there is a need for fast responding alternative energy sources as the production from these methods can fluctuate very rapidly. A solution for this is to use energy storage, which will be further elaborated on later in the report.

9.2.5 Tidal energy

Tidal energy shows a lot of similarities with the aforementioned hydroelectric energy. Both have a reservoir that collects the water and the start-up time depends on the travel time in the penstock and the start-up time of the turbines. The difference, however, as with wind, wave and solar energy, lies in the availability of the source. Tidal energy depends on the head difference between low tide and high tide and therefore has a specific timeframe in which the maximum amount of energy can be harvested until a moment where the inside and outside water levels match and no energy can be harvested. This means a single basin tidal facility has only a limited amount of responsive capabilities to sudden peak energy demands.

Furthermore the change in vertical tide comes with a water flow that brings water into the area or takes it out of it depending on whether the water level rises or falls. This discharge can be used by installing under water wind mills to harvest the stream energy. This is called tidal current energy or tidal stream energy. This type of energy source is predictable due to the predictability of the tide (more predictable than wind energy for example), but also not constantly available in the same quantities due to the harmonic nature of the tide.

9.3 Bridging the gap

Ideally the energy production values would match the energy consumption values. No excess energy would be produced and the available resources would be optimally utilized. In practice, however, this is not the case. There is a large dependency on the conventional combustion plants that produce a constant amount of energy based on the base energy requirement, as to not produce

too little energy, where some use of gas power plants is used to provide the additional energy during peak hours.

This energy production can be divided into three components:

- Base energy production – *The energy needed to fulfil the persistent base energy demand.*
- Off-peak energy production – *The energy needed to fulfil the demand during off-peak hours.*
- Peak energy production – *The energy needed to fulfil all the needs during peak hours.*

Because the production side of the energy spectrum is based on multi-Megawatt installations it is impossible to precisely match the production values with the consumption values. To cover for this difference a practice called “peak-shaving” can be applied. The excess energy that is produced during the off-peak hours (when energy is relatively cheap) is stored and used to supply the demand in the peak hours (when energy is expensive). Figure 26 illustrates this principle. Applying this practice means the overall energy usage is more efficient and the requirement for specific peak energy production facilities is diminished. Of course installations in which the energy can be stored are required.

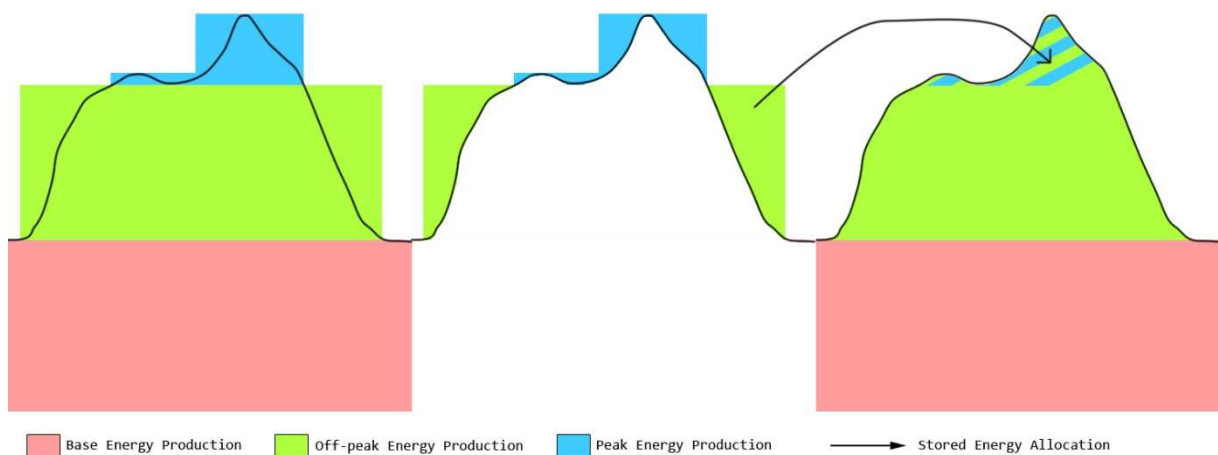


Figure 26 - Peak shaving principle

10 Conclusions on tidal energy scope

The preceding section has sought to establish the application area in which the Tidal Wave Energy Converter can be applied. Firstly a tool to predict the ocean tide in the world's oceans has been found in the Global Inverse Tide Model (Erofeeva, 2002) which uses satellite laser altimetry data to estimate the constituents of the eleven major sinusoids in the tidal motion (Appendix A). This ocean based tidal prediction method is then further detailed into a near shore tidal prediction model which consists of a MatLab script capable of calculating for basins and estuaries how the tidal motion propagates into the coastal anomaly (Appendix B). The tidal prediction scripts can be used to approximate the tidal motion at any given location in the world, which is important for feasibility studies of tidal energy in general and the Tidal Wave Energy Converter in specific.

The created tidal approximation model has been applied to the Dutch hydrologic system where 9 affected locations of interest have been identified as illustrated in Figure 27. From these locations only the Western Scheldt's upstream reaches represent a significant tidal range in the order of 6.6 metres. The basins of the Eastern Scheldt, Haringvliet and Grevelingen show some minor potential with tidal ranges in the order of 3 metres, but the current state of technology does not make such ranges easily feasible.



Figure 27 - Map of the Netherlands with model grid and areas of interest

Lastly this chapter looks into the electric network and the daily trends of supply and demand. These trends show that the demand curve of consumers follows a sinusoidal pattern with peaks of high demand and troughs of low demand. These curves firstly mean that energy production needs to be versatile, but also that the match between conventional energy production methods as well as the tidal motion and the demand curve is far from a perfect match. This means energy storage is essential for matching production and consumption in an efficient manner. The Tidal Wave Energy Converter concept is technically capable of fulfilling this role as well, more on this in chapter 24.

Section 3 – Development framework

| | | |
|------|---|----|
| 11 | Introduction of development framework | 61 |
| 12 | Reference Projects | 63 |
| 12.1 | Marine Energy | 63 |
| 12.2 | Energy Storage | 69 |
| 12.3 | Energy conversion mechanisms | 70 |
| 12.4 | Granted Patents | 74 |
| 13 | Possible host structures for the Tidal Wave Energy Converter..... | 77 |
| 13.1 | Existing projects..... | 77 |
| 13.2 | Planned projects..... | 81 |
| 13.3 | Other products with potential..... | 82 |
| 14 | Generalized boundary conditions | 85 |
| 14.1 | Tide | 85 |
| 14.2 | Soil and bathymetry | 86 |
| 14.3 | Environment | 87 |
| 15 | Program of Requirements | 89 |
| 15.1 | Requirements | 89 |
| 15.2 | Desires | 89 |



11 Introduction of development framework

The previous sections have given an introduction into the subject of the report and aimed to provide a basis to easily estimate the expectations for the tidal motion based on limited data. The next step that needs to be taken before the actual design of the Tidal Wave Energy Converter can begin is to see what developments have been achieved in the field the device will be applied in. To achieve this firstly some reference projects will be investigated in chapter 12. Further on in chapter 13 the possibilities for superstructures will be considered. Namely what existing or future structures can be used as floating objects to attach the Tidal Wave Energy Converter to and what consequences the application would entail. In chapter 14 the boundary conditions under which the device will be designed will be distilled. It is impossible to design a device for every possible specific location, so generalized situations will be constructed to represent different scenarios. Finally in chapter 15 the program of requirements is presented which will serve as a guideline and benchmark for the different requirements the device will have to satisfy. This section also lists some desires that would be preferential to be satisfied but are not too big an issue if they are not met.

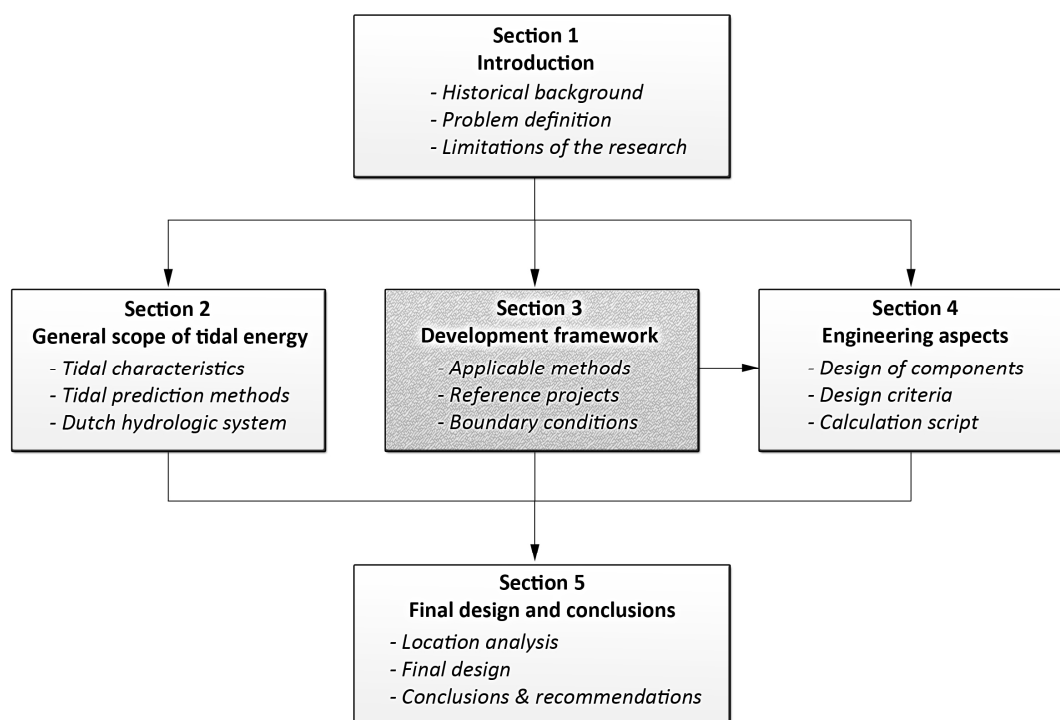


Figure 28 - Structure of the report

12 Reference Projects

Before the design of the Tidal Wave Energy Converter can be started it is important to look at relevant reference projects that the engineering world has already come up with in the past. This process serves two main purposes. The first is to make sure any research regarding relevant aspects to the TWEC that has already been done by others will not have to be repeated, saving valuable time. The second is that comparable projects may serve as inspiration for the design of the TWEC.

Several fields will be looked into in this stage. Firstly Marine Engineering, the field of waterpower engineering related to the energy stored in the oceans. This includes wave energy, tidal stream energy and osmosis energy for instance. The second is that of energy storage. As mentioned before the TWEC may also serve as a means of storing electricity, meaning it is important to know what methods for this are already available and how they may influence this feature of the TWEC. And lastly the existing forms of turbines will be looked into. It will be important to know the characteristics of various types of turbines in order to make a decision on whether or not the current state of technology in these is sufficient to make the TWEC feasibly, if so how and if not what the shortcomings are.

12.1 Marine Energy

Marine Energy is the collective name for all sorts of waterpower energy that originate in the ocean. The large energy potential that the oceanic waters have, in the order of 6000 GW (IEA, 2007), makes it a rapidly expanding field where a lot of innovation is currently taking place to try and extract that potential. Marine energy can be divided into four different categories: Wave energy, tidal energy, osmotic energy, marine current energy and ocean thermal energy. Of these five, the first three are of interest to the TWEC principle and will be looked into further.

12.1.1.1 Wave Energy Convertors

Wave Energy Convertors, or WECs, come in various shapes and sizes. What they all have in common is that they use the energy that is stored in waves to generate electricity. Figure 29 charts the classification of WECs into three specific categories: Oscillating Water Column WECs, Oscillating Body WECs and Overtopping WECs. The following paragraphs will elaborate on what these terms mean.

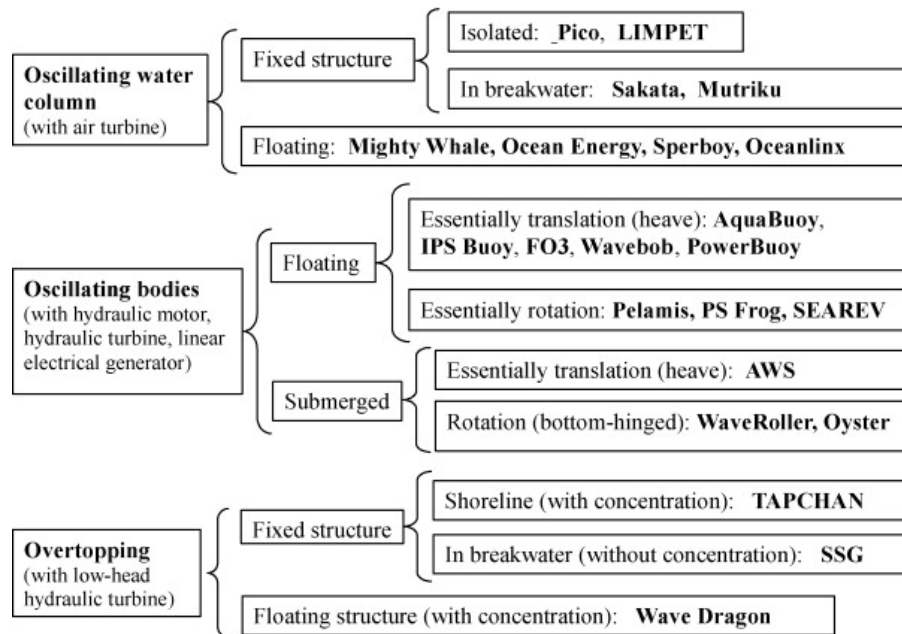


Figure 29 - Classification of Wave Energy Converters (Falcão, 2010)

Oscillating water column wave energy converters

The primary component of Oscillating Water Column wave energy converters is a large air chamber which is on one side bound by the ocean surface and on the other side by an air turbine. The oscillating motion of the wave creates an over- and underpressure in the air chamber as the water moves up and down. This pressure forces an air flow through the turbine on the other end of the chamber. The devices are made of concrete or (stainless) steel and are generally stationary relative to the mean seawater level.

A distinction can be made between floating devices (e.g.: Oceanlinx in Figure 30a and Mighty Whale in Figure 30c) and fixed devices (e.g.: LIMPET in Figure 30b) where the main difference is that the floating devices require a second air chamber to create buoyancy whereas with fixed structures the entire device can be used for energy extraction. Floating devices can, however, operate at a larger variety of locations as they are not bound to the shore and have an operational depth in the order of 10 to 80 meters.

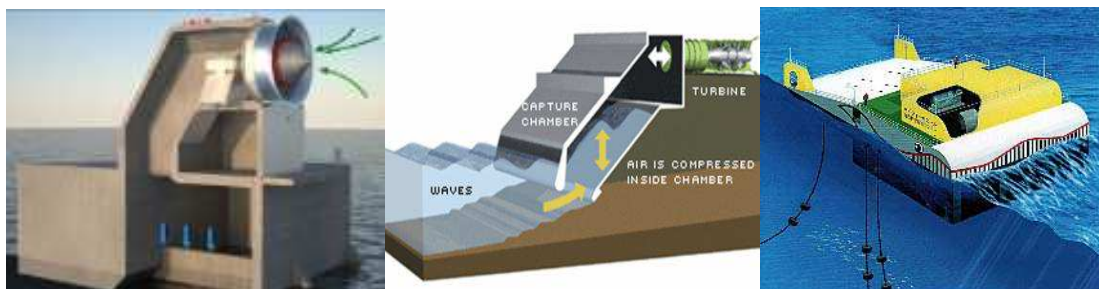


Figure 30 - Oscillating Water Column WECs: a) Oceanlinx b) LIMPET c) Mighty Whale

Oscillating body wave energy converter

Wave energy converters of the oscillating body type are (partially) buoyant devices that move along with the oscillating motion of the water table. Completely floating devices, or buoys, can use the vertical translation (heave) or the rotation (pitch) to extract energy from the wave. An example of the first is the Powerbuoy (Figure 31a), which has a heavy heave plate remaining at a stationary position under water whereas the buoy at the surface moves relative to this plate. The second one has an application in the SEAREV (Figure 31), which has a wheel inside with one heavy side which is always directed downward. As the device rolls over and moves relative to the stationary wheel a set of pistons transfer the energy to a generation device. The operational depth of these devices is in the order of 20 to 60 meters.

Another type of oscillating body WEC is the Oyster WEC (Figure 31b) which has a section anchored to the bottom of the ocean and a big buoyant screen hinged to an edge of its foundation. As the water level rises and falls the screen rotates around this hinge driving a piston that is attached to the foundation layer. This motion can subsequently be used to generate electricity. The operational depth of these devices is smaller at 10 to 30 meters and the influence on the seabed is more severe. They can, however, be applied at a bigger density as their path of motion is fixed.

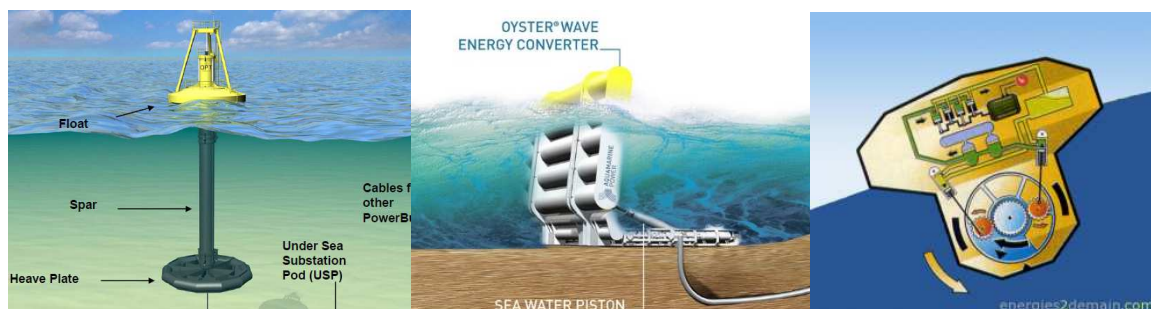


Figure 31 - Oscillating Body WECs: a) Powerbuoy b) Oyster Wave Energy Converter c) SEAREV

Overtopping wave energy converter

Overtopping is what occurs when the run-up of a wave along a slope is higher than the retaining height of the body it runs up against. This principle is used by overtopping wave energy converters to create a water level difference between a reservoir and the mean outside seawater level. A reservoir with an arbitrary retaining height higher than mean seawater level and lower than the wave run up height is constructed. Waves are led up a slope where the excess water higher than the reservoir's walls is deposited in the reservoir for each incoming wave. The summation of all these waves causes the water level inside the basin to be rise creating a head difference, which is subsequently used for electricity production by letting the water flow back out through a turbine.

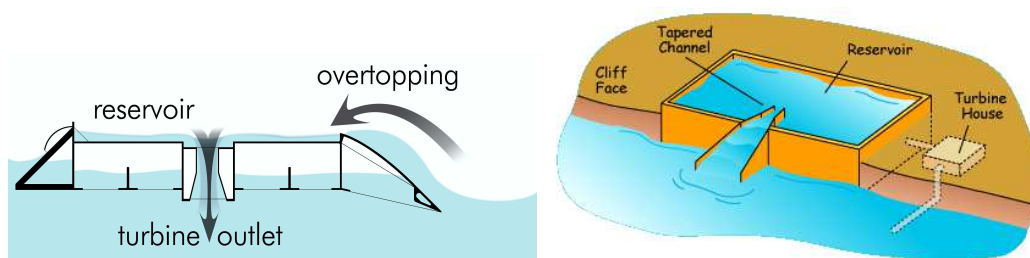


Figure 32 - Overtopping WECs a) Wave Dragon b) TAPCHAN

Overtopping WECs exist in both floating and fixed form where the floating variety (like the Wave Dragon in Figure 32a) has added air pockets in its structure to improve buoyancy. Fixed structures do not require these and can be installed on any shoreline subject to wave action. An example of such a location is a breakwater. Some variants of overtopping WECs have specifically designed converging entry ramps for the waves in which the wave is amplified to a higher level. Doing this means the potential reservoir water level is higher, but with the amount of incoming waves being the same this means it will take longer for the reservoir to fill.

12.1.2 Tidal Energy

The tide is practically a very large wave (order hundreds of kilometres) moving across the globe. It is caused by influences of the sun, the moon and the rotation of the Earth (as explained in Section 2, not included in this document). The Moon being the dominant factor with a diurnal character means the dominant wave period is in the order of 12 hours. The motion of the tide translates into a pair of linked phenomena that can be used for extracting energy. Firstly there is the vertical water level motion caused by the gravitational pull on one side of the Earth and the centrifugal forces in the Earth-Moon system on the other side. The upward and downward motion of the water level goes together with a displacement of water from one point to another, causing a current in the direction of the wave's movement.

Tidal Stream Energy

Harvesting this so called tidal stream energy can be done in a variety of ways. For extracting energy from the currents, Tidal Stream Generators (TSGs) have been developed. These devices are usually applied in areas where the local bathymetry has a funnel effect on the tide, causing an increase in the water's velocity. The most common variety of TSG is that of a large, windmill like, propeller on the bottom of the ocean with an axial turbine. They come in different varieties where some have flow augmenters that direct the flow more towards the blades of the device and others are free to move along with the direction of the tidal current to optimise efficiency. A variety of such a TSG is the Tidal Energy Converter (Figure 33a).

Different types of tidal stream generators exist in cross flow turbines, which operate by letting the tidal current flow into the propeller from a direction perpendicular to the turbine axis. An application of this technology can be found in the helical Gorlov turbine (Figure 33b). A third variety is an oscillating device which operates by letting aerofoil bodies float in the tidal current. The shape of the body makes it oscillate in vertical direction applying a force to a piston.

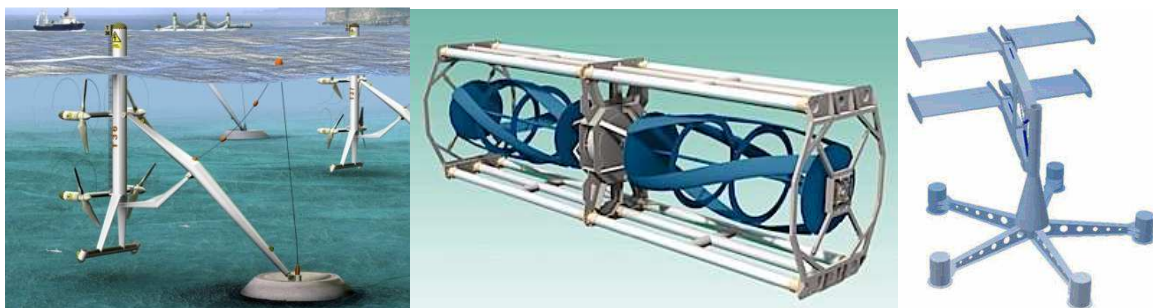


Figure 33 - Tidal Stream Energy: a) Tidal Energy Converter b) Gorlov turbine c) Stingray

Tidal Barrage

Tidal barrages operate by capturing the tidal wave in a basin and letting a head develop. A large dam, or barrage, is constructed on the ocean end of a basin subject to a tidal motion (Figure 34a). When the tide moves in, the water level in the basin rises and an energy potential is built up. When the tide on the Oceanside of the barrage drops again the barrage makes sure the stored water cannot immediately flow out of the basin so that a water level difference between the basin and the outlying ocean is created. Releasing the stored water through turbines when the water level outside has dropped significantly the energy potential can be converted into electricity.

An alternative way of operating such a barrage is through Dynamic Tidal Power (DTP, Figure 34b). Dynamic tidal power also uses the water level difference between high tide and low tide, but instead of blocking an amount of water until the tide drops it uses the travel time of the wave and the according distance between a crest and a trough to create a head. A large barrier is constructed in an area affected by the tide. The tidal wave needs time to travel around the barrier, which causes a water level difference between one side of the barrier and the other. This head can then be used as a regular hydropower dam to generate electricity. Using this method means that there is little to no creation of an extra head, the tide was there already after all, and therefore the requirement for added shoreline protection is limited.

Finally another variant of the tidal barrage can be applied which does not use a naturally existing bathymetric situation but is a complete artificial lake that is made subject to a tidal motion through turbines. This principle, called Tidal Lagoon Power (Figure 34c), can be applied at any given location with a significant tide. The downside of using this, however, is that it costs significantly more due to the added amount of barrage length that needs to be installed.

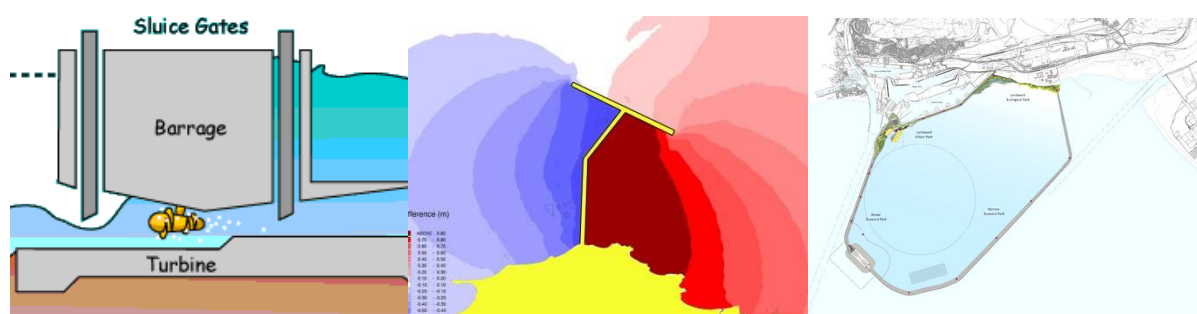


Figure 34 – Tidal Barrage: (a) Barrage cross-section (Green Tech Blog, 2009) (b) Dynamic Tidal Power (c) Tidal Lagoon Power

12.1.3 Osmotic energy

Osmotic or salinity gradient energy is the energy that can be harvested from the mixing of fresh and salt water. It is based on the difference in osmotic pressure between pure water and water with any solution in it. The difference in salinity between fresh water and ocean water means there is also a difference in osmotic pressure between the fluids and a potential for this to be harvested. There are two ways of harvesting this energy, Reverse Electro Dialysis (RED) and Pressure Retarded Osmosis (PRO), of which only the latter bears relevance to the TWEC principle.

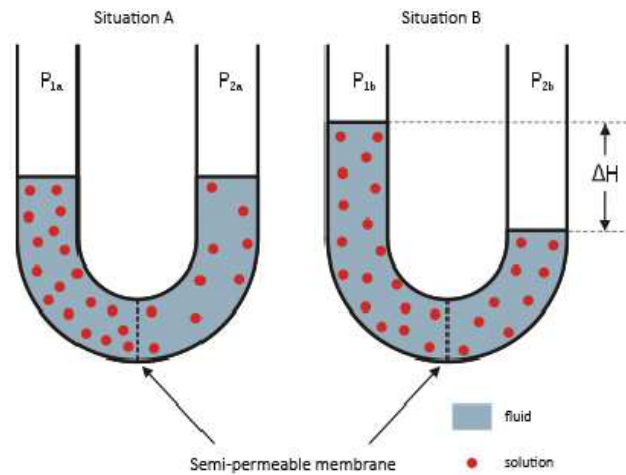


Figure 35 - Osmosis Pressure principle

PRO uses this principle by separating the two solutions with a semi-permeable membrane, which only facilitates water particles flowing through and blocks the salt particles. The fresh water will seek to dilute the saline water until a level of equal salinity is achieved meaning fresh water particles will flow through the membrane into the salt water container (Figure 35). The increase in head this creates in the salt water chamber is subsequently led through a turbine to generate electricity. The theoretical global energy potential for osmotic power is in the order of 1600 TWh per year (Statkraft, 2011).

12.2 Energy Storage

The energy demand varies a lot over time. There are large peaks in the morning and afternoon when many people start actively using electricity for their daily needs, and there are large troughs during the night when everybody is asleep (see also Section 2 chapter 4, not included in this document). Because more conventional means of generating energy do not have an on/off switch but have to produce a constant amount of energy, the capacity of the energy production is adjusted to the peak values of the demand curve. This means that during the off-peak periods a lot of energy is being produced that is not being used.

Furthermore a trend is noticeable towards the use of renewable energy sources, which this research is also a part of. Renewable energy sources are often inconsistent by nature as nature itself too is often inconsistent. The sun does not always shine, the wind does not always blow, and therefore harvesting electricity from them is not as constant as the market demands it to be either.

To optimize the efficiency of energy production, the overproduction of energy during the off-peak periods can either be sold to other countries (like the NorNed cable) or it can be stored to be used as an on-demand means of covering for electricity shortages in peak periods. An important factor for being able to use an energy source on an on-demand basis is the time that is needed to start up the harvesting process, which needs to be very short in order to be an effective means.

Several means of energy storage have been developed over time, of which a selection of inventions relevant to the TWEC research is elaborated on further.

12.2.1 Flywheel energy storage

The first method to go into is that of flywheels (Figure 36). Flywheel Energy Storage (FES) consists of a large disc placed in a vacuum. Excess energy is used to give the disc a rotational velocity which means that energy is stored in the disc in the form of rotational energy. The vacuum serves to minimize friction losses and, in newer devices, the means of propulsion and harvesting is done with magnetic fields for the same purpose.



Figure 36 - Flywheels

12.2.2 Pumped storage hydroelectricity

Pumped Storage Plants (PSPs; Figure 37)) are special cases of reservoir plants. Instead of relying on nature (rivers or tides) to refill the reservoir, they depend on mechanized processes to pump water up to the storage basin. To achieve this excess electricity from the grid can be used, or as is currently being developed wave energy converters can pump water into the reservoir. When the grid is short on electricity the valves are opened again and the water flows through turbines to create electricity.



Figure 37 - Pumped Storage Plant

12.2.3 Gravitational potential energy storage

Gravity power (Figure 38) is much comparable to what a downward directed harvesting process of the TWEC would be like. It uses large cylindrical basins filled with water in which a heavy object is placed such that the water beneath it keeps it lifted. It is not the buoyancy of the object that keeps it lifted, but the water pressure pushing against it from the bottom. By pumping more water underneath the object it can be raised further, and with that the potential energy stored in it is also increased. When energy is needed the water underneath the object is led through turbines where it is converted back into electricity. The analogy with the TWEC is evident in that the pontoon that the TWEC uses is in principle the heavy object in gravity power. The significance difference is that the tide is used to lift the pontoon rather than an insertion of energy through water pressure as is the case with gravity power.

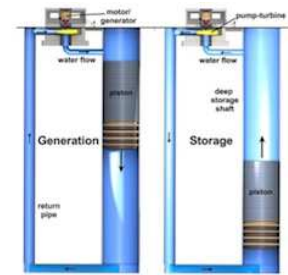


Figure 38 - Gravity power

12.2.4 Compressed air energy storage

Alternatively to using water pressure as a means of storage, also other substances can be interesting. Such means are applied in Hydrostor which uses air as a means of storing energy. The way this is done is by placing large sacks on the bottom of the sea (or any other large water basin) and pumping air into these sacks. The insertion of water into the sacks causes a displacement of the water around it and the weight of the water trying to fill the void inside the sack causes an overpressure in the air sack. When releasing the compressed air from the sack, a turbine can be powered to reclaim the energy that has been stored in the sacks.

12.3 Energy conversion mechanisms

Another important aspect of the Tidal Wave Energy Converter is how the built up pressure is eventually converted into electricity. To get an idea of what means are available for this conversion some known methods are investigated with the pros and cons of their operation and efficiency.

12.3.1 Turbines

A final important aspect to look into is the turbines. They are the heart of any hydroelectric facility and in the case of the TWEC this is no different. The feasibility of the device depends for a large part on the attainable efficiency of the used turbines. The use of turbines is not limited to just hydro purposes. Fluids and gasses of a variety of densities can be used to power a turbine where the density of the turbine material is relevant for the efficiency and durability of the turbine blades. The following paragraphs regarding turbines are written with hydro turbines in mind.

Reaction turbines

Reaction or overpressure turbines are fully submerged turbines with fan type blades. They come in many different shapes and sizes that mainly have an effect on how the water moves around them. The main varieties in these types of turbines are the propeller turbine, the Kaplan turbine and the Francis turbine.

Propeller turbines (Figure 39a) are pretty straight forward and look the same as the propeller of a ship. Except instead of exerting a force on the water to move the ship forward, they are themselves propelled by the moving water to drive a generator. The blades of the propeller turbine are generally fixed in one position so it is inflexible when it comes to adjusting to variations in the flow. A more advanced version of the propeller turbine is the Kaplan turbine (Figure 39b). The pitch of the blades on these propellers is adjustable meaning they are efficient for a more diverse spectrum of water

velocities. The efficiency range of propeller and Kaplan type turbines is in the order of 3 to 60 metres hydraulic head (van Duivendijk, sd).

Another type of submerged turbine is the Francis turbine (Figure 39c). Francis turbines are characterized by a larger amount of blades and a blade orientation that is more parallel to the axis of the turbine. They handle the upper spectrum of high velocity water flows as far as impulse turbines go with an application range of 30 to 600 metres hydraulic head (van Duivendijk, sd). The shape of the turbine is largely influenced by the hydraulic head it is operating for, where the high head turbines show taller blades and a blade orientation less parallel to the axis. This is to optimize the efficiency of the turbine.

Reaction turbines often show a turbine casing that is designed to optimally use the impulse that the water carries. The housing is shaped in such a way that the direction of the flow is aimed in such a way that it falls on the blades in an optimum fashion and that the velocity is kept constant over the circumference of the fan. This is done by decreasing the diameter of the pipeline as it progresses along the circumference. As more water falls into the turbine, the discharge decreases and therefore so would the velocity. The decreasing diameter means the velocity can be kept constant. Typical efficiency of Francis turbines is in the range of 90% for flows close to design flow (Paish, 2002).

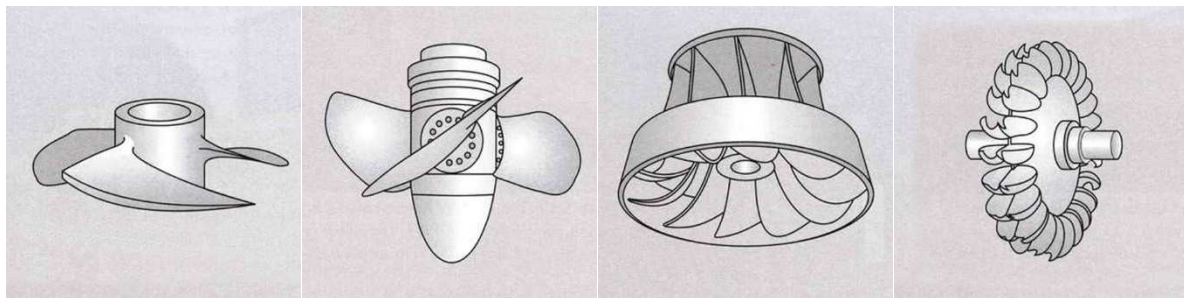


Figure 39 - (a) Propeller turbine (b) Kaplan turbine (c) Francis turbine (d) Pelton turbine (van Duivendijk, sd)

Impulse turbines

With impulse turbines, rapidly moving water is led through one or multiple nozzles and directed at the blades of a wheel type turbine. The wheel of the turbine (and accordingly the nozzles as well) is located above the water level under atmospheric pressure and is rotated by the impulse of the water that the nozzles propel into the bowl-shaped blades on the wheel. Pelton turbines (Figure 39d) are of this sort and are generally used for very large hydraulic heads (order 200 – 1800 metres (van Duivendijk, sd)) as the water velocity needs to be high. This means that the application of these types of turbines for the TWEC is an unlikely solution. Typical efficiency of Pelton turbines is in the range of 80 to 90 percent for flows as low as 25% of the design flow (Paish, 2002).

12.3.2 Scroll expanders

A scroll expander is the inverse application of a scroll compressor. The main application area of these devices is in residential air conditioning and heat pumps where the expansion and compression of air influences the temperature (rapidly expanded air cools down, rapidly compressed air heats up). In these systems it operates by a mechanical force rotating spirals around each other in such a way that the air in between the walls of the spiral is compressed or expanded as it moves inward or outward. Figure 40 illustrates the configuration of the spirals relative to each other.

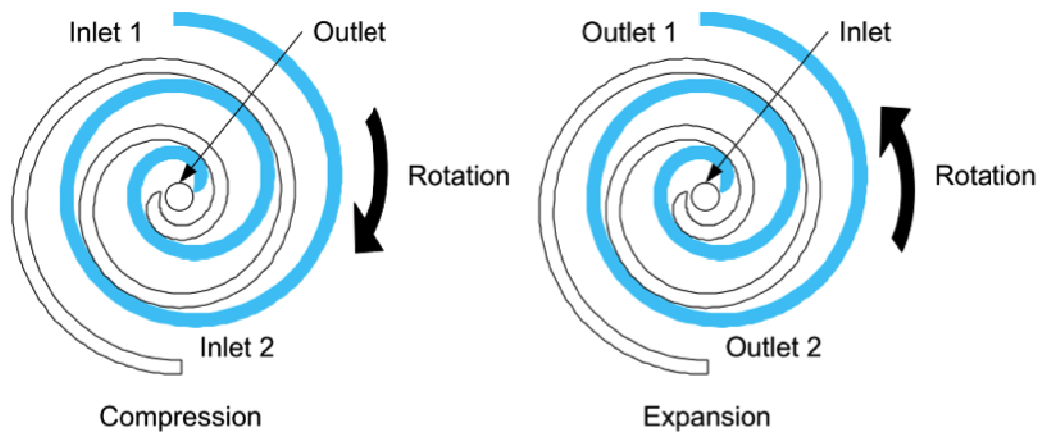


Figure 40 - Scroll expander/compressor

Where the aforementioned applications convert mechanical energy into compression/expansion of air, the inverse can be applied where an under- or overpressure is applied to the inlet of the device and the pressure difference sets the scrolls in motion such that it powers a generator. The efficiency of scroll expanders lies in the range of 50 to 70 percent (Zanelli & Favrat, 1994).

12.3.3 Reciprocating engines

Reciprocating engines, or piston engines, were among the first engines to be developed for converting a pressure difference into mechanical energy. The most commonly known variant of this type of engine is the steam engine. As illustrated in Figure 41 pressure is used to drive a piston back and forth in an airtight cylinder. The translating motion of the piston is then used to power a rotational axis connected to a generator (or in the case of the portrayed image a large wheel which can be used to move a vehicle i.e.). An added rod operates the valve that determines which side of the piston will be powered by the overpressure.

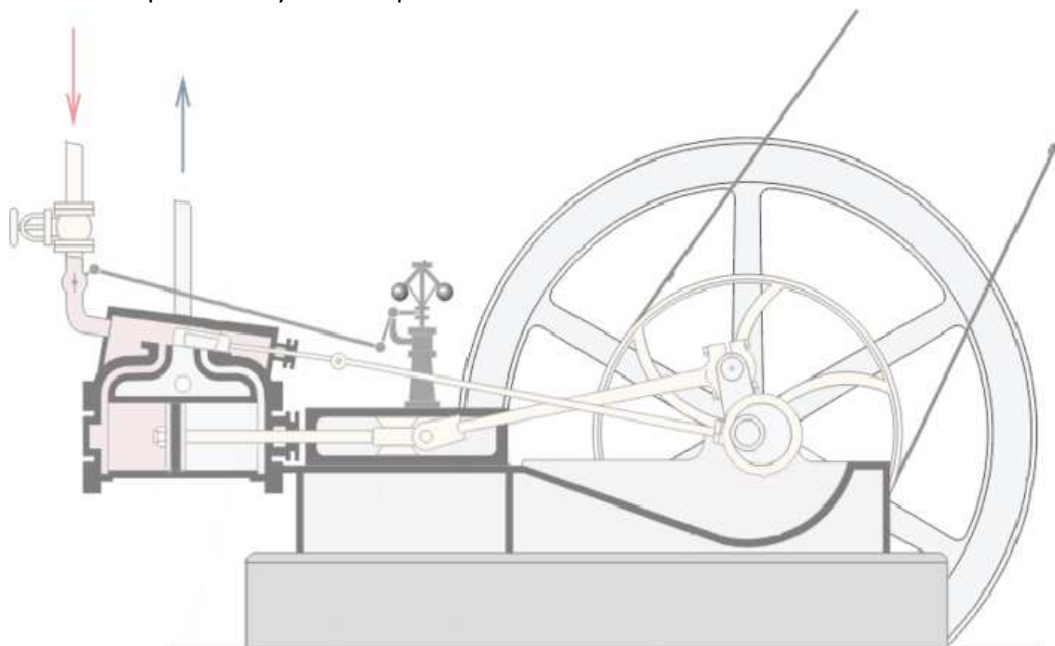


Figure 41 - Reciprocating engine

12.3.4 Hydraulic motor

A hydraulic motor is a device that can convert hydraulic pressure into torque. They exist in a variety of forms and shapes of which there are some common types. The gear motor (Figure 42a), which creates torque through a pressure difference over the tooth (or teeth) of a gear. The vane motor (Figure 42b) works with spring loaded vanes that are bound by a wall and extrude depending on which part of the housing it is pointing towards. A pressure difference over the extruded vanes creates torque. The piston motor (Figure 42c) is theoretically the cheapest and most efficient hydraulic motor and operates by compressing and extruding pistons to create torque. Piston motors exist in many different types such as in-line piston motors (as depicted), radial piston motors (with the pistons mounted in a radial mode around an axis, often used in i.e. airplane propellers) or bent-axis piston motors. A last example is the limited rotation actuator (Figure 42d) which uses an oscillating part with limited movement abilities to create torque by moving back and forth. These types can create relatively high torque.

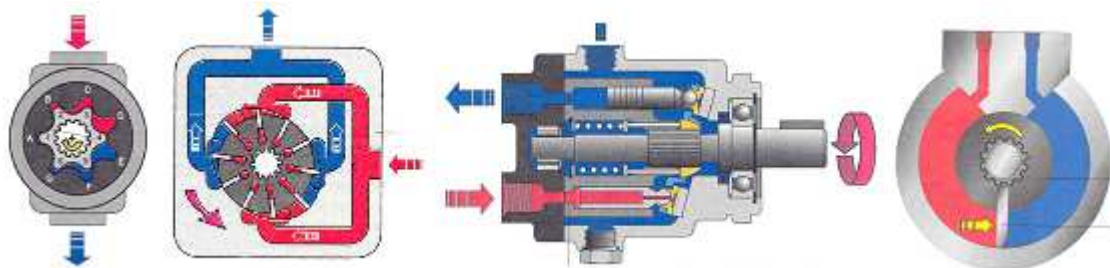


Figure 42 - Hydraulic motors: a) gear motor b) vane motor c) piston motor d) limited rotation actuator

The benefit of hydraulic motors is that they can operate with smaller discharges and therefore do not require the relatively large reservoir that turbine powered systems need to stretch the operation time. Hydraulic efficiency consists of mechanical efficiency and volumetric efficiency where the former decreases as viscosity increases due to friction losses and the latter increases for higher viscosity due to the film thickness. Gear motors typically have an overall efficiency of 70–75% as compared to vane motors which have 75–85% and piston motors having 85–95% (Casey, 2011). The typical features of the various types of hydraulic motors regarding efficiency and costs are illustrated in Figure 43.

| Comparing hydraulic motors | | | | | | |
|----------------------------|---------|------------|--------|------------|------------|-------------|
| | Compact | Reversible | Cost | Efficiency | High speed | High torque |
| Axial piston | No | Yes | High | High | No | Yes |
| Gear motor | Yes | Yes | Low | Low | Yes | No |
| Gerotor motor | Yes | Yes | Medium | Medium | Yes | Yes |
| Radial piston | No | Yes | High | High | No | Yes |
| Vane motor | No | Yes | Medium | Medium | Yes | Yes |

A general summary shows typical features for different hydraulic motors.

Figure 43 - Summary of features for hydraulic motors (Hahn, 2013)

12.4 Granted Patents

Patents are the exclusive rights to a product or process granted for a limited amount of time by a sovereign state to an inventor. These rights include the right to prohibit the use production, use and distribution of an invention without the permission of the inventor. The system of patents was established in 15th century Venice to protect the intellectual property of inventors from potential infringement. Since then patent law has diffused all over the world by Venetian migrants seeking similar protection in their new homelands. Patent law and the protection of intellectual property was one of the foundations on which the first industrial revolution could take place in the late 18th to early 19th century. With the World Trade Organization (WTO) having made it a requirement that all member states have a patent system available the existence of these laws is nowadays widespread over the world.

The validity of a patent is bound to the country the application has been made in. For instance, a Dutch patent is not valid in the United State and vice versa. Because of the costs involved in acquiring a patent it is financially not attractive to apply for a patent in every country in the world, so patents are usually restricted to the countries the inventor has an interest in exploiting it in. This means that the inventions of others can be freely used (but not patented by others) in any other country. Patents are valid for a period of 20 years in most countries and subject to an annual fee to keep the patent. After this time the product is open to be used by others without restrictions.

Besides protecting the intellectual property of inventors patents are also of influence to any newly developed innovation. An idea may be new to one inventor, but may already have been thought up and patented by a different independent inventor in the past. The development of the innovation would therefore potentially be compromised by the previously granted patent. On the other hand the system of patents provides a database of possible solutions to a problem that could assist in solving specific aspects of an innovation. It is therefore essential during the development of any new product to delve into the world of patented products and processes to find out how previous work affects or helps the development of your own.

Table 4 gives an overview of various patents that have been granted in the past that are relevant to the development of the Tidal Wave Energy Converter. A more detailed explanation of what these patents entail can be found in Appendix D. It should be considered during the development of the product that infringement of intellectual property is avoided where necessary, but that relevant previous work also serves as inspiration for improving the TWEC.

| Patent ID | Title |
|----------------------|--|
| CN202579018 | <i>"Tidal wave energy-storing power generation system"</i> |
| US3668412 | <i>"Apparatus for harnessing the vertical movement of ocean tides and utilize the force for generating electrical energy."</i> |
| US4034231 | <i>"Ocean tide and wave energy converter"</i> |
| US4103490 | <i>"Apparatus for harnessing tidal power"</i> |
| US4185464 | <i>"Ocean tide energy converter having improved efficiency."</i> |
| US4208878 | <i>"Ocean tide energy converter"</i> |
| US5184936 | <i>"Multiple gas phase tidal power generation apparatus and method"</i> |
| US5426332 | <i>"Tidal generator"</i> |
| US8347628 | <i>"Power generation directly from compressed air for exploiting wind and solar power"</i> |
| US20020145350 | <i>"Pressure to electric converter PEC"</i> |
| WO2011141691 | <i>"Tidal or wave energy harnessing device"</i> |
| WO2013006088 | <i>"Wave and tidal energy device"</i> |

Table 4 - List of relevant patents

It can be concluded from this patent study that the idea to generate electricity from the vertical motion of the tide is far from new and that some of the relevant patents are still valid in most parts of the world. Especially the two World Intellectual Property Organization (WIPO) patents should be handled with care as they approach the concept of the Tidal Wave Energy Converter closely. The other patents may serve as inspiration and should not pose any possibilities for infringement issues.

13 Possible host structures for the Tidal Wave Energy Converter

There is a large variety in the availability of floating bodies that the Tidal Wave Energy Converter can use as a driving force of the generation procedure. Three types of floating bodies will be discussed in this chapter, two being existing ones that could be used as a body to parasite the TWEC onto, floating houses and redundant marine vessels, and one being floating bodies in their most general form as a specifically designed case to case component.

13.1 Existing projects

Some projects with large floating objects in tidal influenced areas have already been built over the past. A small (but not definitive) sample size of such structures includes floating breakwaters, floating dry docks, floating bridges and as a special case of interest the S.S. Rotterdam, a confined former cruise vessel in the port area of Rotterdam.

13.1.1 Floating breakwaters

Floating breakwaters, as illustrated in Figure 44, are buoyant structures that aim to diminish the severity of the waves between one side of the structure and the other. They can be applied in areas with a moderate wave climate and have significant advantages in terms of ecologic intrusion and construction costs (especially in deeper water). Floating breakwaters can easily be rearranged in case a different layout is required, have a lower visual impact and are less affected by poor foundation possibilities.



Figure 44 - Artist impression of a floating breakwater

On the other hand they suffer high maintenance costs and do not perform well in more severe wave climates. Especially waves with periods in the range of 4 to 6 seconds are hazardous to floating breakwaters. During catastrophic storm conditions they may be susceptible to failure in which case the rampant floating structure becomes a hazard (Farmer, 1999).

These operational conditions still leave plenty of application areas for these types of structures and considering breakwaters are usually constructed in areas that are also subject to a tidal motion they are an interesting application area for vertical tidal power generation as well. Because the dimensions of floating breakwaters very depending on the local conditions a realistic value is distilled from (Foustert, 2006) as is displayed in Table 5. These dimensions are of what would be a compartment of the breakwater as typically breakwaters are in the order of kilometres in length.

| | |
|---------------|---------|
| Width | 34 [m] |
| Draft | 24 [m] |
| Length | 100 [m] |

Table 5 – Approximate floating breakwater dimensions

13.1.2 Dry docks

Dry docks are large structures used to create a dry working environment for ship maintenance. In general two varieties of dry dock can be found in shipyards around the world. The first one is a fixed type (Figure 45a) which consists of an artificial bay enclosed by a door. Once the ship has sailed into the bay the door is closed and the water in the dock is drained to dry up the working environment. The second type is a floating type (Figure 45b) which drains the water from its basin by lifting the base level of the dock above the outside water level.



Figure 45 - Dry docks: a) Fixed dry dock (Ulsan, South Korea) b) Floating dry dock principle

The upside of floating dry docks is that they represent a large, semi-submerged, surface area which could generate significant buoyant forces as well as a significant opposite gravity power whenever a ship has been lifted from the water. The potential energy stored in these situations is vast and could therefore be very interesting for the application of the Tidal Wave Energy Converter. Possible downsides of using dry docks are that they are usually situated in areas that are relatively sheltered from large tidal motions as large tidal fluctuations could complicate working conditions. The operational motions of a dry dock, however, could still be an interesting application case even without the influence of the tide as forcing factor.

| Type | Yard | Length [m] | Width [m] | Draught [m] |
|-------------------|---|------------|-----------|-------------|
| Longest | CIC Shipyards (Shanghai, China) | 410.0 | 70.0 | 18.5 |
| Widest | Keppel Verolme (Rotterdam, Netherlands) | 405.0 | 90.0 | 11.1 |
| Deepest | COSCO (Dalian, China) | 350.0 | 66.0 | 27.0 |
| Shortest | Thales (Sydney, Australia) | 63.0 | 12.9 | 5.0 |
| Narrowest | Thales (Sydney, Australia) | 63.0 | 12.9 | 5.0 |
| Shallowest | Santierul Naval (Constanța, Romania) | 138.0 | 23.0 | 4.0 |

Table 6 - Characteristics of floating dry docks (Wikipedia, 2014)

Many different sizes of dry docks exist to meet the requirements of the large dispersion in ship sizes. This means that some generalized dimensions need to be determined for calculation purposes. Table 6 gives an overview of some of the extreme values that floating dry docks around the world are known to have, evidently fixed dry docks are not of interest to this research. These values are generalized to an upper bound a lower bound and an average value in Table 7.

| | Length [m] | Width [m] | Draught [m] | Volume [m ³] |
|-------------|------------|-----------|-------------|--------------------------|
| Upper bound | 410.0 | 90.0 | 27.0 | 996,300 |
| Average | 236.5 | 51.5 | 15.5 | 188,786 |
| Lower bound | 63.0 | 12.9 | 4.0 | 3,251 |

Table 7 - Generalized characteristics of floating dry docks

13.1.3 Floating / tidal bridge

Floating bridges have been in existence for a significant period of time. Rather than creating a foundation on both ends of the bridge and possibly in between to support the deck of the bridge it floats on the water close to its surface. A famous example of a floating bridge is the Queen Emma Bridge (Figure 46a) in Willemstad, Curaçao, which was built in the late 19th century and is still in operation. The upside of these bridges is that, because of their lack of required foundation, they are relatively cheap. The major downside is evident and is that it has no vertical clearance for ships to pass through. In the example of the Queen Emma Bridge the entire bridge has to sail aside using diesel engine powered propellers whenever a ship needs to pass through (in which case a ferry service takes over transport of pedestrians). Larger, immobile, floating bridges also exist. An example is the Bergsøysundet Bridge in Norway (Figure 46b).



Figure 46 - Floating bridges: a) Queen Emma Bridge b) Bergsøysundet Bridge

A special case of the floating bridge is a so-called tidal bridge (Figure 47). These bridges aim to combine characteristics of the surrounding water body with energy harvesting operations to increase the feasibility of the bridge itself. These types of bridges are an interesting concept for remote island communities who cannot afford the construction of a bridge or justify outside funding. The economic revenue of the added tidal power generation can help their cause.

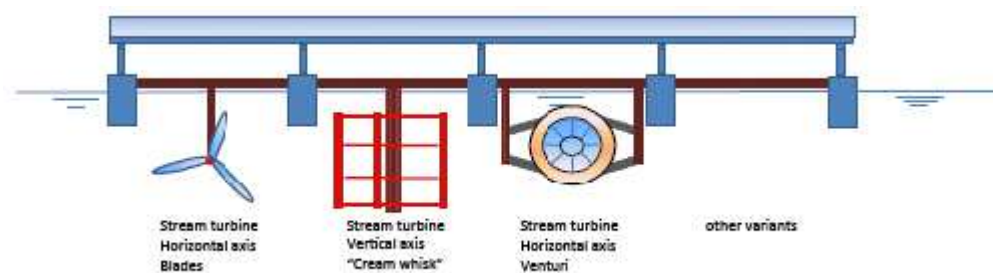


Figure 47 - Tidal bridge components

As example case the aforementioned Bergsøysundet Bridge will be considered. The relevant information on this bridge is given in Table 8.

| | |
|------------------------------------|------------------------|
| Pontoon length | 20.0 [m] |
| Pontoon width | 34.0 [m] |
| Pontoon height | 5.8 [m] |
| Load per pontoon | 750 [ton] |
| Concrete volume per pontoon | 1186 [m ³] |

Table 8 - Characteristics of the Bergsøysundet Bridge (Veritec, 1992)

13.1.4 S.S. Rotterdam

The S.S. Rotterdam is a historic steam powered passenger ship constructed in the late 1960s to be used for ferry services between the port Rotterdam and New York City. It was built by the RDM (Rotterdamse Droogdok Maatschappij) in Rotterdam and, during its time of service, operated by the Holland America Line. During the winter season, when crossing the Atlantic Ocean was impossible due to severe weather conditions, it operated as a cruise liner in South America. Because it was evident by its time of construction that the era of large scale trans-Atlantic passenger transport by sea was bound to end, the ship was very modern for its time with the possibility of easily converting the original two-class configuration to a single class configuration.

After several different owners, a name change (to Rembrandt resp.) and having been confined to port in Halifax, Canada, the ship was bought by a consortium of companies by the name of “Rederij de Rotterdam BV”. The intent of this consortium was to give the ship a permanent place in the port of Rotterdam and to convert it to an event location housing a congress centre, restaurant, hotel and other facilities. Since its renovation it has been anchored at a quay wall in Katendrecht, Rotterdam (Figure 48).



Figure 48 - The S.S. Rotterdam at its anchorage in Rotterdam

The S.S. Rotterdam at its anchorage is subject to a relatively small tidal motion, which makes it an interesting case to consider as application area for the Tidal Wave Energy Converter. Its large submerged volume and weight mean large forces can be created even with relatively small tidal amplitudes. What needs to be considered, however, is that ships are not designed for large point loads on their hull meaning appropriate countermeasures need to be taken to reinforce the structural integrity.

| | |
|---------------------|--------------|
| Length | 228.12 [m] |
| Width | 28.65 [m] |
| Draft | 9.00 [m] |
| Displacement | 31.530 [ton] |

Table 9 - Characteristics of the S.S. Rotterdam (Ward, 1995)

13.2 Planned projects

Contrary to the previously described projects that are already available in the world there are also some projects that have yet to make the transition from the drawing board to the construction site. A concept that has been getting some attention for decades are floating houses and, on a larger scale, entire floating communities.

13.2.1 Floating houses

Floating houses come in various forms and sizes. Because uniformity is important in the analysis of the feasibility of the Tidal Wave Energy Converter it is desired to convert the range of possibilities into a more manageable format rather than a large variety of individual solutions.

Layout and draught

| Name | Floatation system | Surface area [m] | Amount of floors | Draught [m] |
|-----------------|-------------------|------------------|------------------|-------------|
| Booneiland | EPS platform | 12 by 7.8 | 3 | 1.20 |
| De Gouden Ham | Concrete body | 11 by 6 | 3 | 1.50 |
| Olderhuuske | Concrete body | 12 by 5 | 2 | 1.50 |
| Terwijde | Concrete body | 11 by 6 | 2 - 2.5 | 1.25 |
| De Blauwe Stad | Concrete body | 12.6 by 8.7 | 2.5 | 1.20 |
| Waterbuurt Oost | Concrete body | 10 by 7 | 2.5 | 1.50 |
| Waterbuurt West | Concrete body | 10 by 4.9 (6.4) | 2.5 | 1.50 |

Table 10 - Characteristics of floating houses (DeltaSync, 2014)

Data on some varieties of floating houses that have been developed in the Netherlands over the years have been obtained from (DeltaSync, 2014) and are presented in Table 10. This data is summarized into three cases of floating houses which will be used for the evaluation: a lower bound variant, an upper bound variant and an average variant, all with a concrete body type of floatation system.

Generalized layout and draught

| | Surface area [m] | Draught [m] | Volume [m3] | Weight [tons] |
|-------------|------------------|-------------|-------------|---------------|
| Upper bound | 12.6 by 8.7 | 1.5 | 164.43 | 164 |
| Average | 11.23 by 6.49 | 1.38 | 100.58 | 100 |
| Lower bound | 10 by 4.9 | 1.2 | 58.8 | 58 |

Table 11 - Generalized characteristics of floating houses

The generalized characteristics as depicted in Table 11 give a range in which floating houses are being developed. It gives values that can be used both for the gravity based variant of the Tidal Wave Energy Converter as well as the buoyancy based variant.



Figure 49 - Relatively small floating houses (Waterbuurt West) and relatively large floating houses (Booneiland)

13.2.2 Floating cities

Floating cities are in essence idealistic trailer parks of floating houses packed together in the form of municipalities. A preliminary report regarding these types of (mega) structures was made by (Czapiewska, 2013) and describes a floating community which can relocate to other locations in the world depending on the needs of the community. For instance it can be located in a tropical area during the summer and relocate before storm season to a location less prone to severe weather conditions. These cities would produce marine power in various ways and trade with on shore communities for drinking water and other products it cannot produce for itself. In return it would create bio fuels from fish excrements and algae farms, food and organics fertilizer. Figure 50 shows an artist impression of a floating city as envisioned by DeltaSync.



Figure 50 - Artist impression of a floating city

In the foreseeable future floating “cities” will be much less idealistic and will most likely consist of smaller scale communities of floating structures with houses and some mid-sized enterprises. This, however, does not take away the potential of such cities. In the near future by utilizing the motion of smaller pontoons in the tide, but eventually through rogue mega structures roaming the Earth’s oceans.

13.3 Other products with potential

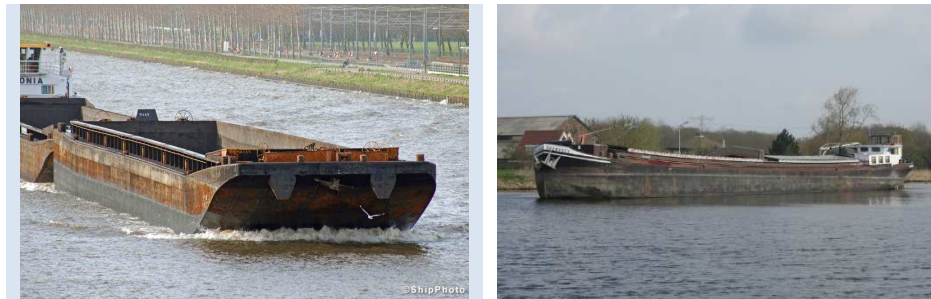
Apart from small and large scale projects with floating pontoons to use as superstructure there are also some other areas of potential interest that should be considered. First of which being redundant marine vessels, which have either been confined to port or unfit for shipping but still retaining their buoyancy. And lastly it is possible to specifically design a floater to use for the buoyancy aspect of the device.

13.3.1 Redundant Marine vessels

The lifetime of marine vessels is not only based on the deterioration of the materials it consists of, but also on the dependency of the system it is operating within. Developments in transport sizes, directions and means or bankruptcy of the sailing firm cause for specific vessels or types of vessels to become redundant long before the materials deteriorate to a degree where it can no longer be used. For the sake of comparison two types of vessels will be considered.

Firstly a regular Rhine push barge will be looked into. Push barges are generally used in convoys and pushed along the river by a towboat. The utilization of these barges largely depends on the demand in the system and often there is an overcapacity. The barges are stored in assigned locations along the river until they are needed again. During this storage time the barges could potentially serve as the driving force for a TWEC installation. Alternatively they can serve this purpose after they have been written off for transport purposes without losing their floatation capacities.

Secondly the “Kempenaar” type vessel will be considered due to its significantly different size from the push barge. This type of vessel belongs to the CEMT class II and has been designed to sail in the Meuse-Scheldt canal in the Netherlands. The southern parts of the Netherlands and Flanders are the areas in which this type of vessel is common.



| | <i>Push barge Europa II class</i> | <i>CEMT Class II - Kempenaar</i> |
|------------------------|-----------------------------------|----------------------------------|
| Length | 76.5 [m] | 50 [m] |
| Width | 11.4 [m] | 6.6 [m] |
| Draught | 3.5 [m] | 2.5 [m] |
| Weight (empty) | 602 [tons] | 425 [tons] |
| Weight (loaded) | 3052 [tons] | 825 [tons] |

Table 12 - Characteristics of considered vessels (Brolsma & Roelse, 2011)

An important aspect to investigate in terms of redundant vessels is not only how much buoyancy or gravitational force they can exert onto the TWEC, but also how they deal with the reaction force that is being dealt upon them. Vessels are designed to withstand a uniform load of the water on its hull rather than the point load that the TWEC exerts. It could be necessary to strengthen the hull of the vessels before using it to load a TWEC or it may fail under the load.

13.3.2 Specifically designed bodies

Apart from using already existing objects to create a load on the TWEC another alternative is to specifically design something that exerts a force. The benefit of this is that the dimensions can be optimized much easier and the choice of material is still open. This means that for a purely buoyancy based structure the material can be minimized, fully utilizing the force of the air, whereas for a purely gravity based solution the weight can be maximized.

14 Generalized boundary conditions

To analyse the operational characteristics of the Tidal Wave Energy Converter it is required to know what the boundary conditions are under which the device is to operate. Aspects like soil conditions, tidal forcing, water quality and neighbouring marine life are of influence and should be taken into consideration. Because, however, these conditions vary depending on what exact location on Earth is being chosen to apply the TWEC it is impossible to consider all possible combinations of boundary conditions. Therefore three very different combinations of conditions will be derived which will serve to provide insight in the design aspects that play a role at different locations.

14.1 Tide

The tide, as described in Appendix A, consists of a large amount of sinusoidal components governed by constituents. These constituents represent how the celestial bodies in the solar system affect the water on the planet and express this in predictions for water height and return period. The main influencing factors on the magnitude of the different constituents are the distance between Earth and the celestial bodies, the speed at which they move relative to the Earth and the local bathymetry. All these aspects vary over the Earth's surface. The main differences that can be used as characterisations for different scenarios are the height of the tide (realistically ranging from 0 to about 15 meters), the return period (once or twice a day) and whether the observed tide is relatively constant over its stretch or has a large variety in height over time. The return period of the tide can be easily observed from graphs but also mathematically determined using Equation 6 (explanation on variables in Section 2, not included in this document). If this ratio is smaller than 0.25 the tide is semi-diurnal, if it is higher than 3.0 the tide is diurnal.

$$F = \frac{K_1 + O_1 + P_1 + Q_1}{M_2 + S_2 + K_2 + N_2}$$

Equation 6 – Diurnality ratio

The first derived tide is a constant low level tide as can be found in for example port basins in Dutch harbours. It is dominated by the semi-diurnal lunar tidal constituent (M_2) resulting in a relatively constant, semi-diurnal amplitude (ratio 0.056). The second tide is a tide loosely based on the tidal motion in the King Sound bay in Western Australia (Australian Bureau of Meteorology, 2014), not included). The tide here is dominantly semi-diurnal (ratio 0.092) and due to all semi-diurnal tidal constituents having large amplitudes its cumulative amplitude varies over time. The third tide is a diurnal tide meaning it has a return period of once a day (ratio 8.2308). The tide is dominated by the arbitrarily chosen diurnal lunisolar tidal constituent (usually the largest diurnal tidal constituent) giving it a constant amplitude.

| | Low semi-diurnal [m] | Mixed semi-diurnal [m] | High diurnal [m] | Phase shift [°] |
|----------------------|----------------------|------------------------|------------------|-----------------|
| M₂ | 1.5 | 3.5 | 0.3 | 40 |
| S₂ | 0.1 | 1.5 | 0.2 | 120 |
| N₂ | 0.1 | 1.0 | 0.1 | 10 |
| K₂ | 0.1 | 1.0 | 0.05 | 120 |
| K₁ | 0.02 | 0.3 | 5.0 | 340 |
| O₁ | 0.02 | 0.2 | 0.2 | 320 |
| P₁ | 0.01 | 0.1 | 0.1 | 350 |
| Q₁ | 0.05 | 0.05 | 0.05 | 310 |
| M_f | 0.01 | 0.01 | 0.01 | 300 |
| M_m | 0.01 | 0.02 | 0.02 | 20 |
| M₄ | 0.03 | 0.3 | 0.3 | 350 |

Table 13 - Amplitudes of generalized constituents (see Appendix A for constituents explanation)

Table 13 gives the constituents of the described tidal motions. The phase shift has been deemed constant for the sake of the generalization; the angular velocity is as given in Section 2 (not included in this document). The resulting tidal responses for the given sets of constituents are displayed in Figure 51.

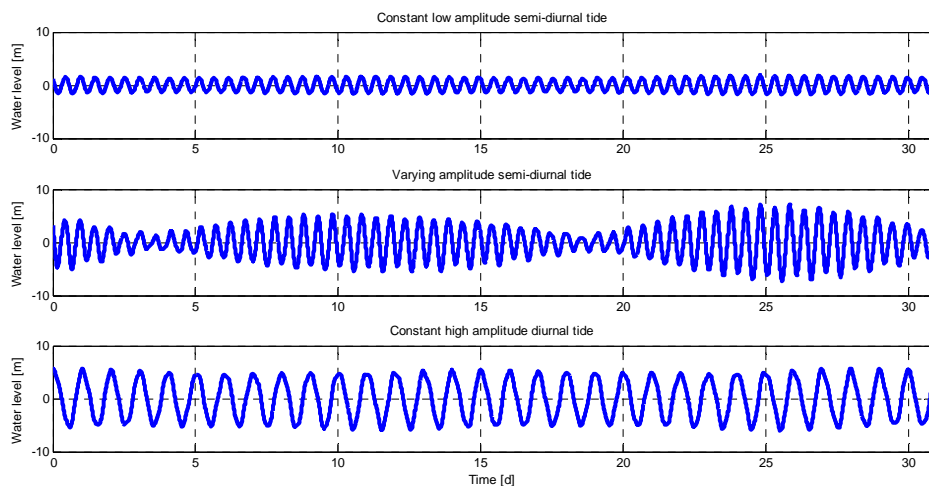


Figure 51 - Plots of generalized tides

14.2 Soil and bathymetry

Generally speaking the soil conditions are determined by two major influences: sediment supply and plate tectonics (Appendix E). It can be seen that along leading edge coastlines coarser sediment and rock formations exist and the occurrence of finer sediment is limited. On trailing edge coastlines the sediment is finer due to wide gentle continental shelves and the influence of rivers. In warmer climates this fine sediment becomes more mud dominated due to chemical and mechanical wearing.

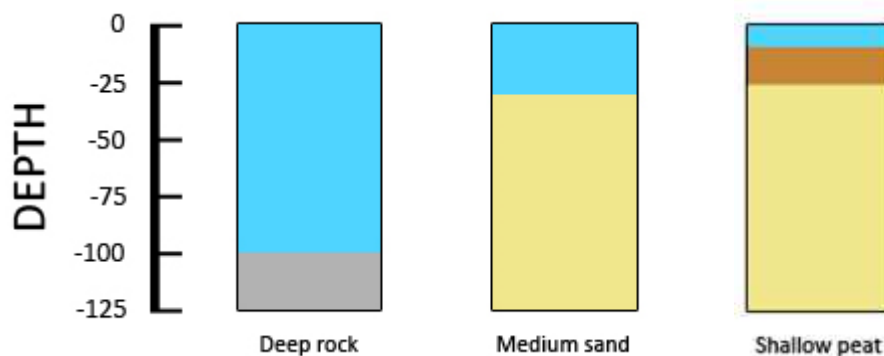


Figure 52 - Depth profiles of considered situations

For the sake of generalization here too three different scenarios will be derived. The first being a leading edge coast with a bottom consisting of rock. Due to the steep continental shelf the water depth is significant and in the order of 100 meters. The second scenario is a trailing edge coast with sandy sediment and a relatively shallow water depth in the order of 30 meters. The third scenario is a manmade port basin of 10 meters deep some distance inland on a trailing edge coastline. Because it is inland there are layers (approximately 25 meters) of compacted organic material (peat) nearer the surface before the sandy sediment from previous geological epoch is reached. Figure 52 illustrates the composition of the different scenarios.

14.3 Environment

The environment is a wide spectrum of things of which not all are of relevance to the in-situ application of the Tidal Wave Energy Converter. The most important of which is the salinity of the surrounding water having its main influence on the corrosion rate of the used materials. The general classification of water salinity consists of fresh water (less than 0.05% saline), brackish water (0.05 to 3% saline), saline water (3 to 5% saline) and brine (over 5% saline). These water salinities have an effect in corrosion rate as well as water density where an increased salinity also increases the density.

A second important environmental factor to take into account is the presence of flora and fauna. Especially when parts are moving plant growth could become problematic and constricting. Furthermore the possibility of using turbines means fish could enter the system and either be damaged by the turbine blades or in turn damage the turbine blades themselves. Adequate countermeasures would be required to counter this risk.

15 Program of Requirements

The program of requirements serves as a benchmark on which the finished product will be tested to see if it is safe and fit for using on in-situ locations. The requirements are based on safety and usability as well as financial motivations. With clearly defined requirements and desires in mind it is easier to design a suitable product from start to finish.

15.1 Requirements

The list of requirements that need to be fulfilled by the final design is as follows:

- Safety valves or releases need to be designed in case excessive conditions occur.
- The structural integrity of the floating body needs to be sufficient to handle the point load(s) of the installed device(s).
- The device needs to be able to handle the added pressures that the operation of it induces.
- The energy conversion mechanism needs to be safe from people or wildlife being harmed by moving parts.
- The energy conversion mechanism needs to be protected against the intrusion of plants and other debris.
- The device needs to be light weight as to limit the effects of it on the buoyancy of the floating body. The maximum added submergence of the floating body due to the device is 1% of the draft.
- The device needs to be accessible for maintenance.
- The stability of the floating body needs to be guaranteed in all construction and operation phases.
- The generator needs to be protected from water intrusion.

15.2 Desires

Apart from requirements there are some wishes that are not essential to be fulfilled but highly desired. For the device it is desired that...

- ...the acceleration of the pontoon is within allowable boundaries of usability at any given time during operation in case the pontoon has a multifunctional use. (0.4 m s^{-2} as per Eurocode)
- ...it is easily scalable for different tidal amplitudes, floating body dimensions and water depths.
- ...it is able to store energy in an efficient manner.
- ...it is constructed with "of the shelf" components.
- ...multiple devices can be attached to a single energy conversion mechanism to optimize the efficiency of the conversion mechanism.
- ...it is easily (dis)mountable so it can be applied on non-permanent floating bodies (e.g.: moored ships).
- ...it is installable without having to extract the floating body from the water.
- ...it is profitable within 10 years.
- ...it is composed of non-corrosive materials.

Section 4 – Engineering aspects

| | | |
|------|---|-----|
| 16 | Introduction of engineering aspects | 93 |
| 17 | Environmental scenarios | 95 |
| 17.1 | Scenario 1: Sheltered manmade port | 95 |
| 17.2 | Scenario 2: Trailing edge estuary | 96 |
| 17.3 | Scenario 3: Leading edge bay | 97 |
| 18 | Limit states | 99 |
| 18.1 | Serviceability limit state | 99 |
| 18.2 | Ultimate limit state..... | 99 |
| 19 | Method of energy conversion | 101 |
| 19.1 | Considered mechanisms for energy conversion | 101 |
| 19.2 | Decision criteria..... | 102 |
| 19.3 | Chosen method | 103 |
| 20 | Operational characteristics | 105 |
| 20.1 | Pontoons used..... | 105 |
| 20.2 | Support and hydraulic motor dimensions..... | 106 |
| 20.3 | System configuration..... | 107 |
| 20.4 | Placement of supports under host structure | 109 |
| 20.5 | Forces for considered scenarios | 110 |
| 21 | Type and dimensions of foundation..... | 111 |
| 21.1 | Early exclusions | 111 |
| 21.2 | Soil characteristics | 113 |
| 21.3 | Steel pipe piles..... | 114 |
| 21.4 | Precast concrete piles | 119 |
| 21.5 | Foundation anchors..... | 121 |
| 21.6 | Shallow foundation | 125 |
| 21.7 | Foundation economics | 126 |
| 21.8 | Influence of soil characteristics on foundation | 127 |
| 22 | Adjustments to the host structure | 129 |
| 22.1 | Barge..... | 129 |
| 22.2 | Breakwater | 130 |
| 23 | Piston and rod dimensions | 133 |
| 23.1 | Piston..... | 133 |
| 23.2 | Rod..... | 135 |
| 23.3 | Connections..... | 137 |
| 24 | Possibilities for energy storage | 139 |
| 25 | Design criteria..... | 141 |
| 25.1 | Design procedure | 141 |
| 25.2 | Device components | 142 |

16 Introduction of engineering aspects

This section elaborates on the important elements of the technical design of the Tidal Wave Energy Converter (TWEK). In the following chapters the various important elements of the device will be considered with various solutions from which the most suitable solution will be chosen. Chapter 17 will give a short recapitulation of what the different design scenarios that have been considered before with the relevant tidal motion and soil characteristics. Chapter 18 will determine what limit states need to be taken into account for different design criteria. These limit states are important to determine what loads the system needs to be able to handle and what these loads consist of.

Following these general considerations the design of the elements as present in the TWEK are determined with first the method of energy conversion in chapter 19. In chapter 20 the operational characteristics such as the used pontoons, the dimensions of the energy conversion mechanism and the location and dimensions of the supports will be determined, with finally the loads these configurations lead to in the aforementioned limit states. Chapter 21 elaborates on the foundation possibilities of the TWEK and concludes on recommendations on what to use in what situation based on financial motivations. Chapter 22 considers the possible adjustments to the used host structures and chapter 23 determines the required dimensions of the used pistons and the rest of the connection between these, the host structure and the foundation.

Finally chapter 24 will textually investigate the possibilities of using the TWEK for the use in combination with energy storage, where either the production of the device itself or external energy input is used to build up storage. Chapter 25 aims to summarize the findings of the chapters that precede it and to derive basic design rules for certain scenarios based on the findings of the followed design steps in previous cases. Furthermore it looks forward to what the concluding section will include. Figure 53 gives an overview of the forces and their directions in both flood and ebb scenarios which will be used to determine the required dimensions of the components.

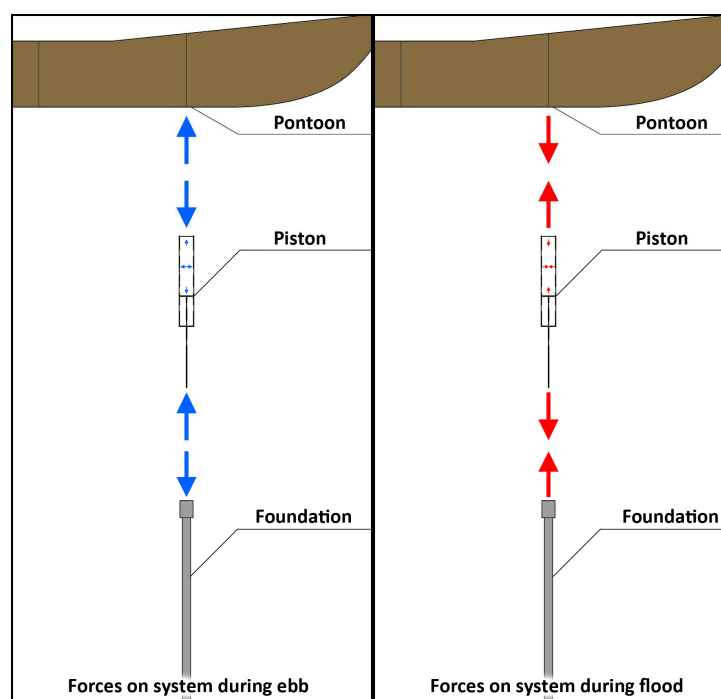


Figure 53 - System forces

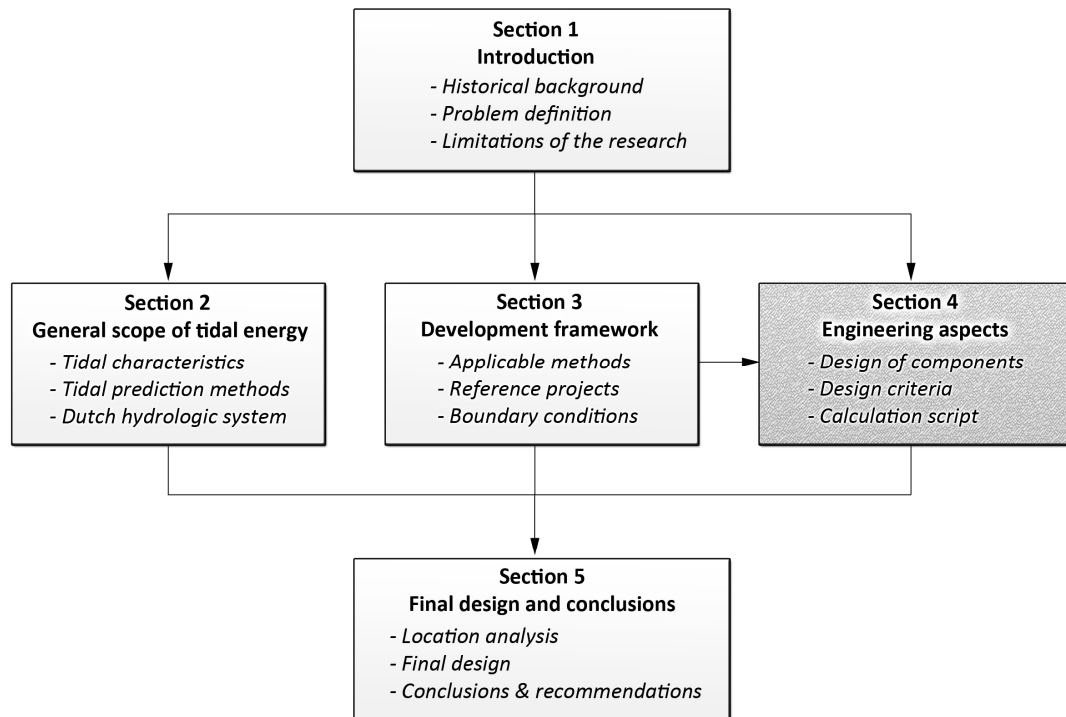


Figure 54 - Structure of the report

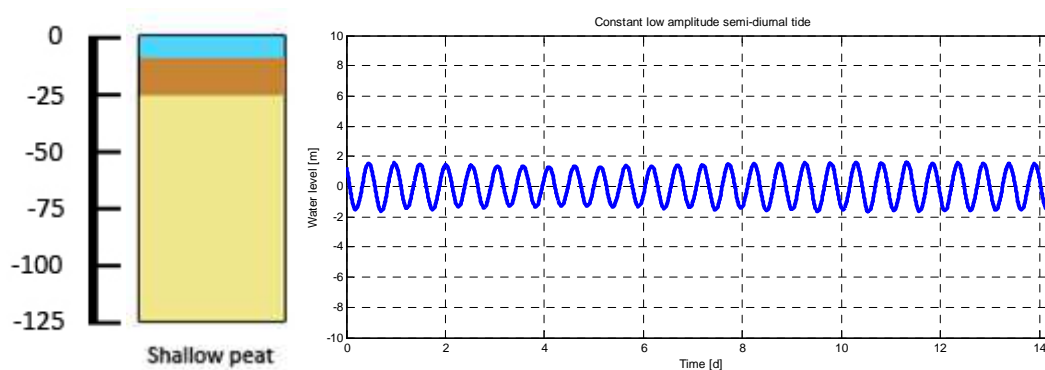
17 Environmental scenarios

The scenarios that will be used for the fictional application of the Tidal Wave Energy Converter have been previously determined in Section 3. Because this section actually applies the knowledge gained in that part a short summary will be given here of what has been derived as being representative application scenarios. The scenarios are:

- Scenario 1: Sheltered manmade port
- Scenario 2: Trailing edge estuary
- Scenario 3: Leading edge bay

17.1 Scenario 1: Sheltered manmade port

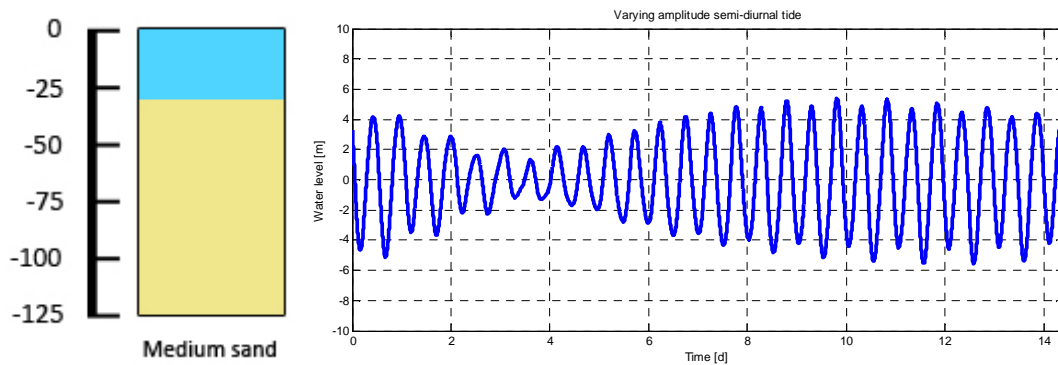
The sheltered manmade port is characterized by a relatively shallow water depth of 10 meters which has been dug by man for shipping activities. Underneath the bottom of the port part of the original clay layer is still found up to a depth of 25 meters after which the bearing sand layer takes over for the rest of the relevant depth. Due to the location being more inland the water is considered to be river dominated and therefore fresh. The tidal range, for the same reasons, is damped down to a dominant lunar amplitude of 1.5 meters with a semi-diurnal (bi-daily) nature.



| Tide: | Amplitude [m] | Phase shift [°] | Soil: | |
|----------------|---------------|-----------------|---------------|----------------------------|
| M ₂ | 1.5 | 40 | Water depth | 10 [m] |
| S ₂ | 0.1 | 120 | Water density | 1000 [kg m ⁻³] |
| N ₂ | 0.1 | 10 | Clay | 10-25 [m] |
| K ₂ | 0.1 | 120 | Sand | 25+ [m] |
| K ₁ | 0.02 | 340 | | |
| O ₁ | 0.02 | 320 | | |
| P ₁ | 0.01 | 350 | | |
| Q ₁ | 0.05 | 310 | | |
| M _f | 0.01 | 300 | | |
| M _m | 0.01 | 20 | | |
| M ₄ | 0.03 | 350 | | |

17.2 Scenario 2: Trailing edge estuary

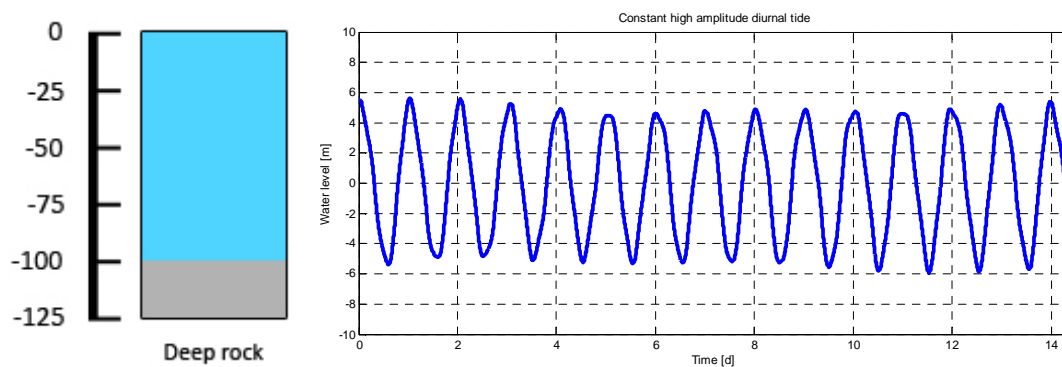
The trailing edge estuary scenario is a naturally existing type of hydraulic phenomenon which occurs in tide dominated river mouths on coasts tectonically moving away from its opposite shore. These types of coasts are characterized by a relatively shallow water depth, in this case 30 meters, and shores of finer sediment. Here the soil is considered to entirely consist of sand without any other soil types occurring. The water is a mixture of salt ocean water and fresh river water, resulting in a brackish water. The tide is influenced by the bathymetry in such a way that it has no dominant diurnal or semidiurnal component resulting in a mixed tide.



| Tide: | Amplitude [m] | Phase shift [°] | Soil: | |
|----------------|---------------|-----------------|---------------|----------------------------|
| M ₂ | 3.5 | 40 | Water depth | 30 [m] |
| S ₂ | 1.5 | 120 | Water density | 1012 [kg m ⁻³] |
| N ₂ | 1.0 | 10 | Sand | 30+ [m] |
| K ₂ | 1.0 | 120 | | |
| K ₁ | 0.3 | 340 | | |
| O ₁ | 0.2 | 320 | | |
| P ₁ | 0.1 | 350 | | |
| Q ₁ | 0.05 | 310 | | |
| M _f | 0.01 | 300 | | |
| M _m | 0.02 | 20 | | |
| M ₄ | 0.3 | 350 | | |

17.3 Scenario 3: Leading edge bay

The leading edge bay scenario is also a naturally occurring hydraulic phenomenon which occurs on the coastlines of shores moving towards its opposite counterpart. These shores are characterized by steeper slopes, and therefore deeper water, and courser bottom material. In this case a water depth of 100 meters has been chosen and a soil consisting of solely rock. The lack of an inflowing river means the water is dominantly salt. Local bathymetry results in a dominantly diurnal (mono-daily) tide with a relatively large amplitude of 5 meters.



| Tide: | Amplitude [m] | Phase shift [°] | Soil: | |
|----------------|---------------|-----------------|---------------|----------------------------|
| M ₂ | 0.3 | 40 | Water depth | 100 [m] |
| S ₂ | 0.2 | 120 | Water density | 1025 [kg m ⁻³] |
| N ₂ | 0.1 | 10 | Rock | 100+ [m] |
| K ₂ | 0.05 | 120 | | |
| K ₁ | 5.0 | 340 | | |
| O ₁ | 0.2 | 320 | | |
| P ₁ | 0.1 | 350 | | |
| Q ₁ | 0.05 | 310 | | |
| M _f | 0.01 | 300 | | |
| M _m | 0.02 | 20 | | |
| M ₄ | 0.3 | 350 | | |

18 Limit states

To properly determine the required dimensions of the components it has to be determined which conditions will be considered normative. A distinction in this can be made between two limit states:

- Serviceability limit state
- Ultimate limit state

18.1 Serviceability limit state

The serviceability limit state is such that the motions of the structure do not become bothersome to the users and mainly relate to sagging and vibrations due to external forcing. Because the actual use of the superstructure is outside the scope of this study it will be assumed that it will be used for civilian use, meaning the building code for floating structures can be used. These guidelines dictate requirements for the acceleration (max. 0.4 m s^{-2}) and the tilt of the pontoon (max 1°) (NEN-8111, 2011) and find their origin in high-rise structures, whom have comparable problems due to wind loads as floating structures have due to wave loads. Furthermore the serviceability limit state involves the capabilities of the device to remain operational, which is assumed to always be the case. At an in-situ location a probabilistic calculation (e.g.: Monte Carlo) could be made to determine how often the device would cease to be operational.

18.2 Ultimate limit state

The ultimate limit state relates to the failure of components due to external forcing. For this limit state the requirements are slightly more ambiguous as there are no specific guidelines available for this type of structure. Real floating structures (as considered in the NEN-code) float relatively freely on the surface and thus lack severe foundation loads, whereas land based structures suffer far greater consequences if the foundation were to fail. Based on the assumption that the superstructure of the Tidal Wave Energy Converter (the design of which is outside the scope of this research) is sufficiently buoyant in its design, the ultimate limit state of the TWEC lies somewhere in between the range of little consequence and severe consequence.

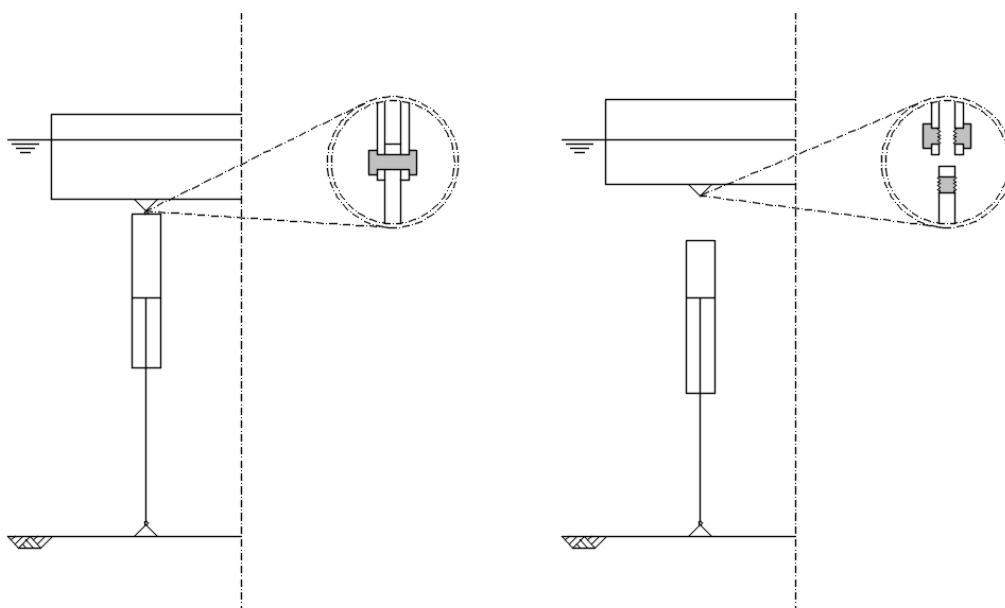


Figure 55 - System failure through sacrificial bolt

The worst case scenario that is used to define the ultimate limit state is chosen as being the situation when a piston breaks and becomes completely inert in one of the extreme operation positions. Seeing as the breaking of a piston does not cease the harmonic load of the tide a situation will develop where the tide is at its highest with the pontoon at its lowest (or vice versa), creating an ultimate worst case force on the foundation and the joints. This limit state causes large additional forces on the foundation and the topside connection meaning the dimensioning of both elements would be greatly exaggerated if this limit state were to be taken as defining. Preferential is to install an added component to the system which breaks at an arbitrary force lower than the ultimate but higher than the daily load. The required amount of force needed to break this sacrificial component is chosen to be a half times greater than the maximum calculated daily load for both tensile and compressive stresses. The design load for the rest of the components will use a regular safety factor of 1.5 on top of the design break load of the safety component. Figure 55 illustrates the considered failure mode.

19 Method of energy conversion

The way in which the energy is converted from the pressure the pontoon creates into electricity is the fundamental characteristic of the Tidal Wave Energy Converter. To obtain a solution on the means of energy conversion a Multi Criteria Decision Analysis (MCDA) is executed which judges various alternatives on a number of relevant decision criteria. The precise decision process is explained in Appendix F.

- Considered mechanisms
- Decision criteria
- Chosen method

19.1 Considered mechanisms for energy conversion

The possible methods of converting a difference in energy head into electricity have been previously discussed in Section 3. To shortly revisit what has been determined there an overview will be given of the methods that will be taken into consideration:

Hydraulic turbines can be divided into two main categories, **Reaction turbines** and **Impulse turbines**. Reaction turbines (Figure 56a) are the most used one and operate in a submerged environment. Water flowing across the blades creates a rotating motion of the turbine and powers a generator. These types of turbines are generally used for smaller heads and can be adjusted in design depending on what exact range is required. Impulse turbines (Figure 56b) use a nuzzle to propel the water into the blades of the propeller to make it rotate. These types of turbines are generally used for significantly larger water heads and can maintain high efficiency grades for flows as low as a quarter of the design flow.

Scroll expanders (Figure 56c) are a pressure to electricity conversion method mostly used in the opposite conversion direction in for instance refrigerators and air conditioners where they change the temperature of a substance by compressing/expanding it. The other way around works as well, however, and reaches efficiencies of up to 70 percent.

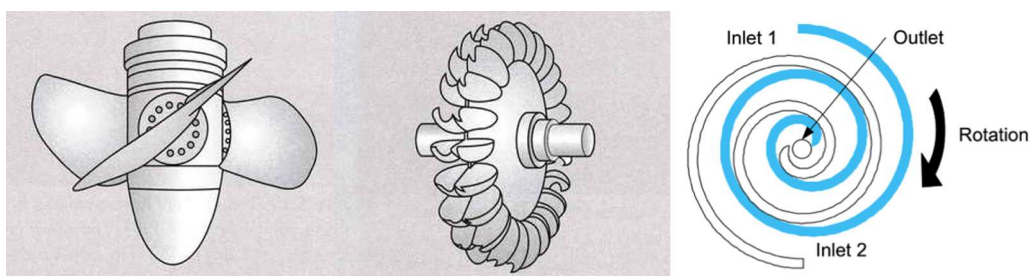


Figure 56 - a) Reaction turbine b) Impulse turbine c) Scroll expander

Hydraulic motors exist in various shapes and sizes and come with the main benefit that they can operate with a significantly smaller discharge than turbines.

The efficiency is generally in the 80% and higher range but differs depending on the type of motor used. **External gear motors and internal gear motors** (Figure 57a) are generally compact and relatively cheap whereas **Piston motors** (Figure 57c) obtain a better top efficiency and higher torque whilst being bigger. **Vane motors** (Figure 57b) are somewhere in the middle.

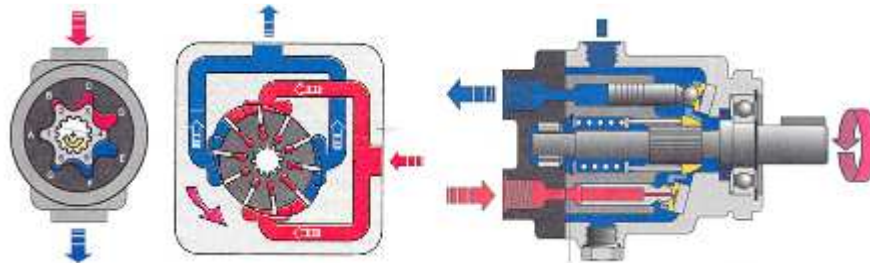


Figure 57 - Hydraulic motors: a) Gear motor b) Vane motor c) Piston motor

19.2 Decision criteria

The decision criteria are chosen such that the important differences between the considered mechanisms can be evaluated in an as objective as possible means. By assembling a comparison matrix giving a point whenever a criterion is more important than one of the others the weight factors can be calculated to determine what criteria will be weighing heavier in the decision. Table 14 gives the matrix and the accompanying weight factors. The decision criteria that are important for this comparison are:

Required discharge - The ability to spread out production: Energy consumption is spread out over the course of the day, which means energy production should be as well. There is no practical use for a certain peak energy harvest if it is produced in a very short time span as the possibilities of matching it with a user would be limited.

Peak efficiency: It is preferable to preserve as much of the potential energy from the wave as possible. Every kWh lost due to an inefficient conversion method means less revenue and further limitation in the feasibility range of the product.

Overall efficiency - The ability to work under different circumstances: The dynamic nature of the tide means the operating pressure will not be consistent. It is therefore preferential to have a device that keeps a high efficiency regardless of the applied energy head differential.

Compactness - Size of the device: The size of the device is important because the pontoon needs to be used for other purposes still as well. Furthermore a bigger device is generally heavier, which affects the maximum freeboard of the pontoon. This size is not only influenced by the device itself, but also by the required reserves to make it operate (e.g.: the reservoir required due to the discharge).

Ecologic/chemical sustainability - Impact on the environment: It would be odd to create a device for green energy production and not take into account the impact it has on the environment. Things that should be taken into account are the harm that can be done to wildlife in a physical manner, as well as the possibilities for toxic pollution.

| | peak efficiency | overall efficiency | chemical sustainability | ecologic sustainability | required discharge | compactness | Sum | factor |
|-------------------------|-----------------|--------------------|-------------------------|-------------------------|--------------------|-------------|-----|--------|
| peak efficiency | 1 | 0 | 1 | 1 | 0 | 1 | 4 | 0.19 |
| overall efficiency | 1 | 1 | 1 | 1 | 0 | 1 | 5 | 0.24 |
| chemical sustainability | 0 | 0 | 1 | 0 | 0 | 0 | 1 | 0.05 |
| ecologic sustainability | 0 | 0 | 1 | 1 | 0 | 0 | 2 | 0.10 |
| required discharge | 1 | 1 | 1 | 1 | 1 | 1 | 6 | 0.29 |
| compactness | 0 | 0 | 1 | 1 | 0 | 1 | 3 | 0.14 |

Table 14 - Determination of MCDA weight factors

19.3 Chosen method

To obtain scores for each of the considered methods points are given on a scale of 1 to 7 (because there are 7 methods) where the best performing method gets 7 points and the second best 6 points and so on to the worst getting 1. If two methods score equal they will get the same score and the next one will be skipped (so if two score 7 points, the third best will get 5). This method is used to take away subjectivity in obtaining the scores as much as possible.

The final score of each conversion method is obtained by multiplying the scores each method obtained for a specific criterion with the weight factor given to that criterion. The sum of all these components is the final score. It can be observed from Table 15 that piston motors and internal gear motors perform the best. They obtain their benefits from performing better on the three main criteria of required discharge and efficiency. Even though piston engines have a slight edge over internal gear motors, the benefits internal gear motors have in terms of costs mean the internal gear motor, or gerotor motor, has a slight advantage and is the preferred choice. This is deemed acceptable due to the lack of consideration for small differences in the determination of scores.

| Conversion method | Score |
|---------------------|-------|
| Reaction turbine | 3.81 |
| Impulse turbine | 4.76 |
| Scroll expander | 2.62 |
| External gear motor | 5.14 |
| Vane motor | 5.10 |
| Internal gear motor | 6.43 |
| Piston motor | 6.57 |

Table 15 - MCDA results

20 Operational characteristics

To be able to obtain dimensioning of the components of the device it is required to know what the forces are that will be exerted on them. These forces are a result of the exertion of the pontoon relative to its equilibrium position in the water. To determine what this relative position is two things need to be known: the motion of the tide and the resulting motion of the pontoon. The motion of the tide has been previously determined in chapter 17, the motion of the pontoon depends on the characteristics of the hydraulic motor and the used piston.

20.1 Pontoons used

The used pontoons are of significant importance as their surface area determines how much vertical force will be created for every unit of length it is pulled under or out of the water. Furthermore pontoons have a specific freeboard that ought to be taken into account to make sure the pontoon is not lifted from the water or completely submerged. For the dimensioning here the pontoons are chosen based on both availability as well as surface dimensions, in case the freeboard is insufficient the pontoon is automatically replaced by a pontoon of equivalent surface area with associated recommendations for increasing the freeboard.

20.1.1 Europa II class barge

Push barges are a common sight in many of the world's largest rivers. The Mississippi River, Rio Paraná and River Rhine are all well known for their inland waterway transport systems and house



Figure 58 - Europa II class push barge

various sizes of barges. On the Rhine one of the most commonly seen barges is the Europa II class push barge (Figure 58), an 11.4 by 76.5 meter vessel that can carry up to 3052 tons. The abundance of these vessels means there is also an abundance of these types of vessels which are damaged or have exceeded their lifespan, which results in a market of such vessels available for use in other fields such as energy conversion.

The upward or downward force of the pontoon on the pistons is determined by the volume of water that is displaced by the barge. Because a barge is designed to move through the water with little resistance the submerged volume is not exactly the same as the product of the length the width and the draught, but needs to be multiplied by a block factor to account for the unused space. For the Europa II class push barge this factor is 0.952 (Tabaczek, et al., 2007). Table 16 lists the relevant dimensions of the barge.

| | |
|--------------------------|-------------------------|
| Length | 76.5 [m] |
| Width | 11.4 [m] |
| Surface area | 872.1 [m ²] |
| Block coefficient | 0.952 |
| Maximum draught | 3.5 [m] |

Table 16 - Dimensions of the Europa II push barge

20.1.2 Floating Breakwaters

Floating breakwaters (Figure 59) are floating structures that aim to reduce the amplitude of swell waves in coastal areas. They generally consist of a buoyant concrete caisson which is kept in place by a



Figure 59 - Floating breakwater

number of anchor lines attaching it to the bottom. They exist in many different sizes depending on the severity of the local waves and potential other uses of the breakwater, which means an example case has to be taken to be used as a host structure.

The considered floating body is determined to have a width of 34 meters and a length of 100 meters, which makes it a significantly larger than the barge. Furthermore the lack of requirements for low resistance movement means the block coefficient for the pontoon is equal to one. The maximum draught is also significantly larger at 24 meters, which means a pontoon with the exact size mentioned can impossibly be applied to shallow areas. For that scenario a caisson with the same surface area but a smaller draught will be considered. What also has to be taken into account with these structures is that the breakwater may not lose its function as wave reduction mechanism, meaning the degree in which it can be pulled under water will be less than the given draught. Table 17 gives the dimensions of floating breakwater units.

| | |
|--------------------------|-------------------------|
| Length | 100 [m] |
| Width | 34 [m] |
| Surface area | 3,400 [m ²] |
| Block coefficient | 1.0 |
| Maximum draught | 24 [m] |

Table 17 - Dimensions of floating breakwater units

20.2 Support and hydraulic motor dimensions

As determined in chapter 19 the energy conversion process will be done through the use of hydraulic motors of the internal gear variety. Because there is a large variety of such motors available the choice has been made to exclusively look at motors produced by Eaton, simply because a complete document with performances of their devices is available. The specific type of motor to be used is the Eaton Gerotor motor of the J-series, which exists for various displacements and can run at various speeds in both directions. The application range of the motors is considered to be in the range of 14 to 140 BAR. This pressure is obtained by dividing the generated load on the system by the surface area of the supports.

Through trial and error calculations (using the MatLab program described in Appendix P for periods of one week) an optimum configuration of a certain displacement, RPM, support diameter and number of supporting pistons can be calculated that yields the best electric revenue. From (Eaton, 2011) the possibilities for applicable displacements and rotations per minute can be obtained, the possibilities in terms of support area and number of supports are considered to be completely open. What can be concluded from this process is that the various components affect the process in the following way:

Pontoon elevation velocity: The elevation velocity is important in the process because it determines how much elevation fits into a tidal window. The faster it rises and falls, the more of the tidal range it will be able to utilise. What is, however, important is that it does not rise or fall faster than the tidal motion itself as this results in difficulties maintaining the required pressure. The elevation velocity is influenced by the combination of the hydraulic motor's discharge and the volume of the piston. A larger piston results in slower velocities and a higher discharge results in larger velocities.

Pressure control: The pressure is controlled by the amount of supports and the surface area of those supports. Controlling the pressure is important because for too high pressure levels (higher than 140 BAR) the hydraulic motor does not suffice anymore. A higher amount of supports of equal diameter increases the bearing surface area and therefore decreases the pressure. What should be taken into account is that increasing the surface area per support also decreases the elevation velocity due to the larger volume it creates at the same height, whereas increasing the amount of supports does not. Increasing the amount of supports has an effect on the costs however.

The chosen hydraulic motors and the according support diameters and numbers of supports are displayed in Table 18.

| Scenario | Motor type | Displacement [cm ³ /rotation] | Rotations per minute [RPM] | Ø Support [m] | Number of supports |
|---|------------|---|-------------------------------|------------------|-----------------------|
| Sheltered manmade port <i>Barge</i> | MOJ05 | 8.2 | 444 | 0.84 | 3 |
| Sheltered manmade port <i>Breakwater</i> | MOJ05 | 8.2 | 810 | 1.04 | 4 |
| Trailing edge estuary <i>Barge</i> | MOJ12 | 19.8 | 550 | 0.90 | 6 |
| Trailing edge estuary <i>Breakwater</i> | MOJ30 | 50 | 220 | 0.90 | 13 |
| Leading edge bay <i>Barge</i> | MOJ05 | 8.2 | 810 | 0.98 | 6 |
| Leading edge bay <i>Breakwater</i> | MOJ30 | 50 | 210 | 0.98 | 13 |

Table 18 - Configuration of pistons and hydraulic motors

20.3 System configuration

The configuration of the Tidal Wave Energy Converter is important in terms of what component of the system is placed where. The hydraulic motors need to be placed at a certain position, as do the pistons which also need to be installed under a certain angle. Table 19 gives the different options that are taken into consideration where:

The **support orientation** indicates which direction the piston is positioned in. Vertical means it goes straight down giving only support in the vertical direction. Diagonal means it is inclined giving it capacities to absorb a horizontal force as well. Lever means the piston is installed in a lever composition meaning the piston size can be reduced and the pressure amplified at the cost of a longer support beam and less ideal forces on the beam.

The **piston position** relates to the location of the piston. It can either be installed underwater without piercing the hull of the host structure, but in a more corrosive environment. Or above water with less corrosion and a necessity to pierce the host structure. The **motor position** is based on the same characteristics that it can be placed either above the water table or beneath it. The motor's position does not include a need to pierce the host structure as its pressure pipes can be led over the side.

| Support orientation | Piston position | Motor position |
|---------------------|------------------------|-----------------|
| 1 - Vertical | α - Above water | A - Above water |
| 2 - Diagonal | β - Under water | B - Under water |
| 3 - Lever | | |

Table 19 - System configuration options

Following the MCDA process as described in Appendix G the conclusion is that the best system is to use variant 1- β -A with a vertical support orientation, the piston under water and the motor above water. A representation of the configuration of this system is given in Figure 60.

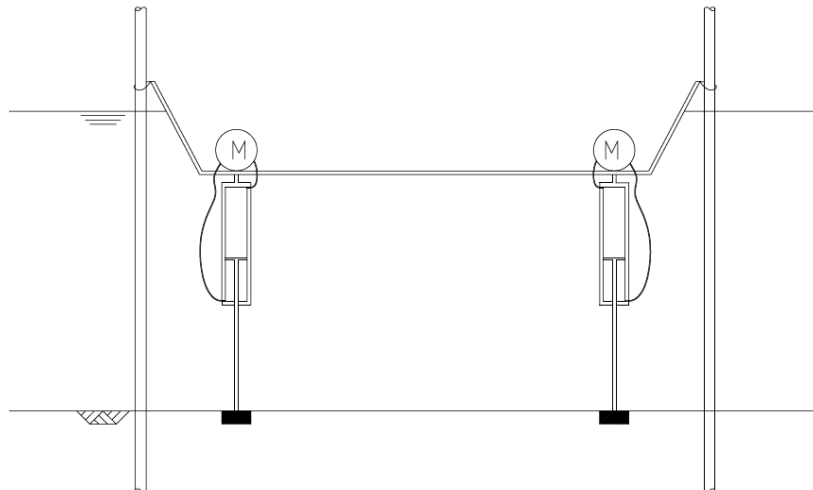


Figure 60 - System configuration 1- β -A

20.4 Placement of supports under host structure

The locations of the supports under the host structure are arbitrary to a degree, where practical reasons dictate they should be at least 1 metre from the side of the structure the rest is a matter of optimising the force distribution.

For the barge scenarios the required amounts of supports are three and six, for which configurations have been presented in Figure 61. In determining these configurations the governing train of thought has been to evenly distribute the supports over the surface whilst placing them as far apart as possible. This is to prevent one side being loaded more significantly leading to a certain tilt, and to prevent the foundations under the supports from influencing each other.

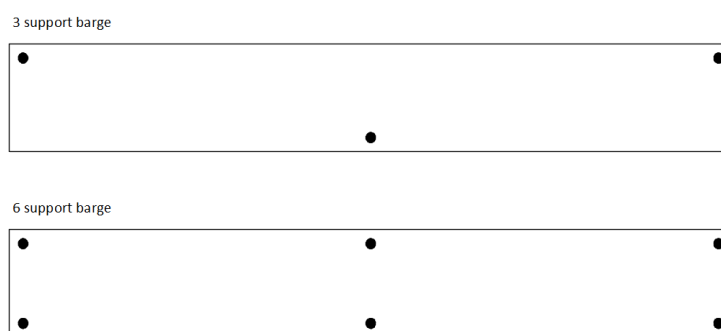


Figure 61 - Barge support configurations

For the breakwaters the same philosophy applies as for the barges where in this case the required amount of supports are four and thirteen. The chosen configurations for these are portrayed in Figure 62.

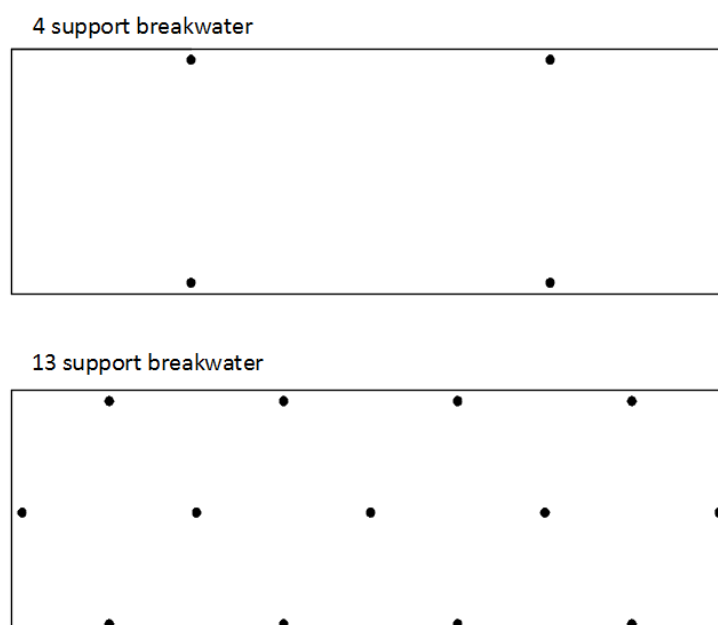


Figure 62 - Breakwater support configurations

20.5 Forces for considered scenarios

Using the same MatLab program as used in chapter 20.2 the operating loads the exerted pontoon applies to the device can be calculated. This time the considered time period is taken as a full year to make sure the maximum values are included in the calculation. Table 20 displays these values as well as the resulting limit state values for the safety bolt and the rest of the structure.

| Scenario | Operation load [kN] Compression [tension] | Bolt failure load [kN] Compression [tension] | Ultimate load [kN] Compression [tension] |
|-------------------------------|--|---|---|
| Sheltered manmade port | 4,229.5 | 6,344.3 | 9,516.4 |
| <i>Barge</i> | [-4,308.8] | [-6,463.2] | [-9,694.8] |
| Sheltered manmade port | 10,557.4 | 15,836.1 | 23,754.2 |
| <i>Breakwater</i> | [-11,022.8] | [-16,534.2] | [-24,801.3] |
| Trailing edge estuary | 9,238.9 | 13,858.4 | 20,787.5 |
| <i>Barge</i> | [-10,206.7] | [15,310.1] | [-22,965.1] |
| Trailing edge estuary | 15,238.4 | 22,857.6 | 34,286.4 |
| <i>Breakwater</i> | [-17,308.7] | [-25,963.1] | [-38,944.6] |
| Leading edge bay | 7,877.9 | 11,816.9 | 17,725.3 |
| <i>Barge</i> | [-7,498.5] | [-11,247.8] | [-16,871.6] |
| Leading edge bay | 11,147.7 | 16,721.6 | 25,082.3 |
| <i>Breakwater</i> | [-8,716.4] | [-13,074.6] | [-19,611.9] |

Table 20 - Calculated forces in limit states

The resulting freeboard in the different scenarios is considered in chapter 22.

21 Type and dimensions of foundation

The type of foundation depends mostly on the manner in which it is loaded, the soil characteristics, the costs and potential construction limitations. The only construction limitation that applies to any of the scenarios is that the foundation has to be laid underwater, there are no height restrictions that apply. In this case the considered possibilities will be:

- Steel pipe piles (tension/compression)
- Precast concrete piles (tension/compression)
- GEWI or rock anchors (only tension)
- Shallow foundations (only compression)

Calculations for all these types of foundations will be made to determine the required dimensions of the entire foundation (piles, pile caps, slab thickness, etc.). After this an evaluation can be made of the costs which when compared to the effect the foundation type has on the revenue will lead to a conclusion on which foundation type is preferential.

21.1 Early exclusions

Without doing any actual calculation on the foundation itself some conclusions can be drawn on whether or not certain types of foundations are possible and/or desirable for certain scenarios. These exclusions are based on the water depth and the soil layers on which the foundation is to be placed. For the water depth the determining excluding factor is the buckling length. For large water depths it is simply too difficult to dimension the piston and the accompanying piston rod in such a way that buckling does not occur. Equation 7 gives the range in which buckling is manageable, where the left boundary is a solid rod with a minimum radius needed such that the yield stress is not exceeded, and the right boundary is a hollow rod of equal diameter as the inside of the piston also with just as much material that the yield stress is not exceeded (derivation in Appendix H).

$$\sqrt{\psi \cdot \omega_{buc} \cdot F_{\max} \cdot \frac{\pi \cdot E_s}{4 \cdot \sigma_s^2}} \leq l_{buc} \leq R_u \cdot \sqrt{\frac{\omega_{buc} \cdot \pi^2 \cdot E_s}{2 \cdot \sigma_s}}$$

ψ = Safety factor [–]
 ω_{buc} = Buckling factor [–]
 F_{\max} = Maximum force [N]
 E_s = Young's modulus [N/mm²]
 σ_s = Yield strength [N/mm²]
 l_{buc} = Buckling length [m]
 R_u = Outside diameter [m]

Equation 7 - Buckling range

Any scenario with a buckling length (much) larger than this considered range is deemed unfit for energy extraction from compression. Table 21 gives an overview of the different scenarios and the buckling ranges that apply to them. From the values presented here it can be observed that the Leading edge bay scenario is unfit for loading in a compressive state because the buckling length is much shorter than the water depth, meaning severe countermeasures would be required to prevent

buckling. The trailing edge estuary scenario is just outside the buckling range, which means some added material might be needed in the rod to prevent buckling.

| | Barge | Breakwater | Depth |
|-------------------------------|--------------------------------------|---------------------------------------|--------|
| Sheltered manmade port | $5.34[m] \leq l_{buc} \leq 22.82[m]$ | $8.44[m] \leq l_{buc} \leq 28.25[m]$ | 10[m] |
| Trailing edge estuary | $7.90[m] \leq l_{buc} \leq 24.45[m]$ | $10.14[m] \leq l_{buc} \leq 24.45[m]$ | 30[m] |
| Leading edge bay | $7.29[m] \leq l_{buc} \leq 26.62[m]$ | $8.67[m] \leq l_{buc} \leq 26.62[m]$ | 100[m] |

Table 21 - Buckling ranges of scenarios

A second exclusion can be made for the sheltered manmade port scenario where the top soil layer consists of clay. The compressive behaviour of clay means it is impossible to construct a shallow foundation in this scenario as it would sink into the ground over time. Furthermore, due to the rock bottom the use of piles in the leading edge bay scenario is inapplicable as well.

Precast concrete piles are generally a go-to solution for foundations. They are common and therefore cheap, as well as easy to use. In the case of underwater application, however, the necessity of a concrete pile cap creates difficulties. Underwater concrete is a possibility but not generally applicable for use as construction material. This means it is virtually impossible to create a sufficient pile cap to handle the required tensile forces without creating a complex and expensive construction pit.

Table 22 summarizes the effects of the aforementioned findings into which foundation method is applicable in what situation.

| | Sheltered manmade port | Trailing edge estuary | Leading edge bay |
|------------------------|------------------------|-----------------------|------------------|
| Compression | | | |
| Steel pipe piles | ✓ | ✓ | ✗ |
| Precast concrete piles | ✓ | ✓ | ✗ |
| Anchors | ✗ | ✗ | ✗ |
| Shallow foundation | ✗ | ✓ | ✗ |
| Tension | | | |
| Steel pipe piles | ✓ | ✓ | ✗ |
| Precast concrete piles | ✗ | ✗ | ✗ |
| Anchors | ✓ | ✓ | ✓ |
| Shallow foundation | ✗ | ✗ | ✗ |

Table 22 - Summary of applicable foundation types

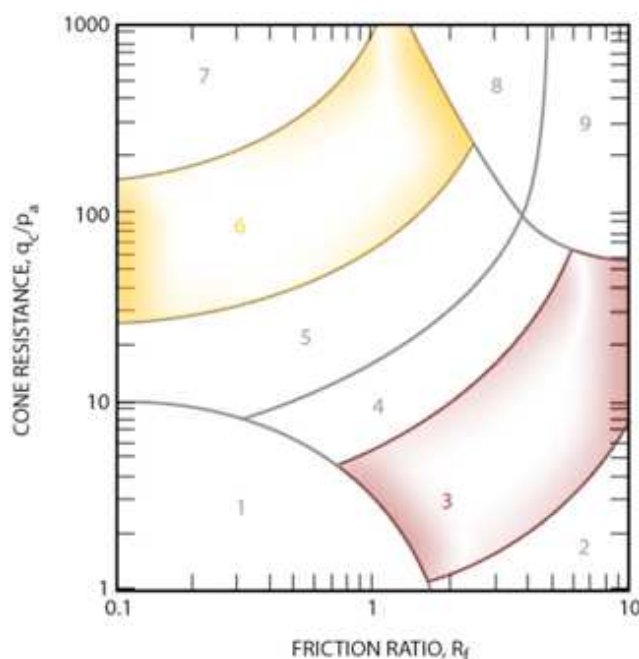
21.2 Soil characteristics

It has been previously determined that it is virtually impossible and undesirable to make designs for soil compositions of every different variety available in the world. For these reasons a set of generalized soil compositions has been derived in Section 3 which will be used now to dimension a proper foundation. The soil characteristics of these compositions are taken to be uniform everywhere along the soil layer, meaning the usual fluctuations in cone resistance and skin friction are neglected. Figure 63 gives an overview of the classification of different types of soils. Because only clay and sand are used in the determined soil profiles the range of areas of interest are numbers 3 and 6.

As can be seen in Figure 63 the range of possible soils even within a certain classification is quite large and cannot be accounted for entirely. For the main calculations an average value for the soil types will be assumed as given in Table 23.

| Soil type | Cone resistance (q_c) | Effective unit weight (γ') | Angle of internal friction (ϕ) |
|-----------|---------------------------|-------------------------------------|---------------------------------------|
| Clay | 2 MPa | 6 [kN m ⁻³] | - |
| Sand | 10 MPa | 10 [kN m ⁻³] | 35° |

Table 23 - Considered soil characteristics



| Zone | Soil Behaviour Type |
|------|---|
| 1 | Sensitive, fine grained |
| 2 | Organic soils - clay |
| 3 | Clay – silty clay to clay |
| 4 | Silt mixtures – clayey silt to silty clay |
| 5 | Sand mixtures – silty sand to sandy silt |
| 6 | Sands – clean sand to silty sand |
| 7 | Gravelly sand to dense sand |
| 8 | Very stiff sand to clayey sand |
| 9 | Very stiff fine grained |

P_a = atmospheric pressure = 100 kPa = 1 tsf

Figure 63 - Soil classification (Robertson, et al., 1986)

For the rock layers different characteristics apply where the important one is that of the working bond stress (τ_b) at the grout-rock interface. This bond stress depends on the type of rock that is considered where granite produces the lowest bond stress (0.55 to 1.0 MPa) and strong rock gives the highest (1.05 to 1.40 MPa) (Wyllie, 1992). For this research a medium to strong rock type is used with a bond stress of 1.05 MPa.

21.3 Steel pipe piles

Steel pipe piles are large tubular steel pipes which can be driven into the ground. The bearing capacity of these types of piles depends on the subsoil behaviour of the pile, and namely that of the soil plug on the inside of it. As illustrated in Figure 64 there are several types of steel pipe piles, of which the open ended type will be considered in this design.

In the compressive state depending on which is the smaller one either the end bearing capacity should be used or the skin friction on the inside of the pile. Added to this the outside skin friction always contributes as well. In the tensile state the inner skin friction is limited by the weight of the plug and the end bearing capacity plays no role. For small piles the contribution of the inside of the pile is negligible.

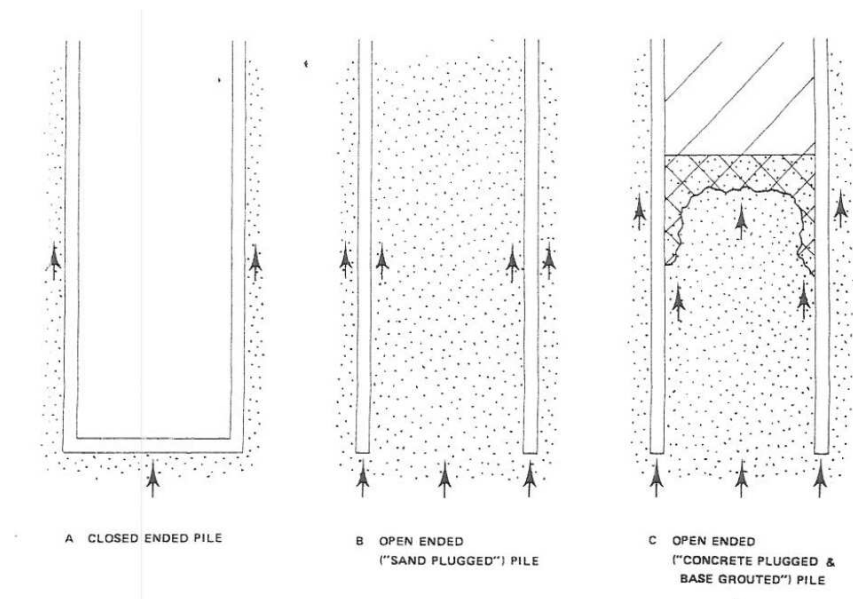
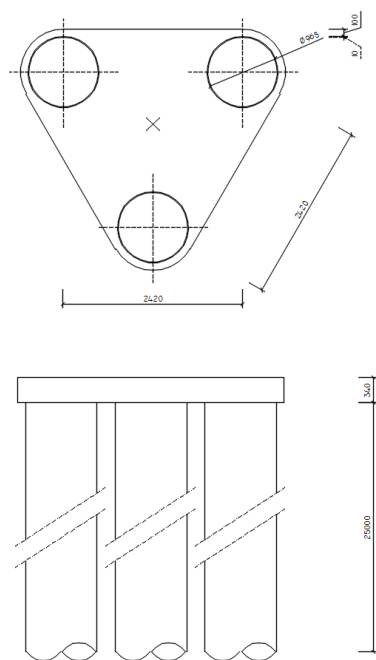


Figure 64 - Types of steel pipe piles

Steel pipe piles are available in a range of pile diameters as given in Appendix H. The distance between piles must be at least 2.5 times the pile diameter. The calculation of the bearing capacity of steel pipe piles is done according to the method of (CUR-2001-8, 2001) which is elaborated on in Appendix H. It is assumed that for plugging to occur a penetration depth of at least 8 times the pile diameter is required. To transfer the load from the piston to the foundation and vice versa a steel slab will be welded onto the piles. Corrosion of the piles and slabs due to the marine environment is taken into account in accordance with Appendix O. The following paragraphs will give the resulting pile and slab dimensions as well as the required numbers of piles for each applicable scenario.

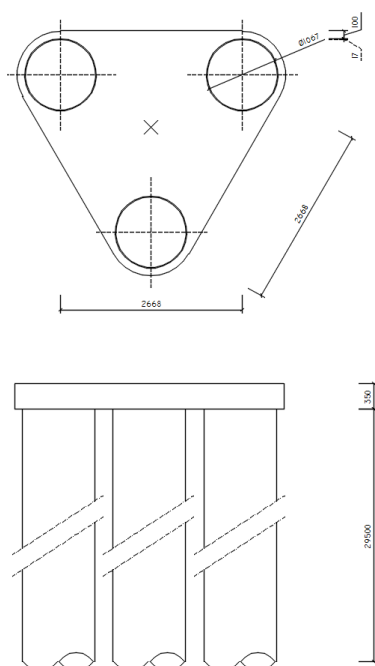
21.3.1 Steel pipe pile foundation in sheltered manmade port

The sheltered manmade port scenario has relatively low tides and therefore the foundation is also subject to relatively low forces. Furthermore it has a 15 metre clay layer before the bearing sand layer is achieved which adds significant skin friction to the pile bearing capacity. The required dimensions and bearing capacities for the different load situations are given in Table 24 through Table 27.



| Scenario | Barge - compression |
|---------------------------|--|
| Required capacity | 9,516.4 [kN] |
| Number of piles | 3 |
| Pile diameter | 0.965 [m] |
| Wall thickness | 0.010 [m] |
| Pile length | 35 [m] |
| Pile depth | 25 [m] |
| Centre-to-centre distance | 2.420 [m] |
| Slab thickness | 0.34 [m] |
| Slab surface area | $0.25 \times \sqrt{3} \times 3.59^2$ [m ²] |
| Capacity per pile | 3,225.1 [kN] |

Table 24 - Steel pipe pile foundation for barge in compression



| Scenario | Barge - tension |
|---------------------------|--|
| Required capacity | 9,694.8 [kN] |
| Number of piles | 3 |
| Pile diameter | 1.067 [m] |
| Wall thickness | 0.017 [m] |
| Pile length | 39.5 [m] |
| Pile depth | 29.5 [m] |
| Centre-to-centre distance | 2.668 [m] |
| Slab thickness | 0.35 [m] |
| Slab surface area | $0.25 \times \sqrt{3} \times 3.89^2$ [m ²] |
| Capacity per pile | 3,241.1 [kN] |

Table 25 - Steel pipe pile foundation for barge in tension

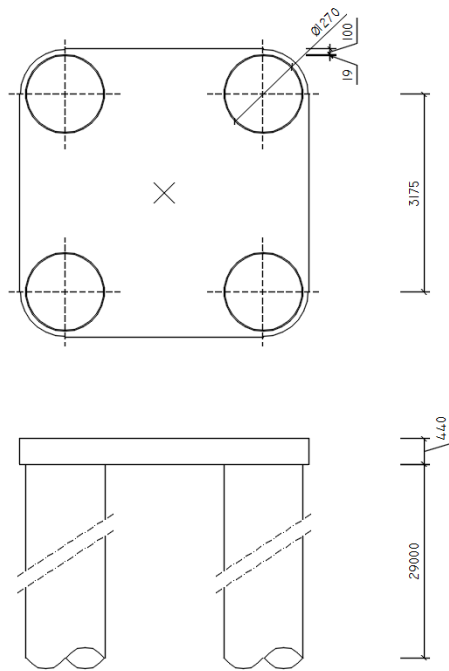


Table 26 - Steel pipe pile foundation for breakwater in compression

| Scenario | Breakwater - compression |
|---------------------------|-------------------------------|
| Required capacity | 23,754.2 [kN] |
| Number of piles | 4 |
| Pile diameter | 1.270 [m] |
| Wall thickness | 0.019 [m] |
| Pile length | 39 [m] |
| Pile depth | 29 [m] |
| Centre-to-centre distance | 3.175 [m] |
| Slab thickness | 0.44 [m] |
| Slab surface area | 4.65 x 4.65 [m ²] |
| Capacity per pile | 5,983.0 [kN] |

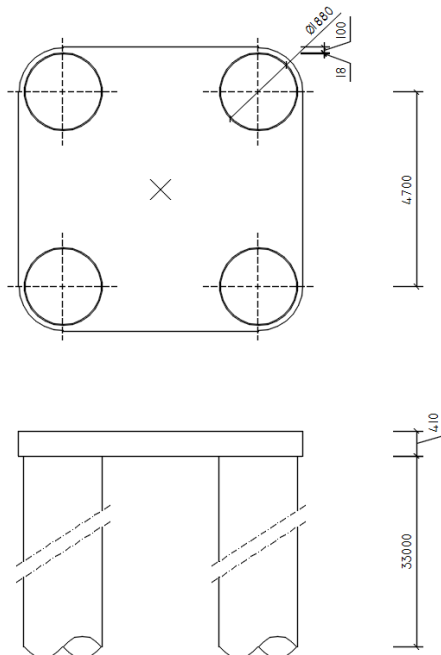


Table 27 - Steel pipe pile foundation for breakwater in tension

| Scenario | Breakwater - tension |
|---------------------------|-------------------------------|
| Required capacity | 24,801.3 [kN] |
| Number of piles | 4 |
| Pile diameter | 1.880 [m] |
| Wall thickness | 0.018 [m] |
| Pile length | 43 [m] |
| Pile depth | 33 [m] |
| Centre-to-centre distance | 4.700 [m] |
| Slab thickness | 0.41 [m] |
| Slab surface area | 6.78 x 6.78 [m ²] |
| Capacity per pile | 6,207.1 [kN] |

21.3.2 Steel pipe pile foundation trailing edge estuary

The trailing edge estuary scenario had a relatively deep water depth which means that the use of piles is somewhat more challenging. An additional pile length of 30 meters is required to make driving the piles possible which means that in some cases multiple segments welded together are required. The lack of a clay layer furthermore means that skin friction will be less and therefore tensile loading is less favourable. Table 28 through Table 31 give the required dimensions for each case.

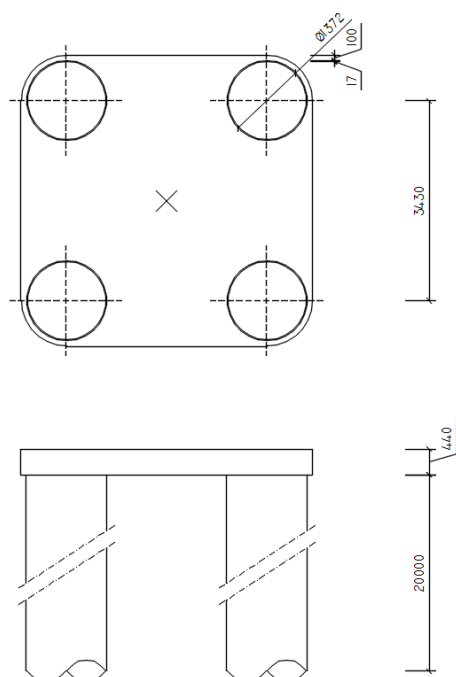


Table 28 - Steel pipe pile foundation for barge in compression

| Scenario | Barge - compression |
|---------------------------|-------------------------------|
| Required capacity | 20,787.5 [kN] |
| Number of piles | 4 |
| Pile diameter | 1.372 [m] |
| Wall thickness | 0.017 [m] |
| Pile length | 50 [m] |
| Pile depth | 20 [m] |
| Centre-to-centre distance | 3.430 [m] |
| Slab thickness | 0.41 [m] |
| Slab surface area | 5.00 x 5.00 [m ²] |
| Capacity per pile | 5,223.3 [kN] |

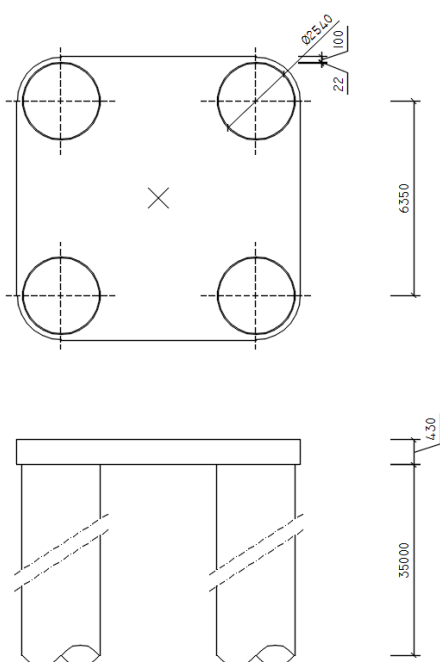
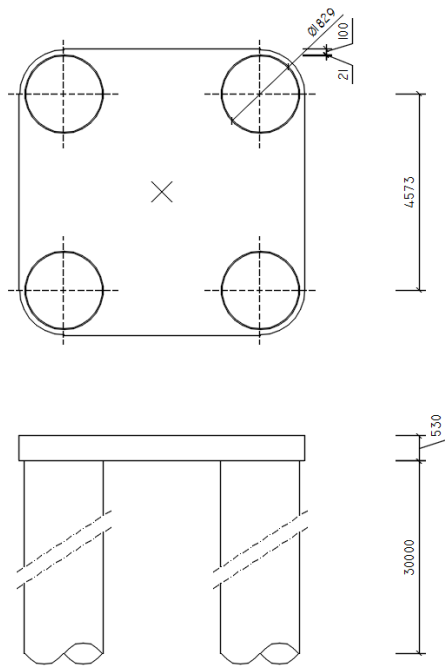


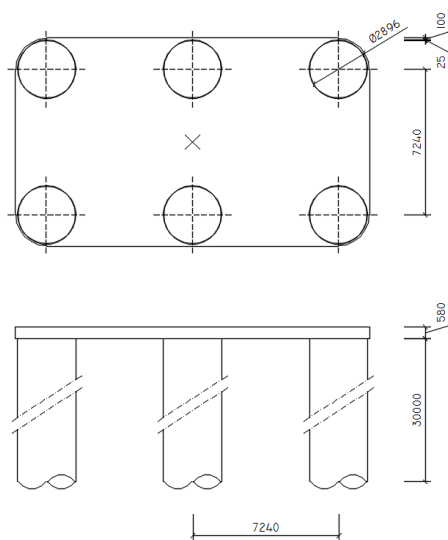
Table 29 - Steel pipe pile foundation for barge in tension

| Scenario | Barge - tension |
|---------------------------|-------------------------------|
| Required capacity | 22,965.1 [kN] |
| Number of piles | 4 |
| Pile diameter | 2.540 [m] |
| Wall thickness | 0.022 [m] |
| Pile length | 65 [m] (2 segments) |
| Pile depth | 35 [m] |
| Centre-to-centre distance | 6.350 [m] |
| Slab thickness | 0.43 [m] |
| Slab surface area | 9.09 x 9.09 [m ²] |
| Capacity per pile | 5,521.9 [kN] |



| Scenario | Breakwater - compression |
|---------------------------|-------------------------------|
| Required capacity | 34,286.4 [kN] |
| Number of piles | 4 |
| Pile diameter | 1.829 [m] |
| Wall thickness | 0.021 [m] |
| Pile length | 52 [m] |
| Pile depth | 22 [m] |
| Centre-to-centre distance | 4.573 [m] |
| Slab thickness | 0.53 [m] |
| Slab surface area | 6.60 x 6.60 [m ²] |
| Capacity per pile | 8,586.6 [m] |

Table 30 - Steel pipe pile foundation for breakwater in compression



| Scenario | Breakwater - tension |
|---------------------------|---------------------------------|
| Required capacity | 38,944.6 [kN] |
| Number of piles | 6 |
| Pile diameter | 2.896 [m] |
| Wall thickness | 0.025 [m] |
| Pile length | 60 [m] (2 segments) |
| Pile depth | 30 [m] |
| Centre-to-centre distance | 7.240 [m] |
| Slab thickness | 0.58 [m] |
| Slab surface area | 17.58 x 10.33 [m ²] |
| Capacity per pile | 6,499.5 [kN] |

Table 31 - Steel pipe pile foundation for breakwater in tension

21.4 Precast concrete piles

Precast concrete piles are among the most used and therefore most cost efficient means of foundation. They are well capable of handling compressive forces and have a limited capability of bearing tensile forces as well. Because, however, the connection between the piles and the structure is difficult to make for tensile forces and near impossible to do so underwater, only the compressive capabilities of the precast concrete piles will be taken into consideration.

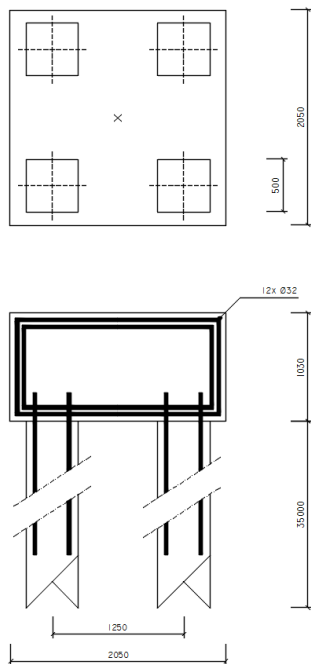
The calculation method used for this type of pile is the empirical Koppejan method as described in Appendix I. For the foundation block a reinforced concrete block is used of which the calculation is also given in the same appendix. The resulting dimensions of the various components in the different considered scenarios are elaborated on in the following paragraphs.

21.4.1 Precast concrete pile foundation in sheltered manmade port

Precast concrete piles get the same benefits from the sheltered manmade port scenario as steel pipe piles in that there is a clay layer providing added skin friction to the bearing capacity. The forces per pile again are relatively low. The required dimensions of the different scenarios are given in Table 32 and Table 33.

| Scenario | | Barge |
|---------------------------|--------------------------------------|-------|
| Required capacity | 9,516.4 [kN] | |
| Number of piles | 2 | |
| Pile diameter | 0.500 [m] | |
| Pile length | 38 [m] | |
| Pile depth | 28 [m] | |
| Centre-to-centre distance | 1.250 [m] | |
| Foundation block | 2.05 x 0.75 x 1.03 [m ³] | |
| Reinforcement area | 13,642.7 [mm ²] (1.6 %) | |
| Rebars (FeB500) | 17 x Ø32 | |
| Capacity per pile | 4,800.0 [kN] | |

Table 32 - Precast concrete pile in barge scenario

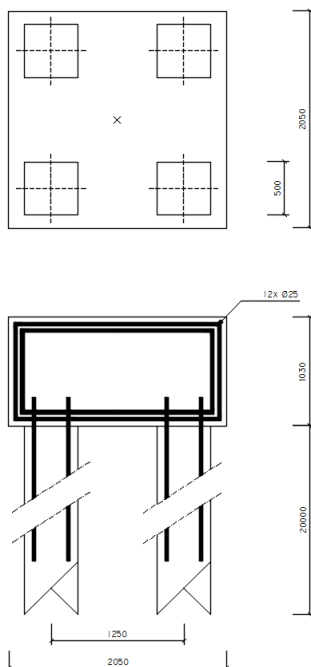


| Scenario | Breakwater |
|---------------------------|-------------------------|
| Required capacity | 23,754.2 [kN] |
| Number of piles | 4 |
| Pile diameter | 0.500 [m] |
| Pile length | 45 [m] |
| Pile depth | 35 [m] |
| Centre-to-centre distance | 1.250 [m] |
| Foundation block | 2.05 x 2.05 x 1.03 [m³] |
| Reinforcement area | 9,438.5 [mm²] (0.4 %) |
| Rebars (FeB500) | 12 x Ø32 |
| Capacity per pile | 5,920.0 kN |

Table 33 - Precast concrete pile in breakwater scenario

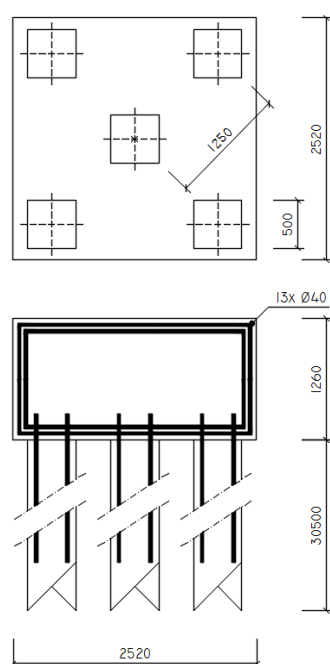
21.4.2 Precast concrete pile foundation in trailing edge estuary

The trailing edge estuary scenario is deeper and has a larger tide, resulting in longer piles and higher loads. Piles are available in sufficiently long lengths so no added difficulties arise there. The resulting dimension requirements are given in Table 34 and Table 35.



| Scenario | Barge |
|---------------------------|-------------------------|
| Required capacity | 20,787.5 [kN] |
| Number of piles | 4 |
| Pile diameter | 0.500 [m] |
| Pile length | 30 [m] |
| Pile depth | 20 [m] |
| Centre-to-centre distance | 1.250 [m] |
| Foundation block | 2.05 x 2.05 x 1.03 [m³] |
| Reinforcement area | 8,259.7 [mm²] (0.3 %) |
| Rebars (FeB500) | 17 x Ø25 |
| Capacity per pile | 5,200.0 [kN] |

Table 34 - Precast concrete pile in barge scenario



| Scenario | Breakwater |
|---------------------------|--------------------------------------|
| Required capacity | 34,286.4 [kN] |
| Number of piles | 5 |
| Pile diameter | 0.500 [m] |
| Pile length | 40.5 [m] |
| Pile depth | 30.5 [m] |
| Centre-to-centre distance | 1.250 [m] |
| Foundation block | 2.52 x 2.52 x 1.26 [m ³] |
| Reinforcement area | 19,548.4 [mm ²] (0.6 %) |
| Rebars (FeB500) | 13 x Ø40 |
| Capacity per pile | 6,880.0 [kN] |

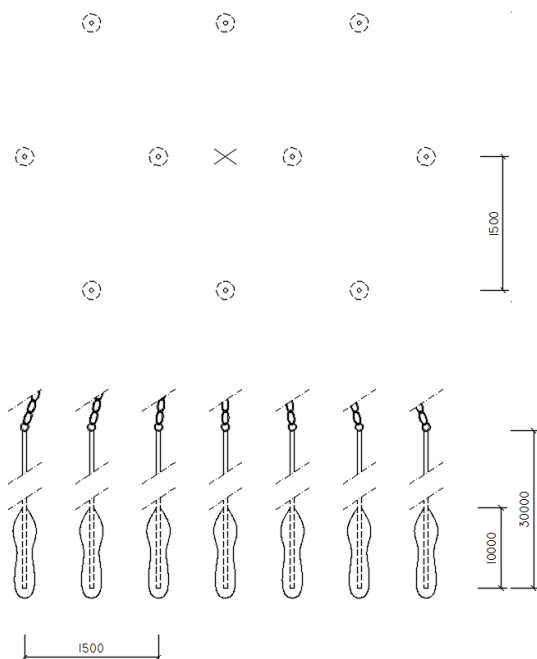
Table 35 - Precast concrete pile in breakwater scenario

21.5 Foundation anchors

To transfer pure tensile forces to the subsoil often the use of anchors is the most efficient manner. The type of anchors that ought to be used differs depending on the type of soil the force needs to be transferred to. For sand layers grout or “GEWI” anchors are the preferred method, whereas rock layers naturally require rock anchors. Both methods in essence consist of a steel rod enclosed in a body of grout connecting to the surrounding soil. In these methods the interaction between soil and grout, grout and steel and the bearing capacity of the rod itself are of relevance. The required calculation method of these types of foundations is given in Appendix J. The anchors are connected to the rest of the structure by strains or chains connected to the top of the foundation anchors and combining at some arbitrary distance from the bottom to lead further up to the piston. The tensile yield stress of the steel is the determining factor for the dimensioning of these. This connection system is considered part of the piston and rod system as elaborated on in Chapter 0. Corrosion of the chains in the marine environment is taken into account in accordance with the numbers discussed in Appendix O.

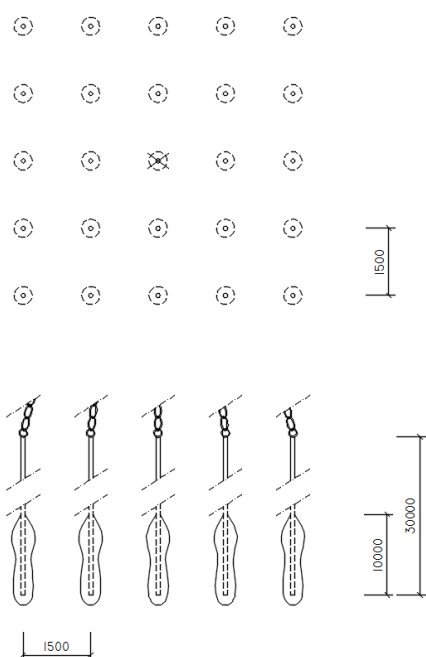
21.5.1 Foundation anchors in sheltered manmade port

The sheltered manmade port has a clay layer of 15 metres before the bearing sand layer begins. The use of GEWI anchors is preferred which means that a load transferring rod will need to be installed connecting the bearing grout body to the device, because the grout body can only build bearing capacity in sand layers. The required anchor dimensions for the different host structures are given in Table 36 and Table 37.



| Scenario | Barge |
|---------------------------|--------------|
| Required capacity | 9,694.8 [kN] |
| Type of anchor | GEWI |
| Number of anchors | 10 |
| Anchor diameter | 0.047 [m] |
| Anchor length | 40 [m] |
| Grout body length | 10 [m] |
| Anchor depth | 30 [m] |
| Centre-to-centre distance | 1.5 [m] |
| Capacity per anchor | 1,000.0 [kN] |

Table 36 - GEWI anchor configuration for barge

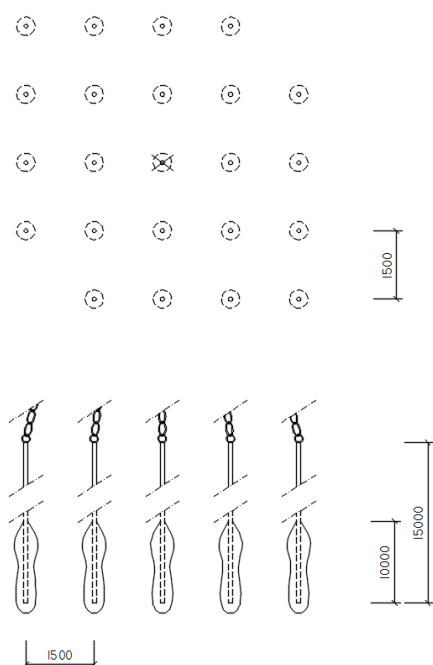


| Scenario | Breakwater |
|---------------------------|---------------|
| Required capacity | 24,801.3 [kN] |
| Type of anchor | GEWI |
| Number of anchors | 25 |
| Anchor diameter | 0.047 [m] |
| Anchor length | 40 [m] |
| Grout body length | 10 [m] |
| Anchor depth | 30 [m] |
| Centre-to-centre distance | 1.5 [m] |
| Capacity per anchor | 1,000.0 [kN] |

Table 37 - GEWI anchor configuration for breakwater

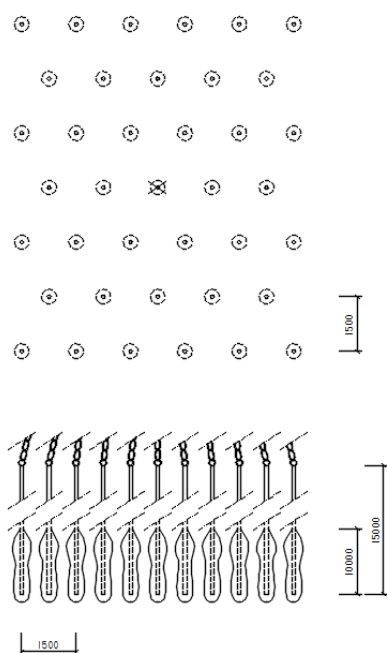
21.5.2 Foundation anchors in trailing edge estuary

The bearing soil layer in the trailing edge estuary scenario is right at the surface of the bottom profile meaning the distance to the grout body is limited. The required dimensions of the anchors are given in Table 38 and Table 39.



| Scenario | Barge |
|---------------------------|---------------|
| Required capacity | 22,965.1 [kN] |
| Type of anchor | GEWI |
| Number of anchors | 23 |
| Anchor diameter | 0.047 [m] |
| Anchor length | 45 [m] |
| Grout body length | 10 [m] |
| Anchor depth | 15 [m] |
| Centre-to-centre distance | 1.5 [m] |
| Capacity per anchor | 1,000.0 [kN] |

Table 38 - GEWI anchor configuration for barge

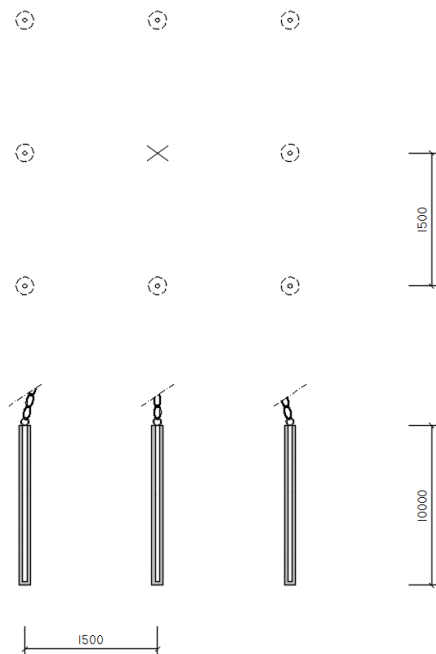


| Scenario | Breakwater |
|---------------------------|---------------|
| Required capacity | 38,944.6 [kN] |
| Type of anchor | GEWI |
| Number of anchors | 39 |
| Anchor diameter | 0.047 [m] |
| Anchor length | 45 [m] |
| Grout body length | 10 [m] |
| Anchor depth | 15 [m] |
| Centre-to-centre distance | 1.5 [m] |
| Capacity per anchor | 1,000.0 [kN] |

Table 39 - GEWI anchor configuration for breakwater

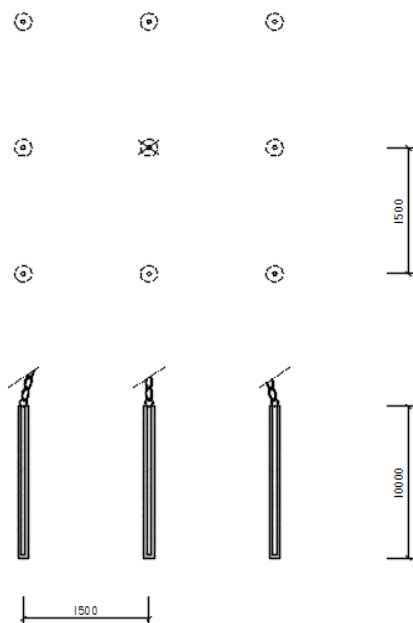
21.5.3 Foundation anchors in leading edge bay

The leading edge bay scenario has a rock layer as the bearing layer which means the use of rock anchors is the preferred foundation method. These anchors have a significantly higher bearing capacity and therefore fewer are needed to handle the applied forces. Table 40 and Table 41 give the determined dimensions required for the different host structures.



| Scenario | Barge |
|---------------------------|-------------------|
| Required capacity | 16,871.6 [kN] |
| Type of anchor | Rock anchor |
| Number of anchors | 8 |
| Anchor diameter | 0.066 / 0.130 [m] |
| Bond length | 7.5 [m] |
| Grout body length | 7.5 [m] |
| Anchor depth | 7.5 [m] |
| Centre-to-centre distance | 1.5 [m] |
| Capacity per anchor | 2,143.1 [kN] |

Table 40 - Rock anchor configuration for barge



| Scenario | Breakwater |
|---------------------------|-------------------|
| Required capacity | 19,611.9 [kN] |
| Type of anchor | Rock anchor |
| Number of anchors | 9 |
| Anchor diameter | 0.068 / 0.130 [m] |
| Bond length | 7.5 [m] |
| Grout body length | 7.5 [m] |
| Anchor depth | 7.5 [m] |
| Centre-to-centre distance | 1.5 [m] |
| Capacity per anchor | 2,285.9 [kN] |

Table 41 - Rock anchor configuration for breakwater

21.6 Shallow foundation

Shallow foundations consist of large blocks that distribute the applied foundation force over the soil in such a way that the maximum soil pressure is not exceeded. In this case a large reinforced concrete block is used for this purpose and due to reasons mentioned before it can only be applied to the trailing edge estuary scenario where a sand layer is present at average depth. The calculation is done according to the Brinch Hansen method and is described in Appendix K. The required dimensions are given in Table 42 and Table 43.

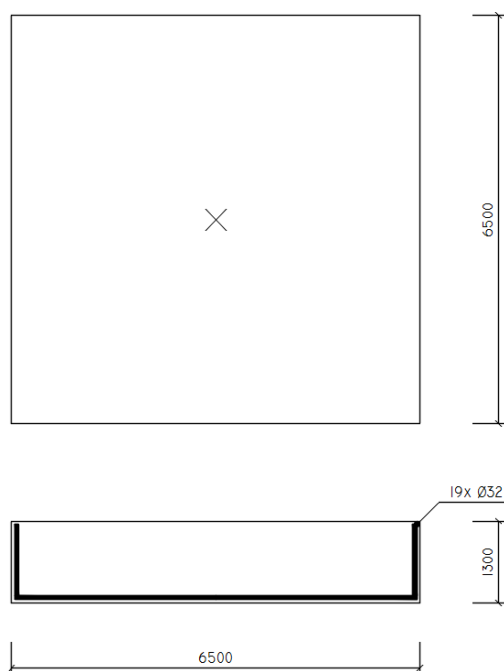


Table 42 - Shallow foundation for barge

| Scenario | Barge |
|-------------------------|--------------------------------------|
| Required capacity | 20,787.5 [kN] |
| Block width | 6.50 [m] |
| Block length | 6.50 [m] |
| Block height | 1.30 [m] |
| Soil stress | 492.0 [kN m ⁻¹] |
| Req. reinforcement area | 5,405.7 [mm ²] (0.6 %) |
| Min. reinforcement area | 15,210.0 [mm ²] (0.18 %) |
| Rebars (FeB500) | 19 x Ø32 |

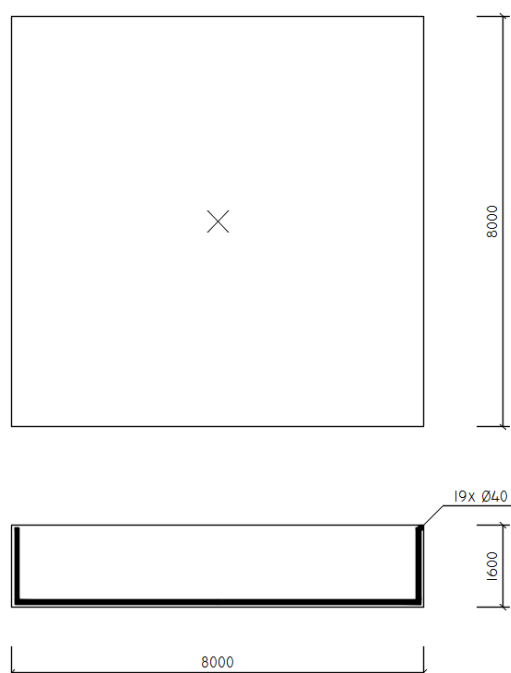


Table 43 - Shallow foundation for breakwater

| Scenario | Breakwater |
|-------------------------|--------------------------------------|
| Required capacity | 34,286.4 [kN] |
| Block width | 8.00 [m] |
| Block length | 8.00 [m] |
| Block height | 1.60 [m] |
| Soil stress | 535.7 [kN m ⁻¹] |
| Req. reinforcement area | 7,244.1 [mm ²] (0.06 %) |
| Min. reinforcement area | 23,040.0 [mm ²] (0.18 %) |
| Rebars (FeB500) | 19 x Ø40 |

21.7 Foundation economics

The choice of the to be used foundation is based on the costs of applying said foundation. The previously determined foundation dimensions can be used to estimate their respective costs per support and based on that the choice of which foundation should be used in what scenario can be derived. All price estimates are courtesy of (Pascha, 2015). Elaboration on how prices are accumulated can be found in Appendix L.

21.7.1 Foundation costs in sheltered manmade port

The costs of the different foundation designs in the sheltered manmade port are given in Table 44. The price of construction steel is significant which is where the large difference in price between the concrete foundation and the steel foundation comes from. Furthermore anchors are much cheaper than steel pipe piles but also quite a bit more expensive than precast concrete piles. The preferred foundation here are precast concrete piles for the compressive load case and if sufficient economic revenue is attained GEWI anchors can be used for tensile loading.

| Type | Barge | Breakwater |
|---|--------------|--------------|
| Steel pipe piles (compression) | € 68.310,79 | € 301.883,26 |
| Steel pipe piles (tension) | € 110.740,38 | € 548.441,50 |
| Precast concrete piles (compression) | € 8.747,11 | € 15.135,45 |
| GEWI anchors (tension) | € 33.000,00 | € 82.500,00 |

Table 44 - Sheltered manmade port foundation costs

21.7.2 Foundation costs in trailing edge estuary

The costs of the different foundation designs in the sheltered manmade port are given in Table 45. The difference between steel foundations and concrete foundations increases significantly with the increase of the required load bearing capacity. The lack of the clay layer is evident as well as the diminished skin friction contribution results in much larger piles. Again the preferred foundation here are precast concrete piles for the compressive load case and if sufficient economic revenue is attained GEWI anchors can be used for tensile loading.

| Type | Barge | Breakwater |
|---|----------------|----------------|
| Steel pipe piles (compression) | € 344.066,57 | € 697.942,75 |
| Steel pipe piles (tension) | € 1.143.215,80 | € 2.867.081,66 |
| Precast concrete piles (compression) | € 21.635,45 | € 26.045,97 |
| GEWI anchors (tension) | € 37.950,00 | € 64.350,00 |
| Shallow foundation (compression) | € 48.019,89 | € 89.526,39 |

Table 45 - Trailing edge estuary foundation costs

21.7.3 Foundation costs in leading edge bay

The costs of the different foundation designs in the sheltered manmade port are given in Table 46. It is evident that because no other types of foundation can be applied the rock anchors are the foundation of choice.

| Type | Barge | Breakwater |
|-------------------------------|-------------|-------------|
| Rock anchors (tension) | € 20.000,00 | € 22.500,00 |

Table 46 - Leading edge bay foundation costs

21.8 Influence of soil characteristics on foundation

The calculations in the previous paragraphs were done assuming a uniform soil composition of a certain quality. This was primarily done because no actual information on the considered locations is available, but it also helps in making the calculations slightly easier. In reality, however, soil characteristics are rarely uniform and this has a certain influence on the bearing capacities of the different calculated foundations. The following paragraphs will shortly address the influences different soil compositions have on the foundation for each of the used soil materials.

21.8.1 Sand

As can be seen in Figure 63 there is a large variety in possible cone resistances in sand ranging from 2.7 up to well over 20 megapascals. Practically 20 megapascals is a realistic cut-off, however, as first of all higher values are uncommon and secondly the used formulae have not been gauged for such high values. This means that bearing capacities of piles and foundations in sand can range from 27% to 200% for precast concrete piles, GEWI anchors and shallow foundations as the cone resistance is proportional to the bearing capacity for those piles. For steel pipe piles the cone resistance is included as a square root, so here bearing capacities range from 52% to 141% of the used value. Figure 65 gives a graph of the bearing capacity per unit area relative to the used value for different sand types.

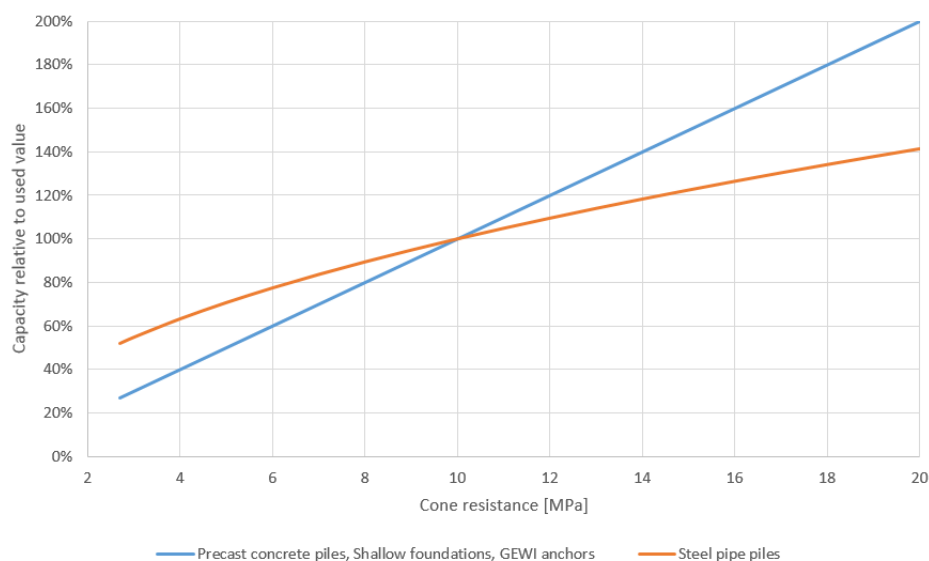


Figure 65 - Relative bearing capacity for different cone resistances

21.8.2 Clay

Clay, contrary to sand, has no real use in end bearing capacity and mostly plays a role in skin friction. For this reason it is of influence to steel pipe piles and precast concrete piles. For both types of foundations the influence is proportional with the cone resistance. With the possible cone resistance of clay ranging from 0.1 to 8 megapascals according to Figure 63 this means the bearing capacity range for clay is between 5% and 400%. This is quite a significant range, but seeing as it applies per unit area it only plays a role if the thickness of the clay layer is significant.

21.8.3 Rock

Rock too exists with different capacities ranging from 0.55 (52%) to 1.40 (133%) megapascals (Wyllie, 1992). The determining factor for the rock's strength that has not been considered in this research is the formation of cracks however. If cracks are present the bearing capacity of the rock reduces to the weight of the block that the anchor is placed in, as there is no possibility for load transfer between one side of the crack and the other. This is why the crack formation inside the rock needs to be mapped accurately before designing and installing the anchors and perhaps countermeasures need to be taken to either drill the holes deeper into another rock formation, reinforce the connection or use another foundation method.

22 Adjustments to the host structure

22.1 Barge

Barges are generally speaking existing structures with no initial necessity for handling the types of forces exerted in them by a Tidal Wave Energy Converter. They are dimensioned for a uniformly distributed load from the bottom upward (the buoyancy force exerted by the water) and a (slightly less) uniformly distributed load from the top downward exerted by the cargo. The point loads the TWEC exerts are outside the barge's capabilities and therefore require adjustments.

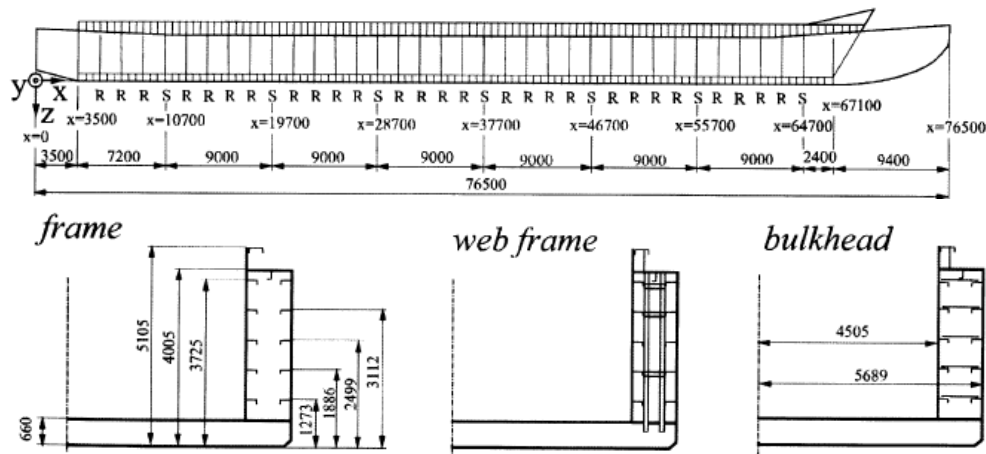


Figure 66 - Push barge cross-section

Figure 66 shows the cross-section of a Europa II class push barge, where the markers S indicate a bulkhead and the markers R indicate a web frame. Because the actual use of these detailed components overcomplicates the calculation it is assumed that the entire barge consists of a cross-section using a rectangular steel box with the freeboard required by the system (so where needed the barge wall is heightened) and a bottom thickness as described in Figure 66. It is assumed that lateral torsional buckling of the walls is sufficiently countered by the presence of the bulkheads. The required height of the barge is equal to the water level at the design failure position added with 1 metre of freeboard for wind and wave action. Above this value the sacrificial structure element will have failed meaning the water level cannot rise further relative to the pontoon. The check is made to see whether the moment of inertia of the adjusted barge is sufficient to handle the created bending moments and shear stresses. Where needed additional walls identical to those in the original design are placed in the interior of the barge.

| | Sheltered port | Trailing estuary | Leading bay |
|-----------------------------------|--|---|---|
| Required height | 3.22 [m] | 11.53 [m] | 9.13 [m] |
| Barge height | 4.005 [m] | 4.005 [m] | 4.005 [m] |
| Added height | - | 7.525 [m] | 5.125 [m] |
| Moment of inertia | 4.6×10^{11} [mm ⁴] | 7.1×10^{12} [mm ⁴] | 3.9×10^{12} [mm ⁴] |
| Maximum bending moment | 100,481.4 [kNm] | 164,594.5 [kNm] | 127,103.6 [kNm] |
| Maximum shear force | 7,265.5 [kN] | 21,515.6 [kN] | 16,614.8 [kN] |
| Required moment of inertia | 1.18×10^{12} [mm ⁴] | 5.1×10^{12} [mm ⁴] | 3.2×10^{12} [mm ⁴] |
| Additional walls required | 5 | - | - |
| Punch reinforcement slab | 16 x 2,022 [mm] | 37 x 4,788 [mm] | 29 x 3,696 [mm] |

Table 47 - Barge adjustments

It can be observed from Table 47 that the retaining walls for the trailing edge estuary and the leading edge bay need to be heightened to handle the water height. These adjusted barges are sufficiently capable of handling the resulting bending moments. The barge in the sheltered manmade port is sufficiently capable of handling the water level fluctuations but cannot process the bending moment. It is interesting to note that this is mainly due to the unfavourable three support configuration, if four supports were used it would be sufficiently stiff on its own.

The punch is calculated in terms of the slab thickness needed to withstand the punch force of the support. Additionally the required diameter of this circular slab is determined required to reduce the load such that it does not punch through the wall of the barge.

22.2 Breakwater

Although floating breakwaters have been applied at various locations in the world to date the consideration here is that any floating breakwater the Tidal Wave Energy Converter is to be applied to will be constructed anew. This means alterations to the reinforcement percentage and wall heights are available as means of adjustment whereas with existing structures adjusting these would be difficult to impossible. Figure 67 gives the considered layout of the breakwater where the surface area dimensions are as given in 20.1.2, the height is considered freely adjustable depending on freeboard requirements.

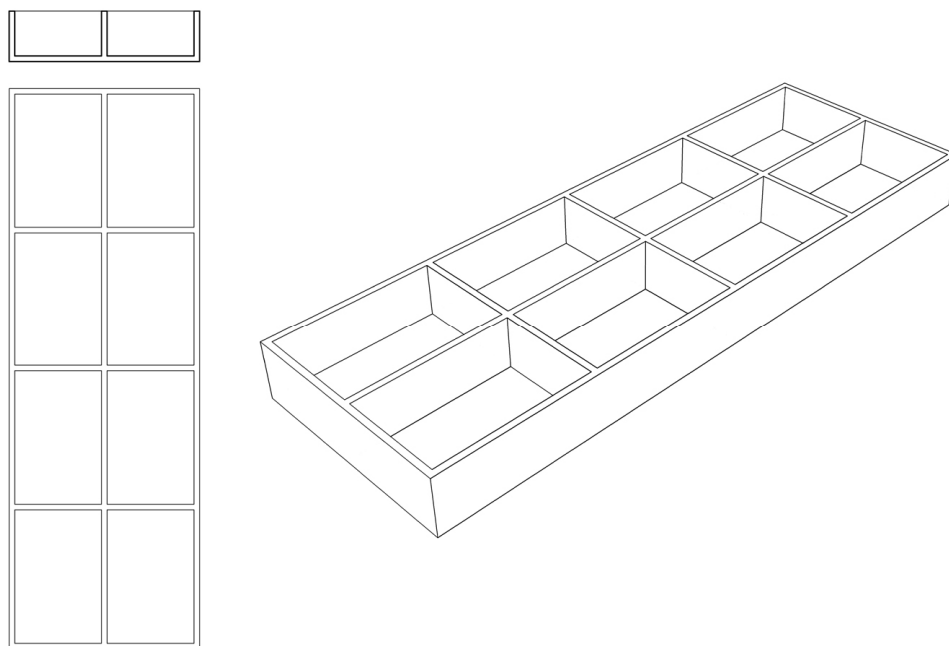


Figure 67 - Floating breakwater

The calculation method for the breakwater's required dimensioned are as given in Appendix M. The governing requirement here is that of the reinforcement percentage which should be between 0.18% and 1.94 % for B35 concrete. The results of the calculation are given In Table 48.

| | Sheltered manmade | Trailing estuary | Leading bay |
|------------------------------------|---------------------------------|---------------------------------|---------------------------------|
| Required caisson height | 3.22 [m] | 11.53 [m] | 9.13 [m] |
| Maximum bending moment | 385,382.5 [kNm] | 202,900.9 [kNm] | 99,918.0 [kNm] |
| Maximum shear force | 18,600.0 [kN] | 46,865.9 [kN] | 23,079.0 [kN] |
| Reinforcement area (FeB500) | 1.042 [m ²] (1.94%) | 0.048 [m ²] (0.41%) | 0.030 [m ²] (0.32%) |
| Resisted bending moment | 74,374.1 [kNm] | 202,900.9 [kNm] | 99,918.0 [kNm] |
| Required additional profile | Too large | - | - |
| Bottom height | - | 1.33 [m] | 0.97 [m] |

Table 48 - Breakwater adjustments

It can be seen that for the sheltered manmade port the required adjustments to sufficiently handle the bending moment induced stresses are too severe to be plausible. Therefore the use of the considered breakwater in this scenario is determined unrealistic and will not be considered further. Smaller floating breakwaters, however, could still be feasible as the created bending moments are less severe. Furthermore a solution with more supports could be an outcome.

23 Piston and rod dimensions

The required diameter of the pistons has been previously determined in 20.2 as the bearing surface area is the same as the inner surface area of the pistons. After all the support will be provided by the hydraulic fluid in the piston. So the inner diameter of the piston and the load on the entire system are known, which leaves to be determined the outer diameter of the piston and the dimensions of whatever connects it to the foundation.

23.1 Piston

The piston itself has no vertical bearing function, so the dimensions of the wall are solely based on its capacity to handle the pressure inside of the piston. The length of the piston is governed by the tidal range, as a piston length shorter than the water level difference would mean that the motion of the pontoon is limited, which is undesirable. Because the tidal range itself is considered to be sufficiently accurate in prediction the only margin that needs to be considered is that of the storm surge. Because actual data about this is unknown this margin is considered to be the minimum value of 1.5 times the tidal range (in accordance with the failure criterion) and the arbitrary limiting value of the tidal range plus 2 metres.

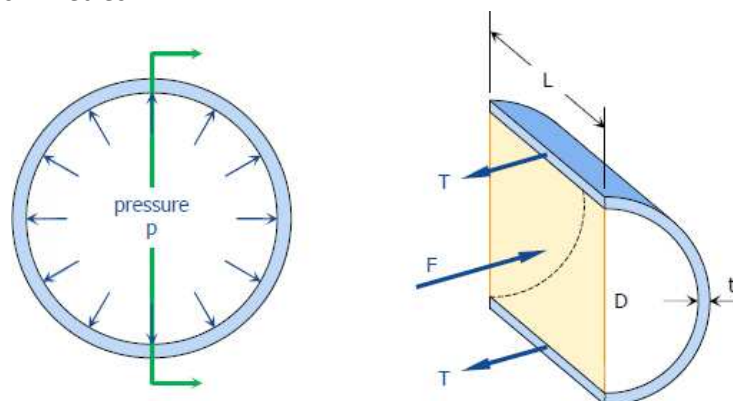


Figure 68 - Force distribution on piston wall

The thickness of the piston wall is determined based on the forces the pressure inside the piston exerts on the walls as illustrates in Figure 68. Along with the aforementioned piston length requirements and the loads as determined in 0 the required dimensions of the pistons can be calculated with the method as given in Appendix N. The results of this for the different scenarios are given in Table 49 through Table 52.

| | Sheltered manmade port | Trailing edge estuary | Leading edge bay |
|----------------------------------|------------------------|------------------------|------------------------|
| Length | 5.55 [m] | 16.72 [m] | 13.93 [m] |
| Load | 9,516.4 [kN] | 20,787.5 [kN] | 17,725.3 [kN] |
| Inner diameter | 0.84 [m] | 0.90 [m] | 0.98 [m] |
| Inner surface area | 0.55 [m ²] | 0.64 [m ²] | 0.75 [m ²] |
| Max. pressure | 17,302 [kPa] | 32,480 [kPa] | 23,634 [kPa] |
| Force on the wall | 7,266.8 [kN] | 14,616.0 [kN] | 11,580.7 [kN] |
| Required thickness (S235) | 0.031 [m] | 0.062 [m] | 0.049 [m] |
| Outer diameter | 0.91 [m] | 1.03 [m] | 1.08 [m] |

Table 49 - Piston dimensions barge (compression)

| | Sheltered manmade port | Trailing edge estuary | Leading edge bay |
|----------------------------------|------------------------|------------------------|------------------------|
| Length | 5.55 [m] | 16.72 [m] | 13.93 [m] |
| Load | 23,754.2 [kN] | 34,286.4 [kN] | 25,082.3 [kN] |
| Inner diameter | 1.04 [m] | 0.90 [m] | 0.98 [m] |
| Inner surface area | 0.85 [m ²] | 0.64 [m ²] | 0.75 [m ²] |
| Max. pressure | 27,946 [kPa] | 53,572 [kPa] | 33,443 [kPa] |
| Force on the wall | 14,531.9 [kN] | 24,107.4 [kN] | 16,387.1 [kN] |
| Required thickness (S235) | 0.062 [m] | 0.103 [m] | 0.070 [m] |
| Outer diameter | 1.16 [m] | 1.10 [m] | 1.12 [m] |

Table 50 - Piston dimensions breakwater (compression)

| | Sheltered manmade port | Trailing edge estuary | Leading edge bay |
|----------------------------------|------------------------|------------------------|------------------------|
| Length | 5.55 [m] | 16.72 [m] | 13.93 [m] |
| Load | 9,694.8 [kN] | 22,965.1 [kN] | 16,871.6 [kN] |
| Inner diameter | 0.84 [m] | 0.91 [m] | 0.98 [m] |
| Inner surface area | 0.55 [m ²] | 0.64 [m ²] | 0.75 [m ²] |
| Max. pressure | 17,627 [kPa] | 35,883 [kPa] | 22,495 [kPa] |
| Force on the wall | 10,492.3 [kN] | 19,935.0 [kN] | 11,022.6 [kN] |
| Required thickness (S235) | 0.045 [m] | 0.084 [m] | 0.047 [m] |
| Outer diameter | 0.93 [m] | 1.08 [m] | 1.08 [m] |

Table 51 - Piston dimensions barge (tension)

| | Sheltered manmade port | Trailing edge estuary | Leading edge bay |
|----------------------------------|------------------------|------------------------|------------------------|
| Length | 5.55 [m] | 16.72 [m] | 13.93 [m] |
| Load | 24,801.3 [kN] | 38,944.6 [kN] | 19,611.9 [kN] |
| Inner diameter | 1.04 [m] | 0.90 [m] | 0.98 [m] |
| Inner surface area | 0.85 [m ²] | 0.64 [m ²] | 0.75 [m ²] |
| Max. pressure | 29,178 [kPa] | 60,851 [kPa] | 26,149 [kPa] |
| Force on the wall | 15,172.6 [kN] | 27,383.0 [kN] | 12,813.0 [kN] |
| Required thickness (S235) | 0.065 [m] | 0.117 [m] | 0.055 [m] |
| Outer diameter | 1.17 [m] | 1.14 [m] | 1.09 [m] |

Table 52 - Piston dimensions breakwater(tension)

23.2 Rod

The dimensions of the rod in compression follow from the buckling calculation as described in Appendix H where the allowed buckling length, the length of each component and the moment of inertia of the piston is known. The moment of inertia of the rod can then be calculated and along with the stress requirements so can the diameters. The rod has to be sufficiently long that it can cover the entire tidal range, meaning it is at a minimum of equal length to the piston length and at maximum equal to the water depth minus half the piston length. The relevant dimensions that need to be determined in the compressive state are illustrated in Figure 69 with the calculated variables for the different scenarios in Table 53 and Table 54.

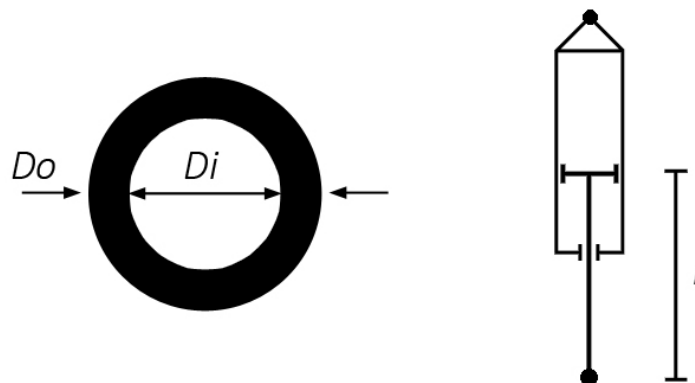


Figure 69 - Relevant rod dimensions

| | Sheltered manmade port | Trailing edge estuary | Leading edge bay |
|----------------------------|-------------------------|-------------------------|------------------|
| Length | 7.23 [m] | 16.72 [m] | × |
| Load | 9,516.4 [kN] | 20,787.5 [kN] | × |
| α | 0.57 | 0.5 | × |
| β | 0.33 | 2.15 | × |
| x | 0.810 | 1.000 | × |
| Outer diameter | 0.40 [m] | 0.82 [m] | × |
| Inner diameter | 0.16 [m] | 0.44 [m] | × |
| Surface area | 0.106 [m ²] | 0.376 [m ²] | × |

Table 53 - Rod dimensions barge (compression)

| | Sheltered manmade port | Trailing edge estuary | Leading edge bay |
|----------------------------|-------------------------|-------------------------|------------------|
| Length | 7.23 [m] | 16.72 [m] | × |
| Load | 23,754.2 [kN] | 34,286.4 [kN] | × |
| α | 0.57 | 0.46 | × |
| β | 0.21 | 2.46 | × |
| x | 0.770 | 1.000 | × |
| Outer diameter | 0.56 [m] | 0.91 [m] | × |
| Inner diameter | 0.40 [m] | 0.32 [m] | × |
| Surface area | 0.121 [m ²] | 0.570 [m ²] | × |

Table 54 - Rod dimensions breakwater (compression)

For the tensile state only the maximum tensile stress is of importance, where either a rod or a chain can be used as load transfer mechanism. In the case of the chain the shear stress is also relevant as the chains of the chain connect to each other and exert a shear force on the material.

Because for both the tensile stress and the shear stress the yield stress of the material is of importance the required area for both phenomena is used. This means that the required area for both is the same. The tensile force in the chains, however, is distributed over two strains whereas the shear force has to be absorbed by one, meaning the minimal thickness as the connections has to be twice as thick as the “vertically” running strains. The required thicknesses are given in Table 55 and Table 56.

| | Sheltered manmade port | Trailing edge estuary | Leading edge bay |
|----------------------------------|-------------------------|-------------------------|-------------------------|
| Length | 7.23 [m] | 21.64 [m] | 91.05 [m] |
| Load | 9,694.8 [kN] | 22,965.1 [kN] | 16,871.6 [kN] |
| Tensile/shear area (S235) | 0.041 [m ²] | 0.098 [m ²] | 0.072 [m ²] |
| Chain diameter | 0.12 [m] | 0.18 [m] | 0.15 [m] |

Table 55 - Rod dimensions barge (tension)

| | Sheltered manmade port | Trailing edge estuary | Leading edge bay |
|----------------------------|-------------------------|-------------------------|-------------------------|
| Length | 7.23 [m] | 21.64 [m] | 91.05 [m] |
| Load | 24,801.3 [kN] | 38,944.6 [kN] | 19,611.9 [kN] |
| Tensile area (S235) | 0.105 [m ²] | 0.166 [m ²] | 0.083 [m ²] |
| Chain diameter | 0.19 [m] | 0.23 [m] | 0.17 [m] |

Table 56 - Rod dimensions breakwater(tension)

23.3 Connections

The connections between the piston/rod combination and the other components of the device are of some importance. Firstly because they need to be dimensioned in such a way that the relevant forces can be properly propagated through the structure, and secondly because the previously determined safety precautions (chapter 18) have to be included in them. For this critical component the most logical solution is to use a bolt loaded on shear strength as a bolt is easily replaceable after failure. Table 57 through Table 60 give the relevant bolt sizes for each scenario. The connection between the failure structure and the rest of the device is as illustrated in Figure 70.

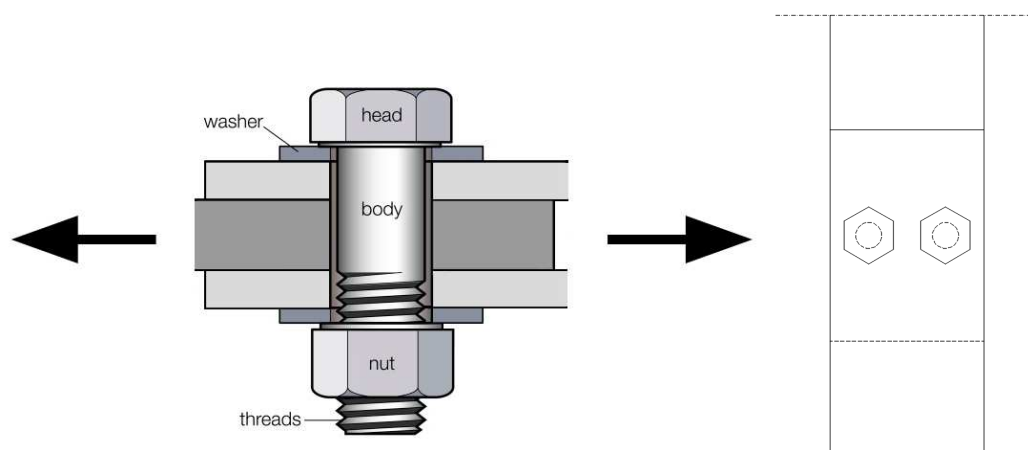


Figure 70 - Failure bolt

| | Sheltered manmade port | Trailing edge estuary | Leading edge bay |
|----------------------------------|-------------------------------|--------------------------------|------------------|
| Failure load | 6,344.3 [kN] | 13,858.4 [kN] | × |
| Tensile/shear area (S235) | 0.027 [m ²] | 0.059 [m ²] | × |
| Bolt diameter | 2 x 0.13 [m] | 2 x 0.20 [m] | × |
| Bearing surface area | 0.46 x 0.23 [m ²] | 0.87 x 0.435 [m ²] | × |
| Bolt length | 0.46 [m] | 0.87 [m] | × |

Table 57 - Bolt dimensions barge (compression)

| | Sheltered manmade port | Trailing edge estuary | Leading edge bay |
|-----------------------------|--------------------------------|--------------------------------|------------------|
| Failure load | 15,836.1 [kN] | 22,857.6 [kN] | × |
| Tensile area (S235) | 0.067 [m ²] | 0.097 [m ²] | × |
| Bolt diameter | 2 x 0.21 [m] | 2 x 0.25 [m] | × |
| Bearing surface area | 0.49 x 0.245 [m ²] | 1.07 x 0.535 [m ²] | × |
| Bolt length | 0.49 [m] | 1.07 [m] | × |

Table 58 - Bolt dimensions breakwater (compression)

| | Sheltered manmade port | Trailing edge estuary | Leading edge bay |
|----------------------------------|--------------------------------|--------------------------------|-------------------------------|
| Failure load | 6,463.2 [kN] | 15,310.1 [kN] | 11,247.8 [kN] |
| Tensile/shear area (S235) | 0.028 [m ²] | 0.065 [m ²] | 0.048 [m ²] |
| Bolt diameter | 2 x 0.13 [m] | 2 x 0.20 [m] | 2 x 0.17 [m] |
| Bearing surface area | 0.29 x 0.145 [m ²] | 0.45 x 0.225 [m ²] | 0.38 x 0.19 [m ²] |
| Bolt length | 0.29 [m] | 0.45 [m] | 0.38 [m] |

Table 59 - Bolt dimensions barge (tension)

| | Sheltered manmade port | Trailing edge estuary | Leading edge bay |
|-----------------------------|--------------------------------|-------------------------------|--------------------------------|
| Failure load | 16,534.4 [kN] | 25,963.1 [kN] | 13,074.6 [kN] |
| Tensile area (S235) | 0.070 [m ²] | 0.110 [m ²] | 0.056 [m ²] |
| Bolt diameter | 2 x 0.21 [m] | 2 x 0.26 [m] | 2 x 0.19 [m] |
| Bearing surface area | 0.49 x 0.245 [m ²] | 0.58 x 0.29 [m ²] | 0.41 x 0.205 [m ²] |
| Bolt length | 0.49 [m] | 0.58 [m] | 0.41 [m] |

Table 60 - Bolt dimensions breakwater (tension)

It should be noted that the yield strength of the steel used in this calculation is the 95% value of steel, meaning 95% of all tested steel has a yield strength stronger than this value. Because in this case, however, the steel is intended to yield it would be preferential to use an inverted value where 95% of all tested steel actually yields below this strength so it can be ensured that the value is not exceeded. Due to the accuracy of steel's yield stress predictability, however, the 95% value is considered sufficient.

24 Possibilities for energy storage

One of the main problems many forms of renewable energy are facing is that the production is irregular and difficult to predict. For instance wind mills only produce electricity when there is a sufficient amount of wind, and the quantity of produced wind energy also depends on the wind speed. Solar energy is only available during the day, and even then the amount fluctuates depending on the weather. The needs of the consumers on the other hand are more on an on-demand bases, they want electricity when they need it rather than when there is sufficient sun or wind. The solution to this problem is to store the energy when a surplus is being produced and use this when there is insufficient production (see also Section 2).

The Tidal Wave Energy Converter has some small scale energy storage in its design as well, albeit for different purposes. As the pontoon is held in place as the tide moves towards its opposite extreme an amount of energy is stored in the extruded pontoon and the pressurized piston. Releasing this energy at a time when consumers need it rather than when the production is optimal would serve as a means of on-demand energy production. Moreover, electricity from the grid can be used in times of surplus (when electricity is cheap) to exert the pontoon independent of the tidal motion, releasing it again during a time of shortage (when electricity is expensive).

Energy storage using the TWEC can be done in two ways. Either the energy can be stored in the pistons, meaning the energy potential at any given time is dependent of the tidal motion. For example, if the pontoon is locked in the low tide position it will not be capable of providing significant on-demand energy during any subsequent low tide period. Alternatively a buffer storage can be used which stores the energy from an optimally operated TWEC in a different manner. A possibility for this would be a secondary pontoon which is pulled under water and released whenever electricity is needed. Both methods can be operated either fully by the tide, or in the aforementioned manner where the pontoon and/or buffer are exerted by cheap energy from the grid.

This means the possibilities for operating the TWEC in terms of energy storage are as follows:

- Tidal extrusion with optimal energy production.
- Tidal extrusion with on-demand energy production.
- Tidal extrusion with on-demand energy production through buffer storage.
- Forced extrusion with on-demand energy production.
- Forced extrusion with on-demand energy production through buffer storage.

The choice between the use of a buffer and the non-use of a buffer can be made on engineering grounds and does not require the use of a decision tool such as an MCDA. Buffer storages allow for the continuous accumulation of harvested energy independent of the tidal forcing on the buffer. The energy is harvested in separate pontoons and transferred to the buffer, which is pulled under water. Whenever energy is required it can be harvested from the storage in this pontoon.

The means of transferring the energy harvested in the separate pontoons to the buffer storage can be done in two ways. One being a cable spanned between the pontoons connected to the bottom through pulleys. This method directly transfers the motion of one pontoon to the other but is limited by the fact that halfway through the exertion a balance of forces will occur and the buffer pontoon will balance with the harvesting pontoon before the full energy potential is transferred.

The second method is to use the energy harvested by the hydraulic motor and transfer this to a pump to move the other pontoon. This is less energy efficient, but it does mean the full amount of harvested energy can be used. Furthermore it is easier to apply added electricity from the grid to the system in order to store that energy in the pontoon's buoyancy.

For the reasons stated above it is preferential to have a separate floating body to use for buffer storage as it gives possibilities for accumulating energy rather than being dependent on the tidal situation at that moment. Furthermore the possibilities of forced extrusion should be involved as it increases the potential of the device and is relatively easy to include when using a motor/pump energy transfer combination.

25 Design criteria

From the design procedures that have been followed in the previous chapters some basic design criteria and procedures can be deducted that ought to be followed when designing a Tidal Wave Energy Converter for any given location. This chapter will include a review of the used design cycle and an evaluation of how it worked and what could be improved. Secondly it will recapitulate on the choices made for certain device components and under what circumstances these can and should be used.

25.1 Design procedure

The followed design procedure in the methods described before are based on a maximum electric revenue basis and is illustrated in Figure 71. The design steps followed in the previous chapters showed that this method can lead to unfavourable load conditions requiring severe structural reinforcements to the host structure and therefore significant added costs. Furthermore a revenue inspired number of supports can lead to significant support forces which in turn leads to unfavourable foundation requirements such as large numbers of piles or anchors per support.



Figure 71 - Initial design cycle

The reviewed design procedure is therefore based on the forces in the system rather than optimal revenue. This may lead to a decreased revenue per cycle, but also results in a significant cost reduction. The use of the designed MatLab program therefore moves from the start of the design cycle towards the end of it. This revised design cycle is illustrated in Figure 72.

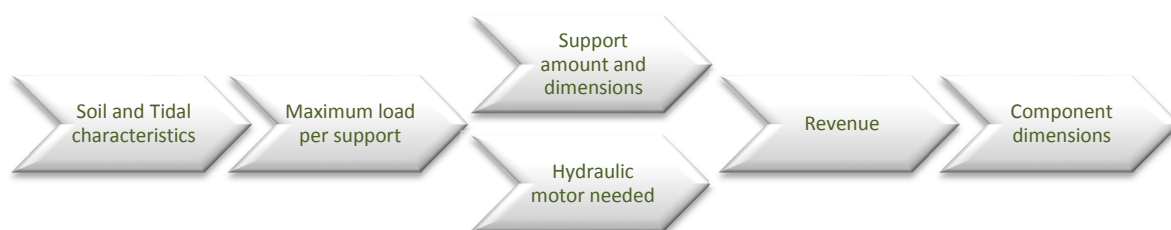


Figure 72 - Revised design cycle

25.2 Device components

The entire device consists of six general components that have been discussed in the previous chapters. From the design procedures followed some conclusions can be drawn on what these components should consist of and how the boundary conditions influence these decisions. Figure 73 gives an illustration of the installed device (in this case that of a barge in the sheltered manmade port location) with indicators of what component is globally located in what place. The following paragraphs will summarize the findings of their characteristics during the executed design cycle.

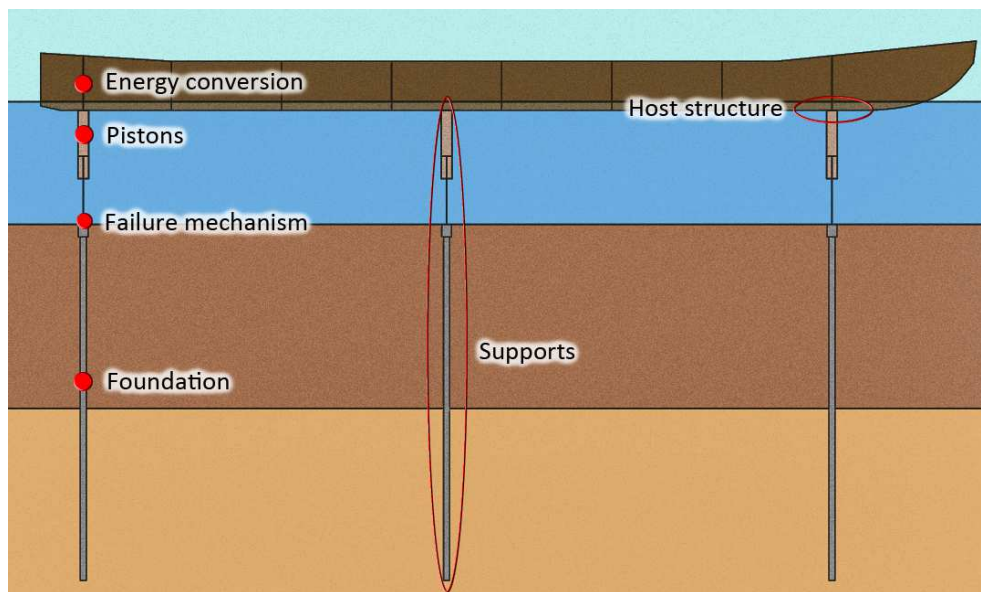


Figure 73 - Tidal Wave Energy Converter components

25.2.1 Host structure

In many cases the host structure can be sufficiently capable of dealing with the added loads of the device's operation within the boundaries of its structure as long as the support layout is done appropriately. Punch is the main structural failure mechanism of concern and can often easily be countered. Another important aspect of the host structure is the ratio between the tidal range and the freeboard as well as the ratio between the water depth and the surface area of the host structure. The freeboard is evidently relevant because it limits the allowed submergence of the pontoon, unless it is made submersible. The surface area is important because for low water depths (and thus logically speaking lower tidal ranges) it means there is insufficient space available for constructive elements handling the bending moments.

25.2.2 Supports

The location and amount of supports is important for the load distribution within the host structure. In 22.1 it can be seen that an unfavourable number and positioning of supports can lead to significant bending moments and shear forces leading to significant required adjustments to reinforce the host structure. A minimum of 4 supports appears to be recommended where the use of more would only positively influence the distribution of forces.

25.2.3 Pistons

The size of the pistons is in relation with the amount of supports and the submergence or emergence of the host structure what determines the pressure build up in the system. The size of the pistons in the considered designs has been taken as completely arbitrary, whereas there are

limitations to the constructability of large diameter pistons. The length leaves little room for limitations due to the fact that any limitation to the freedom of motion of the host structure leads to a significant increase in the load on the system.

25.2.4 Failure mechanism

The bolts that limit the potential maximum load on the system are of straightforward design and did not yield any specific limiting complications or possibilities for improvement. What should be taken into account with these is that they need to be easily accessible so that in case of failure they can be replaced.

25.2.5 Foundation

For the foundation several different possibilities were considered including piles, anchors and a shallow foundation. The considerations that ought to be used when determining a type of foundation have partially been elaborated on in 21.1 and still apply in the general sense. Based on the costs of the foundations in the different scenarios and the unit prices of construction materials it is concluded that for compressive scenarios with penetrable soil precast concrete piles are preferable over shallow foundations and steel pipe piles. For deep waters compressive solutions are undesirable due to buckling.

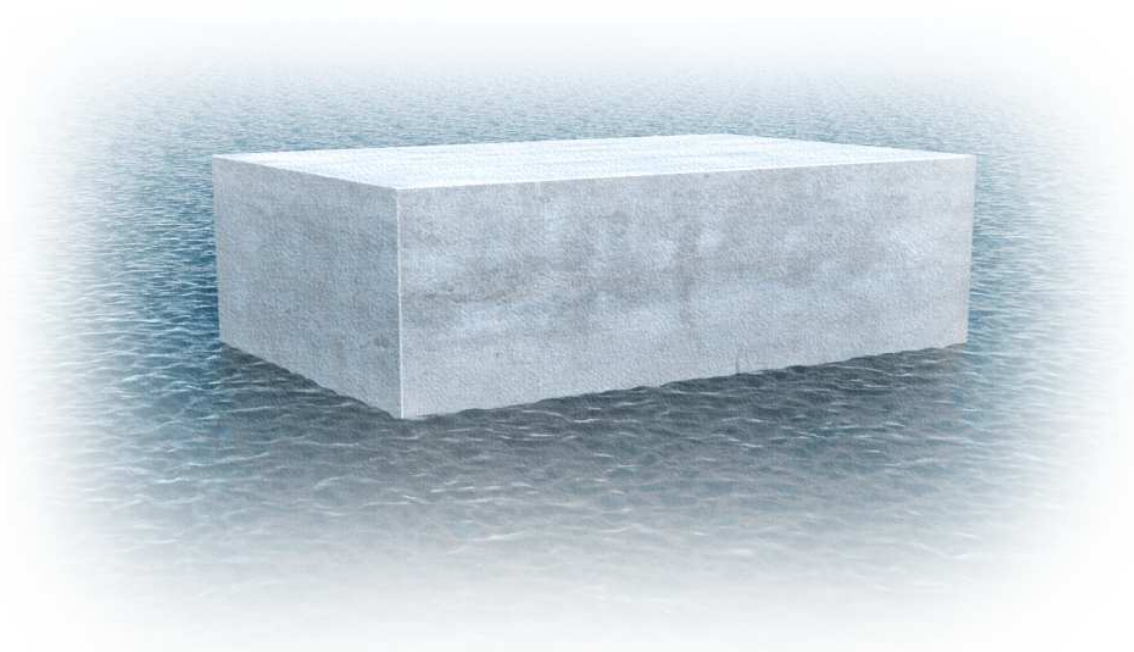
For tensile situations anchors are preferred over tension piles because they are significantly cheaper. Rock anchors can achieve high capacities but are evidently not universally applicable, GEWI anchors are a suitable alternative for weaker soils. Anchors can be installed in most coastal locations, which is sufficient due to the limited tidal range in the deep ocean. Combinations of precast concrete piles and anchors are a possibility in case the revenue is sufficient to maintain feasibility.

25.2.6 Energy conversion

The energy conversion method of choice is the internal gear hydraulic motor because of its size and cost. The motor used in the researched design cycle is that of the Eaton Gerotor series mainly because this is the only type with sufficient available information. The limitations of these motors are that they operate efficiently in a pressure range between 14 and 140 BAR. Motors are available, however, with possibilities for higher pressures which would limit the required size of the pistons.

Section 5 – Final design and conclusions

| | | |
|------|---|-----|
| 26 | Introduction to final design and conclusions | 147 |
| 27 | Location analysis | 149 |
| 27.1 | Tidal climate | 150 |
| 27.2 | Bottom characteristics | 151 |
| 27.3 | Host structure..... | 151 |
| 28 | Specific design: Bay of Fundy | 153 |
| 28.1 | Host structure..... | 153 |
| 28.2 | Support and piston configuration | 154 |
| 28.3 | Foundation | 156 |
| 28.4 | Connection to the host structure | 157 |
| 28.5 | Full configuration of the Tidal Wave Energy Converter | 158 |
| 29 | Financial considerations | 159 |
| 29.1 | Construction costs | 159 |
| 29.2 | Production costs of electricity..... | 160 |
| 30 | Conclusions and recommendations | 161 |
| 30.1 | Conclusions..... | 161 |
| 30.2 | Recommendations..... | 163 |



26 Introduction to final design and conclusions

After having determined the technical design conditions of the Tidal Wave Energy Converter in the previous section the next step is to determine whether this can be implemented in a feasible manner. To determine this a “highest probability location” is determined based on the design conditions as determined before, where a real life location is found such that as many conditions are present in a favourable manner. To find this location the Tidal Model Driver from section 2 is used in order to find an optimal combination of tidal range and return period. Subsequently a suitable host structure is found using the reference projects from section 3.

Once a design location and host structure have been found the work from section 4 is used to design the required TWEC device in terms of the piston diameters, foundation, failure component and connection to the host structure. With this information the TWEC MatLab script can be used to determine the annual electricity production of the device and combined with the costs of building the design TWEC device conclusions are obtained in terms of costs per unit produced electricity and overall feasibility, as well as what possible terms apply to this feasibility or how it can be achieved. To conclude some recommendations are given on how the design and other components of the work in the previous sections can be improved.

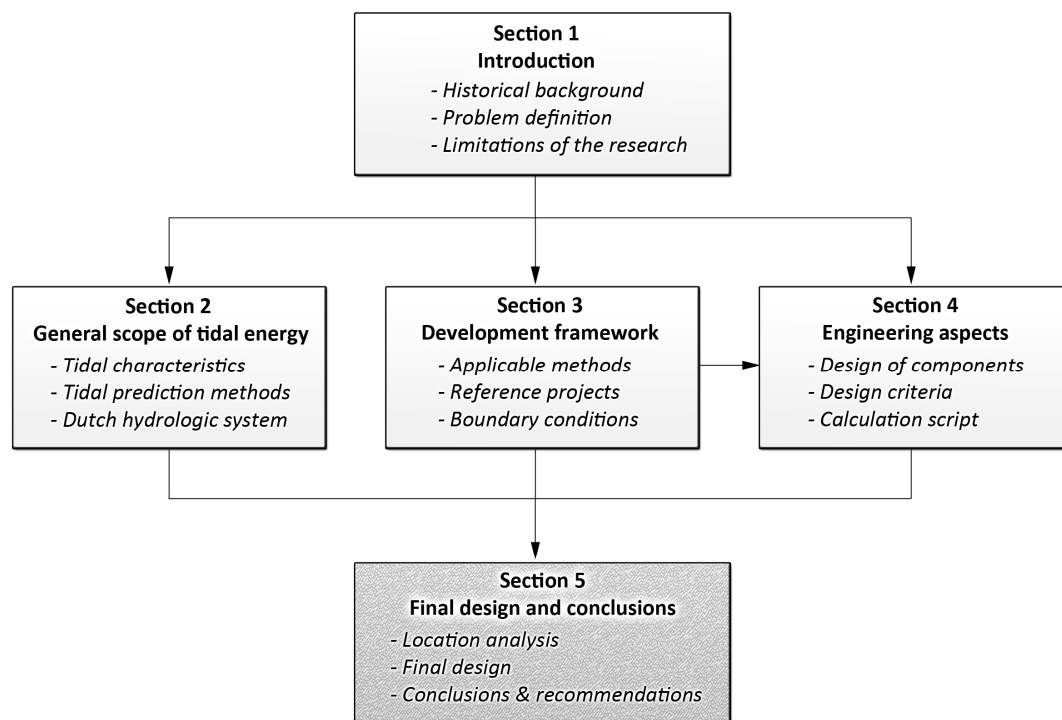


Figure 74 - Structure of the report

27 Location analysis

To choose a location for the high feasibility design cycle previously determined important factors are taken into consideration. The factors regarded as important are:

- Semi-diurnal tide
- Large tidal amplitude
- Constant tidal amplitude

To obtain a location with these characteristics a sieve analysis is done as described in Appendix Q and leads to the resulting location of the Bay of Fundy in between the Canadian mainland and the peninsula of Nova Scotia (Figure 75). This location is well known for its high tidal amplitude and furthermore has a dominantly semi-diurnal nature and is governed by the semi-diurnal lunar tidal constituent with relatively small other constituents, meaning it is of a relatively constant nature.



Figure 75 - Bay of Fundy development location (45°17'38", -65°01'37")

27.1 Tidal climate

The tidal constituents for the considered location can be extracted from the Tidal Model Driver (TMD) as introduced in section 3. It is expected from the sieve analysis done in Appendix Q the dominant tidal constituent will be the lunar semi-diurnal and that this constituent is large relative to all other semi-diurnal as well as all diurnal constituents. Table 61 shows that this is indeed the case and the according tide ratio is 0.062 which is well below the threshold for semi-diurnal classifications at 0.25.

| Constituent | Ang. Vel. [$^{\circ} \text{h}^{-1}$] | Amplitude [m] | Phase shift [$^{\circ}$] |
|----------------------|--|---------------|----------------------------|
| M₂ | 28.984 | 4.1860 | 112.03 |
| S₂ | 30.000 | 0.4325 | 173.24 |
| N₂ | 28.439 | 0.8527 | 74.72 |
| K₂ | 30.082 | 0.1594 | 160.60 |
| K₁ | 15.041 | 0.1707 | 200.00 |
| O₁ | 13.943 | 0.1199 | 181.92 |
| P₁ | 14.958 | 0.0437 | 199.64 |
| Q₁ | 13.399 | 0.0168 | 178.25 |
| M_f | 1.098 | 0.0046 | 239.19 |
| M_m | 0.544 | 0.0035 | 212.72 |
| M₄ | 57.971 | 0.0669 | 63.67 |

Table 61 – Tidal constituents of the Bay of Fundy location ($45^{\circ}17'38''$, $-65^{\circ}01'37''$) (TOPEX/Poseidon, sd)

By plotting the resulting tidal motion, as done in Figure 76, it can be confirmed that the tidal range is indeed significant, shows a dominantly semi-diurnal nature and is relatively constant over time. The minimum tidal range is around 7 metres and the maximum around 12 metres, which gives a difference from the mean tidal motion of around 25%.

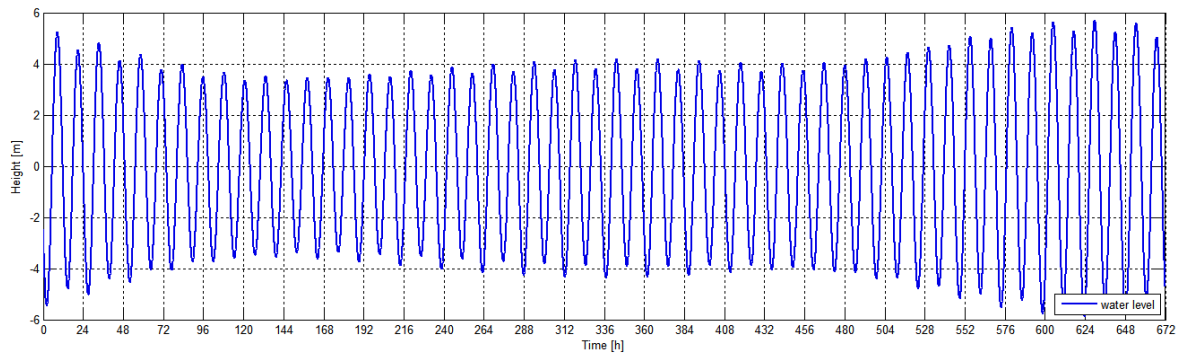


Figure 76 – Water level at the Bay of Fundy location for 1 month duration

27.2 Bottom characteristics

Due to the scientific interest in the tidal propagation in the Bay of Fundy the local bathymetry has been quite well documented. As can be seen in Figure 77 the majority of the water depth along the bay is known with the equilibrium depth at the considered location being approximately 50 metres.

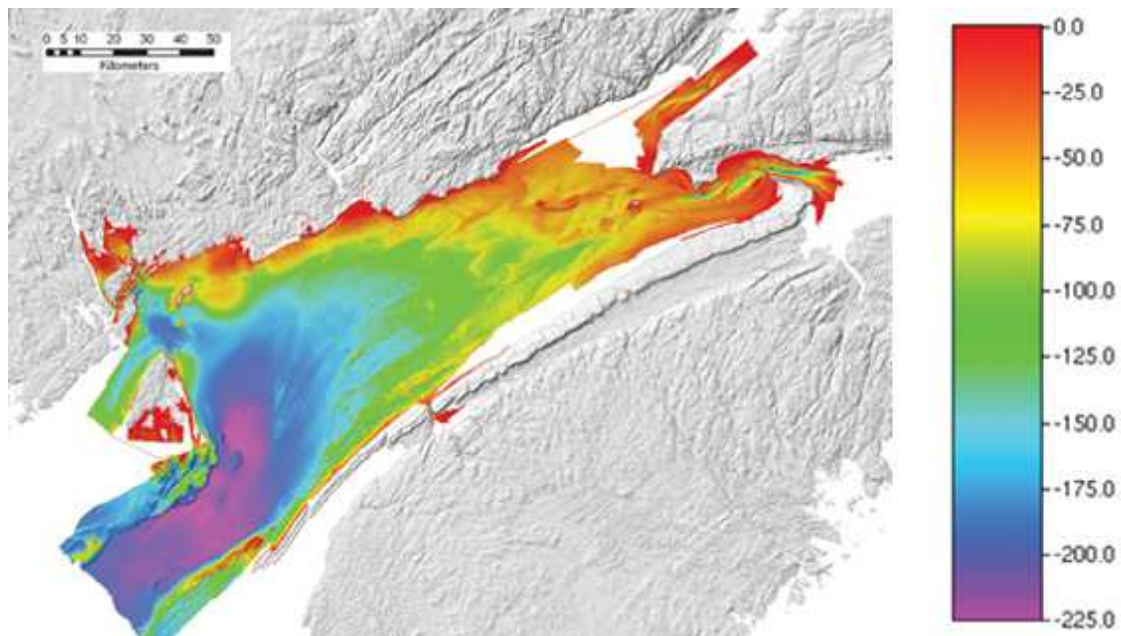


Figure 77 - Bay of Fundy bathymetry (Government of Canada, 2015)

The soil composition along the basin is another story altogether and is not as well documented. According to some sources, such as (Swift & Lyall, 1967), it consists of Triassic bedrock with an arbitrary amount of dynamic sediment subject to the tidal streams in the bay. Because of this mostly unknown soil composition, combined with the conceptual nature of the design, it is assumed that the soil consists of solid bedrock with no noteworthy sediment deposits on top of it. This means that the foundation design will be based entirely on the bedrock layer located at a depth of 50 metres below mean sea level.

27.3 Host structure

In accordance with a realistic location a realistic host structures needs to be determined that could be of use to the chosen location. In section 4 it has been observed that there is a certain correlation between the size of the host structure and its applicability to certain tidal ranges. Small size structures (like the barge) are less applicable to large tidal ranges and large size structures (like the breakwater) are not ideal for small tidal ranges. Because this location has a large tidal range the barge is therefore not a realistic application.

The choice of host structure is a floating bridge between the municipalities of Middleton, Nova Scotia, and Saint Martins, New Brunswick (see Figure 78). Due to the depth of the bay it is deemed realistic to assume a floating bridge would be a realistic solution, and the distance a bridge would cut from the travel time from the Nova Scotia peninsula to the New Brunswick mainland is considered a sufficient motivation to deem a connection somewhat desirable. Currently this function is being fulfilled by a ferry service between Saint John, Nb and Digby, Ns.

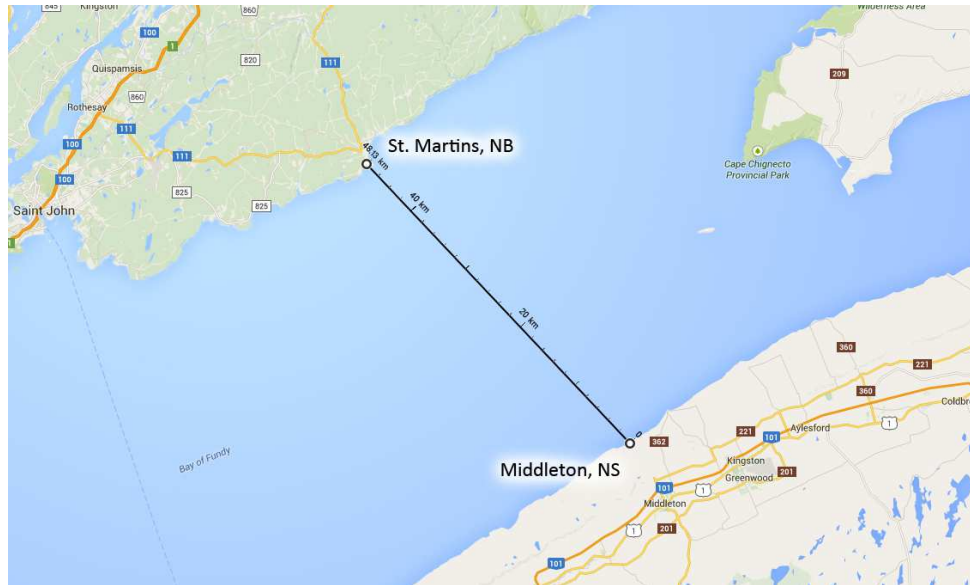


Figure 78 - St. Martins - Middleton floating bridge trajectory

The pontoons on which the bridge is supported consist of reinforced concrete caissons. The dimensions of these caissons are determined by a combination of the local tidal range, the amount of lanes on the bridge and the surcharge by the traffic. Judging from the roads surrounding the design location a bridge for two lanes (one in each direction) should suffice and it does not appear a requirement for expanding this capacity is imminent.

28 Specific design: Bay of Fundy

For the design cycle of the Tidal Wave Energy Converter in the Bay of Fundy the design cycle as revised in Section 4 is used. This design cycle, as illustrated in Figure 79, dictates that the maximum loads on the foundation need to be determined as to minimize the required foundation dimensions. From there an amount of supports and according configuration needs to be determined such that the load distribution is most favourable. From here on the dimensions of the other components can be determined.

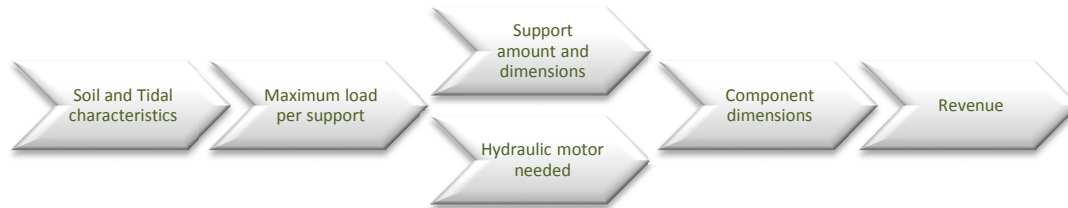


Figure 79 - Design cycle

To follow this design cycle first the boundary conditions must be known. In chapter 27 the boundary conditions of the tide, bathymetry and soil profile have already been determined, which means the host structure's dimensions are the only unknown at this stage. These will be determined first after which subsequently the dimensions of the pistons and their location underneath the pontoon will be calculated. Following this the foundation will be calculated and finally the connections between the components as well as the designed failure module.

28.1 Host structure

The dimensions of the host structure are governed by the local tidal range, the required width of the road and the required buoyant force to keep the bridge afloat. The maximum tidal range is given by the sum of all constituents, after all the amplitude can never be higher than the sum of its components. Equation 8 shows the required calculation and the value for the maximum amplitude at the considered location. The considered range of water levels consequently is thrice the calculated amplitude (twice for the tidal range and a factor one and a half for the safety margin of the safety system) added with a two metre margin for wind set-up.

$$\begin{aligned}\eta_{\max} &= \eta_{M_2} + \eta_{S_2} + \eta_{N_2} + \eta_{K_2} + \eta_{K_1} + \eta_{O_1} + \eta_{P_1} + \eta_{Q_1} + \eta_{M_f} + \eta_{M_m} + \eta_{M_4} \\ &= 6.0567 [m]\end{aligned}$$

Equation 8 - Maximum tidal amplitude

From (Eurocode 1, 2010) it follows that the bridge width should be at least 6 metres with a traffic load of 9 [kN/m²] over one half and 2.5 [kN/m²] over the other. Any further width margin would be devoid of this load. Due to this eccentric nature of the load the pontoon needs to be slightly wider than the width of the load to maintain stability. To slightly accelerate the design process the Bergsøydundet bridge as mentioned in is used which also facilitates two lane traffic. This means the dimensions of the considered pontoons are as given in Table 62. Here it is assumed that the height of the pontoon may not exceed its width in any direction for stability considerations, so the length is slightly altered to reflect this.

| | |
|---------------------|--------------------------|
| Length | 22.00 [m] |
| Width | 34.00 [m] |
| Height | 20.17 [m] |
| Surface area | 748.00 [m ²] |

Table 62 - Floating bridge pontoon dimensions

It is assumed that the weight of the pontoon is such that in the equilibrium position the weight of the pontoon and the load of the bridge upon it balance out with the buoyant force of the semi-submerged pontoon.

28.2 Support and piston configuration

The conclusion from Section 4 is that the configuration of the supports underneath the pontoon are of significant importance to the required adjustments. If sufficient supports are placed in the correct positions virtually no added adjustments need to be made to the existing structure. Symmetry was found to be an important requirement in placing the supports and the minimum amount of supports should be equal to the amount of corners the structure has.

The size of the pistons is dictated by the required buckling length, as a fitting combination of piston and rod is difficult to determine if the inner diameter of the piston is fixed. To obtain a combination of piston size and rod size an iterative process is used with the method as described in Section 4. Table 63 gives the values required for the Tidal Wave Energy Converter MatLab script as given in Appendix P.

| Variable | Value |
|---|-------|
| Displacement [cm³ rev⁻¹] | 12.9 |
| Rotations per minute [min⁻¹] | 810.0 |
| Support surface [m²] | 0.54 |
| Floating surface [m²] | 748.0 |
| Block coefficient [-] | 1.0 |
| Number of supports [-] | 6.0 |

Table 63 - Design values for MatLab script

From the simulation done by the script over the time period of a year (8760 hours) the maximum values for the tensile and compressive forces can be extracted. In accordance with the limit states as defined in chapter 18 the loads required to break the safety bolt as well as the design load for the rest of the structure can be calculated (Table 64).

| | Operation load [kN] | Bolt failure load [kN] | Ultimate load [kN] |
|--------------------|---------------------|------------------------|--------------------|
| Compression | 5,925.76 | 8,888.64 | 13,332.96 |
| Tension | 5,920.93 | 8,881.40 | 13,322.09 |

Table 64 - Forces in different limit states

To obtain such an equal distribution of forces over the supports the area over which each support transfers the distributed load needs to be equally large as well. With the use of six supports this means six areas of equal size need to be identified on the pontoon with the supports being placed in the centres of each of these areas. This configuration is illustrated in Figure 80.

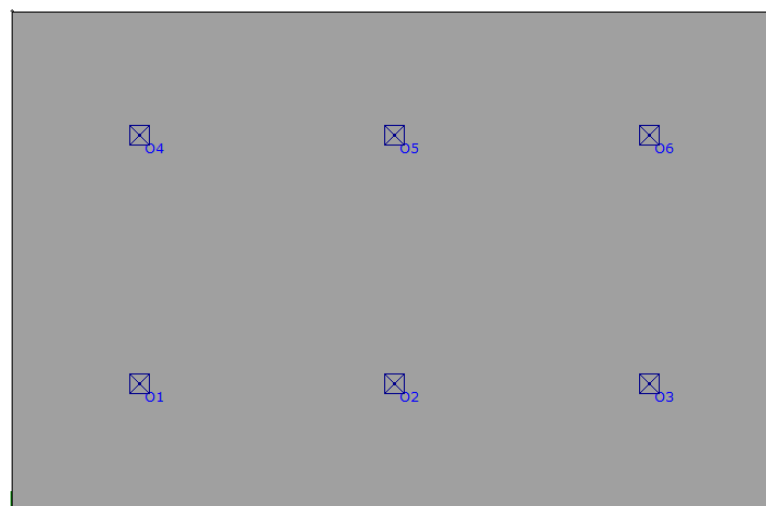


Figure 80 - Support configuration (plan view)

Knowing the forces on the support the required piston dimensions can be determined. For the length of the piston the same theory holds as for the required height of the pontoon meaning it is to be thrice as large as the maximum tidal amplitude. The inner diameter follows from the calculations done with the TWEC script and the wall thickness depends on the maximum pressure within the piston. The calculation method is as was used in chapter 23 leading to the results as given in Table 65. Due to the higher pressure a steel type with a higher yield stress is used, in this case 500 [MPa] (Ovako, sd).

| | |
|----------------------------------|----------|
| Maximum pressure [kPa] | 24,690.7 |
| Piston length [m] | 20.17 |
| Inner diameter [m] | 0.81 |
| Outer diameter [m] | 0.99 |
| Piston wall thickness [m] | 0.030 |
| Rod length [m] | 29.83 |
| Rod diameter [m] (solid) | 0.81 |

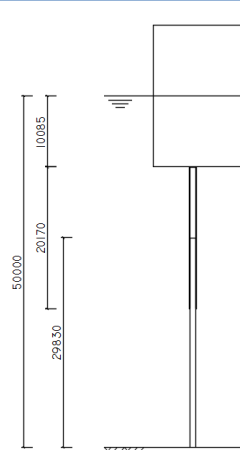


Table 65 - Piston dimensions

The dimensions of the rod connecting the piston to the foundation and ensuring the pumping motion of the piston are determined based on the local water depth and the buckling force on the system. The length of the rod needs to be at least as long as the piston itself as to not limit the freedom of motion. Its maximum length is dictated by the equilibrium water depth minus the piston length. This takes into account that the rod penetrates the piston to the halfway point in the equilibrium position, as the draught of the pontoon in that case is also that same length.

28.3 Foundation

Because the chosen location has a bottom profile consisting of bedrock, the use of piles as a foundation method is not preferred. The preferred solution for tensile forces is the use of rock anchors as discussed in chapter 21.5, whereas the compressive force can theoretically be transferred to the sub soil by placing the lower end of the piston rod straight on the bedrock. To limit the potential for failure due to the rod slipping away, however, it is preferred to penetrate the bottom end of the rod into the bedrock a certain amount as to prevent the rod slipping away horizontally. The calculation results as done for the foundation as well as the failure mechanism are given in Table 66.

| | |
|---|-----------|
| Maximum bond stress [N m⁻²] | 1050 |
| Steel yield stress [MPa] | 630 |
| Grout yield stress [MPa] | 30 |
| Total force [kN] | 13,322.09 |
| Force per anchor [kN] | 2,285.90 |
| Number of anchors | 6 |
| Drill hole diameter [m] | 0.13 |
| GEWI bar diameter [m] | 0.068 |
| Anchor length [m] | 8 |
| Failure bolts [mm] | 2x Ø160 |
| Chain diameter [mm] | 0.055 |

Table 66 - Foundation characteristics

The orientation of the anchors relative to the support as well as how this configuration looks from the side are illustrated in Figure 81. It can be seen that the anchors have a polar orientation relative to the support and that the anchors are drilled in under an angle such that the anchor chain makes a straight line towards its connection point. At the connection point a protruding ring is attached to the bottom section of the pillar which the chains are attached through. The failure bolts are installed such that after failure the top section of the pillar can use freely in vertical direction and the bottom section remains stationary.

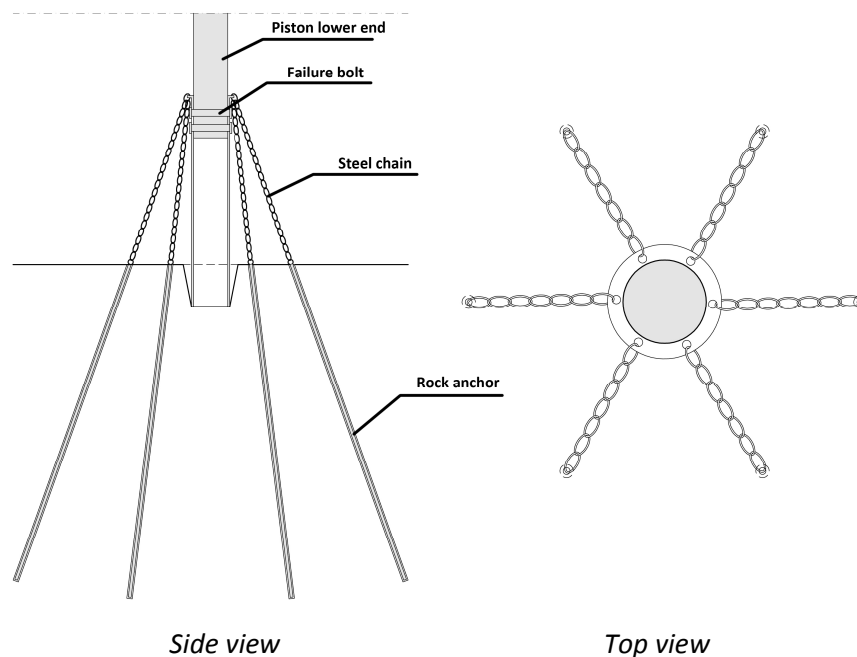


Figure 81 - Side and top view of foundation

28.4 Connection to the host structure

The connection to the host structure is made up of bolts welded to the piston and penetrating the bottom of the caisson. Because these bolts threaten the buoyancy of the structure it is essential to take precautionary actions to ensure a water tight fit is made. To do this rubber slabs are placed on both sides of the penetrated concrete mass creating a water tight fit as they are compressed by the bolts. Four bolts are used with a diameter of 14 centimetres each. The use of multiple bolts ensures stability of the connection. The layout of this connection is as given in Figure 82.

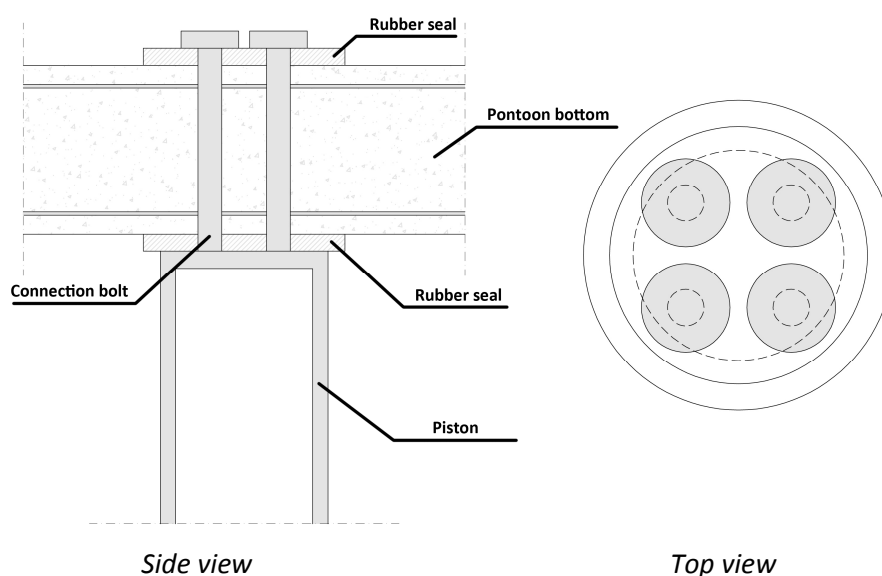


Figure 82 - Side and top view of connection to pontoon

28.5 Full configuration of the Tidal Wave Energy Converter

An illustration of the side view and top view of the entire system as designed in the previous paragraphs is given in Figure 83. It can be seen that the foundation of each support does not interfere with that of others as the distance between the ends of the anchors is always more than the minimum required 1.5 metres.

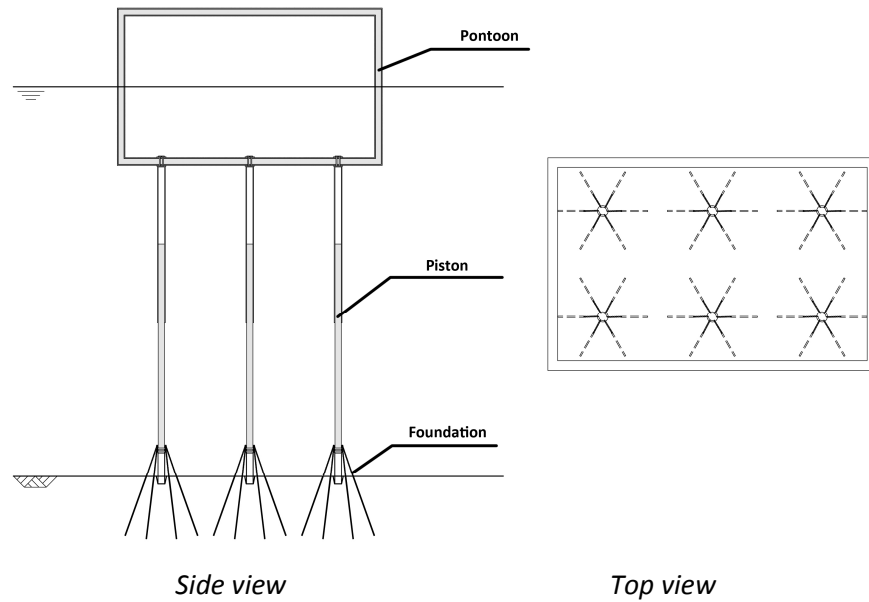


Figure 83 - Full system configuration side and top view

29 Financial considerations

Having designed the required extra work to build the Tidal Wave Energy Converter onto an existing structure, the costs attached to these alterations can be determined. From here the costs per kWh can be calculated from which it is possible to compare to the costs of harvesting existing energy sources and from there conclude on whether or not it is feasible to use the TWEC, and if so under what conditions.

29.1 Construction costs

The construction costs are calculated similarly to the method used in chapter 21.7 although due to the lack of different foundation types also fewer different types of materials are used. The required prices of key materials are given in Table 67.

| Material | Unit | Price per unit |
|---------------------------|------|----------------|
| Construction steel | [kg] | €2.50 |
| Rock anchor | [-] | €2500.00 |
| Eaton J05 Hydraulic motor | [-] | €270.00 |

Table 67 - Unit costs of construction materials (Pascha, 2015)

From here on the costs of the entire structure can be determined through the specific quantities of materials involved. The quantities are determined based on the dimensions as given in the previous paragraphs and combined with the unit prices to determine the costs. The cost of maintenance is estimated to be 1% of the construction costs annually during the lifetime of the structure. Assuming a rate of interest of 4% this means that for every euro of construction costs a total of €0.081 in maintenance costs will have to be paid over the lifetime of the structure. The results of the cost calculation are given in Table 68.

| Component | Material | Quantity | Costs |
|--------------------------------|--------------------|-----------------|----------------------|
| Anchors | Rock anchor | 6 | €15,000.00 |
| Failure bolts | Construction steel | 288.6 [kg] | €721.50 |
| Chains | Construction steel | 1,912.45 [kg] | €4,781.12 |
| Rod lower end | Construction steel | 5,268.45 [kg] | €13,171.12 |
| Rod upper end | Construction steel | 107,436.90 [kg] | €268,592.26 |
| Piston (Bitter, 2015) | Construction steel | | €218,180.00 |
| Connection bolts | Construction steel | 624.37 [kg] | €1,560.93 |
| Hydraulic motor | Motor | | €270.00 |
| Total per support | | | €522,276.93 |
| Maintenance per support | | | €42,304.43 |
| Total | | | €3,387,488.17 |

Table 68 - Construction costs

29.2 Production costs of electricity

The production cost of electricity is determined by dividing the costs of construction during its considered lifespan by the amount of electricity that is produced during that time. The produced electricity in turn can be calculated with the Tidal Wave Energy Converter calculation script as described in Appendix P. The results of this calculation are given in Table 69.

| | |
|--|---------------|
| Construction costs | €3,387,488.17 |
| Annual electricity production [kWh] | 22,875.8 |
| Lifetime electricity production [kWh] | 228,758.0 |
| Production cost per kWh | €14,81 |

Table 69 - Production costs

It is assumed that the costs of producing electricity in Canada and the United States are comparable due to their proximity to each other, and because of the availability of data from the United States this data is used. From (US Energy Information Administration, 2014) the production prices of common types of electricity sources are obtained. Given the exchange rate of the USD at the time of writing these prices are approximately the same in Euros as in USD (Wisselkoers.nl, 2015). Figure 84 gives these production costs sorted from cheapest to most expensive, with the costs for producing electricity with the Tidal Wave Energy Converter included as reference.

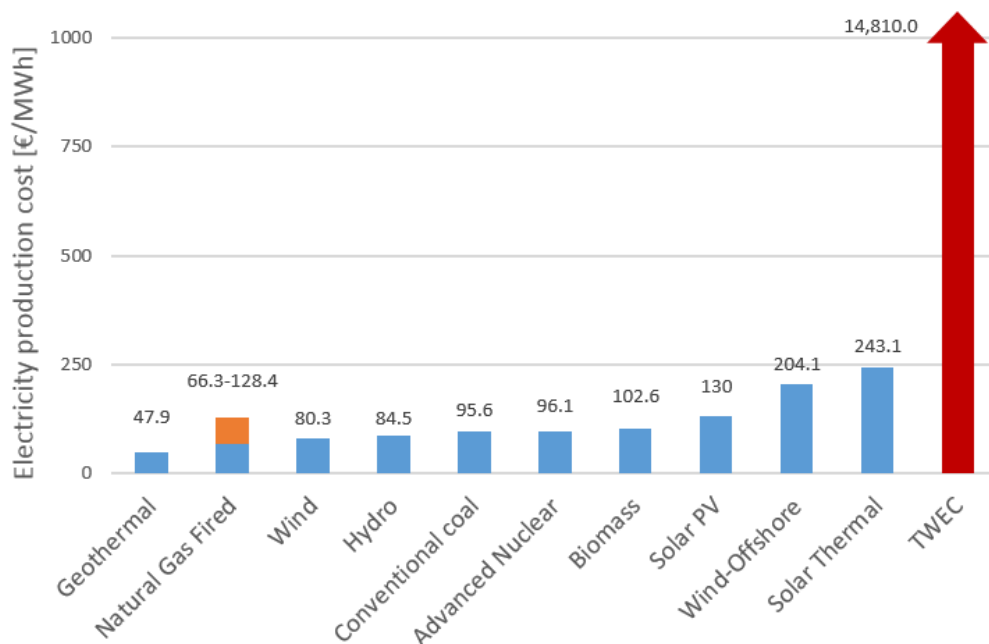


Figure 84 - Production costs per MWh of common energy sources after (US Energy Information Administration, 2014)

These results have been obtained for the use of the Tidal Wave Energy Converter in a situation where both tension and compression are used for energy generation. In case tension only was used for this the required rod diameter would reduce as buckling would no longer be an issue. This adjustment would mean the “Rod upper end” component would be dimensioned smaller and the costs of that would approximately disappear, making the construction costs cut in half. With the production also cutting in half this would yield approximately the same production cost per unit of electricity production.

30 Conclusions and recommendations

Following the structural and financial considerations on the high probability location of the Bay of Fundy in Canada, as well as with the information gathered in Sections 2 through 4, conclusions on the feasibility of the Tidal Wave Energy Converter can be derived and recommendations for further research or possible improvement can be given. The following two paragraphs expand on this.

30.1 Conclusions

To come to a proper solution of the report the main question as posed in chapter 4 needs to be answered. To refresh, the main question reads:

How, if at all, can the Tidal Wave Energy Converter be made a financially and technically feasible means of harvesting energy from (relatively small) tidal motions?

This question can be split into two parts, the technical feasibility and the financial feasibility.

30.1.1 Technical feasibility

For the technical feasibility it can be concluded that it is possible to construct a device capable of extracting a certain amount of energy from the vertical motion of the tide. The calculations in section 4 show that for a variety of boundary conditions a working solution can be designed that suffices for that scenario. There are several things regarding the technical design that need to be taken into account:

- ***The technologically optimum extraction method is the use of hydraulic motors*** due to the limited reservoir requirements and efficient energy conversion. Hydraulic motors furthermore take up relatively little space and can easily be controlled in terms of discharge. This controllability of the discharge means the harvesting period can be stretched out over a longer period of time and the rise and fall velocity and acceleration of the pontoon can be kept within serviceable bounds.
- ***Due to the effect of buckling the direction of energy harvesting depends on the local water depth***, for relatively shallow waters both ebb (downward, compression) and flood (upward, tension) extraction are possible whereas for deeper water only flood harvesting is an option as the pistons would buckle under the exerted load if the depth exceeds the buckling length of the system.
- ***A component needs to be designed specifically to fail at a certain, limited load***. This ensures that the required force resistance does not become excessive in the case a single component blocks or fails, thereby severely reducing the required design dimensions. Without the safety component the pontoon would be able to sink or rise above the equilibrium water level much further than during its normal operation, significantly increasing the forces exerted on the device.

30.1.2 Financial feasibility

From Figure 84 in the previous paragraph it can be seen that the cost per unit of produced electricity is in the order of 60 to 300 times as expensive for the TWEC as for any other common form of electricity generation. This means that it is evidently unfeasible in any location with access to the grid to use the Tidal Wave Energy Conversion as an energy solution. The possibilities for application of the device are therefore limited to non-existent and hinge on the following requirements:

- **A remote, off grid area** exists where the costs of transporting fuel to the location are so high that the cost per unit of produced energy exceed the local cost of use for the Tidal Wave Energy Converter. These would have to be remote and badly accessible areas with a suitable, preferably bedrock, soil composition where a significant tidal motion is present. Furthermore a necessity for a floating structure needs to be present or a cheap floating body solution available. It is not realistic such a location exists.
- **The production price of other energy sources drastically increases** due to a shortage of resources. This may be a remote possibility if fossil fuel supplies get depleted and there is insufficient renewable energy capacity, but does not appear feasible in the near future. Furthermore the production price of renewable energy sources will likely only decrease further with the advancement of technology rather than increase.
- **The material costs of the used materials drops drastically.** The price of steel and pistons is a severe influence on the construction costs of the device, if the costs of obtaining and installing steel were to drop, or an alternative construction material with similar properties were to become available for a cheaper price, the cost per unit of produced electricity would decrease.
- **More elements of the device are paid for in the host structure.** If a pontoon is laid in the tide and already needs a hydraulic system to manoeuvre it, this could be used in a more cost effective way to harvest energy. It would mean the costs of the piston and the foundation are accounted for and at worst only minor adjustments need to be paid for. This would, however, be unfit if the hydraulic system needs to be used regularly.

It follows that the technical feasibility is in order, but the financial feasibility leaves a lot to be desired. It is virtually impossible to find a location where the conditions apply that are required to lower the price per kWh such that it comes within the range of other energy sources meaning it is unlikely to find consumers interested in installing the device.

30.2 Recommendations

Albeit the Tidal Wave Energy Converter has been deemed an unfeasible application in the previous paragraph, there are still some recommendations that apply to the work in this report that may improve the design or prove useful to certain aspects.

- **Improve the tidal propagation prediction in estuaries to include all tidal constituents.** At the moment of writing no research was available for tidal propagation in estuaries with multiple constituents, if this were to come available in the future this should be included in the prediction script. Currently it uses the dominant tidal constituent wherein the calculation method has an error margin that compensates for the missing constituents.
- **Look into the use of suction piles as a means of foundation.** Suction piles are widely used in the offshore industry to form a foundation for temporary structures, as well as in port areas to anchor buoys. They have not been considered in this research because there is not enough scientific background available to properly analyse them, but due to their wide availability they may present a relatively cheap solution for foundations in sandy soil types.
- **Look into the use of a mechanical, movement based energy conversion mechanism rather than a hydraulic, pressure based one.** The use of pistons has turned out to be expensive despite being the best choice of the considered alternatives. The use of a mechanical conversion method rather than a pressure based one was not considered and may yet provide a feasible solution. For example a system with gears that rotate as the pontoon rises or falls could be considered and investigated.
- **Look into the use of a failure element that forewarns failure and releases the pontoon more slowly.** The failure bolts used are loaded on shear force and have a sudden and brittle failure type. This means that if they break the pontoon may accelerate rapidly, which is undesirable for an inhabited structure. A failure mechanism that absorbs some of the buoyant energy and warns when failure is close would be preferential, although likely more expensive. Research should be done to determine such a system if a Tidal Wave Energy Converter were to be constructed.
- **Investigate possible host structures that require fewer additions.** The main cost components are in the pistons and the foundation, if a host structure exists which already requires these elements for its own operation this would drastically increase feasibility. Research could be done to find a host structure that fits this requirement.
- **Research the required probability of failure and adjust the limit states accordingly.** Due to a lack of available knowledge on such systems the limit states have been chosen arbitrarily (albeit based on reference requirements of other structures). This means a total safety margin of 2.25 times the actual load is applied to the majority of the structure. More research could lead to a lower safety margin requirement and therefore lower construction costs.
- **Include swell and wind waves in the harvesting spectrum.** Swell waves and wind waves are significantly smaller than tidal waves but also occur significantly more often (in the order of seconds). The pontoon may be affected by these waves as well creating additional energy potential. This has not been taken account in this design but could improve the electric revenue of the device if added to its functionality.

Reflection

After the conclusion of the report it is important to take a moment and look back at what's been done and where there's room for improvement on how it was handled. This chapter seeks to provide that reflection on the work done and comment on what could or should have been done differently if the research was to be done again.

Firstly I would like to list the things that warrant improvement. In the MCDA stage of the energy conversion mechanism I underestimated the cost influence of using pistons, which in the end turned out to be half the cost of the total device. In hindsight it would have been better to include this into the decision tool. I spent a lot of time waiting for others to have the time to advise me on for example the foundation and the host structure. Despite having been able to use this time to create the Graphic User Interface for the calculation script it may have been preferential to move on to different sources sooner and save some time in the progress.

I spend some time looking into the possibilities of the Dutch hydrologic system, but in the end did fairly little with this information. This is in part due to the low tidal potential found here and the lack of feasibility even on high potential tidal locations, but the time spent on that could have been spend trying to find a more feasible conversion mechanism.

What did go well is that I believe I managed to put together a research that manages to include a wide variety of off the shelf solutions and compare them in terms of technical applicability. I believe I have derived a good method for determining the tidal range at locations of interest which can be easily used in the early stages of a project. The method used with different sections and according deadlines also worked well to keep the pace of progress controlled and the amount of work that needed to be done clear.

All in all I personally believe to have written a clear and mostly complete report which, despite having some influential flaws, manages to explain clearly whether the concept is feasible or not. Furthermore the process of writing this report and researching the concept has taught me a great deal about fields I have not come into contact with during the rest of my studies involving mechanical engineering, estuary dynamics and many others. I am happy to have chosen this subject and would do so again if given the choice.

Bibliography

- Anon., 2014. *Milieu Centraal*. [Online]
 Available at: <http://www.milieucentraal.nl/themas/energie-besparen/gemiddeld-energieverbruik-in-huis/energieprijzen>
- ArcelorMittal, 2015. *Spiral welded steel tubes*. [Online]
 Available at:
http://ds.arcelormittal.com/projects/europe/foundationsolutions/EN/steel_tubes_spiral.htm
- Australian Bureau of Meteorology, 2014. *Major tidal constituents, Derby*, Kent Town: National Tidal Center, Ocean Services Section.
- Bitter, G., 2015. *Costs of pistons* [Interview] (3 2015).
- Brolsma, J. & Roelse, K., 2011. *Waterway Guidelines 2011*, Delft: RWS Centre for Transport and Navigation.
- Cai, H., Savenije, H. H. & Toffolon, M., 2012. A new analytical framework for assessing the effect of sea-level rise and dredging on tidal damping in estuaries. *Journal of Geophysical Research: Oceans*.
- Campbell University, 2015. *Summary of the enzyme classes and major subclasses*. [Online]
 Available at: http://web.campbell.edu/faculty/nemecz/323_lect/enzyme_mech/mech_chapter.html [Accessed 2015].
- Casey, B., 2011. *Hydraulic Pumps and Motors: Considering Efficiency*. [Online]
 Available at: <http://www.machinerylubrication.com/Read/28430/hydraulic-pump-motors-maintenance>
- Chief inspector of shipping, 2001. *Beleidsregel verdubbelingen op bodem-, kim- en zijbeplating van de scheepshuid van schepen voor de Rijn- en binnenvaart*, s.l.: Directoraat-Generaal Goederenvervoer.
- Cleveland, C. J., 2013. *Bay of Fundy*. [Online]
 Available at: <http://www.eoearth.org/view/article/150449/>
- CUR166, 2012. *Damwandconstructies*, s.l.: CUR.
- CUR-2001-8, 2001. *Bearing capacity of steel pipe piles*, s.l.: CUR.
- Czapiewska, K., 2013. *Seasteady Implementation Plan: Final Report*, Delft: DeltaSync BV.
- DeltaSync, 2014. s.l.: DeltaSync.
- Eaton, 2011. *Low Speed, High Torque Motors*, s.l.: Eaton.
- Enerdata, 2013. *Average household electricity consumption*. [Online]
 Available at: <http://shrinkthatfootprint.com/average-household-electricity-consumption>
- Erofeeva, L., 2002. *Global Inverse Model*, Seattle: Earth & Space Research.
- Eurocode 1, 2010. *Eurocode 1: Actions on structures - Part 2: Traffic loads on bridges*, s.l.: s.n.
- Eurocode 2, 1992. *Design of concrete structures*. s.l.: s.n.
- EWA, 2008. *Energie uit water*. [Online]
 Available at: <http://www.energieuitwater.nl/EWA>
- Falcão, A. F. d. O., 2010. Wave energy utilization: A review of the technologies. *Renewable and Sustainable Energy Reviews*, p. 899–918.
- Farmer, A. L., 1999. *Investigation Into Snap Loading of Cables Used in Moored Breakwaters*, Blacksburg: Virginia Tech.
- Foustert, M. W., 2006. *Floating Breakwater: Theoretical study of a dynamic wave attenuating system*, Delft: Delft University of Technology.
- Government of Canada, 2015. *Fisheries and Oceans Canada*. [Online]
 Available at: <http://www.dfo-mpo.gc.ca/science/Publications/annualreport-rapportannuel/ar-ra0708/sect2-eng.htm>

- Green Tech Blog, 2009. *Tidal power barrages and ebb generation*. [Online]
Available at: <http://lifekills.me/2009/02/13/tidal-power-barrages-and-ebb-generation/>
[Accessed 2015].
- Hahn, D. L., 2013. *When electric motors won't do*. [Online]
Available at: <http://machinedesign.com/motorsdrives/when-electric-motors-won-t-do>
- Hayes, M. O., 1967. Relationship between coastal climate and bottom sediment type on the inner continental shelf. *Marine Geology*, pp. 111-132.
- Horrevoets, A., Savenije, H., Schuurman, J. & Graas, S., 2004. The influence of river discharge on tidal damping in alluvial estuaries. *Journal of Hydrology*, p. 213–228.
- Houghton, J. et al., 2001. *Climate Change 2001: The Scientific Basis*. Cambridge: Cambridge University Press.
- IEA, 2007. Implementing Agreement on Ocean Energy Systems (IEA-OES). *International Energy Agency Annual Report 2007*.
- Imambaks, R., 2013. *Energy Storage / Gravity Power Storage*, Delft: Delft University of Technology.
- Inman, D. L. & Nordstrom, C. E., 1971. On the Tectonic and Morphologic Classification of Coasts. *Jour. Geol.*, pp. 1-21.
- International Energy Agency, 2010. *IEA Key stats 2010*. [Online]
Available at: <http://www.iea.org/publications/freepublications/publication/kwes.pdf>
- Itaipu Binacional, 2013. *Itaipu Binacional*. [Online]
Available at: <https://www.itaipu.gov.br/en>
- Ligthart, P., 2012. *Kieuwbalg* [Interview] 2012.
- NEN-6720, 1995. *Voorschriften Beton - Constructieve eisen en rekenmethoden*, s.l.: NEN.
- NEN-6743, 1991. *Geotechniek - Berekeningsmethode voor funderingen op palen*, s.l.: NEN.
- NEN-6786, 2001. *Rules for the design of movable bridges*, s.l.: NEN.
- NEN-8111, 2011. *NTA 8111:2011 Drijvende bouwwerken*, s.l.: s.n.
- NUFFIC, 2013. *Key Figures 2013; Internationalisation in higher education*, s.l.: s.n.
- Ovako, n.d. *Steel for hydraulic applications from Ovako*, s.l.: Ovako.
- Paish, O., 2002. Small hydro power: technology and current status. *Renewable and Sustainable Energy Reviews*, p. 537–556.
- Pascha, K., 2015. *Cost estimates of Tidal Wave Energy Converter components* [Interview] (3 2015).
- Pelletier, B. & McCullen, R., 1972. Sedimentation Patterns in the Bay of Fundy and Minas Basin. In: *Tidal Power*. Halifax: Springer US, pp. 153-187.
- Port of Rotterdam, 2014. *Operationeel stromingsmodel*, s.l.: s.n.
- Renewable Energy Policy Network for the 21st Century, 2010. *Renewables 2010 Global Status Report*, s.l.: s.n.
- Ridderinkhof, H., 1988. Tidal and residual flows in the Western Dutch Wadden Sea I: Numerical model results. *Netherlands Journal of Sea Research*, p. 1–21.
- Robertson, P., Campanella, R., Gillespie, D. & Greig, J., 1986. Use of Piezometer Cone. *Use of In-situ testing in Geotechnical Engineering*, pp. 1263-1280.
- Savenije, H., 2014. [Interview] 2014.
- Savenije, H. H., Toffolon, M., Haas, J. & Veling, E. J., 2008. Analytical description of tidal dynamics in convergent estuaries. *Journal of Geophysical Research: Oceans*.
- Schuttelaars, H. M., de Jonge, V. N. & Chernetsky, A., 2011. *Influence of the length of an estuary on tidal*, Delft: Delft University of Technology.
- Statkraft, 2011. *Osmotic Power - Developing a new, renewable energy source*, s.l.: s.n.

- Swift, D. J. & Lyall, A. K., 1967. Origin of the Bay of Fundy, an interpretation from subbottom profiles. *Marine Geology*, pp. 331 - 343.
- Tabaczek, T., Kulczyk, J. & Zawislak, M., 2007. Analysis of hull resistance of pushed barges in shallow water. *Polish Maritime Research*, pp. 10 - 15.
- The Oildrum, 2012. *World Energy Consumption - Beyond 500 Exajoules*. [Online]
Available at: <http://www.theoildrum.com/node/8936>
- TOPEX/Poseidon, n.d. *Sea surface height altimetry data*, s.l.: s.n.
- US Energy Information Administration, 2014. *Levelized Cost of New Generation Resources in the Annual Energy Outlook 2014*, s.l.: U.S. Department of Energy.
- van Duivendijk, J., n.d. *Waterpower Engineering Principles and Characteristics*. Delft: VSSD.
- Veritec, 1992. *Bergsøysundet floating bridge*, s.l.: s.n.
- Volker Staal en Funderingen, 2015. *Grout (injectie) ankers*. [Online]
Available at: <http://www.vsf.nl/nl/funderingen/ankers/grout-injectie-ankers/grout-injectie-ankers>
- Vroom Funderingstechnieken, 2015. *Prefab betonpalen*. [Online]
Available at: <http://www.vroom.nl/nl/products/15-prefab-betonpalen>
- Ward, D., 1995. *Berlitz Complete Guide to Cruising & Cruise Ships*. Oxford: Berlitz.
- Welleman, J., Dolfing, A. & Hartman, J., 2001. *Basisboek Toegepaste Mechanica*. Delft: Waltman.
- Wikipedia, 2014. *List of dry docks*. [Online]
Available at: http://en.wikipedia.org/wiki/List_of_dry_docks
- Wisselkoers.nl, 2015. *Koers dollar (USD)*. [Online]
Available at: <http://www.wisselkoers.nl/dollar>
- Wyllie, D. C., 1992. *Foundations on Rock (First Edition)*. London: E & FN Spon.
- Wyre Tidal Energy, 2014. *La Rance Barrage*. [Online]
Available at: <http://www.wyretidalenergy.com/tidal-barrage/la-rance-barrage>
- Zanelli, R. & Favrat, D., 1994. *Experimental investigation of a hermetic scroll expander-generator*. s.l., s.n.

Appendices

| | | |
|------------|--|-----|
| Appendix A | The Tide | 173 |
| Appendix B | Near shore tide approximation models | 177 |
| Appendix C | Locations of interest and their tidal constituents | 183 |
| Appendix D | Patents..... | 185 |
| Appendix E | Coastal soil composition..... | 197 |
| Appendix F | Elaboration on energy conversion MCDA | 201 |
| Appendix G | Elaboration on system configuration MCDA..... | 205 |
| Appendix H | Steel pipe piles..... | 211 |
| Appendix I | Precast concrete piles | 219 |
| Appendix J | Foundation anchors..... | 225 |
| Appendix K | Shallow foundation | 229 |
| Appendix L | Financial considerations | 231 |
| Appendix M | Host structure adjustments..... | 235 |
| Appendix N | Piston and rod dimensioning..... | 241 |
| Appendix O | Corrosion of steel elements | 249 |
| Appendix P | Tidal Wave Energy Converter calculation script..... | 251 |
| Appendix Q | Sieve analysis..... | 255 |
| Appendix R | Preliminary feasibility study | 259 |

Appendix A The Tide

The tide is a result of the interaction of the sun and the moon with the water on earth. The gravity of both stellar bodies pulls the water towards them, and the centrifugal force of the sun-earth and moon-earth system pushes it away. This means that the water level is raised in the direction facing the stellar body as well as the direction facing away from it. Subsequently the water level is lowered in the directions perpendicular to the line between those points, as the water flows away from these areas. Figure 85 illustrates how the forces of the lunar tide and the solar tide interact to create neap tide (the lowest possible tide) and spring tide (the highest possible tide).

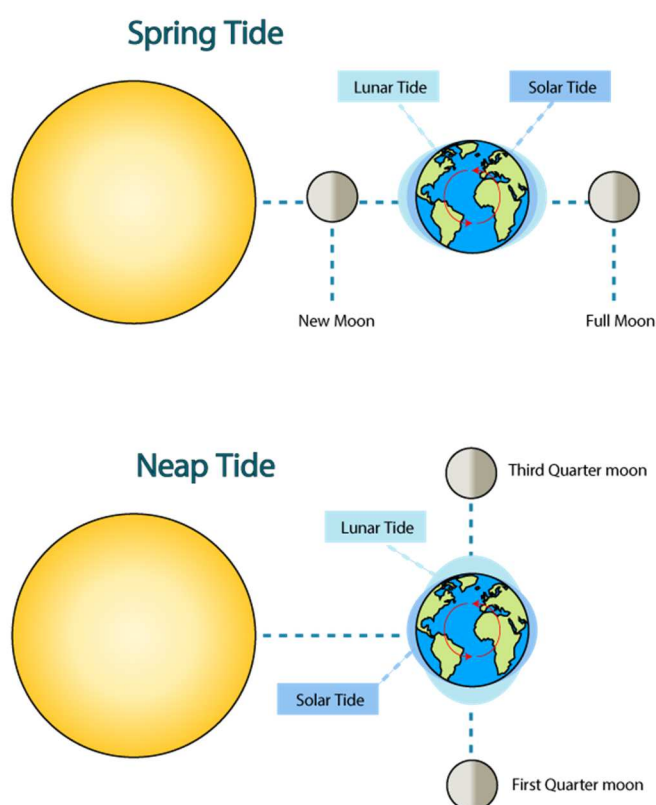


Figure 85 - Workings of the tide

A.1 Primary constituents

The tide consists of a set of eleven primary tidal constituents that make up a large sinusoidal function as given in Equation 9. The eleven primary tidal constituents are M_M , M_F , K_1 , O_1 , P_1 , Q_1 , M_2 , S_2 , N_2 , K_2 and M_4 . The periods and angular velocities of these constituents are given in Table 70 along with the names of the constituents. In the following paragraphs an explanation will be given regarding what these constituents actually represent.

$$z(t) = z_0 + \sum_{i=1}^{11} A_n \cdot \cos(\omega_n + \varphi_n)$$

$$z = \text{waterlevel} [m]$$

$$A = \text{amplitude} [m]$$

$$\omega = \text{rotationalvelocity} [^\circ/hr]$$

$$\varphi = \text{phaseshift} [^\circ]$$

Equation 9 – Summation of harmonic motion

| Constituent | Abbreviation | T [h] | ω [$^\circ \text{ h}^{-1}$] |
|-----------------------------------|--------------|----------|--------------------------------------|
| Semidiurnal lunar | M_2 | 12.4206 | 28.984 |
| Semidiurnal solar | S_2 | 12.0000 | 30.000 |
| Larger lunar elliptic semidiurnal | N_2 | 12.6583 | 28.439 |
| Lunisolar semidiurnal | K_2 | 11.9672 | 30.082 |
| Lunisolar diurnal | K_1 | 23.9345 | 15.041 |
| Lunar diurnal | O_1 | 25.8193 | 13.943 |
| Solar diurnal | P_1 | 24.0659 | 14.958 |
| Larger lunar elliptic diurnal | Q_1 | 26.8684 | 13.399 |
| Forthnightly lunar | M_f | 327.8599 | 1.098 |
| Monthly lunar | M_m | 661.3112 | 0.544 |
| Shallow water lunar overtide | M_4 | 6.2103 | 57.971 |

Table 70 - Periods and angular velocities of primary tidal constituents

A.2 Semi-diurnal tides

M_2 is the semi-diurnal lunar tidal constituent. It is determined through the idealised situation where the earth is completely covered by water and the earth-lunar system creates two bulges as previously described. This means that its high tide occurs twice within a full rotation of the earth around its axis and has a period of once every 12.42 hours. S_2 is the semi diurnal solar tidal constituent. Its basic principle is the same as the earth rotates once a day and the sun's gravitational force therefore also revolves around the earth's axis once a day. The previously explained bulges pass each location on earth twice a day. The period of this constituent is once every 12 hours. N_2 is the larger lunar elliptic semi-diurnal and simulates the cycle of perigee to perigee. It is an artificial constituent that compensates for the monthly varying difference in the distance between the earth and the moon from perigee to perigee. Together with the, usually negligible, L_2 smaller elliptic tidal constituent it is in phase at perigee (moon closest to Earth) and out of phase at apogee (moon furthest from Earth) each occurring once every anomalistic month. Its period is once every 12.66 hours. The K_2 lunisolar semidiurnal tidal constituent is the modulation of the M_2 and S_2 tides for the declination of the earth.

A.3 Diurnal tides

K_1 , O_1 and P_1 are respectively the diurnal lunisolar, diurnal lunar and diurnal solar tidal constituent compensate for diurnal inequality. Because the moon and the sun's orbit are slightly tilted relative to the earth's equator the tidal bulges are unequal to each other. The K_1 tidal constituent has a period of once every 23.93 hours, the O_1 constituent has a period of 25.82 hours and the P_1 tidal constituent has a period of 24.07 hours. These constituents are in phase (K_1 with O_1 and K_1 with P_1 not necessarily simultaneously) once every half of a tropical month (the time between crossings of the moon across the equator) when the gravitational pull of the stellar body they relate to is maximal. Q_1 is the larger lunar elliptic diurnal and compensates for the inequality of the bulges created by N_2 . Its period is 26.87 hours.

A.4 Long period tides

M_M is the monthly lunar tidal constituent compensating for the varying distance between the moon and the earth. The elliptical shape of the moon's orbit around the earth means it is not equally close and does not exert an equal force on the ocean waters at all times. Once a month, at perigee, the moon is closest to the Earth and the forces are largest. Once a month exactly in between two perigees, at apogee, the gravitational pull by the moon is smallest. This tidal constituent has a period of 661.31 hours (27.55 days).

M_F is the fortnightly lunar tidal constituent. A fortnight being old English for a period of two weeks means this tidal constituent has a period of 327.86 hours (13.66 days). The constituent is caused by the declination of the moon's orbit relative to the earth's equator meaning that half of its orbit it is closer to the northern hemisphere and the other half it is closer to the southern hemisphere.

A.5 Shallow water tides

Shallow water tides occur when the tidal waves reaches shallow water conditions and the shape of the wave changes. Shallow water occurs when the water depth is much smaller than half the wave length. For semi-diurnal tides this means the water is considered shallow when its depth is much smaller than a quarter of the Earth's circumference (in the order of 10,000 km), which comes down to being everywhere on Earth. The dominant and usually only relevant shallow water tidal constituent is the M_4 lunar overtide with a period of 6.21 hours.

Appendix B Near shore tide approximation models

B.1 Basin model mathematical background

The model for open basins is based on a simple storage equation as depicted in Equation 10.

$$B \cdot \frac{\partial h}{\partial t} = \mu \cdot A_s \cdot \sqrt{2 \cdot g \cdot (|h_{basin} - h_{ocean}|)} + Q_r$$

B = storage area

μ = contraction coefficient

A_s = flow area

Q_r = river discharge

$$z(t) = z_0 + \sum_{i=1}^{11} A_n \cdot \cos(\omega_n + \varphi_n)$$

z = water level

A = amplitude

ω = rotational velocity

φ = phase shift

Equation 10 – Storage equation and summation of harmonic motion

B.2 Estuary model mathematical background

The estuary model is based on the research of Prof. dr. ir. H.H.G. Savenije which was done in 2008 and is described in (Savenije, Toffolon, Haas, & Veling, 2008). It uses a set of iterative dimensionless formulae to calculate the tide in subsequent upstream intervals based on the damping number (δ), the phase lag between high water and high water slack (ϵ), the celerity number (λ) and the velocity number (μ). Through the iterative equations for these variables and the determining factors of the shape number (γ) and the friction number (χ) these equations can calculate the damping in an estuary in amplitude as well as velocity. Equation 11 shows these characteristic relations of the estuary and basic equations.

$$\chi = r_s \cdot f \cdot \frac{c_0}{\omega \cdot h} \cdot \zeta \quad \gamma = \frac{c_0}{\omega \cdot b} \quad \zeta = \frac{\eta}{h}$$

$$f = \frac{g}{K^2 \cdot \frac{1}{h^3}} \cdot \frac{1}{1 - \left(\frac{4 \cdot \eta}{3 \cdot h} \right)^2} \quad c_0 = \sqrt{\frac{g \cdot h}{r_s}}$$

Equation 11 – Characteristic estuary relations

A distinction in this can be made between mixed waves and standing waves, in which mixed waves propagate along the estuary and standing waves do not have a moving location of their peaks and troughs, they are also characterised by the lack of phase lag between the tidal velocity oscillation and amplitude oscillation. This distinction is made through the critical estuary number in

which standing waves occur when the estuary number is higher than this critical value and the wave is mixed when the estuary number is smaller than the critical value. Equation 12 shows the equation that determines the critical estuary number.

$$\gamma_c = \frac{1}{3 \cdot \chi} \cdot \left[\frac{m_1}{2} - 1 + 2 \cdot \frac{12 \cdot \chi^2 + 1}{m_1} \right]$$

$$m_1 = \left[36 \cdot \chi^2 \cdot (3 \cdot \chi^2 + 8) - 8 + 12 \cdot \chi \cdot \sqrt{3} \cdot \sqrt{(\chi^2 - 2)^2 \cdot (27 \cdot \chi^2 - 4)} \right]^{\frac{1}{3}}$$

Equation 12 – Critical estuary number

The first family of equations is for the mixed waves and applies when $\gamma < \gamma_c(\chi)$. Equation 13 gives the relations for this scenario.

$$\mu_m = \sqrt{\frac{1}{3 \cdot \chi} \cdot \left(m - \gamma + \frac{\gamma^2 - 6}{m} \right)}$$

$$m = \left[27 \cdot \chi + (9 - \gamma^2) \cdot \gamma + 3 \cdot \sqrt{3} \cdot \sqrt{27 \cdot \chi^2 + 2 \cdot (9 - \gamma^2) \cdot \gamma \cdot \chi + 8 - \gamma^2} \right]^{\frac{1}{3}}$$

$$\delta = \frac{\gamma - \chi \cdot \mu^2}{2}$$

$$\tan(\varepsilon) = \frac{\lambda}{\gamma - \delta}$$

$$\lambda = \sqrt{(1 - \delta)(\gamma - \delta)}$$

Equation 13 – First family estuary tidal propagation coefficients

The second family of equations is for standing waves and applies when $\gamma > \gamma_c(\chi)$. Equation 14 gives the, much simpler, relations for this scenario.

$$\mu = \delta = \frac{\gamma}{2} - \frac{1}{2} \cdot \sqrt{\gamma^2 - 4}$$

$$\lambda = \varepsilon = 0$$

Equation 14 – Second family estuary tidal propagation coefficients

By iteratively solving the aforementioned equations and accounting for the possible changing nature of the wave along the estuary the damping number, celerity number, velocity number and phase lag can be calculated and subsequently the tidal amplitude as it propagates along the estuary can be calculated through Equation 15.

$$\frac{\partial \eta}{\partial x} = \eta \cdot \frac{\omega}{c_0} \cdot \delta$$

$$\eta_{i+1} = \eta_i + \eta_i \cdot \frac{\omega}{c_0} \cdot dx \cdot \delta$$

Equation 15 – Iterative tidal wave propagation

B.3 Basin model MatLab code

```

%% Basin
clear,clc
L=40000;           % Length of the basin           [m]
B=9000;            % Width of the basin           [m]
mu=1;              % Contraction coefficient       [-]
g=9.81;            % Gravitational constant       [m s^-2]
Qr=0;              % River discharge           [m^3s^-2]
Bs=L*B;            % Storage area           [m^2]
t=0;               % Start time           [s]
Hm=0;              % Mean seawater level       [m]
h3=0;              % Initial water level in bay [m]
Hd=-20;            % Height of the inflow bottom [m]
As=(Hm-Hd)*4000;   % Flow area of the canal      [m^2]

%Tidal Constituents%
omegaM2 = 28.984;   % Angular velocity of the M2 tide [deg/h]
omegaS2 = 30.000;   % Angular velocity of the S2 tide [deg/h]
omegaN2 = 28.439;   % Angular velocity of the N2 tide [deg/h]
omegaK2 = 30.082;   % Angular velocity of the K2 tide [deg/h]
omegaK1 = 15.041;   % Angular velocity of the K1 tide [deg/h]
omegaO1 = 13.943;   % Angular velocity of the O1 tide [deg/h]
omegaP1 = 14.958;   % Angular velocity of the P1 tide [deg/h]
omegaQ1 = 13.399;   % Angular velocity of the Q1 tide [deg/h]
omegamf = 01.098;   % Angular velocity of the mf tide [deg/h]
omegamm = 00.544;   % Angular velocity of the mm tide [deg/h]
omegaM4 = 57.971;   % Angular velocity of the M4 tide [deg/s]
phiM2 = 40.72;      % Phase shift of the M2 tide      [deg]
phiS2 = 101.69;     % Phase shift of the S2 tide      [deg]
phiN2 = 31.96;      % Phase shift of the N2 tide      [deg]
phiK2 = 120.56;     % Phase shift of the K2 tide      [deg]
phiK1 = 350.68;     % Phase shift of the K1 tide      [deg]
phiO1 = 187.44;     % Phase shift of the O1 tide      [deg]
phiP1 = 358.45;     % Phase shift of the P1 tide      [deg]
phiQ1 = 129.83;     % Phase shift of the Q1 tide      [deg]
phimf = 249.54;     % Phase shift of the mf tide      [deg]
phimm = 199.35;     % Phase shift of the mm tide      [deg]
phiM4 = 88.11;      % Phase shift of the M4 tide      [deg]
AM2 = 1.2855;       % Amplitude of the M2 tide        [m]
AS2 = 0.3104;       % Amplitude of the S2 tide        [m]
AN2 = 0.1622;       % Amplitude of the N2 tide        [m]
AK2 = 0.0832;       % Amplitude of the K2 tide        [m]
AK1 = 0.0756;       % Amplitude of the K1 tide        [m]
AO1 = 0.0871;       % Amplitude of the O1 tide        [m]
AP1 = 0.0106;       % Amplitude of the P1 tide        [m]
AQ1 = 0.0280;       % Amplitude of the Q1 tide        [m]
Amf = 0.0097;       % Amplitude of the mf tide        [m]
Amm = 0.0081;       % Amplitude of the nn tide        [m]
AM4 = 0.1097;       % Amplitude of the M4 tide        [m]

```

```
%Calculation%

for i=1:1:24*4440
    dt=1/360;

H1(i)=Hm+AM2*cosd(omegaM2*t+phiM2)+AS2*cosd(omegaS2*t+phiS2)+AN2*cosd(omegaN2*t+phiN2)+AK2*cosd(omegaK2*t+phiK2)+AK1*cosd(omegaK1*t+phiK1)+A01*cosd(omegaO1*t+phiO1)+AP1*cosd(omegaP1*t+phiP1)+AQ1*cosd(omegaQ1*t+phiQ1)+Amf*cosd(omegamf*t+phimf)+Amm*cosd(omegamm*t+phimm)+AM4*cosd(omegaM4*t+phiM4);
    d(i)=Hd;
    if h3>=H1(i)
        if h3-Hd>=(2/3)*(H1(i)-Hd)
            dh3(i)=-(mu*As*sqrt(2*g*abs((h3-H1(i))))-Qr)/Bs;
        else
            dh3(i)=-(mu*As*sqrt(2*g*abs(((H1(i)-Hd)-(2/3)*(H1(i)-Hd))))-Qr)/Bs;
        end
    else
        if h3-Hd>=(2/3)*(H1(i)-Hd)
            dh3(i)=(mu*As*sqrt(2*g*abs((H1(i)-h3)))+Qr)/Bs;
        else
            dh3(i)=(mu*As*sqrt(2*g*abs(((H1(i)-Hd)-(2/3)*(H1(i)-Hd))))+Qr)/Bs;
        end
    end
    Q(i)=dh3(i)*Bs;
    h(i)=h3+dh3(i);
    h3=h(i);
    tt(i)=t;
    t=t+dt;
    nul(i)=0;
    d(i)=Hd;
    He(i)=abs(H1(i)-h(i));
    P(i)=8*Q(i)*He(i);
end

per=max(h)/max(H1);
per2=min(h)/min(H1);
pksH1 = findpeaks(H1);
pksh = findpeaks(h);
H1r=(max(pksH1)+min(pksH1))/2;
hr=(max(pksh)+min(pksh))/2;

figure(1)
plot(tt,h,'-c',tt,H1,'-b','linewidth',3);
legend('Tide inside the basin','Ocean tide');
grid on
```

B.4 Estuary model MatLab code

```

%% Estuary (Eems-Dollard)
clear,clc
dx=100;
h0=13;
g=9.81;
a1=30000;
a2=30000;
rs=1.4;
omega=2*3.14/((360/28.984)*3600);
eta(1)=1.35;
K=38;
h(1)=h0;
c0(1)=sqrt(g*h(1)/rs);

for i=1:1:90000/dx
    x(i)=i*dx;
    rs=1.4;
    if x<20000
        h(i)=h0-(x(i)/4000);
        gamma(i)=c0(i)/(omega*a1);
    elseif x<25000
        h(i)=h0-(20000/4000)-((x(i)-20000)/10000);
        gamma(i)=c0(i)/(omega*a1);
    elseif x<35000
        h(i)=h0-(20000/4000)-(5000/10000)-((x(i)-25000)/10000);
        rs=2;
        gamma(i)=c0(i)/(omega*a1);
    elseif x<60000
        h(i)=h0-(20000/4000)-(15000/10000)-((x(i)-35000)/10000);
        gamma(i)=c0(i)/(omega*a1);
    elseif x<70000
        h(i)=h0-(20000/4000)-(5000/10000)-(35000/10000)+((x(i)-
60000)/10000);
        gamma(i)=c0(i)/(omega*a1);
    else
        h(i)=h0-(20000/4000)-(5000/10000)-
(35000/10000)+(10000/10000);
        gamma(i)=c0(i)/(omega*a2);
    end

    c0(i+1)=sqrt(g*h(i)/rs);
    zeta(i)=eta(i)/h(i);
    f(i)=(g/(K^2*h(i)^(1/3)))*(1/(1-(4*eta(i)/(3*h(i)))^2));
    chi(i)=rs*f(i)*c0(i)*zeta(i)/(omega*h(i));

```

```

    m1(i)=(36*chi(i)^2*(3*chi(i)^2+8)-
8+12*chi(i)*sqrt(3)*sqrt((chi(i)^2-2)^2*(27*chi(i)^2-4)))^(1/3);
    gammac(i)=(m1(i)/2-1+2*(12*chi(i)^2+1)/m1(i))/(3*chi(i));

    q(i)=gamma(i)-gammac(i);

    if gamma(i)<gammac(i)
        %Savenijeb 2008
        m(i)=(27*chi(i)+(9-
gamma(i)^2)*gamma(i)+3*sqrt(3)*sqrt(27*chi(i)^2+2*(9-
gamma(i)^2)*gamma(i)*chi(i)+8-gamma(i)^2))^(1/3);
        mu(i)=sqrt((m(i)-gamma(i)+(gamma(i)^2-6)/m(i))/(3*chi(i)));
        delta(i)=(gamma(i)-chi(i)*mu(i)^2)/2;
        lambda(1)=1;
        lambda(i+1)=sqrt(1-delta(i)*(gamma(i)-delta(i)));
        epsilon(i)=atan(lambda(i)/(gamma(i)-delta(i)));
    else
        mu(i)=(gamma(i)-sqrt(gamma(i)^2-4))/2;
        delta(i)=mu(i);
        lambda(i+1)=0;
        epsilon(i)=0;
    end
    nu(i)=mu(i)*rs*eta(i)*c0(i)/h(i);
    eta(i+1)=eta(i)+eta(i)*omega*dx*delta(i)/c0(i);
    etah(i)=eta(i);
    etal(i)=-eta(i);
    hm(i)=0;
    xk(i)=x(i)/1000;

end
x(i+1)=x(i)+dx;
xk(i+1)=x(i+1)/1000;
delta(i+1)=delta(i);
q(i+1)=q(i);
h(i+1)=h(i);
etah(i+1)=etah(i);
etal(i+1)=etal(i);
nu(i+1)=nu(i);
hm(i+1)=0;

figure(1);
plot(xk,etah,'-b',xk,etal,'-c',xk,-h,'-k','linewidth',3);
axis([0 90 -15 5])
legend('maximum water level','minimum water level','bottom profile')
grid on
xlabel('Upstream distance [km]')
ylabel('Water level [m]')

```

Appendix C Locations of interest and their tidal constituents

For the determined locations of interest in the Dutch hydrologic system the latitude and longitude are obtained from Google Maps. These values have subsequently been inserted into the Tidal Model Driver to obtain the values for the tidal amplitudes and phase shifts. The results are displayed in Table 71. It should be noted that the phase shift is determined to fit the curve of the tidal motion with the tide at the moment of extracting data, so for two different requests at the same location the phase shift would vary. For the application of these constituents, however, the relative shift of the constituents to each other gives sufficient data.

| Location | | Western Scheldt | Eastern Scheldt | Grevelingen | Haringvliet | Nieuwe Waterweg | Lauwersmeer | Eems |
|----------------------|---|-----------------|-----------------|--------------|--------------|-----------------|--------------|---------|
| Type | | Estuary | Open basin | Closed basin | Closed basin | Estuary | Closed basin | Estuary |
| Latitude | | 51.4382 | 51.6329 | 51.7674 | 51.8621 | 51.9840 | 53.4194 | 53.4962 |
| Longitude | | 3.4044 | 3.6893 | 3.8267 | 4.0148 | 4.0718 | 6.1688 | 6.9296 |
| M₂ | A | 1.5335 | 1.2845 | 1.2154 | 1.1284 | 0.8927 | 0.9725 | 0.9962 |
| | φ | 20.88 | 42.04 | 51.45 | 66.94 | 76.57 | 250.07 | 275.88 |
| S₂ | A | 0.4147 | 0.3097 | 0.2837 | 0.2523 | 0.1967 | 0.1978 | 0.1887 |
| | φ | 78.40 | 102.09 | 113.65 | 132.62 | 141.64 | 316.16 | 343.81 |
| N₂ | A | 0.2234 | 0.1618 | 0.1484 | 0.1367 | 0.1126 | 0.0943 | 0.0891 |
| | φ | 8.38 | 32.37 | 45.18 | 65.51 | 76.55 | 242.31 | 278.59 |
| K₂ | A | 0.1163 | 0.0830 | 0.0762 | 0.0705 | 0.0572 | 0.0579 | 0.0542 |
| | φ | 94.25 | 121.02 | 135.41 | 157.92 | 170.53 | 331.99 | 8.21 |
| K₁ | A | 0.0685 | 0.0757 | 0.0782 | 0.0801 | 0.0816 | 0.0675 | 0.0567 |
| | φ | 349.16 | 350.71 | 351.21 | 352.72 | 352.09 | 11.23 | 18.38 |
| O₁ | A | 0.0833 | 0.0871 | 0.0884 | 0.0885 | 0.0883 | 0.0674 | 0.0647 |
| | φ | 183.67 | 187.50 | 188.53 | 191.29 | 190.29 | 213.57 | 228.56 |
| P₁ | A | 0.0094 | 0.0106 | 0.0110 | 0.0113 | 0.0113 | 0.0095 | 0.0092 |
| | φ | 352.43 | 358.53 | 0.15 | 4.20 | 4.00 | 16.90 | 24.18 |
| Q₁ | A | 0.0278 | 0.0280 | 0.0280 | 0.0277 | 0.0271 | 0.0144 | 0.0131 |
| | φ | 124.27 | 129.92 | 131.73 | 135.96 | 135.88 | 172.58 | 185.93 |
| M_F | A | 0.0096 | 0.0097 | 0.0098 | 0.0098 | 0.0098 | 0.0107 | 0.0109 |
| | φ | 250.75 | 249.53 | 249.08 | 249.15 | 249.06 | 238.69 | 238.58 |
| M_M | A | 0.0080 | 0.0081 | 0.0082 | 0.0082 | 0.0082 | 0.0088 | 0.0089 |
| | φ | 199.69 | 199.35 | 199.25 | 199.33 | 199.36 | 198.71 | 199.23 |
| M₄ | A | 0.1213 | 0.1100 | 0.1235 | 0.1229 | 0.1161 | 0.0553 | 0.0432 |
| | φ | 38.38 | 88.79 | 104.84 | 120.26 | 115.84 | 45.16 | 115.21 |

Table 71 - Locations and constituents of research locations

Appendix D Patents

| | |
|----------------------|--|
| Title: | <i>"Tidal wave energy-storing power generation system"</i> |
| Patent Number: | CN202579018 (U) |
| Patent office: | China Patent & Trademark Office |
| Date of application: | December 5 th 2012 |
| Abstract: | <p>The utility model relates to the technical field of a power generation device, in particular to a tidal wave energy-storing power generation system. The tidal wave energy-storing power generation system comprises devices for converting water energy to air pressure, an air storing device, a device for converting the air pressure into electric energy, and a detection control device, wherein each device for converting the water energy to the air pressure comprises a water turbine and a spiral air compressor; an output end of each spiral air compressor is communicated with an input end of the air storing device; the air storing device is connected with the device for converting the air pressure into the electric energy; and each spiral air compressor is electrically connected with the detection control device. Compared with the prior art, according to the tidal wave energy-storing power generation system disclosed by the utility model, the energy of tidal waves is converted into compressed air potential energy and the air potential energy is converted into mechanical energy of a flywheel; then the mechanical energy is converted into the electric energy by a generator and the electric energy is stably output through controlling output frequency and voltage of the generator with the corresponding power; and the tidal wave energy-storing power generation system has the characteristic of environment-friendly power generation.</p> |

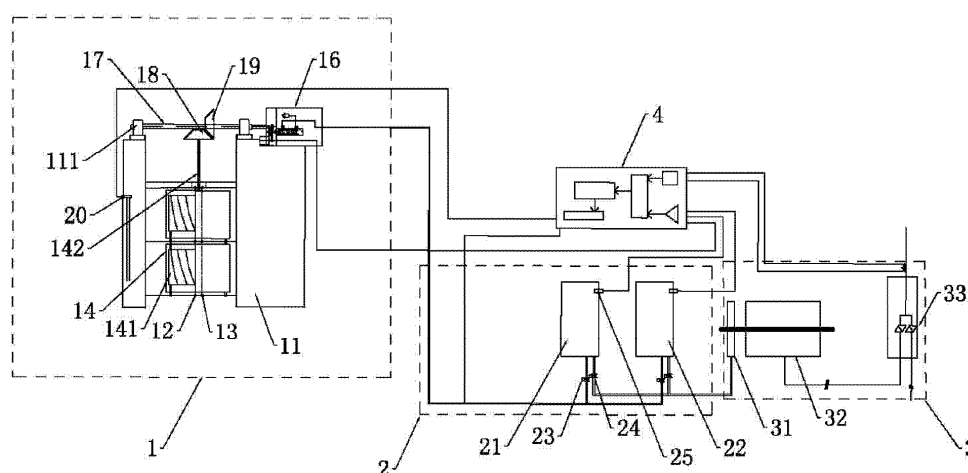


Figure 86 - Schematic drawing of the Tidal wave energy-storing power generation system

| | |
|----------------------|--|
| Title: | <i>"Apparatus for harnessing the vertical movement of ocean tides and utilize the force for generating electrical energy."</i> |
| Patent Number: | US3668412 |
| Patent office: | United States Patent and Trademark Office |
| Date of application: | June 6 th 1972 |
| Abstract: | An apparatus for harnessing the vertical movement of ocean tides and utilize the force for generating electrical energy, the apparatus being based upon the principal of a large float which exerts force upwardly at a time of a risen tide and a downward force due to gravity at a time of a fallen tide, said float is first securely captivated to the level of the prevailing low tide and which is then released at the height of the tide in order to contribute its full built up force of available energy, the vertical movements of the float being transmitted from a vertical superstructure mounted upon the float to a rotatable gear mounted upon a rotatable horizontal shaft journalled in stationary stanchions, and the rotatable shaft thus driving an electrical generator or performing other useful work. |

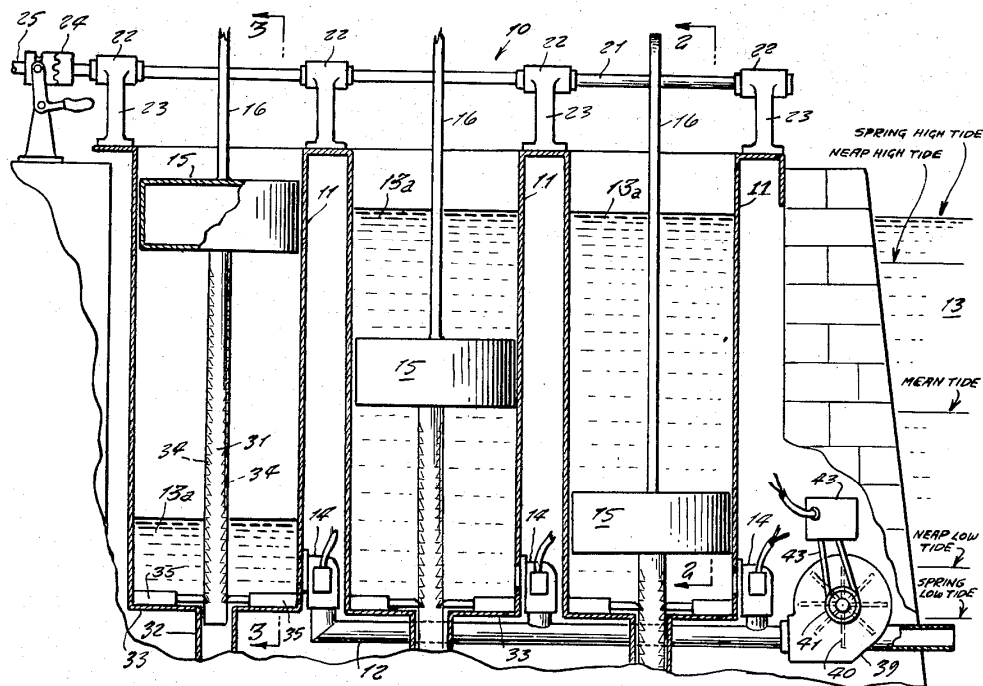


Figure 87 - Schematic drawing of the apparatus

| | |
|----------------------|--|
| Title: | "Ocean tide and wave energy converter" |
| Patent Number: | US4034231 |
| Country of Origin: | United States Patent and Trademark Office |
| Date of application: | July 5 th 1977 |
| Abstract: | A machine for harnessing the motion of ocean waves in order to convert the motion energy into useful electrical power; the machine consisting of a large V-shaped frame, submerged near a beach, having its apex pointed away from the beach, and the frame supporting a series of water turbines connected to an electric generator so that incoming waves toward a beach move along the outer side of the frame while turning the turbine rotors, and outgoing waves moving along the inner side of the frame so to likewise influence turning the turbine rotors. |

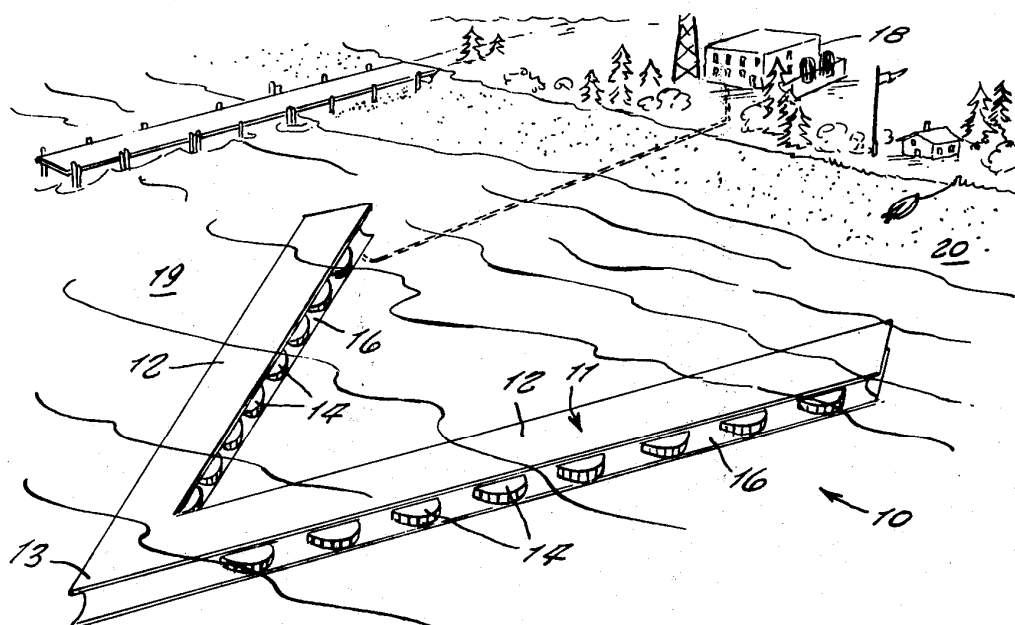


Figure 88 - Schematic drawing of the ocean tide and wave energy converter

| | |
|----------------------|--|
| Title: | "Apparatus for harnessing tidal power" |
| Patent Number: | US4103490 |
| Patent office: | United States Patent and Trademark Office |
| Date of application: | August 1 st 1978 |
| Abstract: | An apparatus for harnessing and extracting a portion of the power generated by the rise and fall of ocean tides. A tidal chamber is provided wherein the rise of the tide creates positive air pressure within the tidal chamber and the fall of the tide creates a partial vacuum within the tidal chamber. The pressure and partial vacuum are, through appropriate valving, used to drive a pair of reciprocating, fluid-coupled rod and float assemblies, the motions of which can be harnessed to operate an air compressor, crank shaft, flywheel or other suitable mechanical device. |

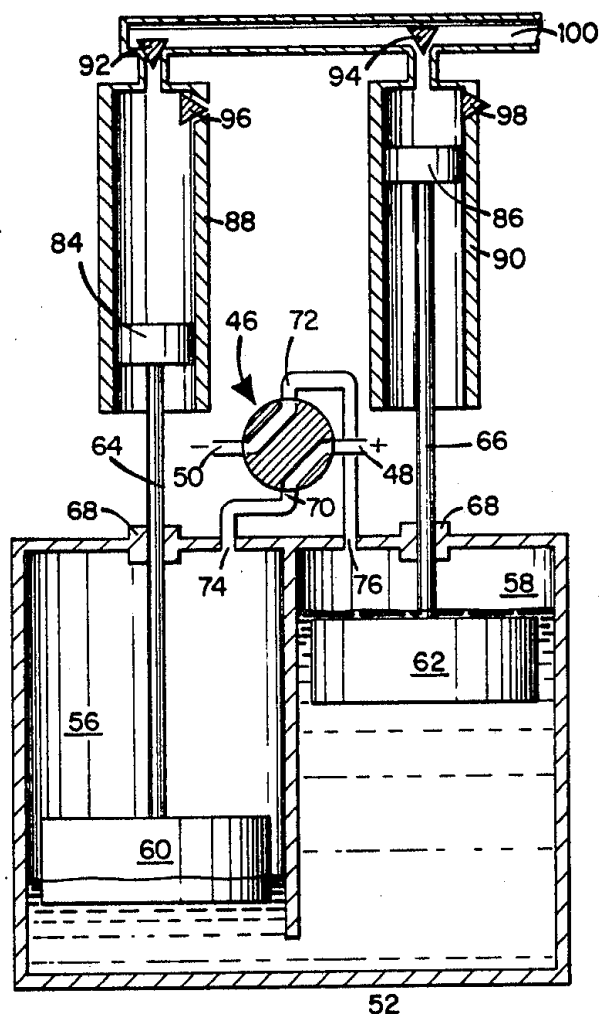


Figure 89 - Schematic drawing of the apparatus

| | |
|----------------------|---|
| Title: | <i>"Ocean tide energy converter having improved efficiency."</i> |
| Patent Number: | US4185464 |
| Patent office: | United States Patent and Trademark Office |
| Date of application: | January 29 th 1980 |
| Abstract: | <p>A tide motor useful for converting periodic rising and falling water levels to useful work such as electric power generation includes a primary piston having a large enclosed chamber that can selectively be filled with air for generation of upward thrust when submerged in rising tidal water or filled with water for generating downward gravitational thrust when the piston is suspended in air above a dropping tidal water level. Cyclic filling and emptying of the chamber is programmed to coordinate piston positions and water level positions, and the piston can be locked in either up or down position to achieve maximum floatation and gravitational thrust forces. An auxiliary piston is connected to the lower area of the primary piston chamber by a valve conduit so the primary piston chamber can be filled with water at its high position while it is locked up by releasing the auxiliary piston to float upwardly with its water chamber filled, and placing the primary and auxiliary piston chambers in communication with each other so water flows from the latter into the former until the primary piston chamber is filled with water before it begins its downward stroke after the water level has dropped below it. After the primary piston has completed its downward stroke, its interior chamber is drained and sealed in preparation for its next upward stroke on the next rising tide, and the water chamber of the auxiliary piston is refilled in preparation for the next cycle of operation.</p> |

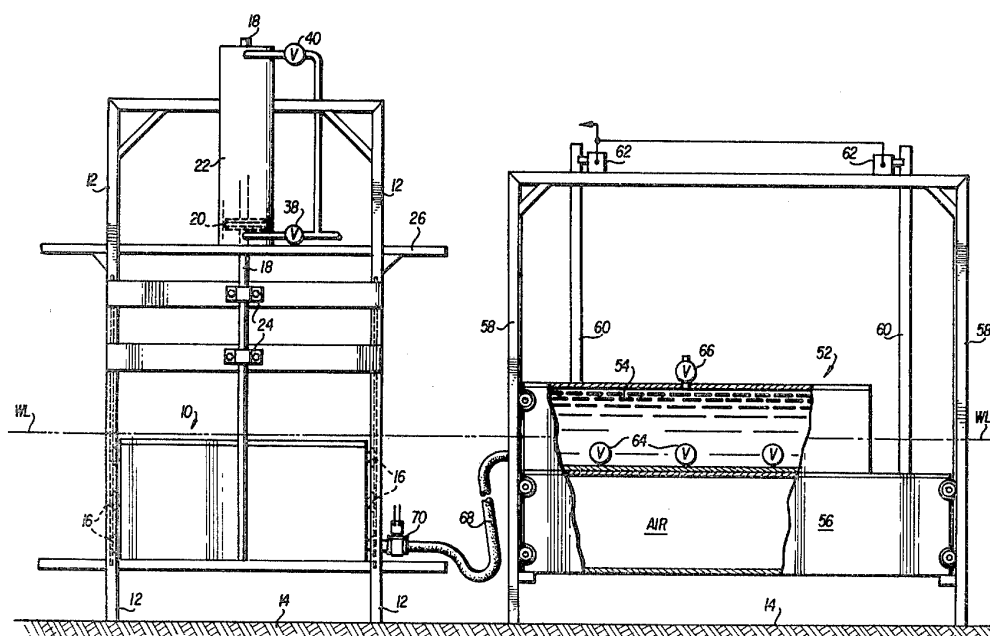


Figure 90 - Schematic drawing of the ocean tide energy converter

| | |
|----------------------|--|
| Title: | "Ocean tide energy converter" |
| Patent Number: | US4208878 |
| Patent office: | United States Patent and Trademark Office |
| Date of application: | June 24 th 1980 |
| Abstract: | <p>A tide motor energy source includes a tidal piston with a valved chamber. The piston drives a hydraulic ram to generate electrical power through a pressure accumulator and hydraulic motor. The ram can be locked hydraulically to enable the tidal piston to be held fixed at a desired elevation and the valves in the chamber permit it to be filled with water or air. The piston with its chamber filled with air at its low tide position and then released for controlled ascent while submerged acts as a submerged float for driving the ram upwardly while the tide runs in during one phase of its operation. The piston with its chamber filled with water while locked at its highest position as the tide begins to run out, and then released to fall under control acts as a weight suspended in air after the water level drops below the piston for driving the ram downwardly during the second phase of its operation. The rising and falling motion of the tidal piston is used as the energy source.</p> |

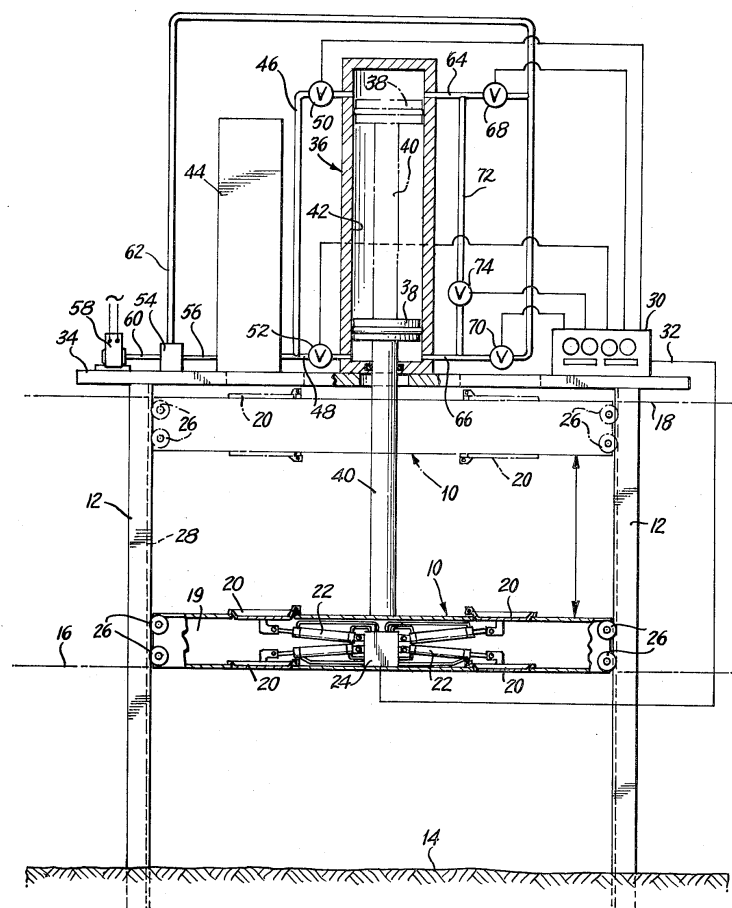


Figure 91 - Schematic drawing of the ocean tide energy converter

| | |
|----------------------|--|
| Title: | <i>"Multiple gas phase tidal power generation apparatus and method"</i> |
| Patent Number: | US5184936 |
| Patent office: | United States Patent and Trademark Office |
| Date of application: | February 9 th 1993 |
| Abstract: | <p>A tidal power generation apparatus includes a first group of containers fixed in plural piles in a natural sea having a tidal difference in sea level height, which containers are spaced in parallel to one another at fixed intervals, each container of which is opened at a lower side thereof and is capable of holding air therein, a second group of containers fixed in plural piles in tideless water within an artificial dam, which second group of containers are spaced parallel to one another at fixed intervals, each container of which is opened at a lower side thereof and is capable of holding air therein, and air pipes providing communication between the respective containers of the first group in the natural sea and respective containers of the second group within the artificial dam. With the apparatus, the energy in a tide is collected in the form of energy in compressed air created by water pressure at high tide. The compressed air is stores within the artificial dam and, at low tide, is transferred to a container situated at a relatively deeper position in the natural sea to obtain compressed air of even larger energy at the next high tide. Repetition of the above steps enables gathering of tidal energy otherwise dispersed over a wide area.</p> |

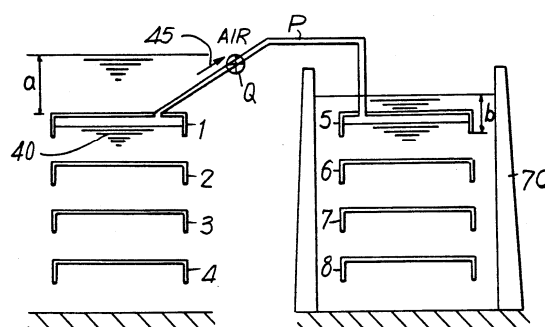


FIG. 2

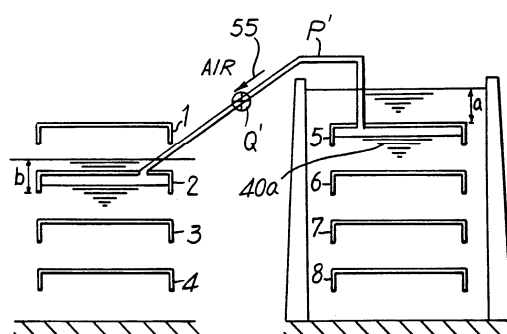


FIG. 3

Figure 92 - Schematic drawing of the apparatus

| | |
|----------------------|--|
| Title: | "Tidal generator" |
| Patent Number: | US5426332 |
| Patent office: | United States Patent and Trademark Office |
| Date of application: | June 20 th 1995 |
| Abstract: | An electric power generator apparatus that generates electrical power from the tidal movements of a body of water by employing multiple energy producing systems. Those energy producing systems include: (1) a moveable tank system associated with hydraulic cylinders in which the upward and downward movements of the tank relative to the tide are used to generate electrical power; (2) an enclosure system in which the controlled inflow and outflow of water between the enclosure and the surrounding body of water is used to generate electrical power; (3) a bellows system in which the effects of the tidal movements are used to force water from the bellows tank through a generator thereby producing electrical power; and (4) a buoyant mass-actuated piston system in which the movement of floating objects (such as docked ships) relative to the tide is used to generate electrical power. |

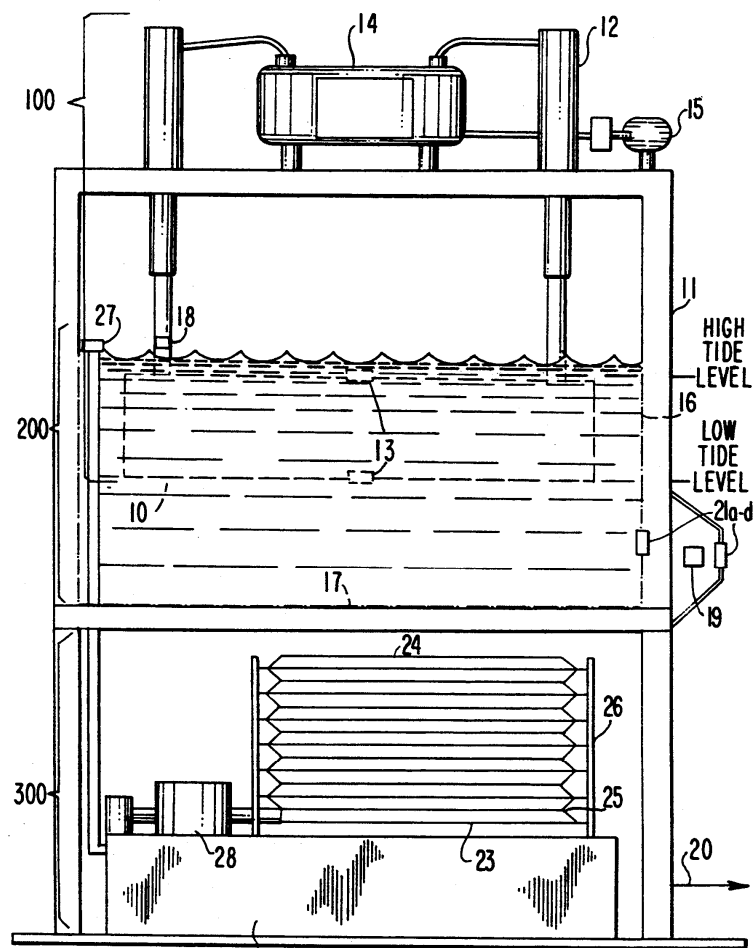


Figure 93 - Schematic drawing of the tidal generator

| | |
|----------------------|---|
| Title: | <i>"Power generation directly from compressed air for exploiting wind and solar power"</i> |
| Patent Number: | US8347628 |
| Patent office: | United States Patent and Trademark Office |
| Date of application: | January 8 th 2013 |
| Abstract: | This invention relates to a Compressed Air Turbine-Generator, or CAT-G that will enable the ability to manage energy gathered from ecologically friendly sources, such as solar and wind power. Compressed Air Energy Storage, (C.A.E.S.), is a promising mode of clean energy storage. A major challenge facing this technology is the need to efficiently convert the compressed air energy into electricity. Conventionally, high-pressure air is used only to improve the efficiency of a conventional hot powered turbine generator. The focus herein is on a new technology that efficiently converts the energy stored in compressed air directly into electrical power without producing greenhouse by-product gases or other pollutants. This new capability will add important flexibility to the optimization of ecologically friendly energy systems. |

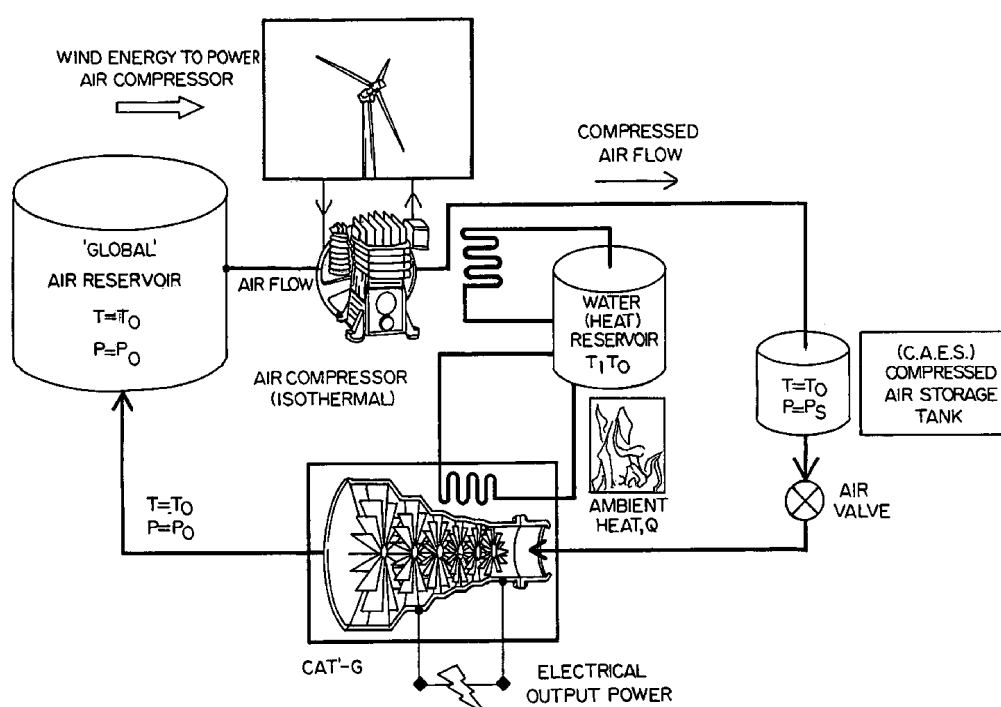


Figure 94 - Schematic drawing of the process

| | |
|----------------------|---|
| Title: | <i>"Pressure to electric converter PEC"</i> |
| Patent Number: | US20020145350 |
| Patent office: | United States Patent and Trademark Office |
| Date of application: | October 10 th 2002 |
| Abstract: | <p>The PEC is utility device designed to convert intermittent pressure into electrical charges. It may be implemented in a variety of forms. The easiest to describe is the mechanical floor plate. It consists of depress-able track mounted plates with small barrel electrical generators attaches to the bottom and geared to turn downward step pressure into rotational energy for the generators. This implementation is inexpensive to manufacture, as it uses off the shelf components, and would be ideal in third world applications where components are difficult to obtain. It would be useful in animal movement applications, like the herding of livestock for transport or processing. The current generated is stored in a separate battery assembly, and the flooring is designed to lock together on all four sides With the electrical transport channel outlets available on all sides as well. The piezoelectric implementation can be implemented with piezoelectric film or ceramics, the relevant design considerations are for step comfort and trip avoidance. Both of these considerations are addressed by the choice of materials for the top insulating plate, and a bevelling of edges of the same.</p> |

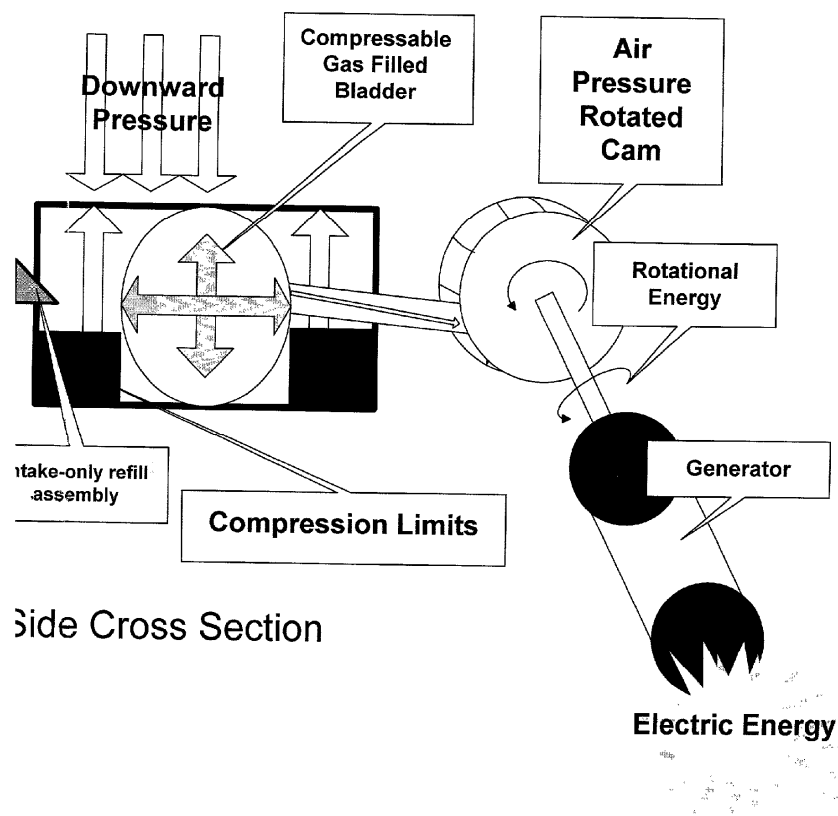


Figure 95 - Schematic drawing of the pressure to electric converter

| | |
|----------------------|---|
| Title: | <i>"Tidal or wave energy harnessing device"</i> |
| Patent Number: | WO2011141691 (A2) |
| Patent office: | World Intellectual Property Organization |
| Date of application: | November 17 th 2011 |
| Abstract: | <p>A tidal or wave energy harnessing device comprises a float; and a pump arranged to be driven by tidal or wave motion of a body of water. The pump comprises a piston chamber, connected to the float and having a first inlet, a second inlet, a first outlet and a second outlet. The pump further comprises a piston comprising a piston head which is movably received within the piston and which has first and second pressure faces, the piston being configured to be anchored to a floor supporting said body of water. The piston head is movable relative to the piston chamber as a result of movement of the piston chamber resulting from the tidal or wave motion of said body of water.; The first inlet and the first outlet are in fluid communication with the first pressure face of the piston head, and the second inlet and second outlet are in fluid communication with the second pressure face of the piston head. In use, the piston chamber is substantially submerged in the body of water.</p> |

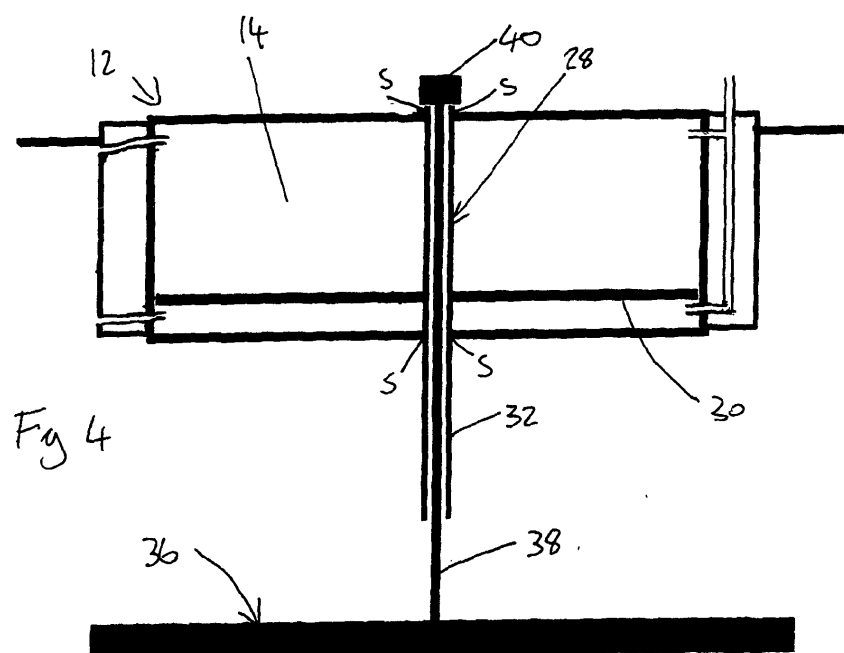


Figure 96 - Schematic drawing of the wave energy harnessing device

| | |
|----------------------|--|
| Title: | <i>"Wave and tidal energy device"</i> |
| Patent Number: | WO2013006088 (A1) |
| Patent office: | World Intellectual Property Organization |
| Date of application: | January 10 th 2013 |
| Abstract: | <p>The invention relates to hydroelectric engineering and, in particular, to wave and tidal energy devices. The wave and tidal energy device comprises a floating pontoon with a pulley fastened thereon, and a vertical cylinder with positive buoyancy which is located underwater and is connected by a flexible coupling to an anchor moored to the sea floor. A piston is disposed inside the cylinder such as to be capable of downward reciprocating movement under the effect of its own weight, a spring or another retracting mechanism, and upwards movement by the displacement of the floating pontoon. This enables working fluid to be drawn into and expelled from the cylinder and supplied to an electrical generator or to shore. A flexible coupling is slung over the pulley, one end of which is connected to the cylinder and the other to the rod of the piston. The wave and tidal energy device provides for an increased device efficiency coefficient due to an increase in the oscillation amplitude of the piston.</p> |

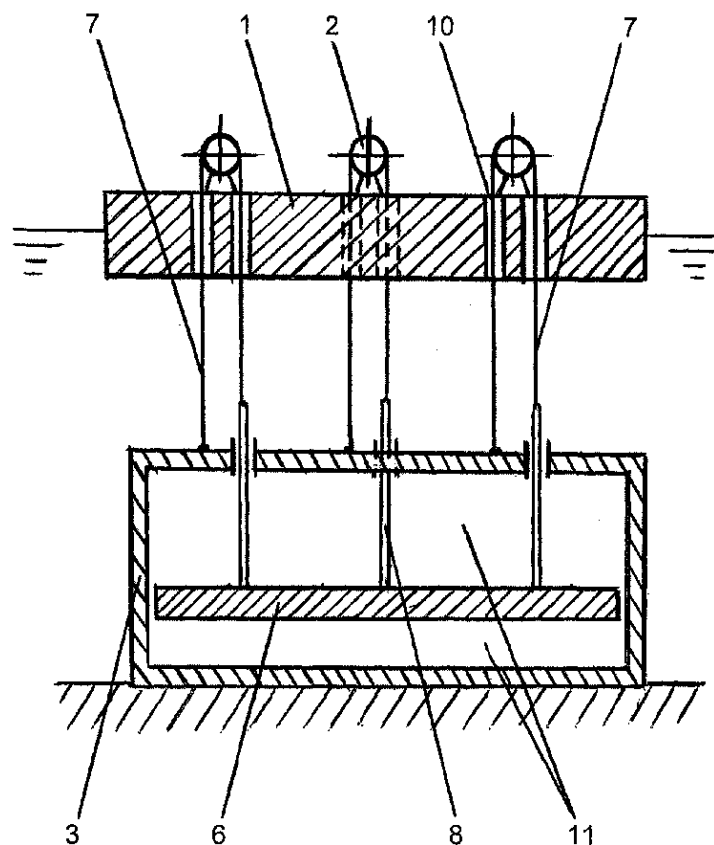


Figure 97 - Schematic drawing of the wave and tidal energy device

Appendix E Coastal soil composition

Two major aspects play a role in the general soil composition along the world's coastlines: plate tectonics and sediment composition. A combination of the theories on both means a reasonable estimation can be made regarding the soil composition at any arbitrary coastal location.

E.1 Plate tectonics

The soil compositions along the coastlines in the world are influenced by their orientation regarding the tectonic movements of the Earth's crust (Inman & Nordstrom, 1971). Three different main categories of coastlines can be distinguished with very specific types of cost. The classification of coastlines over the world is illustrated in Figure 98.

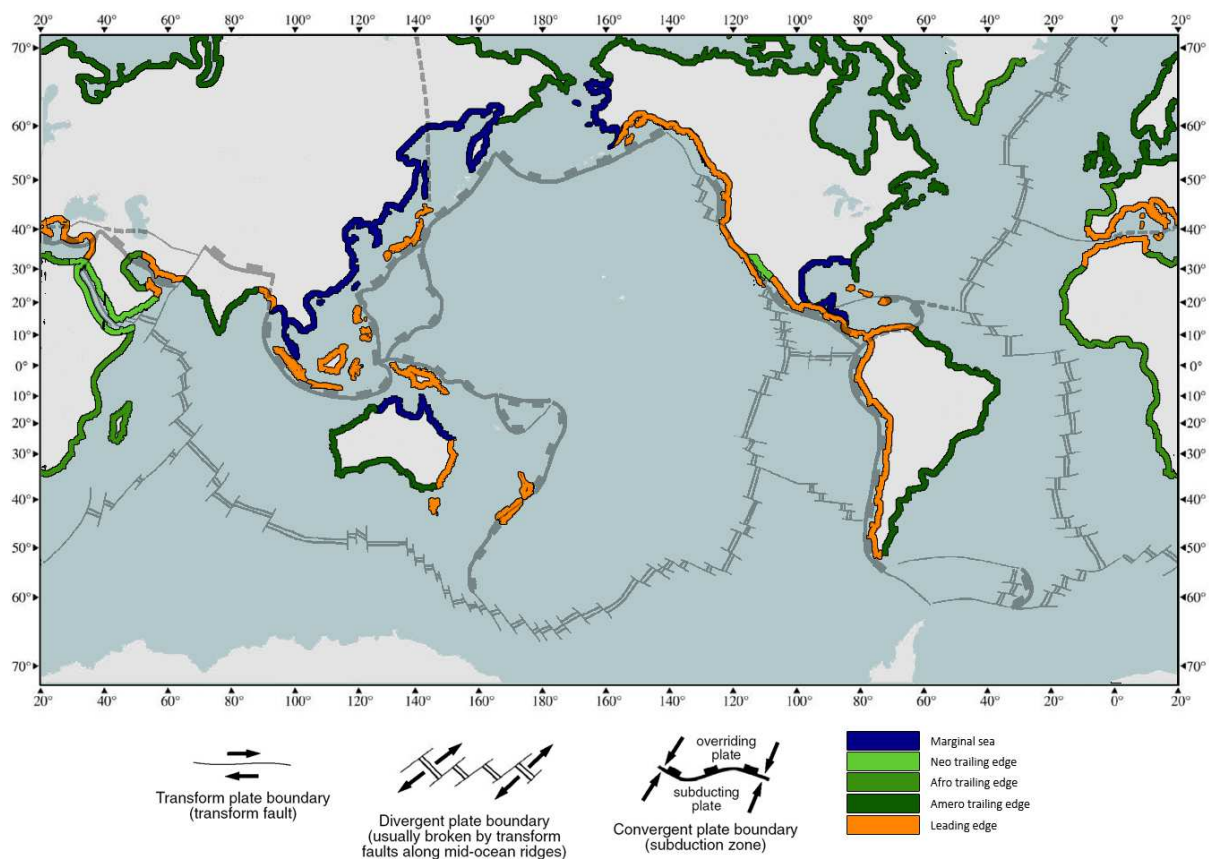


Figure 98 - Tectonic based classification of coasts (redrawn from (Inman & Nordstrom, 1971))

- ▶ **Leading edge or collision coasts** occur on the edge of a tectonic plate that converges with another. The collision of the coastlines causes trenches as one plate slides under another. Leading edge coastlines are characterised by rugged, cliffed coastlines with tectonic activity and a narrow continental shelf.
- ▶ **Trailing edge coastlines** occur on the side of the tectonic plate that diverges from another. As plates diverge they create a tear in the Earth's crust where magma surfaces and solidifies into new land. These tears usually occur in the middle of the ocean. Coastlines facing these areas are tectonically stable and characterised by wide continental shelves. A distinction can be made between three types of trailing edge coast:

- Neo trailing edge coasts: These are relatively new coastlines that have formed at a later stage in history and are therefore less mature in their development. They are typically steep with beaches backed by sea cliffs. Examples can be found along the Red Sea and the Sea of Aken
 - Afro-trailing edge coasts: Found where the opposite side of the continent also has a trailing edge coasts. The continent lacks significant mountainous areas due to the lack of converging plate tectonics meaning river catchment areas are limited and sediment supply is also relatively small. They are generally less mature and lack sedimentary features such as deltas. As the name suggests these coastlines mostly exist along the African continent.
 - Amero-trailing edge coasts: When the opposite coastline of the continent has converging plate tectonics and mountain ridges these types of coastlines develop. They have the most mature coastal systems that are being fed by sediment supply of large meandering rivers that have developed over millions of years. Their coastal plains are broad with little relief. They can be found along the Eastern coast of the Americas and Northern Eurasia.
- Marginal coastlines are coastlines that do not directly face a fault line but are protected by an offshore island ridge at converging plate boundaries. They are the most diverse of coastal types as they are mainly influenced by local processes.

E.2 Sediment distribution

Sediment distribution along the coastlines is highly dependent on local climate conditions. Four types of sediment can be distinguished which are created by different conditions of temperature and historic development. Figure 99 shows the relative frequency of sediment types based on latitude.

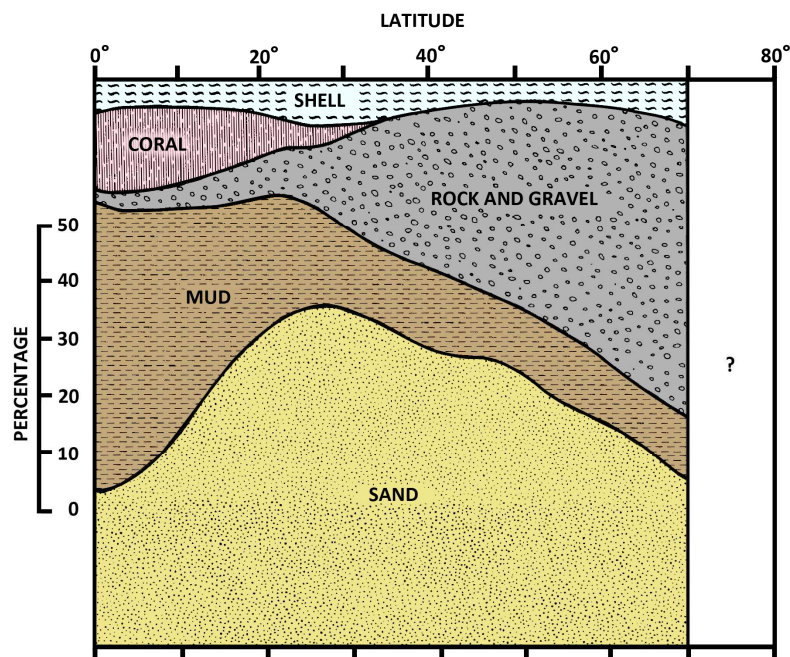


Figure 99 - Relative frequency of inner continental sediment types by latitude (redrawn from (Hayes, 1967))

- Mud is in abundance in areas with severe rainfall and warm, humid climates. Chemical weathering in tropical areas is more severe than in other areas causing the sediment supply in these areas to consist mostly of mud.
- Sand is supplied to the coastline by rivers and is the result of a lengthy process of mechanical weathering along the course of the river from the mountains to the mouth. This type of sediment occurs everywhere in the world but has a stronger presence in the subtropics due to larger river discharges in these areas.
- Rock and gravel are the result of Pleistocene glaciation and therefore occur mostly in the polar and sub-polar areas. Gravel is generally too coarse to be transported to the coast by rivers in the more gently sloped rivers of trailing-edge coasts but does occur in the steeper topographies of leading edge coastlines.
- Coral and carbonate sands (classified under sand) are the result of living organisms that thrive in relatively warmer seawater. These means that they are mostly found in relatively shallow tropical waters and at places of oceanic volcanic activity.
- Shells occur everywhere along coastlines independent of latitude.

Appendix F Elaboration on energy conversion MCDA

F.1 Selection criteria

To obtain a justifiable choice in a Multiple-criteria decision analysis (MCDA) criteria have to be devised that both differentiate the considered mechanisms or products and are relevant to the operational purpose. In the case of selecting the energy conversion mechanism the criteria that will be used for judging are the peak efficiency, the overall efficiency, the chemical sustainability, the ecologic sustainability, the required discharge and the compactness of the device. Each conversion method will be given a score for these criteria graded on a scale of 1 to 7 (because there are 7 criteria). The score each methods gets is the inverse of the rank it is placed in for the specific criterion (so the best scoring method gets 7 points and the worst scoring 1 point).

F.2 Weight factor determination

Because not all criteria are of equal importance to the decision process it is important to assign a weight factor to each selection criterion. This could be done of the top of the head, but it is more accurate to make a comparison chart in which the importance of factors is weighed directly against each other. By determining how the importance of one criterion stacks against that of others in this way a reliable factor can be attained. The factors should be normalized so that the sum of all factors is 1. The table to determine these weight factors is given in Table 72.

| | peak efficiency | overall efficiency | chemical sustainability | ecologic sustainability | required discharge | compactness | sum | factor |
|--------------------------------|-----------------|--------------------|-------------------------|-------------------------|--------------------|-------------|-----|--------|
| peak efficiency | 1 | 0 | 1 | 1 | 0 | 1 | 4 | 0.19 |
| overall efficiency | 1 | 1 | 1 | 1 | 0 | 1 | 5 | 0.24 |
| chemical sustainability | 0 | 0 | 1 | 0 | 0 | 0 | 1 | 0.05 |
| ecologic sustainability | 0 | 0 | 1 | 1 | 0 | 0 | 2 | 0.10 |
| required discharge | 1 | 1 | 1 | 1 | 1 | 1 | 6 | 0.29 |
| compactness | 0 | 0 | 1 | 1 | 0 | 1 | 3 | 0.14 |

Table 72 - Determination of MCDA weight factors for conversion mechanism

F.2.1 Peak efficiency (19/100)

| Conversion method | Efficiency [-] | Score |
|--------------------------------------|----------------|-------|
| Reaction turbine | 0.90 | 6 |
| Impulse turbine | 0.90 | 6 |
| Scroll expander | 0.75 | 1 |
| External gear motor | 0.85 | 3 |
| Vane motor | 0.85 | 3 |
| Piston motor | 0.91 | 7 |
| Internal gear motor (Gerotor) | 0.90 | 6 |

Table 73 - Scores on peak efficiency

The peak efficiency is the maximum efficiency the specific energy conversion mechanism can achieve. It is based on ideal circumstances of flow velocity, rotations per minute and pressure. Turbines can reach high peak efficiencies when operating close to their design discharge (Figure 100), the same goes for the various types of hydraulic motors. Especially internal gear motors and piston motors are very efficient. Scroll expanders are relatively less efficient.

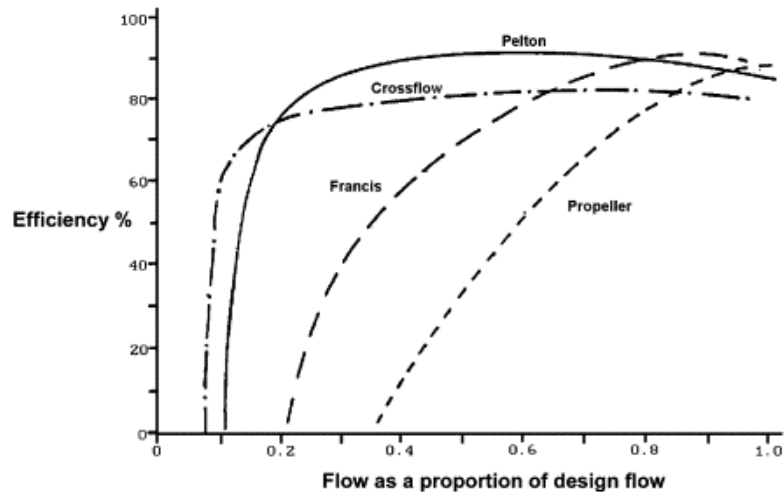


Figure 100 - Efficiency of turbines as proportion of design flow

F.2.2 Overall efficiency (24/100)

| Conversion method | Efficiency [-] | Score |
|-------------------------------|---------------------------------------|-------|
| Reaction turbine | >0.8 from 20% of design flow | 2 |
| Impulse turbine | >0.8 from 60% of design flow | 6 |
| Scroll expander | 0.75 | 1 |
| External Gear motor | 0.70-0.85 depending on rpm and torque | 3 |
| Vane motor | 0.75-0.85 depending on rpm and torque | 4 |
| Piston motor | 0.85-0.91 depending on rpm and torque | 7 |
| Internal gear motor (Gerotor) | 0.80-0.90 depending on rpm and torque | 6 |

Table 74 - Scores on overall efficiency

Because the pressure level will vary greatly over the operation of the device (ranging from a maximum value at the maximum extrusion to 0 when the floater is at the water surface) the efficiency outside the peak value is very important. Impulse turbines are relatively good at maintaining efficiency outside the design discharge whereas reaction turbines are not. Scroll expanders maintain approximately the same, low efficiency. The efficiency of hydraulic motors is slightly lower but still of a respectable level for most varieties. Especially the piston motor and the internal gear motor (alongside the impulse turbine) perform well across the board.

F.2.3 Chemical sustainability (5/100)

| Conversion method | Chemical substance | Score |
|-------------------|--------------------|-------|
| Reaction turbine | None | 7 |
| Impulse turbine | None | 7 |
| Scroll expander | None | 7 |

| | | |
|--------------------------------------|-----------------|---|
| External Gear motor | Hydraulic fluid | 4 |
| Vane motor | Hydraulic fluid | 4 |
| Piston motor | Hydraulic fluid | 4 |
| Internal gear motor (Gerotor) | Hydraulic fluid | 4 |

Table 75 - Scores on chemical sustainability

The use of hydraulic fluids or other chemicals could pose a hazard if it leaks into the surrounding environment. Chemical spills are harmful to the surrounding wildlife and therefore undesirable. Turbines generally do not have any significant chemicals playing a role in their operation; at most there will be some oil in the moving parts to reduce friction. Hydraulic motors, however, use hydraulic fluid which can be hazardous to downright toxic if they leak from the otherwise closed system.

F.2.4 Ecologic sustainability (10/100)

| Conversion method | Type of open water connection | Score |
|--------------------------------------|-------------------------------|-------|
| Reaction turbine | Rotating blades | 3 |
| Impulse turbine | Rotating vanes | 3 |
| Scroll expander | Compacting chambers | 3 |
| External Gear motor | Closed system | 7 |
| Vane motor | Closed system | 7 |
| Piston motor | Closed system | 7 |
| Internal gear motor (Gerotor) | Closed system | 7 |

Table 76 - Scores on ecologic sustainability

Ecologic sustainability entails the damage the system can do in a physical sense to the surrounding wildlife. This involves fish swimming into the turbine blades and being chopped to pieces. Because all hydraulic motors are closed systems it is practically impossible for any physical harm to be done to the local wildlife. Turbines as mentioned before have blades that could pose a threat and scroll expanders too have compacting chambers in their system that could be harmful to creatures entering the system.

F.2.5 Required discharge (29/100)

| Conversion method | Required discharge | Score |
|--------------------------------------|--------------------|-------|
| Reaction turbine | Large | 3 |
| Impulse turbine | Large | 3 |
| Scroll expander | Large | 3 |
| External Gear motor | Small | 7 |
| Vane motor | Small | 7 |
| Piston motor | Small | 7 |
| Internal gear motor (Gerotor) | Small | 7 |

Table 77 - Scores on required discharge

The required discharge is one of the most (if not the most) relevant aspects that need to be taken into consideration. Considering the Tidal Wave Energy Converter is a device with a finite supply of fluid to be used requiring less discharge lengthens the amount of time needed to empty a reservoir, which in turn reflects on the reservoir size, costs, and peak pressure. Turbines generally need larger discharges to be able to yield respectable revenues, hydraulic motors can make do with relatively

much smaller ones and have the added benefit that hydraulic fluid can have a higher density and therefore store more energy per volumetric unit.

F.2.6 Compactness (14/100)

| Conversion method | Compact | Score |
|-------------------------------|---------|-------|
| Reaction turbine | No | 5 |
| Impulse turbine | No | 5 |
| Scroll expander | No | 5 |
| External Gear motor | Yes | 7 |
| Vane motor | No | 5 |
| Piston motor | No | 5 |
| Internal gear motor (Gerotor) | Yes | 7 |

Table 78 - Scores on compactness

Compactness is relevant mostly when the device is installed on board the floater. It is undesirable to have large components on board as it influences the buoyancy and compromises the amount of space that can be used for other functional aspects. It is also influenced by the size of the needed reservoir as especially turbine based systems need relatively large reservoirs to ensure a certain operational capacity. It can be concluded that turbine based systems are not compact and that of the hydraulic motor systems only the gear motors (external and internal) are compact (Figure 101).

| Comparing hydraulic motors | | | | | | |
|----------------------------|---------|------------|--------|------------|------------|-------------|
| | Compact | Reversible | Cost | Efficiency | High speed | High torque |
| Axial piston | No | Yes | High | High | No | Yes |
| Gear motor | Yes | Yes | Low | Low | Yes | No |
| Gerotor motor | Yes | Yes | Medium | Medium | Yes | Yes |
| Radial piston | No | Yes | High | High | No | Yes |
| Vane motor | No | Yes | Medium | Medium | Yes | Yes |

A general summary shows typical features for different hydraulic motors.

Figure 101 - Characteristics of hydraulic motors

Appendix G Elaboration on system configuration MCDA

To further progress on the design of the Tidal Wave Energy Converter it is important to look at the layout of the device's components. This section will look into the positioning of the pistons, the motors and the rods that connect the device to the pistons and the foundation layer. The motors as well as the pistons can be placed either in a dry or wet environment, having an effect on the environmental impact as well as the use of space. The orientation of the rods can vary between a vertical orientation, a diagonal orientation or a lever system. The first two are pretty straight forward where the piston is placed along the axis of the rods and contracts and expands in that same direction. The diagonally placed rods would give some more horizontal stability whereas the vertical ones use less material. The lever system would contain a diagonally placed rod where the piston is placed at some arbitrary point along its axis operating in vertical direction. This would result in more material use and an additional load on the foundation, but would also have the possibility of amplifying the force the pontoon exerts on the piston depending on what the relative arms are of the piston and the pontoon compared to the fulcrum. Table 79 gives an overview of the options that are considered for the different variants. The indications for the variant designations will be based on the characters assigned in this table. Figure 102 illustrates what the variants look like. Because it is illogical to combine a piston above the water table with a motor underneath the water table this combination has been neglected for consideration.

| Support orientation | Piston position | Motor position |
|---------------------|------------------------|-----------------|
| 1 - Vertical | α - Above water | A - Above water |
| 2 - Diagonal | β - Under water | B - Under water |
| 3 - Lever | | |

Table 79 - Options for layout variants

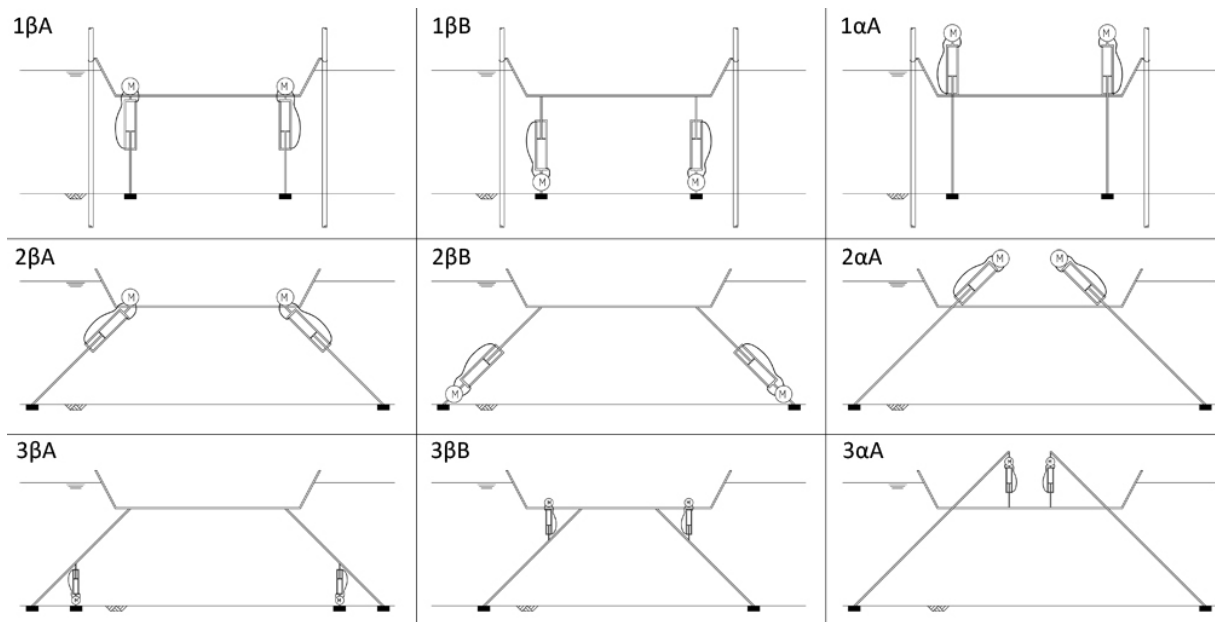


Figure 102 - Schematic representation of the various variants

G.1 Weight factor determination

Because not all criteria are of equal importance to the decision process it is important to assign a weight factor to each selection criterion. This could be done of the top of the head, but it is more accurate to make a comparison chart in which the importance of factors is weighed directly against each other. By determining how the importance of one criterion stacks against that of others in this way a reliable factor can be attained. The factors should be normalized so that the sum of all factors is 1. The table to determine these weight factors is given in Table 72.

| | Durability | Sustainability | Aesthetics | Load amplification | Combined harvesting | Compactness | Pontoon stability | Safety | Load distribution | Sum | Factor |
|----------------------------|------------|----------------|------------|--------------------|---------------------|-------------|-------------------|--------|-------------------|-----|--------|
| Durability | 1 | 1 | 1 | 0 | 1 | 0 | 1 | 0 | 0 | 5 | 0.11 |
| Sustainability | 0 | 1 | 1 | 0 | 0 | 0 | 0 | 0 | 0 | 2 | 0.04 |
| Aesthetics | 0 | 0 | 1 | 0 | 0 | 0 | 0 | 0 | 0 | 1 | 0.02 |
| Load amplification | 1 | 1 | 1 | 1 | 1 | 0 | 1 | 0 | 0 | 6 | 0.13 |
| Combined harvesting | 0 | 1 | 1 | 0 | 1 | 0 | 1 | 0 | 0 | 4 | 0.09 |
| Compactness | 1 | 1 | 1 | 1 | 1 | 1 | 1 | 0 | 0 | 7 | 0.16 |
| Pontoon stability | 0 | 1 | 1 | 0 | 0 | 0 | 1 | 0 | 0 | 3 | 0.07 |
| Safety | 1 | 1 | 1 | 1 | 1 | 1 | 1 | 1 | 1 | 9 | 0.20 |
| Load distribution | 1 | 1 | 1 | 1 | 1 | 1 | 1 | 0 | 1 | 8 | 0.18 |

Table 80 - Determination of MCDA weight factors for layout

G.1.1 Durability (11/100)

| Variant | Score |
|------------------|-------|
| 1 - α - A | 9 |
| 1 - β - A | 6 |
| 1 - β - B | 3 |
| 2 - α - A | 9 |
| 2 - β - A | 6 |
| 2 - β - B | 3 |
| 3 - α - A | 9 |
| 3 - β - A | 6 |
| 3 - β - B | 3 |

Table 81 - Scores on durability

Durability relates to the lifespan of the device and expresses itself in maintenance and replacement costs. Elements of the structure that are exposed to a corrosive environment degrade quicker and are therefore more expensive to maintain and need to be replaced sooner. It is logical to conclude that the variants which have the motor as well as the pistons in a dry environment do better in terms of durability than variants having submerged components. Variants that have either one or the other submerged score average.

G.1.2 Sustainability (4/100)

| Variant | Score |
|------------------|-------|
| 1 - α - A | 9 |
| 1 - β - A | 6 |
| 1 - β - B | 6 |
| 2 - α - A | 9 |
| 2 - β - A | 6 |
| 2 - β - B | 6 |
| 3 - α - A | 9 |
| 3 - β - A | 6 |
| 3 - β - B | 6 |

Table 82 - Scores on sustainability

Sustainability pertains to the effect the device has on its surroundings. This relates mostly to the possibilities of the hydraulic fluid which is being used leaking into the surrounding water body. Any variant having hydraulic components in contact with the water body will score worse than variants being fully emerged from the water. No distinction is made between how many hydraulic components are submerged.

G.1.3 Aesthetics (2/100)

| Variant | Score |
|------------------|-------|
| 1 - α - A | 6 |
| 1 - β - A | 9 |
| 1 - β - B | 9 |
| 2 - α - A | 6 |
| 2 - β - A | 9 |
| 2 - β - B | 9 |
| 3 - α - A | 6 |
| 3 - β - A | 9 |
| 3 - β - B | 9 |

Table 83 - Scores on aesthetics

Aesthetics relate to the manner in which the device is pleasing to the eye. Any part of the construction protruding from the water surface or outside of the pontoon will affect the visible landscape in a negative manner. Therefore variants with large components above the water line will score badly on aesthetics whereas variants mostly under the water line will score better.

G.1.4 Load amplification (13/100)

| Variant | Score |
|------------------|-------|
| 1 - α - A | 3 |
| 1 - β - A | 3 |
| 1 - β - B | 3 |
| 2 - α - A | 6 |
| 2 - β - A | 6 |
| 2 - β - B | 6 |

| | |
|------------------------------------|---|
| 3 - α - A | 9 |
| 3 - β - A | 9 |
| 3 - β - B | 9 |

Table 84 - Scores on load amplification

This factor rates the way the created load is transferred to the pistons and the supports. The lever variants have the possibility to increase the load exerted by the tidal motion due to the leverage effect, this means the pressure in the pistons is higher and shorter pistons can be used. The diagonally places pistons also have a slightly higher force exerted upon them due to the influence of horizontal forces this configuration induces, the resulting exertion and compression of the pistons is, however, smaller.

G.1.5 Possibilities for combined harvesting (9/100)

| Variant | Score |
|------------------------------------|-------|
| 1 - α - A | 6 |
| 1 - β - A | 6 |
| 1 - β - B | 9 |
| 2 - α - A | 6 |
| 2 - β - A | 6 |
| 2 - β - B | 9 |
| 3 - α - A | 6 |
| 3 - β - A | 6 |
| 3 - β - B | 9 |

Table 85 - Scores on possibilities for combined harvesting

For the sake of efficiency and to reduce required investment costs it may be interesting to combine the pressurised hydraulic fluid of multiple pistons into one larger motor. Combining the flows from various devices on separate pontoons is only practical if the pipelines run over the bottom, especially if those pontoons have some distance between them. Having the motor close to the bottom is preferential in such a case as it limits the distance the pipelines have to bridge. Motors that are in the dry environment on the pontoon are least suitable as the pipelines would either have to bridge a big distance or travel above the water table.

G.1.6 Compactness (16/100)

| Variant | Score |
|------------------------------------|-------|
| 1 - α - A | 7 |
| 1 - β - A | 9 |
| 1 - β - B | 9 |
| 2 - α - A | 4 |
| 2 - β - A | 6 |
| 2 - β - B | 6 |
| 3 - α - A | 1 |
| 3 - β - A | 3 |
| 3 - β - B | 3 |

Table 86 - Scores on compactness

The available basin may be limited and/or the floating bodies may be in close proximity to one another. This means it is important that the device does not consume a lot of area both in the horizontal as well as the vertical plane. In the horizontal plane the basin walls may constrict applicability as well as devices of piles of neighbouring pontoons or structures. In the vertical plane the area on top of the floating body may need to be used for residential, industrial or other purposes in which case the extrusion of any device related infrastructure is an obstructing factor.

G.1.7 Pontoon stability (7/100)

| Variant | Score |
|------------------|-------|
| 1 - α - A | 3 |
| 1 - β - A | 3 |
| 1 - β - B | 3 |
| 2 - α - A | 9 |
| 2 - β - A | 9 |
| 2 - β - B | 9 |
| 3 - α - A | 9 |
| 3 - β - A | 9 |
| 3 - β - B | 9 |

Table 87 - Scores on pontoon stability

The pontoon needs to be stable in both horizontal and vertical direction. The vertical stability is guaranteed by the influence of the pistons and the buoyant forces of the water in all variants. For the horizontal stability, however, this is not the case. Regulations prescribe that a floating structure that is being used for residential or industrial purposes needs to be secured at, at least, two opposing corners of the pontoon. Usually this is done by driving piles next to the pontoon and anchoring the pontoon to that. In the case of vertical supports this is still required as the pistons and rods do not sufficiently prevent horizontal movement. In the case of diagonal pistons and rods, however, the pistons could serve a second role to stabilise the horizontal movements of the pontoon as well.

G.1.8 Safety (20/100)

| Variant | Score |
|------------------|-------|
| 1 - α - A | 3 |
| 1 - β - A | 9 |
| 1 - β - B | 9 |
| 2 - α - A | 3 |
| 2 - β - A | 9 |
| 2 - β - B | 9 |
| 3 - α - A | 3 |
| 3 - β - A | 9 |
| 3 - β - B | 9 |

Table 88 - Scores on safety

Safety in the considered sense relates to leakage and sinking of the pontoon (rather than sudden accelerations due to failure of the rods or pistons). All variants which have the piston in a dry environment require some sort of holes in the hull to be created through which the piston rod can reach the piston. The other variants do not require the hull of the barge to be punctured and are therefore relatively safer.

G.1.9 Load distribution (18/100)

| Variant | Score |
|------------------|-------|
| 1 - α - A | 9 |
| 1 - β - A | 9 |
| 1 - β - B | 9 |
| 2 - α - A | 6 |
| 2 - β - A | 6 |
| 2 - β - B | 6 |
| 3 - α - A | 3 |
| 3 - β - A | 3 |
| 3 - β - B | 3 |

Table 89 - Scores on load distribution

Different configurations of the supports result in different load distributions. Vertical supports result in nearly exclusively vertical loads meaning the rods are only subject to compressive and tensile forces. For diagonal supports there is an added rotating motion of the rods resulting in a bending moment in the supports or otherwise added load scenarios that need to be accounted for. Moreover the added horizontal stresses this configuration induces means added material will be needed in the foundation as well as in the pontoon. The lever system introduces shear stresses in the rods as well as requiring a second point load in either the floating body or the foundation.

G.2 MCDA result

| Variant | Score |
|------------------|-------|
| 1 - α - A | 5.96 |
| 1 - β - A | 7.07 |
| 1 - β - B | 7.00 |
| 2 - α - A | 5.76 |
| 2 - β - A | 6.87 |
| 2 - β - B | 6.80 |
| 3 - α - A | 5.16 |
| 3 - β - A | 6.27 |
| 3 - β - B | 6.20 |

Table 90 - Results of the MCDA for layout

The result of the MCDA, as presented in Table 90, clearly indicates that variants with the piston above the water table are not preferred. This mainly has to do with the safety concerns involved in this due to the perforation of the pontoon's hull. Furthermore variants with vertical supports get better scores mostly because they do well in terms of load distribution and the amount of required space. The chosen variant is for these considerations variant 1 - β - A with a vertical support structure, piston below the water table and the motor in a dry environment.

Appendix H Steel pipe piles

H.1 Pile calculation

The calculation of steel pipe piles is done through the method as described in (CUR-2001-8, 2001). It is separated in calculations for piles in sand and piles in clay as well as for compression and tension. For compression the skin friction is calculated with Equation 16.

$$f_{c,sand} = \begin{cases} \frac{q_c}{\gamma_m} \cdot 0.08 \cdot \left(\frac{\sigma_v'}{p_a} \right)^{0.05} \cdot \left(\frac{h}{R^*} \right)^{-0.90}, & \text{for } \frac{h}{R^*} \geq 4 \\ \frac{q_c}{\gamma_m} \cdot 0.08 \cdot \left(\frac{\sigma_v'}{p_a} \right)^{0.05} \cdot \left(\frac{h}{R^*} \right)^{-0.90} \cdot \left(\frac{h}{R^*} \right), & \text{for } \frac{h}{R^*} < 4 \end{cases}$$

$$f_{c,clay} = \frac{q_c}{\gamma_m} \cdot 0.03$$

$$R^* = 0.5 \cdot D_o \cdot \sqrt{DR}$$

$$DR = 1 - \left(\frac{D_i}{D_o} \right)^2$$

f_c = Outside skin friction in compression [kN/m']

q_c = Cone resistance at considered depth [kPa]

γ_m = Material factor [-] = 1.25

σ_v' = Vertical effective soil stress [kN/m³]

p_a = Atmospheric pressure [100kPa]

h = Distance between considered point and pile tip [m]

R^* = Effective pile radius [m]

DR = Displacement ratio [-]

D_o = Outer pile diameter [m]

D_i = Inner pile diameter [m]

Equation 16 - Steel pipe pile skin friction equations

In compression the end bearing capacity of the pile also contributes to the bearing capacity and is calculated as depicted in Equation 17.

$$q_{eb,sand} = \frac{p_a}{\gamma_m} \cdot 8.5 \cdot \left(\frac{\bar{q}_c}{p_a} \right)^{0.5} \cdot (DR)^{0.25}$$

$$q_{eb,clay} = 9 \cdot \frac{c_u}{\gamma_m}$$

Equation 17 - End bearing capacity of steel pipe piles

A distinction here can be made between plugging pipes and non-plugging pipes. Whether a pipe plugs or not depends on the relation between the skin friction inside the pile and the end bearing capacity of the plug. If the end bearing capacity of the pile is larger than the inner skin friction the

plug will not be able to hold and the inner skin friction becomes dominant. Equation 18 gives this relation.

$$Q_{eb} = 0.25 \cdot \pi \cdot D_o^2 \cdot q_{eb} < \left(\pi \cdot D_i \cdot \int_0^{\text{pile tip}} f_c(z) dz + Q_{eb, wall} \right)$$

Equation 18 - Plugging relation

To calculate the bearing capacity from these relations the equations as given in Equation 19 can be used. The contribution of the clay layers on the bearing capacity may be used under the following conditions:

- The clay layer is directly above the bearing sand layer
- The cone resistance of the clay layer is over 2 MPa
- The contribution of the clay layer on the capacity is at most 50% of the total capacity
- At most 50% of the clay layer's bearing capacity can be utilized

$$Q_{eb} = 0.25 \cdot \pi \cdot D_o^2 \cdot q_{eb}$$

$$Q_{fr;c} = \pi \cdot D_o \cdot \int_0^{\text{Pile tip}} f_c(z) dz$$

$$Q_c = Q_{eb} + \sum Q_{fr;c}$$

$$= 0.25 \cdot \pi \cdot D_o^2 \cdot q_{eb} + \pi \cdot D_o \cdot \int_0^{d_{clay}} f_{c;clay}(z) dz + \pi \cdot D_o \cdot \int_{d_{clay}}^{d_{clay} + d_{sand} - 4 \cdot R^*} f_c(z) dz + \pi \cdot D_o \cdot \int_{d_{clay} + d_{sand} - 4 \cdot R^*}^{d_{clay} + d_{sand}} f_c(z) dz$$

Equation 19 - Bearing capacity calculation in compression

For pile loading in friction the formulas are slightly different as presented in

$$f_{t,sand} = \frac{q_c}{\gamma_m} \cdot 0.045 \cdot \left(\frac{\sigma_v'}{p_a} \right)^{0.15} \cdot \left(\frac{h}{R^*} \right)^{-0.85}, \text{ for } \frac{h}{R^*} \geq 4$$

$$f_{t,clay} = \frac{q_c}{\gamma_m} \cdot 0.03$$

$$\gamma_m = \text{Material factor [-]} = 1.40$$

Equation 20 - Skin friction in tension

The calculation of the bearing capacity in tension is similar to that in compression with the exception that there is no end bearing capacity. The equations are given in Equation 21.

$$\begin{aligned}
 Q_{eb} &= 0.25 \cdot \pi \cdot D_o^2 \cdot q_{eb} \\
 Q_{fr;c} &= \pi \cdot D_o \cdot \int_0^{\text{Pile tip}} f_c(z) dz \\
 Q_t &= \sum Q_{fr;t} + \sum F_{g;plug} \\
 &= \pi \cdot D_o \cdot \int_0^{d_{clay}} f_{t,clay}(z) dz + \pi \cdot D_o \cdot \int_{d_{clay}}^{d_{clay} + d_{sand} - 4 \cdot R^*} f_{t,sand}(z) dz
 \end{aligned}$$

Equation 21 - Bearing capacity calculation in tension

H.2 Slab calculation

To transfer the force from the pistons to the piles and vice versa large steel slabs will be welded to the top of the pile foundation. To determine the thickness of these slabs a number of things has to be checked. The maximum bending moment in the slab being the first (Equation 22), and the shear stress being the other (Equation 23). For either failure mode it is important to know the load distribution in the slab for each load case.

$$\begin{aligned}
 \sigma_{\max} &= \frac{M_z \cdot z_{\max}}{I_{zz}} \\
 M_z &= \text{Bending moment [kNm]} \\
 z_{\max} &= \text{Distance from center of cross section [m]} \\
 I_{zz} &= \text{Moment of inertia [m}^4\text{]}
 \end{aligned}$$

Equation 22 - Stress due to bending moment

$$\begin{aligned}
 \sigma &= -\frac{V_z \cdot S_z^a}{b^a \cdot I_{zz}} \\
 S_z^a &= A^a \cdot z_C^a \\
 A^a &= \text{Area of cross section [m}^2\text{]} \\
 z_C^a &= \text{Distance from center of cross section [m]} \\
 V_z &= \text{Shear force [kN]} \\
 S_z^a &= \text{Static moment [m}^3\text{]} \\
 b^a &= \text{Width [m]} \\
 I_{zz} &= \text{Moment of inertia [m}^4\text{]}
 \end{aligned}$$

Equation 23 - Stress due to shear forces

The following paragraphs give the required calculation tools for steel slabs over three piles, four piles and six piles.

H.2.1 Three piles

The three pile configuration as shown in Figure 103 equally distributes the applied force among the three piles installed underneath the slab. The considered force distribution is a statically undetermined system which can be modelled by two perpendicular two support systems where one is situated along the centre from the bottom pile to the line in between the centres of the upper piles loaded by the actual force. The length of this system is four third times the centre-to-centre distance of the piles. And the other is the two support system between those two piles loaded by the upper support reaction of the vertical system of which the length is equal to the centre-to-centre distance of the piles.

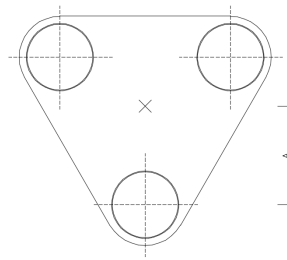


Figure 103 - Three pile configuration

The resulting bending moment and shear force lines are given in Figure 104. In these figures F is the total force applied on the system.

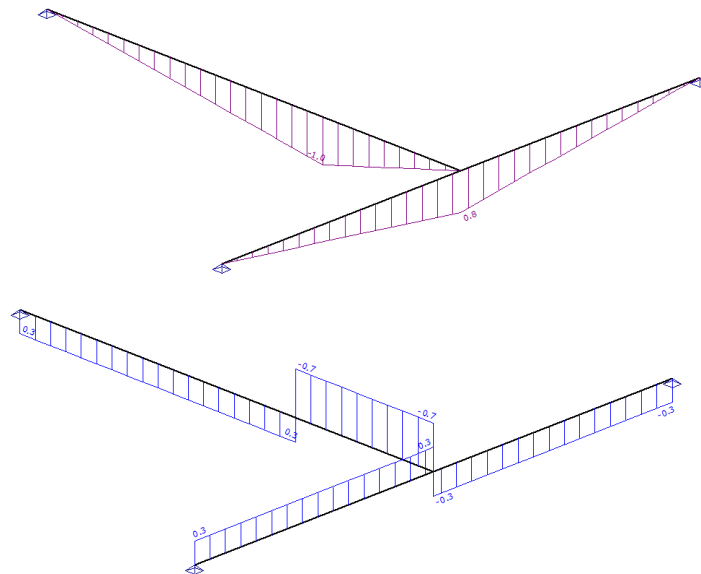


Figure 104 - a) Moment distribution b) Shear force distribution of three pile configuration

$$\sigma_{\max} = \frac{M_z \cdot z_{\max}}{I_{zz}} = \frac{\frac{2 \cdot F}{3} \cdot \sqrt{\frac{3}{4} \cdot \frac{l}{3} \cdot \frac{d}{2}}}{\frac{1}{12} \cdot b \cdot d^3} = \frac{4\sqrt{3} \cdot F \cdot l}{6 \cdot b \cdot d^2} \leq 235 \cdot 10^6 \rightarrow d \geq \sqrt{\frac{4\sqrt{3} \cdot F \cdot l}{6 \cdot b \cdot 235 \cdot 10^6}}$$

$$\sigma_{\max} = \frac{V_z \cdot A^a \cdot z_C^a}{b^a \cdot I_{zz}} = \frac{\frac{2 \cdot F}{3} \cdot b \cdot d \cdot \frac{d}{4}}{b \cdot \frac{1}{12} \cdot b \cdot d^3} = \frac{2 \cdot F}{b \cdot d} \leq 235 \cdot 10^6 \rightarrow d \geq \frac{2 \cdot F}{b \cdot 235 \cdot 10^6}$$

d = Slab thickness [m]

F = Force [N]

b = Pile diameter [m]

l = Centre - to - centre distance [m]

Equation 24 - Required slab thickness for three pile configuration

H.2.2 Four piles

The four pile configuration as shown in Figure 105 equally distributes the applied force among the four piles installed underneath the slab. The considered force distribution is as marked grey and simplifies to a beam on two supports.

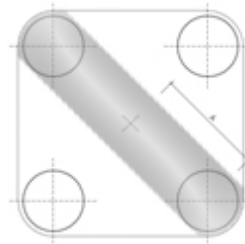


Figure 105 - Four pile configuration

Figure 106 gives the resulting moment distribution and shear force distribution of the considered two support configuration. It should be noted that, because half the piles of the total configuration are in this system, half the total force is what is being applied to this system (F).

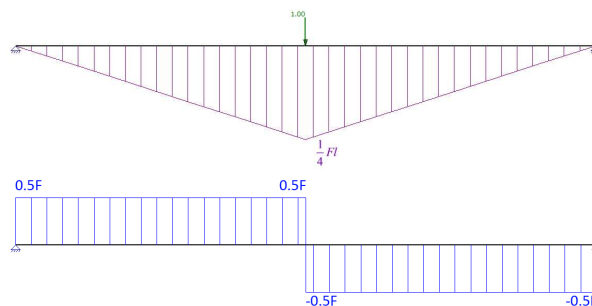


Figure 106 - a) Moment distribution b) Shear force distribution of four pile configuration

The derivation of the requirements for the slab thickness is given in Equation 25, in which F this time is the total load on the system.

$$\sigma_{\max} = \frac{M_z \cdot z_{\max}}{I_{zz}} = \frac{\frac{1}{4} \cdot \left(\frac{1}{2} \cdot F\right) \cdot l \cdot \frac{d}{2}}{\frac{1}{12} \cdot b \cdot d^3} = \frac{3 \cdot F \cdot l}{4 \cdot b \cdot d^2} \leq 235 \cdot 10^6 \rightarrow d \geq \sqrt{\frac{3 \cdot F \cdot l}{940 \cdot 10^6 \cdot b}}$$

$$\sigma_{\max} = \frac{V_z \cdot A^a \cdot z_C^a}{b^a \cdot I_{zz}} = \frac{\frac{1}{2} \cdot \left(\frac{1}{2} \cdot F\right) \cdot b \cdot d \cdot \frac{d}{4}}{b \cdot \frac{1}{12} \cdot b \cdot d^3} = \frac{3 \cdot F}{4 \cdot b \cdot d} \leq 235 \cdot 10^6 \rightarrow d \geq \frac{3 \cdot F}{940 \cdot 10^6 \cdot b}$$

d = Slab thickness [m]

F = Force [N]

b = Pile diameter [m]

l = Centre-to-centre distance [m]

Equation 25 - Required slab thickness for four pile configuration

This leads to the conclusion that for relatively small centre to centre distances the shear force is the determining factor for the slab thickness, whereas for larger centre to centre distances the bending moment becomes the relevant one.

H.2.3 Six piles

The six pile configuration as shown in Figure 107 equally distributes the applied force among the four piles installed underneath the slab. The considered force distribution is as marked grey and simplifies to a beam fixed on one end and free on the other, with the support force of one pile applied to the end.

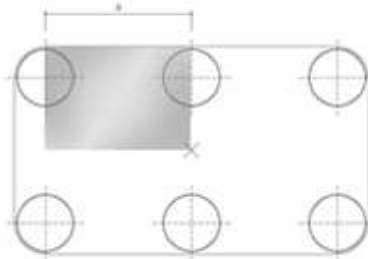


Figure 107 - Six pile configuration

Figure 108 gives the resulting moment distribution and shear force distribution of the considered one support configuration. It should be noted that, because only one of the piles of the total configuration is in this system, a sixth of the total force is what is being applied to this system (F).

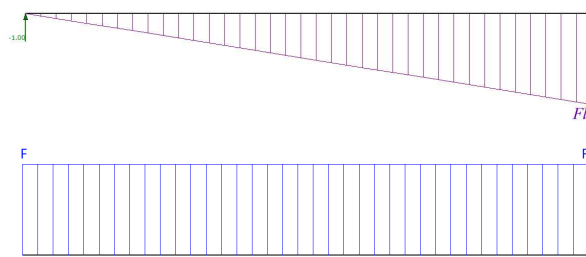


Figure 108a) Moment distribution b) Shear force distribution of six pile configuration

The derivation of the requirements for the slab thickness is given in Equation 26, in which F this time is the total load on the system.

$$\sigma_{\max} = \frac{M_z \cdot z_{\max}}{I_{zz}} = \frac{\frac{1}{6} \cdot F \cdot l \cdot \frac{d}{2}}{\frac{1}{12} \cdot b \cdot d^3} = \frac{F \cdot l}{b \cdot d^2} \leq 235 \cdot 10^6 \rightarrow d \geq \sqrt{\frac{F \cdot l}{235 \cdot 10^6 \cdot b}}$$

$$\sigma_{\max} = \frac{V_z \cdot A^a \cdot z_C^a}{b^a \cdot I_{zz}} = \frac{\frac{1}{6} \cdot F \cdot b \cdot d \cdot \frac{d}{4}}{b \cdot \frac{1}{12} \cdot b \cdot d^3} = \frac{F}{2 \cdot b \cdot d} \leq 235 \cdot 10^6 \rightarrow d \geq \frac{F}{470 \cdot 10^6 \cdot b}$$

d = Slab thickness[m]

F = Force[N]

b = Pile diameter[m]

l = Centre-to-centre distance[m]

Equation 26 - Required slab thickness for six pile configuration

H.3 Dimensions

To get an idea of the availability of steel pipe piles the catalogue of ArcelorMittal has been consulted. Figure 109 gives a sheet of what the common production sizes are.

| weight (kg/m pipe) | wall thickness (mm & inch) | | wall thickness (mm & inch) | | | | | | | | | | | | | | | | | | |
|-----------------------|----------------------------|-------|----------------------------|------|------|------|------|------|------|------|------|------|------|------|------|------|------|------|------|--|--|
| | | | 9 | 10 | 11 | 12 | 13 | 14 | 15 | 16 | 17 | 18 | 19 | 20 | 21 | 22 | 23 | 24 | 25 | | |
| | mm | inch | 0.35 | 0.39 | 0.43 | 0.47 | 0.51 | 0.55 | 0.59 | 0.63 | 0.67 | 0.71 | 0.75 | 0.79 | 0.83 | 0.87 | 0.91 | 0.94 | 0.98 | | |
| 864 | 34 | 1 3/8 | 190 | 211 | 231 | 252 | 273 | 293 | 314 | 334 | 355 | 375 | 396 | 416 | 436 | | | | | | |
| 914 | 36 | 1 3/8 | 201 | 223 | 245 | 267 | 289 | 311 | 333 | 354 | 376 | 398 | 420 | 441 | 463 | 484 | | | | | |
| 965 | 38 | 1 5/8 | 212 | 236 | 259 | 282 | 305 | 328 | 352 | 375 | 398 | 420 | 443 | 466 | 489 | 512 | | | | | |
| 1016 | 40 | 1 5/8 | 224 | 248 | 273 | 297 | 322 | 346 | 370 | 395 | 419 | 443 | 467 | 491 | 515 | 539 | 563 | 587 | 611 | | |
| 1067 | 42 | 1 7/8 | 235 | 261 | 286 | 312 | 338 | 363 | 389 | 415 | 440 | 466 | 491 | 516 | 542 | 567 | 592 | 617 | 642 | | |
| 1118 | 44 | 1 7/8 | 246 | 273 | 300 | 327 | 354 | 381 | 408 | 435 | 461 | 488 | 515 | 541 | 568 | 594 | 621 | 648 | 674 | | |
| 1168 | 46 | 1 7/8 | 257 | 286 | 314 | 342 | 370 | 399 | 427 | 455 | 483 | 511 | 539 | 566 | 594 | 622 | 650 | 677 | 705 | | |
| 1219 | 48 | 1 7/8 | 269 | 298 | 328 | 357 | 387 | 416 | 445 | 475 | 504 | 533 | 562 | 591 | 621 | 650 | 679 | 707 | 736 | | |
| 1270 | 50 | 1 7/8 | | 311 | 342 | 372 | 403 | 434 | 464 | 495 | 525 | 556 | 586 | 617 | 647 | 677 | 707 | 737 | 768 | | |
| 1321 | 52 | 2 | | 323 | 355 | 387 | 419 | 451 | 483 | 515 | 547 | 578 | 610 | 642 | 673 | 705 | 736 | 768 | 799 | | |
| 1372 | 54 | 2 | | 336 | 369 | 402 | 436 | 469 | 502 | 535 | 568 | 601 | 634 | 667 | 699 | 732 | 765 | 798 | 830 | | |
| 1422 | 56 | 2 | | 348 | 383 | 417 | 452 | 486 | 521 | 555 | 589 | 623 | 658 | 692 | 726 | 760 | 794 | 828 | 862 | | |
| 1473 | 58 | 2 1/8 | | | | 432 | 468 | 504 | 539 | 575 | 611 | 646 | 681 | 717 | 752 | 787 | 823 | 858 | 893 | | |
| 1524 | 60 | 2 1/8 | | | | 447 | 484 | 521 | 558 | 595 | 632 | 669 | 705 | 742 | 778 | 815 | 851 | 888 | 924 | | |
| 1575 | 62 | 2 1/8 | | | | 462 | 501 | 539 | 577 | 615 | 653 | 691 | 729 | 767 | 805 | 842 | 880 | 918 | 956 | | |
| 1626 | 64 | 2 1/2 | | | | 478 | 517 | 556 | 596 | 635 | 674 | 714 | 753 | 792 | 831 | 870 | 909 | 948 | 987 | | |
| 1676 | 66 | 2 1/2 | | | | 493 | 533 | 574 | 615 | 655 | 696 | 736 | 777 | 817 | 857 | 898 | 938 | 978 | 1018 | | |
| 1727 | 68 | 2 1/2 | | | | 508 | 550 | 592 | 633 | 675 | 717 | 759 | 800 | 842 | 884 | 925 | 967 | 1008 | 1049 | | |
| 1778 | 70 | 2 3/4 | | | | 523 | 566 | 609 | 652 | 695 | 738 | 781 | 824 | 867 | 910 | 953 | 995 | 1038 | 1081 | | |
| 1829 | 72 | 2 3/4 | | | | 538 | 582 | 627 | 671 | 715 | 760 | 804 | 848 | 892 | 936 | 980 | 1024 | 1068 | 1112 | | |
| 1880 | 74 | 2 3/4 | | | | 553 | 598 | 644 | 690 | 735 | 781 | 826 | 872 | 917 | 963 | 1008 | 1053 | 1098 | 1143 | | |
| 1930 | 76 | 2 3/4 | | | | 568 | 615 | 662 | 709 | 755 | 802 | 849 | 896 | 942 | 989 | 1035 | 1082 | 1128 | 1175 | | |
| 1981 | 78 | 2 3/4 | | | | 583 | 631 | 679 | 727 | 775 | 823 | 871 | 919 | 967 | 1015 | 1063 | 1111 | 1158 | 1206 | | |
| 2032 | 80 | 2 3/4 | | | | 598 | 647 | 697 | 746 | 795 | 845 | 894 | 943 | 992 | 1041 | 1091 | 1140 | 1188 | 1237 | | |
| 2083 | 82 | 2 3/4 | | | | 613 | 664 | 714 | 765 | 816 | 866 | 917 | 967 | 1017 | 1068 | 1118 | 1168 | 1219 | 1269 | | |
| 2134 | 84 | 2 3/4 | | | | 628 | 680 | 732 | 784 | 836 | 887 | 939 | 991 | 1042 | 1094 | 1146 | 1197 | 1249 | 1300 | | |
| 2184 | 86 | 2 3/4 | | | | 643 | 696 | 749 | 803 | 856 | 909 | 962 | 1015 | 1068 | 1120 | 1173 | 1226 | 1279 | 1331 | | |
| 2235 | 88 | 2 3/4 | | | | 658 | 712 | 767 | 821 | 876 | 930 | 984 | 1038 | 1093 | 1147 | 1201 | 1255 | 1309 | 1363 | | |
| 2286 | 90 | 2 3/4 | | | | 673 | 729 | 784 | 840 | 896 | 951 | 1007 | 1062 | 1118 | 1173 | 1228 | 1284 | 1339 | 1394 | | |
| 2337 | 92 | 2 3/4 | | | | 688 | 745 | 802 | 859 | 916 | 973 | 1029 | 1086 | 1143 | 1199 | 1256 | 1312 | 1369 | 1425 | | |
| 2388 | 94 | 2 3/4 | | | | 703 | 761 | 820 | 878 | 936 | 994 | 1052 | 1110 | 1168 | 1226 | 1283 | 1341 | 1399 | 1457 | | |
| 2438 | 96 | 2 3/4 | | | | 718 | 778 | 837 | 896 | 956 | 1015 | 1074 | 1134 | 1193 | 1252 | 1311 | 1370 | 1429 | 1488 | | |
| 2489 | 98 | 2 3/4 | | | | 733 | 794 | 855 | 915 | 976 | 1036 | 1097 | 1157 | 1218 | 1278 | 1339 | 1399 | 1459 | 1519 | | |
| 2540 | 100 | 2 3/4 | | | | 748 | 810 | 872 | 934 | 996 | 1058 | 1120 | 1181 | 1243 | 1305 | 1366 | 1428 | 1489 | 1551 | | |
| 2591 | 102 | 2 3/4 | | | | 763 | 826 | 890 | 953 | 1016 | 1079 | 1142 | 1205 | 1268 | 1331 | 1394 | 1456 | 1519 | 1582 | | |
| 2642 | 104 | 2 3/4 | | | | 778 | 843 | 907 | 972 | 1036 | 1100 | 1165 | 1229 | 1293 | 1357 | 1421 | 1485 | 1549 | 1613 | | |
| 2692 | 106 | 2 3/4 | | | | 793 | 859 | 925 | 990 | 1056 | 1122 | 1187 | 1253 | 1318 | 1383 | 1449 | 1514 | 1579 | 1645 | | |
| 2743 | 108 | 2 3/4 | | | | 808 | 875 | 942 | 1009 | 1076 | 1143 | 1210 | 1276 | 1343 | 1410 | 1476 | 1543 | 1609 | 1676 | | |
| 2794 | 110 | 2 3/4 | | | | 823 | 892 | 960 | 1028 | 1096 | 1164 | 1232 | 1300 | 1368 | 1436 | 1504 | 1572 | 1639 | 1707 | | |
| 2845 | 112 | 2 3/4 | | | | 838 | 908 | 977 | 1047 | 1116 | 1186 | 1255 | 1324 | 1393 | 1462 | 1532 | 1601 | 1670 | 1739 | | |
| 2896 | 114 | 2 3/4 | | | | 853 | 924 | 995 | 1066 | 1136 | 1207 | 1277 | 1348 | 1418 | 1489 | 1559 | 1629 | 1700 | 1770 | | |
| 2946 | 116 | 2 3/4 | | | | 868 | 940 | 1012 | 1084 | 1156 | 1228 | 1300 | 1372 | 1443 | 1515 | 1587 | 1658 | 1730 | 1801 | | |
| 2997 | 118 | 2 3/4 | | | | 883 | 957 | 1030 | 1103 | 1176 | 1249 | 1322 | 1395 | 1468 | 1541 | 1614 | 1687 | 1760 | 1832 | | |

Figure 109 - Steel pipe pile dimensions (ArcelorMittal, 2015)

These piles are available in steel qualities S235, S275, S355, S420 and S460 and can be applied up to a length of 53 meters. Longer lengths are possible by welding piles together.

Appendix I Precast concrete piles

I.1 Pile calculation

Because it is very difficult for precast concrete piles to be dimensioned for tensile forces under water, they will only be considered for loading in compressive state. The calculation is done using the empirical Koppejan formula as further described in (NEN-6743, 1991). The relevant formulae of this method are given in Equation 27. It is assumed that square, symmetric piles with no foot are used.

$$p_{r;\max;tip} = \alpha_p \cdot \beta \cdot s \cdot 0.25 \cdot \left(\frac{q_{c;I;gem} + q_{c;II;gem} + 2 \cdot q_{c;III;gem}}{\gamma_m} \right)$$

$$F_{r;\max;tip} = 0.25 \cdot \pi \cdot D_o^2 \cdot p_{r;\max;tip}$$

$$p_{r;\max;shaft} = \frac{\alpha_c \cdot q_c}{\gamma_m}$$

$$F_{r;\max;shaft} = \pi \cdot D_o \cdot \int_0^{\text{Pile tip}} p_{r;\max;shaft}(z) dz$$

$$\gamma_m = 1.25 \quad \alpha_{c;sand} = 0.010 \quad \alpha_p = 1.0$$

$$s = 1.0 \quad \alpha_{c;clay} = 0.007 \quad \beta = 1.0$$

p_r = Unit bearing capacity [kPa]
 F_r = Bearing capacity [kN]
 q_c = Cone resistance [kPa]
 D_o = Outer pile diameter [m]
 α_c = Friction factor [–]
 α_p = Penetration type factor [–]
 β = Foot factor [–]
 s = Pile shape factor [–]
 γ_m = Material factor [–]

Equation 27 - Precast concrete pile calculation

Regarding the clay layer the same restrictions apply as for steel pipe piles. The contribution of the clay layers on the bearing capacity may be used under the following conditions:

- The clay layer is directly above the bearing sand layer
- The cone resistance of the clay layer is over 2 MPa
- The contribution of the clay layer on the capacity is at most 50% of the total capacity
- At most 50% of the clay layer's bearing capacity can be utilized

The minimum required centre-to-centre distance of the piles again is 2.5 times the nominal pile diameter.

I.2 Foundation block calculation

The used pile configurations are of two piles, four piles and five piles and they are solely loaded on compression. The calculation for such structures is done according to the (NEN-6720, 1995) regulations.

I.2.1 Two piles

The two pile configuration as shown in Figure 110 distributes the force of the load equally over the two installed piles. For the calculation method to be valid the system has to be stocky meaning the length may not exceed twice the height. Reinforcement steel needs to be applied to handle the tensile forces in the block for which FeB500 steel is used. Furthermore B35 concrete is used meaning the minimum reinforcement percentage is 0.18%. The angle of the compression diagonal (α) must be between 30° and 60° in order to be valid. The minimum reinforcement percentage is 0.18%.

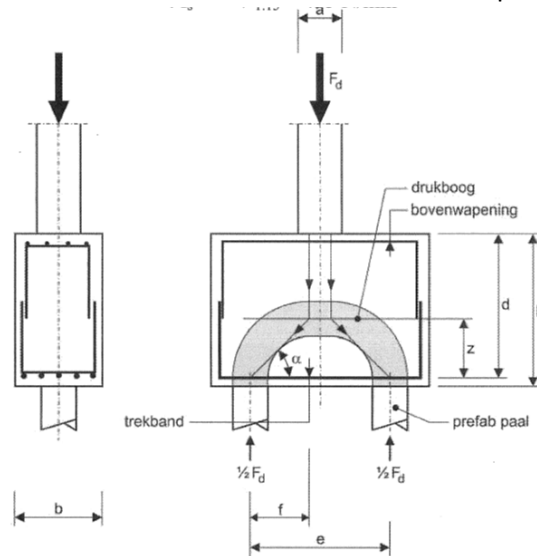


Figure 110 - Two pile foundation block

Equation 28 gives the calculation method required for calculating the amount of required reinforcement steel in the block. The height of the block follows directly from the slenderness requirement (the height is at least half the centre-to-centre distance). The width of the block is determined by constructability requirements and exceeds the pile width by 100 mm on either side added with 50 mm to account for rebar cover. The length is considered as the centre-to-centre distance added with once the pile diameter and the cover margin.

$$z = 0.2 \cdot l + 0.4 \cdot h$$

$$M = \frac{1}{4} \cdot F \cdot l$$

$$T = \frac{M}{z}$$

$$A_s = \frac{T}{435 \cdot 10^6}$$

l = Centre - to - centre distance [m]
 h = Height of the block [m]
 z = Internal lever arm [m]
 M = Bending moment [Nm]
 F = Force [N]
 T = Tensile force [N]
 A_s = Reinforcement steel area [m²]

Equation 28 - Two pile reinforcement calculation

1.2.2 Four piles

The four pile configuration as shown in Figure 111 distributes the force of the load equally over the four installed piles. For the calculation method to be valid the system has to be stocky meaning the length may not exceed twice the height. Reinforcement steel needs to be applied to handle the tensile forces in the block for which FeB500 steel is used. The angle of the compression diagonal (α) must be between 30° and 60° in order to be valid.

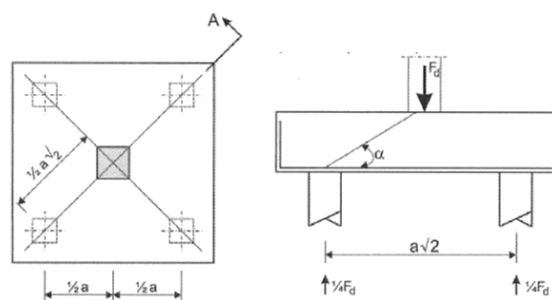


Figure 111 - Four pile foundation block

The moment distribution for a four support system has been previously determined in H.2.2 meaning the maximum bending moment is known. This means the required reinforcement steel can be calculated with Equation 29. The height of the block follows directly from the slenderness requirement. The length and width of the block are determined by constructability requirements and exceeds the pile width by 100 mm on either side added with 50 mm to account for rebar cover. Furthermore the centre-to-centre distance as well as once the pile diameter.

$$z = 0.8 \cdot h$$

$$M = \frac{1}{8} \cdot F \cdot l$$

$$T = \frac{M}{z}$$

$$A_s = \frac{T}{435 \cdot 10^6}$$

l = Centre - to - centre distance [m]
 h = Height of the block [m]
 z = Internal lever arm [m]
 M = Bending moment [Nm]
 F = Force [N]
 T = Tensile force [N]
 A_s = Reinforcement steel area [m²]

Equation 29 - Four pile block reinforcement calculation

Reinforcement should be installed in both directions perpendicular to each other due to the symmetry of the foundation block.

1.2.3 Five piles

The five pile configuration as shown in Figure 112 distributes the force of the load equally over the five installed piles. For the calculation method to be valid the system has to be stocky meaning the length may not exceed twice the height. Reinforcement steel needs to be applied to handle the tensile forces in the block for which FeB500 steel is used. The angle of the compression diagonal (α) must be between 30° and 60° in order to be valid.

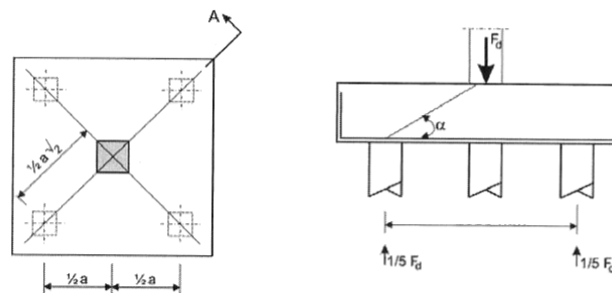


Figure 112 - Five pile foundation block

The moment distribution for a five support system is similar to that of the six pile system that has been previously determined in H.2.3, except with the cross section being along the main diagonal. This means the maximum bending moment is known and the required reinforcement steel can be calculated with Equation 30. The height of the block follows directly from the slenderness requirement. The length and width of the block are determined by constructability requirements and exceeds the pile width by 100 mm on either side added with 50 mm to account for rebar cover. Furthermore the longest centre-to-centre distance as well as once the pile diameter.

$$z = 0.8 \cdot h$$

$$M = \frac{1}{5} \cdot F \cdot l$$

$$T = \frac{M}{z}$$

$$A_s = \frac{T}{435 \cdot 10^6}$$

l = Centre - to - centre distance [m]
 h = Height of the block [m]
 z = Internal lever arm [m]
 M = Bending moment [Nm]
 F = Force [N]
 T = Tensile force [N]
 A_s = Reinforcement steel area [m²]

Equation 30 - Five pile block reinforcement calculation

Reinforcement should be installed in both directions perpendicular to each other due to the symmetry of the foundation block.

I.3 Pile dimensions

Prefab concrete piles are made in a number of conventional sizes and can be applied to depths of up to 90 times the pile diameter. The possible sizes are given in Table 91 (Vroom Funderingstechnieken, 2015).

| Pile diameter [mm] | Maximum length [m] |
|--------------------|--------------------|
| 180 x 180 | 16.2 |
| 220 x 220 | 19.8 |
| 250 x 250 | 22.5 |
| 290 x 290 | 26.1 |
| 320 x 320 | 28.8 |
| 350 x 350 | 31.5 |
| 380 x 380 | 34.2 |
| 400 x 400 | 36.0 |
| 420 x 420 | 37.8 |
| 450 x 450 | 40.5 |
| 500 x 500 | 45.0 |

Table 91 - Precast concrete pile dimensions

Appendix J Foundation anchors

J.1 GEWI anchors

The use of GEWI anchors is widespread in foundation technology. They are relatively cheap to construct, easily applicable and very capable of transferring tensile forces to the subsoil. There are some design requirements that need to be taken into account when designing a GEWI anchor. These are illustrated in Figure 113 and read as follows:

- The grout body of the anchor is between 4 and 10 meters.
- The top of the grout body has to be at least 5 meters beneath the surface.
- The top of the grout body has to be at least 1 meter below any weak soil layer.
- The anchor can only be applied in sand layers.
- The minimum centre-to-centre distance of the anchors is 1.5 meters.

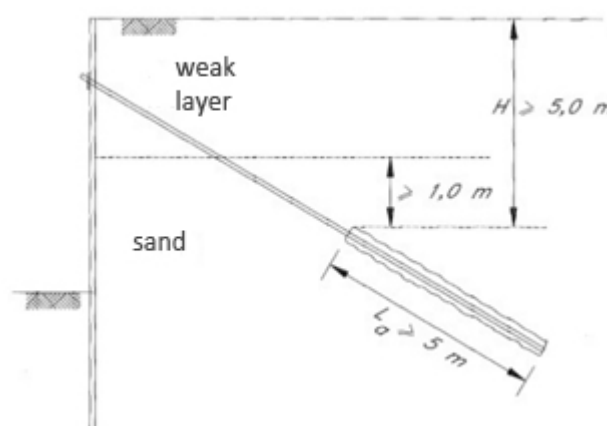


Figure 113 - Design requirements of GEWI anchors

Calculation of the bearing capacity of GEWI anchors is done using the method as described in (CUR166, 2012). This method is displayed in Equation 31.

$$Q_{r;\max;shaft} = f_{k;rep} \cdot L_a$$

$$Q_{r;\max;shaft} = \text{Bearing capacity [kN]}$$

$$f_{k;rep} = \text{Unit skin friction [kN/m']}$$

$$L_a = \text{Anchor length [m]}$$

Equation 31 - GEWI anchor calculation

The unit skin friction is an empirical value according to Table 92.

| Cone resistance [MPa] | Unit skin friction [kN/m'] |
|-----------------------|----------------------------|
| 5 - 10 | 65 - 100 |
| 10 - 15 | 100 - 135 |
| 15 - 20 | 135 - 170 |

Table 92 - Empirical skin friction relations for GEWI anchors

Anchors exist in various sizes based on the diameter of the central steel pipe. The available pipe diameters for use are 26.5, 32, 36, 40 and 47 mm with steel quality Fep 950 (Volker Staal en Funderingen, 2015).

J.2 Rock anchors

Rock anchors are commonly used in mining operations and consist of a GEWI bar fixed with mortar into a drilled hole in the rock. The load is supported by the weight of the rock it is drilled into meaning this method is sensitive to cracks in the rock layer. The actual bearing capacity (when the rock layer is sufficiently pure) is determined by the interaction between the steel and the grout as well as the grout-rock interaction. Figure 114 gives a side view of a rock anchor in installed form.

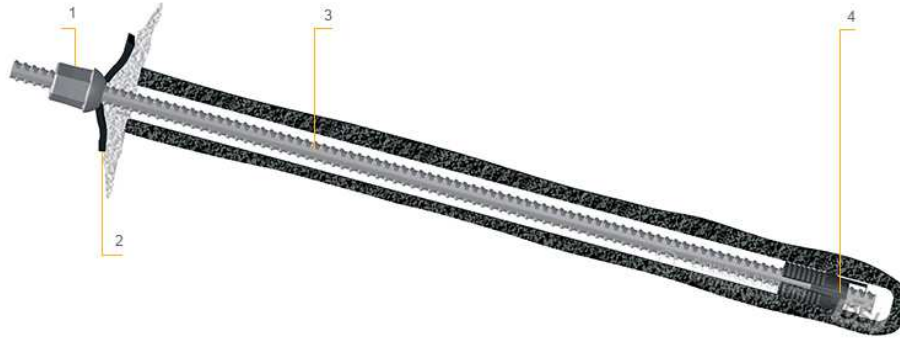


Figure 114 - Rock anchor

The bearing capacity of the rock anchor is determined as in Equation 32. It should be noted in this that the diameter and the bond length are not free to choose. The practical limit for the bond length is in the order of 8 – 10 meters and the maximum applicable drill hole diameter is 150 mm, the approximate diameter of the anchor rod is in the order of 0.4 to 0.6 times the drill hole diameter with anchor diameters of up to 55 mm (Wyllie, 1992). This means the according maximum applicable drill hole diameter is approximately 130 mm. The required calculation for the bond length needed to obtain a certain bearing capacity is given in Equation 32.

$$l_b = \frac{\gamma_m \cdot Q}{\pi \cdot d \cdot \tau_a}$$

$$l_b = \text{Bond length [m]}$$

$$Q = \text{Bearing capacity [N]}$$

$$d = \text{Drilled hole diameter [m]}$$

$$\tau_a = \text{Maximum bond stress [N/m}^2\text{]}$$

$$\gamma_m = \text{Material factor [-]} = 1.5$$

Equation 32 - Required bond length of rock anchors

Furthermore it should be checked that the working bond stress at the rock-grout interface does not exceed the bond stress at the grout-steel interface. To check this the development length is determined which indicates how much length is required to develop the full strength of the bar with an appropriate safety factor. The equation for this is given in Equation 33.

For 35 mm diameter bars and smaller

$$l_d = \gamma_m \cdot \frac{0.019 \cdot A_b \cdot \sigma_y}{\sqrt{\sigma_{uc}}}$$

but no less than

$$l_d = \gamma_m \cdot 0.058 \cdot d_b \cdot \sigma_y$$

For 45 mm diameter bars

$$l_d = \gamma_m \cdot \frac{26 \cdot \sigma_y}{\sqrt{\sigma_{uc}}}$$

For 55 mm diameter bars

$$l_d = \gamma_m \cdot \frac{34 \cdot \sigma_y}{\sqrt{\sigma_{uc}}}$$

l_d = Development length [mm]

A_b = Cross-sectional area [mm²]

σ_y = Yield stress of bar [MPa]

σ_{uc} = Compressive strength of grout [MPa]

d_b = Diameter of bar [mm]

Equation 33 - Development length of grout-steel interaction

These equations mean a graph can be made of the development length as a function of the anchor rod diameter for given values of the steel yield stress and the compressive strength of the grout. For a yield stress of 630 MPa (Fep 950) and a compressive strength of 30 MPa (which will also be used for the anchors) this graph is given in Figure 115. For larger diameter rods the trend lines can be used to estimate the required development length.

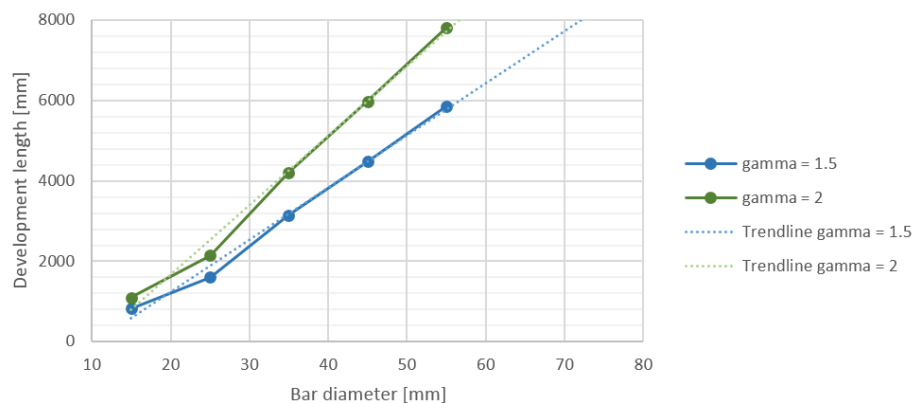


Figure 115 - Relation between rod diameter and development length

Appendix K Shallow foundation

The calculation of a shallow foundation is based on placing a large concrete block at the bottom of the ocean which spreads the load out over the bottom in such a way that the soil can bear it. For this type of foundation two things need to be determined: The bearing capacity of the soil (using the Brinch-Hansen method) and the dimensioning of the reinforced concrete block.

K.1 Brinch-Hansen

The Brinch-Hansen method is based on an empirically derived equation by Prantl, which has been refined using a variety of adjustment factors. The method is based on the shear resistance for certain slide plains in which the unit weight of the soil, the cohesion and the possible load caused by weak layers is included. Figure 116 illustrates this and Equation 34 gives the mathematical background of this process.

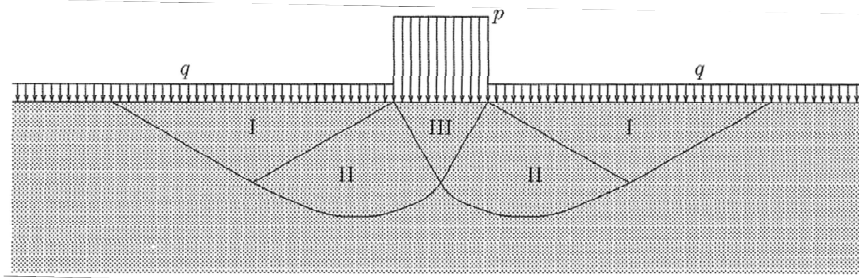


Figure 116 - Brinch-Hansen shallow foundation model

$$F = \frac{B \cdot L}{\gamma_m} \cdot \left(i_c \cdot s_c \cdot c \cdot N_c + i_q \cdot s_q \cdot q \cdot N_q + i_\gamma \cdot s_\gamma \cdot \frac{1}{2} \cdot \gamma' \cdot B \cdot N_\gamma \right)$$

$$i_c = \frac{\tau}{c + \sigma_n \cdot \tan \phi} \quad i_q = i_c^2 \quad i_\gamma = i_c^3$$

$$s_c = 1 + 0.2 \cdot \frac{B}{L} \quad s_q = 1 + \frac{B}{L} \cdot \sin \phi \quad s_\gamma = 1 - 0.3 \cdot \frac{B}{L}$$

$$N_q = \frac{1 + \sin \phi}{1 - \sin \phi} \cdot e^{\pi \cdot \tan \phi} \quad N_c = (N_q - 1) \cdot \cot \phi \quad N_\gamma = 2 \cdot (N_q - 1) \cdot \tan \phi$$

$$\gamma_m = 1.25$$

F = Bearing capacity [kN]

B = Footing width [m]

L = Footing length [m]

i = Load direction factors [–]

s = Footing shape factors [–]

N = Load coefficients [–]

c = Cohesion [kPa]

q = Side load [kN/m²]

γ' = Effective soil weight [kN/m³]

Equation 34 - Brinch-Hansen method

K.2 Foundation block calculation

The shallow foundation block that is placed upon the soil is as illustrated in Figure 117. It is assumed in this that the width of the column (e) is infinitely small and the imposed load is an ideal point load. This is acceptable because it leads to a slight overdimensioning without added failure hazards. Furthermore the soil stress is considered constant along the cross section where in reality there would be a slight increase underneath the column.

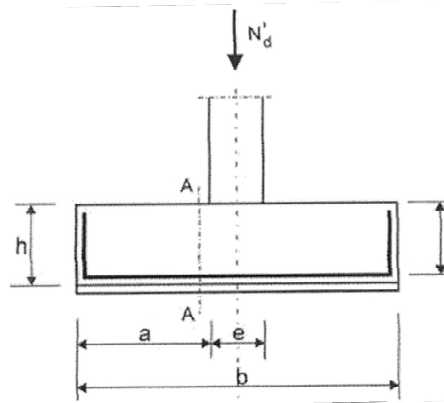


Figure 117 - Shallow foundation block

Using the above schematisation the required height of the foundation block can be calculated as well as the required reinforcement steel. Here too steel of the FeB500 type is used. Equation 35 gives the required formulae for calculating the dimensions and the required steel. Furthermore B35 concrete is used meaning the minimum reinforcement percentage is 0.18%. The horizontal dimensions of the block are known from K.1.

$$h = \frac{0.5 \cdot b}{2.5}$$

$$M = \frac{1}{2} \cdot \sigma_g \cdot 0.25 \cdot b^2$$

$$N_s = \frac{M}{0.85 \cdot h}$$

$$A_s = \frac{N_s}{435 \cdot 10^6}$$

h = Height of the block [m]
 b = Width of the block [m]
 M = Bending moment [Nm]
 σ_g = Soil stress [N/m²]
 N_s = Tensile force [N]
 A_s = Steel surface area [m²]

Equation 35 - Shallow foundation block calculation

Appendix L Financial considerations

L.1 Foundation economics

| Item | Unit | Price per unit |
|--------------------------|-------------------|----------------|
| Construction steel | [kg] | € 2.50 |
| Reinforcement steel | [kg] | € 1.85 |
| Precast concrete pile | [m'] | € 100.00 |
| Concrete | [m ³] | € 500.00 |
| Shallow foundation block | [m ³] | € 800.00 |
| GEWI anchor | [m'] | € 110.00 |
| Rock anchor | | € 2500.00 |

**) Prices include installation costs*

Table 93 - Unit price of construction materials

L.1.1 Barge shallow manmade port

| | Steel pipe piles (c) | Steel pipe piles (t) | Precast concrete piles | Shallow foundation | Anchors |
|--------------------------|----------------------|----------------------|------------------------|--------------------|--------------------|
| Construction steel | 27,324.3 [kg] | 106,756.0 [kg] | - | - | - |
| Reinforcement steel | - | - | 198.9 [kg] | - | - |
| Precast concrete pile | - | - | 2 | - | - |
| Concrete | - | - | 1.56 [m ³] | - | - |
| Shallow foundation block | - | - | - | - | - |
| GEWI anchor | - | - | - | - | 10 |
| Rock anchor | - | - | - | - | - |
| Costs | € 68,310.79 | € 110,740.38 | € 8,747.11 | - | € 33,000.00 |

L.1.2 Breakwater shallow manmade port

| | Steel pipe piles (c) | Steel pipe piles (t) | Precast concrete piles | Shallow foundation | Anchors |
|--------------------------|----------------------|----------------------|------------------------|--------------------|-------------|
| Construction steel | 120,753.3 [kg] | 252,658.7 [kg] | - | - | - |
| Reinforcement steel | - | - | 543.7 [kg] | - | - |
| Precast concrete pile | - | - | 4 | - | - |
| Concrete | - | - | 4.26 [m ³] | - | - |
| Shallow foundation block | - | - | - | - | - |
| GEWI anchor | - | - | - | - | 25 |
| Rock anchor | - | - | - | - | - |
| Costs | € 301,883.26 | € 548,441.50 | € 15,135.45 | - | € 82,500.00 |

L.1.3 Barge trailing edge estuary

| | Steel pipe piles (c) | Steel pipe piles (t) | Precast concrete piles | Shallow foundation | Anchors |
|--------------------------|----------------------|----------------------|------------------------|-------------------------|-------------|
| Construction steel | 75,166.8 [kg] | 457,286.3 [kg] | - | - | - |
| Reinforcement steel | - | - | 543.7 [kg] | 6,480.6 [kg] | - |
| Precast concrete pile | - | - | 4 | - | - |
| Concrete | - | - | 4.26 [m ³] | - | - |
| Shallow foundation block | - | - | - | 45.04 [m ³] | - |
| GEWI anchor | - | - | - | - | 23 |
| Rock anchor | - | - | - | - | - |
| Costs | € 344,066.57 | € 1,143,215.80 | € 21,135.45 | € 48,019.89 | € 37,950.00 |

L.1.4 Breakwater trailing edge estuary

| | Steel pipe piles (c) | | Steel pipe piles (t) | Precast concrete piles | Shallow foundation | Anchors |
|--------------------------|----------------------|------------------|----------------------|------------------------|-------------------------|---------|
| Construction steel | 245,895,0 [kg] | 1,146,832.7 [kg] | - | - | - | - |
| Reinforcement steel | - | - | 1,005.0 [kg] | 12,082.2 [kg] | - | - |
| Precast concrete pile | - | - | - | 5 | - | - |
| Concrete | - | - | - | 7.87 [m ³] | - | - |
| Shallow foundation block | - | - | - | - | 83.97 [m ³] | - |
| GEWI anchor | - | - | - | - | - | 39 |
| Rock anchor | - | - | - | - | - | - |
| Costs | € 697,942.75 | € 2,867,081.66 | € 26,045.97 | € 89,526.39 | € 64,350.00 | |

L.1.5 Barge leading edge bay

| | Steel pipe piles (c) | | Steel pipe piles (t) | Precast concrete piles | Shallow foundation | Anchors |
|--------------------------|----------------------|---|----------------------|------------------------|--------------------|---------|
| Construction steel | - | - | - | - | - | - |
| Reinforcement steel | - | - | - | - | - | - |
| Precast concrete pile | - | - | - | - | - | - |
| Concrete | - | - | - | - | - | - |
| Shallow foundation block | - | - | - | - | - | - |
| GEWI anchor | - | - | - | - | - | - |
| Rock anchor | - | - | - | - | - | 8 |
| Costs | - | - | - | - | € 20,000.00 | |

L.1.6 Breakwater leading edge bay

| | Steel pipe piles (c) | Steel pipe piles (t) | Precast concrete piles | Shallow foundation | Anchors |
|--------------------------|----------------------|----------------------|------------------------|--------------------|-------------|
| Construction steel | - | - | - | - | - |
| Reinforcement steel | - | - | - | - | - |
| Precast concrete pile | - | - | - | - | - |
| Concrete | - | - | - | - | - |
| Shallow foundation block | - | - | - | - | - |
| GEWI anchor | - | - | - | - | - |
| Rock anchor | - | - | - | - | 9 |
| Costs | - | - | - | - | € 22,500.00 |

L.2 Pistons

Pistons of the size considered in this design are generally not available on the market and need to be custom made. This also means that no set price is known and the cost of the pistons needs to be extrapolated from known prizes of smaller pistons. The piston costs used for this extrapolation have been given in Table 94 (Bitter, 2015).

| Diameter | Length | Cost |
|----------|---------|--------------|
| 0.3 [m] | 4.0 [m] | € 50,000.00 |
| 0.5 [m] | 4.0 [m] | € 80,000.00 |
| 0.5 [m] | 9.0 [m] | € 100,000.00 |

Table 94 - Estimated costs of pistons

It can be loosely concluded from this that when doubling the diameter of the piston the costs also double. Furthermore a doubling in length leads to an increase of approximately 20% in the costs. A formula for the calculation of the piston costs that is consistent with the values in Table 94 is given in Equation 36.

$$C = 4,000 \cdot L + 150,000 \cdot D - 11,000$$

$$C = \text{Piston costs [€]}$$

$$L = \text{Piston length [m]}$$

$$D = \text{Piston diameter [m]}$$

Equation 36 - Piston cost formula

Appendix M Host structure adjustments

M.1 Barge

The cross section of the barge can be simplified to a system of for upright metal girders positioned at a certain horizontal distance from each other and connected by flanges. This means the moment of inertia of the girders on both sides of the barge and the application of the Steiner rule should be applied to calculate the moment of inertia of the barge over the cross-section as in Equation 37.

$$\begin{aligned}
 I_{zz} &= \sum (I_{zz(\text{self})} + I_{zz(\text{steiner})}) \\
 &= \sum \left(\frac{1}{12} \cdot b_n \cdot h_n^3 + z_{C;n}^2 \cdot A_n \right) \\
 I_{zz} &= \text{Moment of inertia} [m^4] \\
 b &= \text{Width} [m] \\
 h &= \text{Height} [m] \\
 z_C &= \text{Distance in z direction from neutral center} [m] \\
 A &= \text{Surface area} [m^2]
 \end{aligned}$$

Equation 37 - Moment of inertia

Beside the bending moment punch could also be a failure mechanism, meaning the shear capacity of the bottom profile needs to be sufficient to withstand the support forces.

$$\sigma_{\max} = \frac{F}{\pi \cdot D \cdot d}$$

For the calculation it is assumed that the entire barge simplifies to a slab with a moment of inertia as described above supported by the Tidal Wave Energy Converter units and loaded with a uniform load determined by the added weight or buoyancy created by the extruding barge. For any excess forces the preferred solution is to create a shoe structure of girders welded underneath the barge which can be installed in-situ. This shoe structure needs to be able to add the required extra moment of inertia and shear capacity.

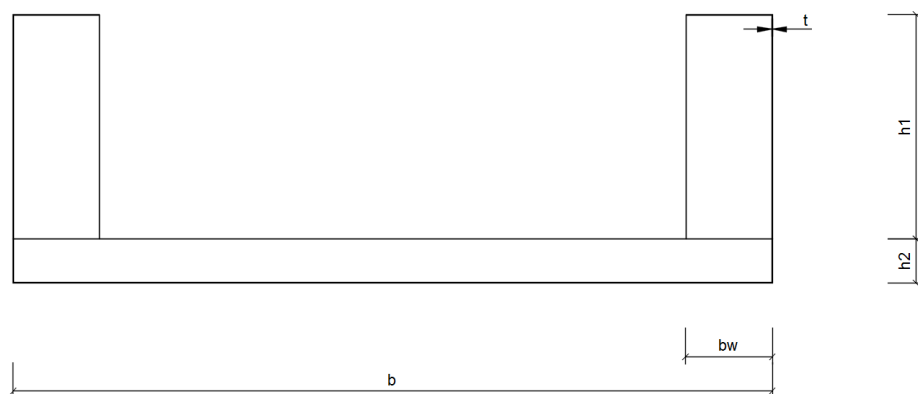


Figure 118 - Cross sectional composition of barge

The minimum skin thickness of inland vessels is 3 mm (Chief inspector of shipping, 2001), the value actually used for vessels is in the order of 5 to 8 mm, however, so an intermediate value of 6.5 mm will be used for the barges. Because the design wave height is unknown and therefore the required freeboard cannot be accurately determined it is assumed that a freeboard of 1 metre above the maximum water level relative to the barge is sufficient. The moment of inertia of the cross-section as illustrated in Figure 118 can be calculated with the formula as given in Equation 38.

$$z_c = \frac{4 \cdot h_1 \cdot t \cdot \frac{h_1}{2} + 2 \cdot h_2 \cdot t \cdot \left(h_1 + \frac{h_2}{2}\right) + b \cdot t \cdot \left(h_1 + \frac{t}{2}\right) + b \cdot t \cdot \left(h_1 + h_2 + \frac{t}{2}\right) + 2 \cdot b_w \cdot t \cdot \frac{t}{2}}{4 \cdot h_1 \cdot t + 2 \cdot h_2 \cdot t + 2 \cdot b \cdot t + 2 \cdot b_w \cdot t}$$

$$I_{zz} = 4 \cdot \frac{1}{12} \cdot t \cdot h_1^3 + 2 \cdot \frac{1}{12} \cdot t \cdot h_2^3 + 2 \cdot \frac{1}{12} \cdot b \cdot t^3 + 2 \cdot \frac{1}{12} \cdot b_w \cdot t^3 + 4 \cdot \left(\frac{h_1}{2} - z_c\right)^2 \cdot h_1 \cdot t$$

$$+ 2 \cdot \left(\frac{t}{2} - z_c\right)^2 \cdot b_w \cdot t + \left(h_1 + \frac{t}{2} - z_c\right)^2 \cdot b \cdot t + 2 \cdot \left(h_1 + \frac{h_2}{2} - z_c\right)^2 \cdot h_2 \cdot t + \left(h_1 + h_2 + \frac{t}{2} - z_c\right)^2 \cdot b \cdot t$$

Equation 38 - Moment of inertia of cross-section

Using the MatrixFrame software the bending moments and shear forces in a system of girders can be calculated. For the barge this has been done with the walls representing the girders and the bending moments and shear stresses being absorbed by those. The resulting moment and shear force distributions for this have been given in Figure 119.

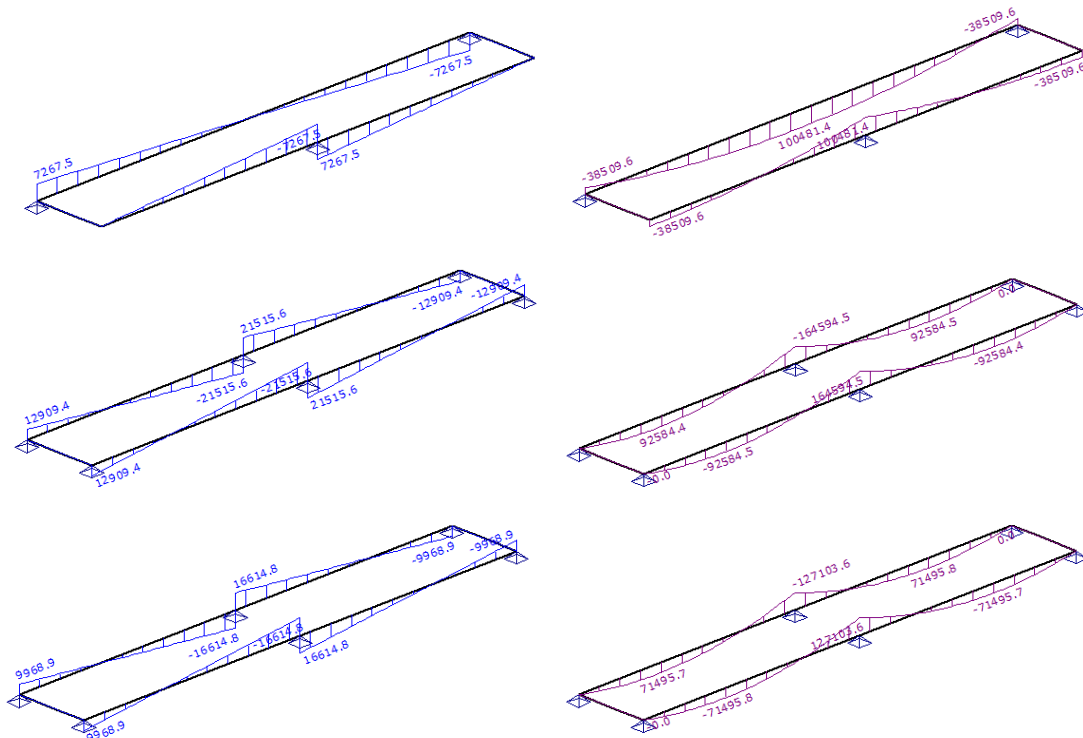


Figure 119 - Load distributions for various barge scenarios

With the bending moments and shear stress known the calculation can be made whether the structure is sufficient to withstand these loads. For this calculation Equation 39 is used. In case the

stresses in the system exceed the maximum yield stress of the steel adjustments to the barge are needed to make it sufficiently capable of handling the forces.

$$\sigma_{\max} = \frac{M_z \cdot z_{\max}}{I_{zz}} = \frac{M_z \cdot z_{\max}}{(I_{zz, \text{barge}} + I_{zz, \text{profile}})} \rightarrow I_{zz, \text{profile}} = \frac{M_z \cdot z_{\max}}{\sigma_{\max}} - I_{zz, \text{barge}}$$

$$\sigma_{\max} = \frac{V_z \cdot A^a \cdot z_C^a}{b^a \cdot (I_{zz, \text{barge}} + I_{zz, \text{profile}})} \rightarrow I_{zz, \text{profile}} = \frac{V_z \cdot A^a \cdot z_C^a}{\sigma_{\max} \cdot b^a} - I_{zz, \text{barge}}$$

d = Slab thickness [m]
 F = Force [N]
 b = Pile diameter [m]
 l = Centre-to-centre distance [m]

Equation 39 - Tension calculation for steel barge profiles

M.2 Breakwater

A floating breakwater is in essence a large concrete caisson designed to reduce the wave height in a sheltered area like a port or marina. Their design is already based on similar scenarios to the Tidal Wave Energy Converter's purpose where they are placed in tidal areas and fixed to the bottom with anchors. It is therefore thought reasonable to design a regular caisson for the specific scenarios anchored to the bottom with TWECs, meaning the caisson needs to be properly dimensioned for the relevant water pressures, the created bending moments through the supports and the shear stress/punch forces. Because the design wave height is unknown and therefore the required freeboard cannot be accurately determined it is assumed that a freeboard of 1 metre above the maximum water level relative to the caisson is sufficient. The bending moments and shear stresses are again calculated through the MatrixFrame software where this time three girders have been modelled. This too has to do with the configuration of the walls within the caisson as well as with the support placement underneath the caisson. The results are given in Figure 120.

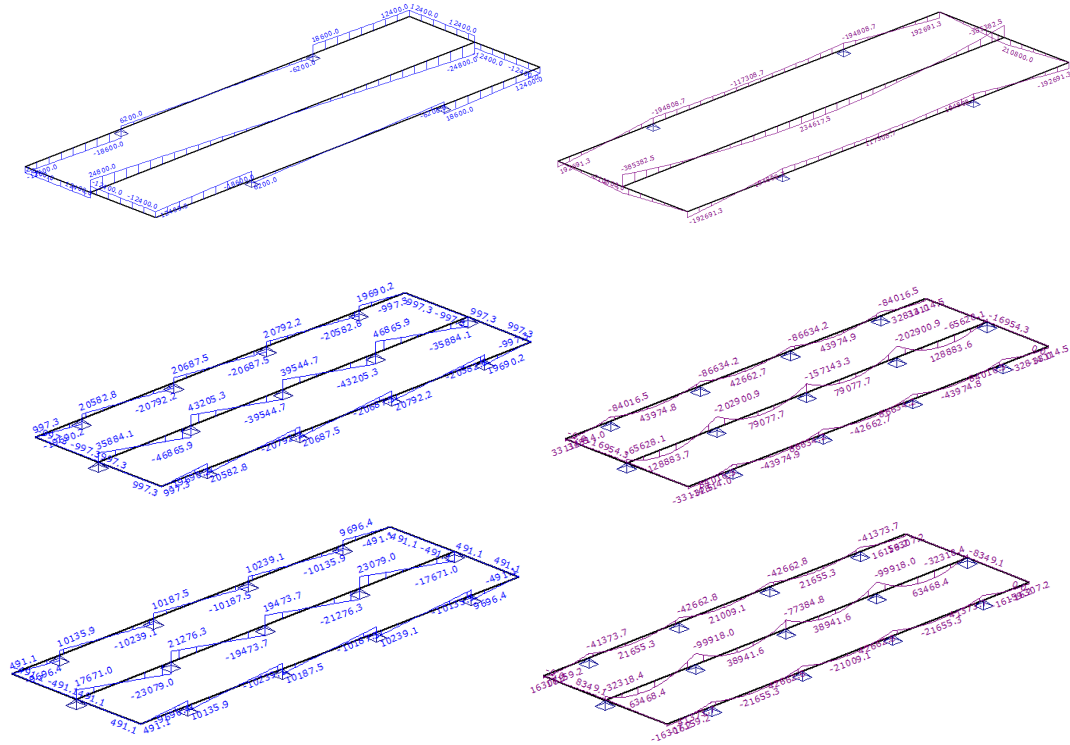


Figure 120 - Load distributions for various breakwater scenarios

To counter the bending moment reinforcement is used. The calculation of this is given in Equation 40. The reinforcement percentage herein must be between 0.18% and 1.94% for B35 concrete.

$$M = \frac{1}{8} \cdot q \cdot l^2$$

$$N_s = \frac{M}{0.85 \cdot h}$$

$$A_s = \frac{N_s}{435 \cdot 10^6}$$

$$0.18\% \leq \omega = \frac{A_s}{h} \cdot 100\% \leq 1.94\%$$

q = Distributed load $[N/m']$

l = Length of the span $[m]$

h = Height of the slab $[m]$

M = Bending moment $[Nm]$

N_s = Tensile force $[N]$

A_s = Steel surface area $[m^2]$

ω = Reinforcement percentage

Equation 40 - Reinforcement calculation for concrete elements

Lastly the punch needs to be calculated to ensure the supports do not punch through the bottom of the structure. This is done through Equation 41.

$$\tau_d \leq \tau_1$$

$$\tau_d = \frac{F_d}{\pi \cdot (a + d) \cdot d}$$

$$\tau_1 = \text{Tensile strength of concrete} = 4.20 \cdot 10^6 \left[N/m^2 \right]$$

$$\tau_d = \text{Shear stress} \left[N/m^2 \right]$$

$$F_d = \text{Applied force} \left[N \right]$$

$$a = \text{Column diameter} \left[m \right]$$

$$d = \text{Slab height} \left[m \right]$$

Equation 41 - Punch calculation for concrete elements

Appendix N Piston and rod dimensioning

N.1 Piston wall thickness

The thickness of the piston is governed by the pressure inside it as the piston itself does not have any forces applied to it in the longitudinal direction. This means that the wall thickness can be determined through half the force (the other half is handled by the wall on the other side) of the entire force pushing outward in the piston as shown in Figure 121.

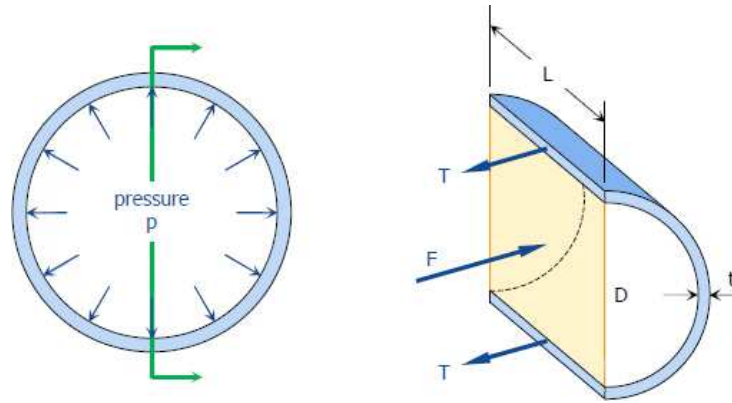


Figure 121 - Pressure distribution in pipe wall

The calculation for the wall thickness of the piston is given in Equation 42.

$$p = \frac{F_{\max}}{0.25 \cdot \pi \cdot D_i^2}$$

$$F_{\text{wall}} = \frac{1}{2} \cdot \frac{p}{D_i}$$

$$t_{\text{wall}} = \frac{F_{\text{wall}}}{\sigma_s}$$

$$\sigma_s = \text{Tensile strength } [N/mm^2]$$

$$F_{\max} = \text{Maximum force } [N]$$

$$F_{\text{wall}} = \text{Force in the wall } [N]$$

$$t_{\text{wall}} = \text{wall thickness } [m]$$

Equation 42 - Piston wall thickness

N.2 Buckling range estimation

The material use of the device is based on several components. For the determination of what part of the tidal wave to use, however, not all of these components are relevant. The important differentiating factors between the two processes are the tensile/compressive strength and the buckling strength. The tensile/compressive strength is present in both load scenarios and is limited by the maximum tensile strength of the used material (e.g.: 235 N/mm² for steel). This means that for a given force exerted by the floating body, the required load bearing surface can be easily calculated with Equation 43.

$$\sigma = \frac{F_{\max}}{A}$$

σ = tensile strength $[N/mm^2]$
 F_{\max} = maximum force $[N]$
 A = load bearing area $[mm^2]$

Equation 43 – Tensile strength formula

For the load scenario with the up going tidal motion, when the pistons are loaded on compression, the effect of buckling also needs to be taken into account. In this calculation the exact modelling of the pistons in its complete installation is relevant as the effect of a fixed, spring or free connection to the pontoon and the foundation is of influence on the buckling force. Because in this phase this exact configuration is unknown the ideal Euler buckling formula will be used as presented in Equation 44.

$$F_{buc} = \frac{\omega_{buc} \cdot \pi^2 \cdot EI_{zz}}{\psi \cdot l_{buc}^2}$$

F_{buc} = buckling force $[N]$
 ω_{buc} = buckling factor $[-]$
 E = Young's modulus $[N/mm^2]$
 I_{zz} = moment of inertia $[mm^4]$
 ψ = load factor $[-]$
 l_{buc} = buckling length

Equation 44 – Eulerian buckling load

Ideally the same structure can be used for both energy extractions during flood as well as during ebb. This is the case when the buckling force for the structure dimensioned for the tension based structure exceeds the actual load on the system. Following the same principle this means that the length of the loaded rods in the system may not be longer than the theoretical buckling length. The force on the system (which for calculating the buckling length is assumed to be the buckling force) and the Young's modulus for the materials are fixed, meaning that the only remaining variable to influence the buckling length is the moment of inertia. Assuming equal surface areas for both scenarios, and therefore equal costs (Pascha, 2015), the moment of inertia can be increased by making the rod hollow (as illustrated in Figure 122). The rod length as found in the fully extruded position of the piston is considered to be the dominant length to be considered, the piston is considered to be at the outer end of the draught beneath the floater either at the bottom or at the top. The buckling length is also illustrated in Figure 122.

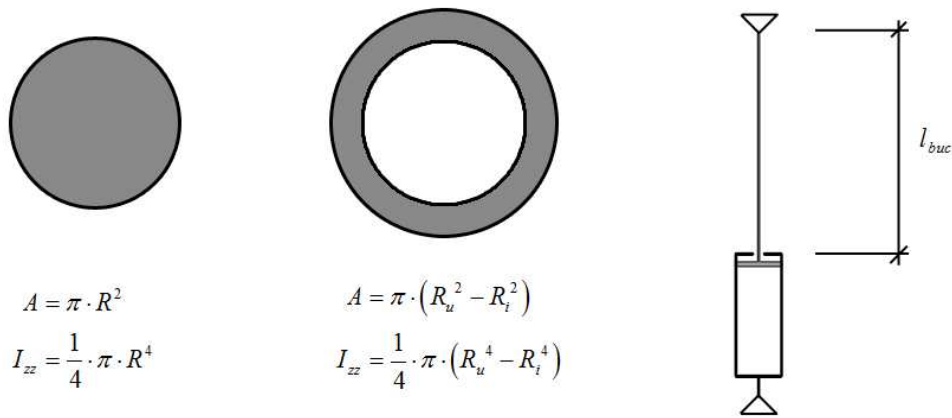


Figure 122 - Different rod styles and buckling length

The dimensions of the hollow area within the rod provide an indication of the range from the minimum (solid rod) to the maximum obtainable buckling length (outer diameter equal to support area). It should be noted that the actual buckling length differs slightly due to the influence of the piston, for this estimation tool it is, however, assumed that the piston is relatively short and narrow. Albeit not entirely accurate it is a sufficiently valid assumption as long as the method is used only as an indicative method for whether it will buckle or not and not as a definitive calculation. Equation 45 derives a formula for the calculation of the buckling length of a solid rod. It can be observed that this buckling length is only dependent on a set of fixed material characteristics and the loading force on the system. The width of the rod is still present as a hidden influence, however, due to the validity requirement that the surface area is sufficient to bear the compressive load.

$$\begin{aligned}
 A &= \frac{\psi \cdot F_{\max}}{\sigma} \\
 R_u &= \sqrt{\frac{A}{\pi}} = \sqrt{\frac{\psi \cdot F_{\max}}{\sigma \cdot \pi}} \\
 I_{zz} &= \frac{1}{4} \cdot \pi \cdot R_u^4 = \frac{1}{4} \cdot \pi \cdot \sqrt{\frac{\psi \cdot F_{\max}}{\sigma \cdot \pi}}^4 = \frac{\psi^2 \cdot F_{\max}^2}{4 \cdot \sigma^2 \cdot \pi} \\
 l_{buc;solid} &= \sqrt{\frac{\omega_{buc} \cdot \pi^2 \cdot E \cdot I_{zz}}{\psi \cdot F_{\max}}} = \sqrt{\frac{\omega_{buc} \cdot \pi^2 \cdot E \cdot \frac{\psi^2 \cdot F_{\max}^2}{4 \cdot \sigma^2 \cdot \pi}}{\psi \cdot F_{\max}}} = \sqrt{\psi \cdot \omega_{buc} \cdot F_{\max} \cdot \frac{\pi \cdot E}{4 \cdot \sigma^2}}
 \end{aligned}$$

Equation 45 – Solid rod buckling length

The maximum value for the buckling length is obtained when the outer diameter of the rod is equal to the bearing surface of the piston. This value is obtained through the process in which the operating pressure is calibrated with the characteristics of the hydraulic motor. For all practical applications the rod in this scenario can be modelled as thin, which means the buckling length can be calculated with the simplified formula as derived in Equation 46. It can be observed that the buckling length in this scenario is dependent on the same set of material characteristics as in the previous derivation, with the difference that the rod diameter is the only variable rather than the force. Again, the load is a hidden influence through the load bearing requirement.

$$\begin{aligned}
 A &= \frac{\psi \cdot F_{\max}}{\sigma} \\
 t &= \frac{A}{2 \cdot \pi \cdot R_u} = \frac{\psi \cdot F_{\max}}{2 \cdot \pi \cdot R_u \cdot \sigma} \\
 I_{zz} &= \pi \cdot R_u^3 \cdot t = \pi \cdot R_u^3 \cdot \frac{\psi \cdot F_{\max}}{2 \cdot \pi \cdot R_u \cdot \sigma} = \frac{R_u^2 \cdot \psi \cdot F_{\max}}{2 \cdot \sigma} \\
 l_{buc;thin} &= \sqrt{\frac{\omega_{buc} \cdot \pi^2 \cdot E \cdot I_{zz}}{\psi \cdot F_{\max}}} = \sqrt{\frac{\omega_{buc} \cdot \pi^2 \cdot E \cdot \frac{R_u^2 \cdot \psi \cdot F_{\max}}{2 \cdot \sigma}}{\psi \cdot F_{\max}}} = R_u \cdot \sqrt{\frac{\omega_{buc} \cdot \pi^2 \cdot E}{2 \cdot \sigma}}
 \end{aligned}$$

Equation 46 – Thin walled rod buckling length

The solution in between the two extremes, when the rod cannot be considered thin, is more complex and derived in Equation 47. As is to be expected it is dependent on not only the material characteristics, but also on both the rod diameter and the load.

$$\begin{aligned}
 A &= \frac{\psi \cdot F_{\max}}{\sigma} \\
 R_i &= \sqrt{R_u^2 - \frac{A}{\pi}} = \sqrt{R_u^2 - \frac{\psi \cdot F_{\max}}{\sigma \cdot \pi}} \\
 I_{zz} &= \frac{1}{4} \cdot \pi \cdot (R_u^4 - R_i^4) = \frac{1}{4} \cdot \pi \cdot \left(R_u^4 - \sqrt{R_u^2 - \frac{\psi \cdot F_{\max}}{\sigma \cdot \pi}}^4 \right) \\
 &= \frac{1}{4} \cdot \pi \cdot \left(R_u^4 - \left(R_u^2 - \frac{\psi \cdot F_{\max}}{\sigma \cdot \pi} \right)^2 \right) \\
 l_{buc;hollow} &= \sqrt{\frac{\omega_{buc} \cdot \pi^2 \cdot E \cdot I_{zz}}{\psi \cdot F_{\max}}} = \sqrt{\frac{\omega_{buc} \cdot \pi^3 \cdot E \cdot \left(R_u^4 - \left(R_u^2 - \frac{\psi \cdot F_{\max}}{\sigma \cdot \pi} \right)^2 \right)}{4 \cdot \psi \cdot F_{\max}}}
 \end{aligned}$$

Equation 47 – Hollow rod buckling length

From these derivations it can be concluded that the maximum length of the rod can be made to have a workable value in the range as given in Equation 48. This means that as long as the required rod length is lower than the upper bound of the range, it can operate on pressure (and tension) with hollow rods; and if the rod length is lower than the lower bound of the range it can also be done with solid rods.

$$\sqrt{\psi \cdot \omega_{buc} \cdot F_{\max} \cdot \frac{\pi \cdot E}{4 \cdot \sigma^2}} \leq l_{buc} \leq R_u \cdot \sqrt{\frac{\omega_{buc} \cdot \pi^2 \cdot E}{2 \cdot \sigma}}$$

Equation 48 – Buckling range

N.3 Actual buckling force

The actual buckling force of a rod/piston combination is different from the Eulerian buckling load as derived above. The moments of inertia of the piston and the rod are of importance as are the relative lengths of each section. The calculation of such a piston/rod system is given in (NEN-6786, 2001) and is as depicted in Equation 49.

$$\sqrt{\frac{I_1}{I_2}} \cdot \tan\left(\frac{\pi}{x} \cdot \frac{l_1}{l}\right) = -\tan\left(\frac{\pi \cdot \left(1 - \frac{l_1}{l}\right) \cdot \sqrt{\frac{I_1}{I_2}}}{x}\right)$$

$$I_{circle} = \frac{1}{4} \cdot \pi \cdot (R_u^4 - R_i^4)$$

$$l_{buc} = x \cdot l$$

$$I_n = \text{Moment of inertia } [m^4]$$

$$l_n = \text{Length } [m]$$

Equation 49 – Buckling ratio for pistons

The explanation of what areas the different variables relate to is given in Figure 123.

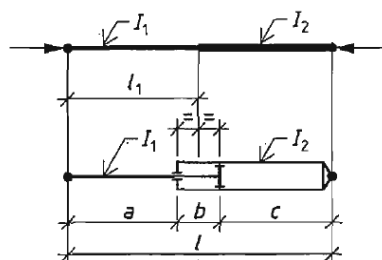


Figure 123 – Explanation of variables for buckling ratio for pistons

The values for x for different values of α (l_1/l) and β (I_1/I_2) are given in Table 95.

| $\alpha \backslash \beta$ | 0.05 | 0.10 | 0.20 | 0.30 | 0.40 | 0.50 | 0.60 | 0.70 | 0.80 | 0.90 |
|---------------------------|-------|-------|-------|-------|-------|-------|-------|-------|-------|-------|
| 0.05 | 0.226 | 0.317 | 0.448 | 0.548 | 0.633 | 0.707 | 0.775 | 0.837 | 0.895 | 0.949 |
| 0.10 | 0.249 | 0.329 | 0.454 | 0.552 | 0.636 | 0.709 | 0.776 | 0.838 | 0.895 | 0.949 |
| 0.20 | 0.392 | 0.426 | 0.506 | 0.585 | 0.659 | 0.726 | 0.788 | 0.846 | 0.900 | 0.951 |
| 0.30 | 0.541 | 0.561 | 0.608 | 0.660 | 0.713 | 0.765 | 0.816 | 0.865 | 0.912 | 0.957 |
| 0.40 | 0.672 | 0.686 | 0.716 | 0.749 | 0.784 | 0.820 | 0.857 | 0.893 | 0.929 | 0.965 |
| 0.50 | 0.783 | 0.792 | 0.812 | 0.833 | 0.855 | 0.878 | 0.901 | 0.926 | 0.950 | 0.975 |
| 0.60 | 0.872 | 0.878 | 0.889 | 0.902 | 0.914 | 0.928 | 0.941 | 0.955 | 0.970 | 0.985 |
| 0.70 | 0.938 | 0.941 | 0.946 | 0.952 | 0.959 | 0.965 | 0.972 | 0.979 | 0.985 | 0.993 |
| 0.80 | 0.979 | 0.980 | 0.962 | 0.984 | 0.986 | 0.988 | 0.991 | 0.993 | 0.995 | 0.998 |
| 0.90 | 0.997 | 0.997 | 0.997 | 0.998 | 0.998 | 0.998 | 0.999 | 0.999 | 0.999 | 1.000 |

Table 95 - Buckling ratio

Applying the newly obtained buckling ratio for pistons to the Eulerian buckling load gives the expression as given in Equation 50.

$$F_{buc} = \frac{\omega_{buc} \cdot \pi^2 \cdot EI_{zz}}{\psi \cdot (x \cdot l)^2} = \frac{\omega_{buc} \cdot \pi^2 \cdot EI_{zz}}{\psi \cdot x^2 \cdot l^2}$$

Equation 50 - Buckling load for pistons

N.4 Buckling factor

The buckling factor as mentioned in Equation 44 is a factor that accounts for the inhomogeneous nature of the used material, the shape of the used material and the proximity to the yield stress. The equation that gives the relation between a triplicate of variables and the buckling factor is given in Equation 51 and illustrated in Figure 124 for symmetric cross sections (Welleman, et al., 2001). In this equation λ_{rel} is the relative slenderness of the structure, a ratio between the slenderness of the structure and the minimal slenderness based on the yield stress. The variables α_k and λ_0 depend on the shape of the cross section. For symmetric cross sections such as the one being used these values are respectively 0.21 for α_k and 0.2 for λ_0 .

$$\alpha_k = 0.21 \quad \lambda_0 = 0.2 \quad \lambda_{rel} = 1$$

$$\omega_{buc} = \frac{1 + \alpha_k \cdot (\lambda_{rel}^2 - \lambda_0) + \lambda_{rel}^2}{2 \cdot \lambda_{rel}^2} - \frac{\sqrt{(1 + \alpha_k \cdot (\lambda_{rel}^2 - \lambda_0) + \lambda_{rel}^2)^2 - 4 \cdot \lambda_{rel}^2}}{2 \cdot \lambda_{rel}^2} = 0.67$$

Equation 51 – Buckling factor

The relation between the slenderness and the buckling factor is given in Figure 124. The load factor as mentioned in Equation 44 depends on the classification of the superstructure. It is reasonable to assume that the use of the superstructure will at most consist of small scale residential buildings the classification is CC1b. This means the required load factor for all variable loads is 1.5 (Eurocode 2, 1992). The material factor is included in the representative material characteristics of the used materials. (e.g.: for steel the material factor is 1.0 and for concrete 1.5).

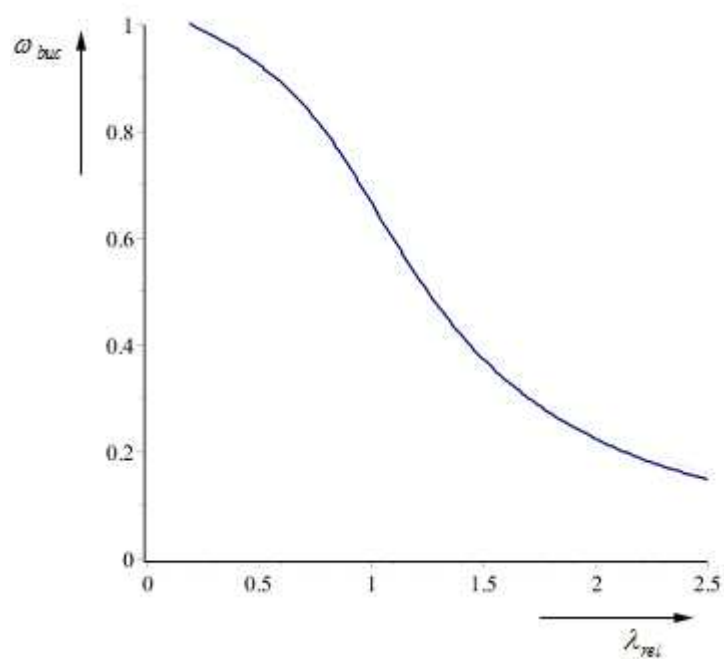


Figure 124 - Relation between ω_{buc} and relative slenderness

Appendix O Corrosion of steel elements

Steel elements in marine environments are subject to a certain amount of corrosion. The magnitude of this corrosion depends on the salinity of the water, the location of the corroding element relative to the water table and according splash zone and the time of exposure. Figure 125 illustrates the locations of the different water zones (CUR166, 2012).

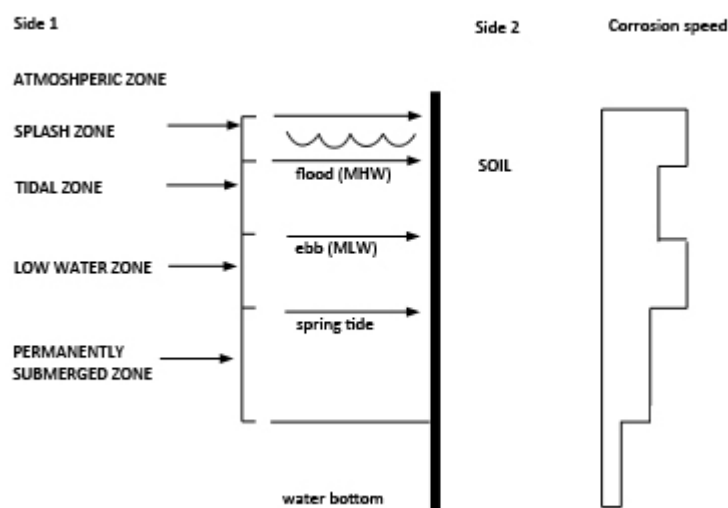


Figure 125 - Water zones for corrosion

The amount of corrosion of steel elements over a certain amount of time depends on the number of years of exposure and the type of exposure. Table 96 gives these rates of decay in mm for combinations of exposure duration and type for an exposed surface of steel.

| Desired lifespan (years) | 5 *) | 25 *) | 50 | 75 | 100 |
|---|------|-------|------|------|------|
| Clean, fresh water (around the water table) | 0.15 | 0.55 | 0.90 | 1.15 | 1.40 |
| Contaminated fresh water (around the water table) | 0.30 | 1.30 | 2.30 | 3.30 | 4.30 |
| Salt water (splash and low water zone) | 0.55 | 1.90 | 3.75 | 5.60 | 7.50 |
| Salt water (permanently submerged) | 0.25 | 0.90 | 1.75 | 2.60 | 3.50 |

*) Values for 5 and 25 years have been measured, the rest is extrapolated from these.

Table 96 - Corrosion rates in different zones in mm

Appendix P Tidal Wave Energy Converter calculation script

Because the tide is an inhomogeneous phenomena that is never quite the same over a certain period of time it is difficult to determine a uniform representation of the electric revenue and the applied loads. Therefore a script has been written that can determine the tidal forcing and the according electric revenue for any desired period of time. Because some trial and error is required to optimize the process a Graphic User Interface (GUI), as shown in Figure 126, has been created to make the process easier. The following paragraphs elaborate on what input data is given and what output data the script provides.

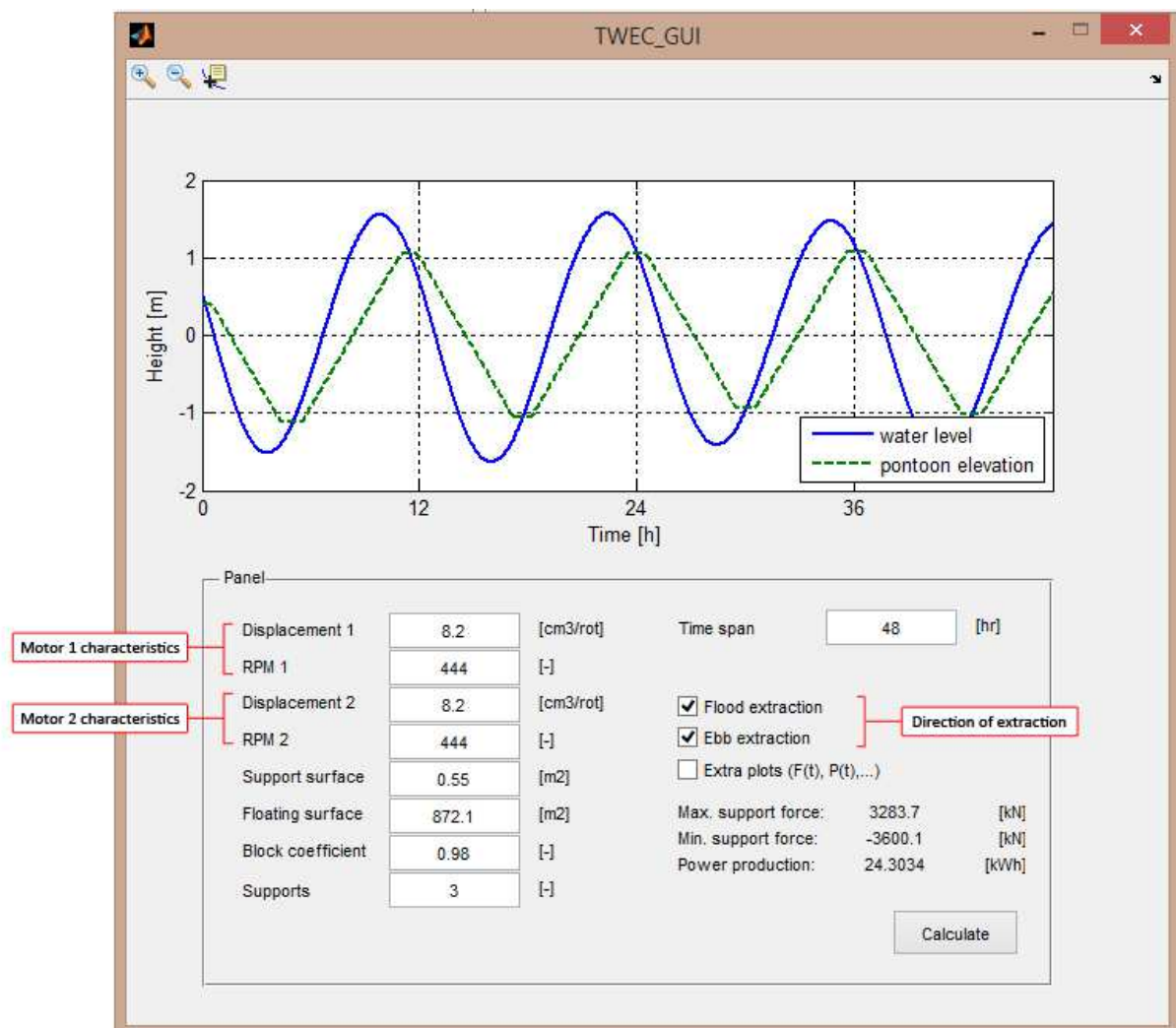


Figure 126 - TWEC script Graphic User Interface

P.1 Input data

There are three different ways in which input data is supplied to the script. Firstly and most evident are the input boxes in the GUI which account for the motor's displacement and rotations per minute, the bearing surface area of the supports (or the inner surface area of the pistons), the surface area of the host structure, the block coefficient of the host structure, the number of supports over which the load is (equally) distributed and the amount of time over which results are desired. Furthermore the direction of energy extraction can be determined through a checkbox. Also through a checkbox a number of extra plots like the exerted force over time and the amount of generated power over time can be generated. The script holds the possibility to use two different motors based

on the rise- and fall velocity of the host structure, but usually the use of a single type of motor is preferential.

The second method of inputting data is through the data.out file which is generated by the Global Inverse Tide Model (as described in Section 2). This file contains the relevant characteristics of the 11 major tidal constituents (amplitude, angular velocity and phase shift) which are read by the script and combined into a complete plot of the tidal motion. In principle this file is filled out automatically by the GITM, but manual manipulation is possible as well as long as the format is not altered. Figure 127 shows what this file looks like.

| | Latitude | Longitude | Parameter | Con | Ampl/MajAxis | Phase(o, GMT) | MinAxis | Incl(o, GMT) |
|----|----------------------|-----------|-----------|-----|--------------|---------------|---------|--------------|
| 1 | 04-Nov-2014 14:49:53 | | | | | | | |
| 2 | 53.1840 | 5.1060 | z (m) | m2 | 1.5000 | 040.00 | | |
| 3 | 53.1840 | 5.1060 | z (m) | s2 | 0.1000 | 120.00 | | |
| 4 | 53.1840 | 5.1060 | z (m) | n2 | 0.1000 | 010.00 | | |
| 5 | 53.1840 | 5.1060 | z (m) | k2 | 0.1000 | 120.00 | | |
| 6 | 53.1840 | 5.1060 | z (m) | k1 | 0.0200 | 340.00 | | |
| 7 | 53.1840 | 5.1060 | z (m) | o1 | 0.0200 | 320.00 | | |
| 8 | 53.1840 | 5.1060 | z (m) | p1 | 0.0100 | 350.00 | | |
| 9 | 53.1840 | 5.1060 | z (m) | q1 | 0.0500 | 310.00 | | |
| 10 | 53.1840 | 5.1060 | z (m) | mf | 0.0100 | 300.00 | | |
| 11 | 53.1840 | 5.1060 | z (m) | mm | 0.0100 | 020.00 | | |
| 12 | 53.1840 | 5.1060 | z (m) | m4 | 0.0300 | 350.00 | | |
| 13 | | | | | | | | |
| 14 | | | | | | | | |

Figure 127 - Tidal constituents input file

The final method of inputting data is by hard coding it into the script. Because doing this decreases the ease of use of the program the amount of hard coded data input has been kept to a minimum. The only thing that is actually hard coded into the script is the efficiency curve of the hydraulic motors, which is derived based on performance data provided by Eaton, the manufacturer of the considered hydraulic motors. This efficiency curve depends on the applied pressure and is given in Equation 52. The efficiency is limited between 14 and 140 BAR outside of which the efficiency is zero.

$$\eta(p) = 3 \cdot 10^{-7} \cdot p^3 - 0.001 \cdot p^2 + 0.0101 \cdot p + 0.05784$$

$$\eta = \text{efficiency}[-]$$

$$p = \text{pressure}[BAR]$$

Equation 52 - Motor efficiency curve

P.2 Output data

The data that can be obtained from the GUI is printed in the lower right corner and consists of the electric revenue during the considered timespan and the maximum compressive and tensile forces that occur during that time. Furthermore plots are available for the water level, the pontoon elevation, the power production and the forces on the system. Further numbers, like pontoon elevation, could be obtained fairly easily but would require (minor) additional coding to be added.

P.3 Code

The code included in the discussed GUI, without the code required to make the GUI work is as given in the following text boxes.

```
% Read constituents file
fileID = fopen('data.out', 'rt');
NumHeaders = 2;
NumDataLines = 11;
ColNum = 5;
fmt = [ repmat('%s',1,ColNum-1), '%f%[\n]' ];
data = textscan(fileID, fmt, NumDataLines, 'HeaderLines', NumHeaders);
A=data{1};
P=cellfun(@str2double, data{2});
fclose(fileID);
% Angular velocities of tidal constituents
O = [28.984; 30.000; 28.439; 30.082; 15.041; 13.943; 14.958; 13.399; 1.098;
0.544; 57.971];
% Calculation loop
handles.x = 0:1/handles.N:1;
for i = 1:1/60:(handles.N)
    handles.t(j)=i-1;
    handles.z(j)=sum(A .* cosd(O .* (i-1) + P));
    handles.h(1)=0.7*handles.z(1)
    handles.p(j)=0.00001*9.81*1000*(handles.Af/handles.sup)*(handles.h(j)-
handles.z(j))*handles.Cb/handles.Ab
    if 0 < abs(handles.p(j)) && abs(handles.p(j)) < 14
        alpha=0;
        beta=0;
    elseif abs(handles.p(j)) >= 140
        alpha=0;
        beta=0;
    else
        if handles.p(j) < 0
            alpha=1;
            beta=1*handles.Eflood;
        else
            alpha=-1;
            beta=-1*handles.Eebb;
        end
    end
    handles.eta(j)=(3*10^-7)*(abs(handles.p(j)))^3-
0.0001*(abs(handles.p(j)))^2+0.0101*abs(handles.p(j))+0.5784;
handles.Ph(j)=handles.sup*abs(beta*handles.eta(j)*(handles.Dis*handles.RPM/1000)
*handles.p(j)/600);
handles.h(j+1)=handles.h(j) + (alpha * handles.Dis * handles.RPM / 1000000)
/ handles.Ab;
handles.z(j+1)=sum(A .* cosd(O .* (i-1) + P));
handles.Ph(j+1)=handles.sup*abs(beta*handles.eta(j)*(handles.Dis*handles.RPM/100
0)*handles.p(j)/600);
handles.t(j+1)=(i-1)+1/60;
handles.eta(j+1)=(3*10^-7)*(abs(handles.p(j)))^3-
0.0001*(abs(handles.p(j)))^2+0.0101*abs(handles.p(j))+0.5784;
handles.F(j)=(handles.z(j)-handles.h(j))*9.81*handles.Af/handles.sup;
handles.F(j+1)=(handles.z(j+1)-handles.h(j+1))*9.81*handles.Af/handles.sup;
j=j+1;
handles.Pt = sum(handles.Ph)/60;
handles.Fm = max(handles.F);
handles.Fmin = min(handles.F);
set(handles.text20, 'String', handles.Pt);
set(handles.text25, 'String', handles.Fm);
set(handles.text28, 'String', handles.Fmin);
end
```

```
% Plot creation
plot(handles.t, handles.z, '-', handles.t, handles.h, '--', 'Linewidth', 2)
set(0, 'DefaultAxesColorOrder', [0 0 0.9; 0 0.5 0])
axis 'auto y'
xlim([0 handles.N-1])
set(gca, 'XTick', 0:12:handles.N-1);
grid on
legend('water level', 'pontoon elevation', 'Location', 'southeast')
xlabel('Time [h]')
ylabel('Height [m]')

% Extra plots creation
if handles.Eplots > 0

    figure(1)

    subplot(2,1,1)
    plot(handles.t, handles.Ph, 'Linewidth', 2)
    xlabel('Time [h]')
    ylabel('Power [kW]')
    axis 'auto y'
    xlim([0 handles.N-1])
    set(gca, 'XTick', 0:12:handles.N-1);
    grid on

    subplot(2,1,2)
    plot(handles.t, handles.F, 'Linewidth', 2)
    xlabel('Time [h]')
    ylabel('Force [kN]')
    axis 'auto y'
    xlim([0 handles.N-1])
    set(gca, 'XTick', 0:12:handles.N-1);
    grid on

    figure(2)

    plot(handles.t, handles.z, '-', handles.t, handles.h, '--', 'Linewidth', 2)
    set(0, 'DefaultAxesColorOrder', [0 0 0.9; 0 0.5 0])
    axis 'auto y'
    xlim([0 handles.N-1])
    set(gca, 'XTick', 0:12:handles.N-1);
    grid on
    legend('water level', 'pontoon elevation', 'Location', 'southeast')
    xlabel('Time [h]')
    ylabel('Height [m]')
```

Appendix Q Sieve analysis

To determine a location with a highest probability of feasibility a sieve analysis can be executed to rule out low potential locations and pinpoint those with high potential. The important aspects that ought to be taken into account to determine a suitable location are the type of tide (diurnal, semi-diurnal or mixed) and the relevant tidal amplitudes. As was determined in chapter 25 it is favourable to have a constant semi-diurnal type of tide with a high amplitude as this means there are more repetitions of the height difference with little variations in revenue over time. Figure 128 gives the classifications of tides over the world as rendered with information of (TOPEX/Poseidon, sd).

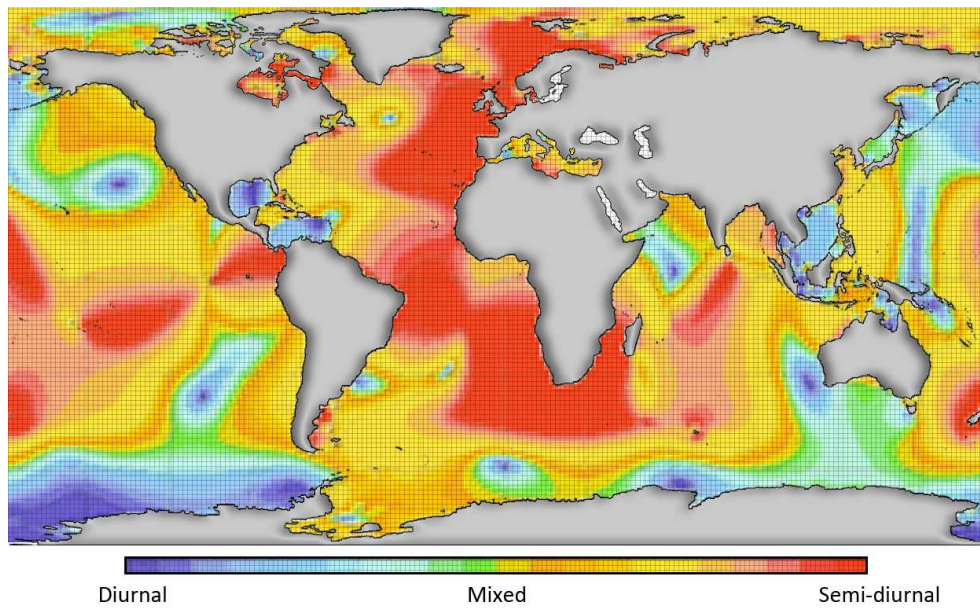


Figure 128 - Classification of tides over the world

The classification of the tide is determined based on the ratio between the diurnal and the semi-diurnal constituents according to Equation 53. Values of F smaller than 0.25 mean the tide is semi-diurnal, values higher than 4 mean it is diurnal. Anything in between is mixed with a certain bias based on which constituents are larger. So for an ideal location the map in Figure 128 would be coloured red as this illustrates a purely semi-diurnal tidal motion.

$$F = \frac{K_1 + O_1 + P_1 + Q_1}{M_2 + S_2 + K_2 + N_2}$$

Equation 53 - Tide classification formula

The second important tidal element is the amplitude of the relevant constituents. Through Figure 128 the influence of the diurnal constituents has been taken out of consideration, as a location will be picked where the semi-diurnal constituents are dominant, meaning the amplitudes of the dominant semi-diurnal constituents (M_2 and S_2) need to be known. Figure 129 gives the amplitudes of the semi-diurnal lunar tide over the world (M_2) and Figure 130 gives that of the semi-diurnal solar tide (S_2) (TOPEX/Poseidon, sd). Because there is a slight difference in angular velocity between the solar tide and the lunar tide both being of equal magnitude means they would cancel each other out at certain time intervals resulting in an inconsistent tidal window. Ideally therefore either one of

these constituents has to be larger than the other. From Figure 129 and Figure 130 this means a location needs to be selected where either one or the other shows values in the red.

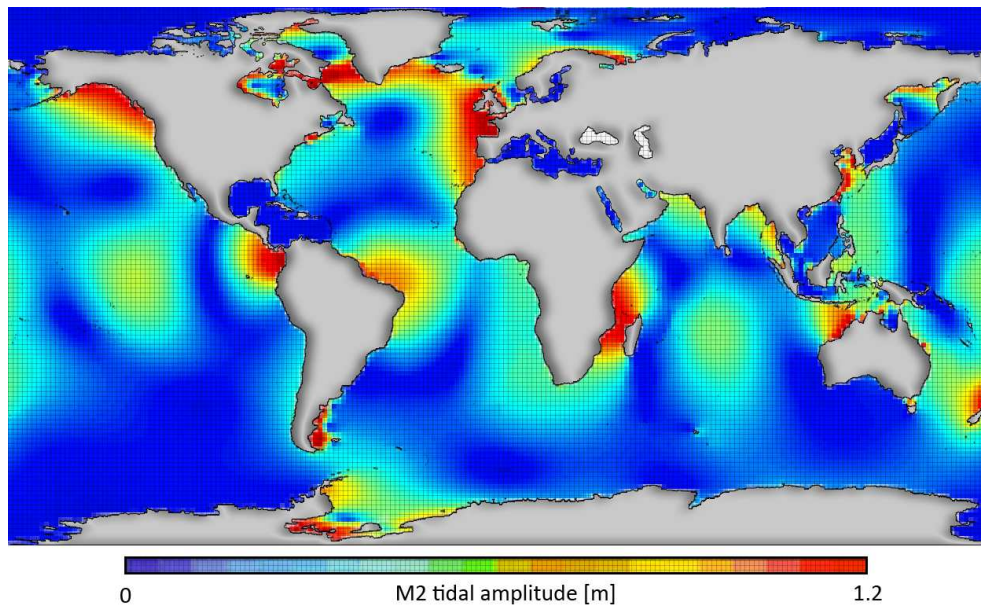


Figure 129 - Tidal amplitude of semi-diurnal lunar constituent

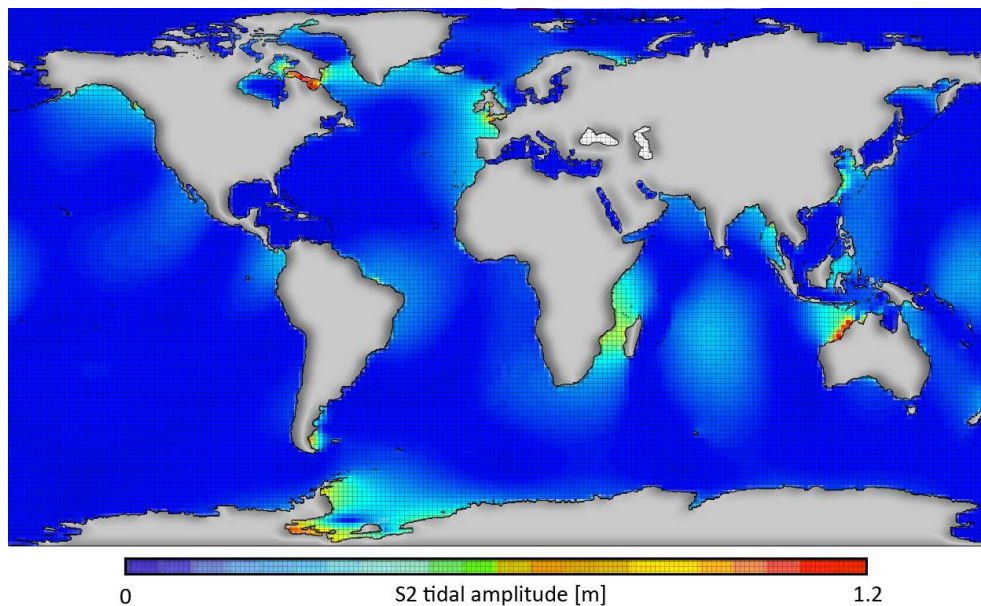


Figure 130 - Tidal amplitude of semi-diurnal solar constituent

It can be observed that in most areas where the lunar tidal constituent is high, the solar constituent is elevated as well, which makes it tough to identify a location where either one is elevated and the other is not. There are some areas, however, where the elevation of the solar tide is relatively small compared to the lunar tide and the tide is dominantly semi-diurnal.

From the analysis done a number of locations can be identified which have potential in terms of a constant, high amplitude tide with bi-daily high tides and low tides. These locations are illustrated on the world map in Figure 131 and listed as:

- Colombian Pacific Coast, Colombia
- Bay of Biscay, France
- Bay of Fundy, Canada
- Tasman Sea, New Zealand
- Mozambique Channel, Madagascar
- Barents Sea, Russia
- Patagonian Sea, Argentina

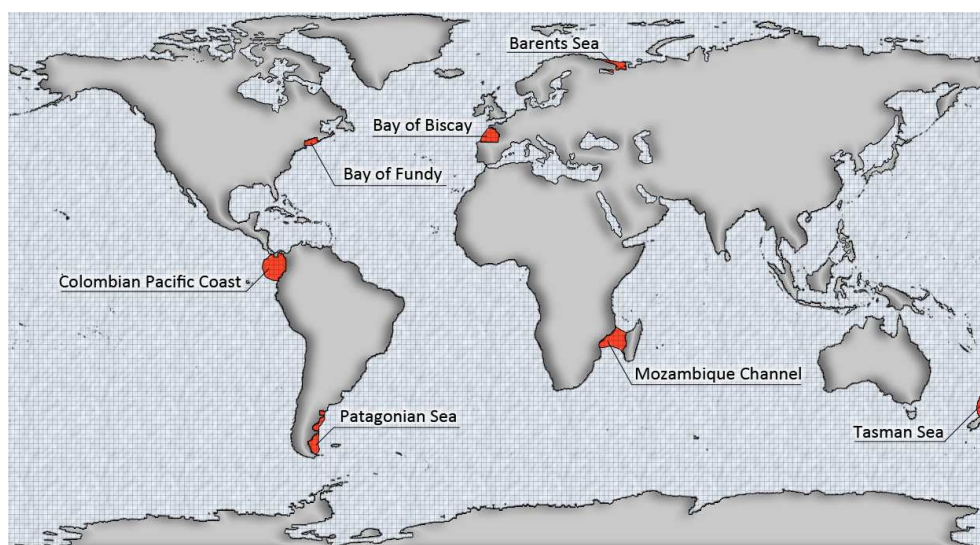


Figure 131 - Selection of possible locations

The choice of location from here on is arbitrary, any of the locations should provide an interesting and favourable tide to work with. Several locations are less favourable however due to natural conditions. The Barents Sea and the Patagonian Sea are subject to extremely low temperatures and could suffer from ice loads, introducing added stresses that are not accounted for. The Colombian Pacific Coast and the Tasman Sea are on or near fault lines, which are not necessarily a problem for the pontoons but could negatively impact the foundation. Finally the Mozambique Channel is on a trailing edge coastline in the tropical zone (between 30° N and 30° S) meaning it is subject to very fine sediment.

The chosen location is in the Bay of Fundy in Canada because its dominant tidal constituents are significantly larger than in the other remaining possible locations in the Bay of Biscay, France. This may seem like an obvious go-to location at first sight, given it is notorious for its high tides, but it also makes sense given the requirements of being semi-diurnal and relatively constant.

Appendix R Preliminary feasibility study

Before the actual design phase of the Tidal Wave Energy Converter can be initiated it is important to determine to what degree the concept is feasible. Because this feasibility study is done at the start of the design process there is not much information available in terms of what the specific boundary conditions of the tide, the bathymetry and the water quality are. Some educated assumptions will have to be made to facilitate the preliminary calculation. The preliminary calculation will be loosely based on the test case of the Rijnhaven in Rotterdam. This location is chosen because there is a sincere possibility it will, in the future, be used to facilitate floating houses, which would make an ideal situation for the Tidal Wave Energy Converter to potentially be applied to.

R.1 Deriving a simplified tidal motion

The Rijnhaven location has a tide consisting of 94 constituents (R.5), which can be summed up to the actual tidal motion using Equation 54, is much too detailed to use for a preliminary consideration. Ideally the formula would consist of a single sinusoidal equation rather than a combination of ninety-four.

$$z(t) = z_0 + \sum_{i=1}^{94} A_n \cdot \cos(\omega_n \cdot t + \phi_n)$$

z = water level

A = amplitude

ω = rotational frequency

ϕ = phase shift

Equation 54 – Summation of harmonic motion

As can be seen in Figure 132 (blue line) the tide is dominated by the semi-diurnal lunar tide (recognizable by the 12 our wave period), which means that the period and the phase shift of this tidal constituent are also the logical dominant factors in the simplified tidal range. The amplitude, however, is of larger influence on the overall tide meaning the 93 other components have to be taken into account there as well. This is done through manually plotting the complete tidal motion in a figure with the simplified tide and fitting it such that the resulting tidal graph is deemed a good enough representation of the tide.

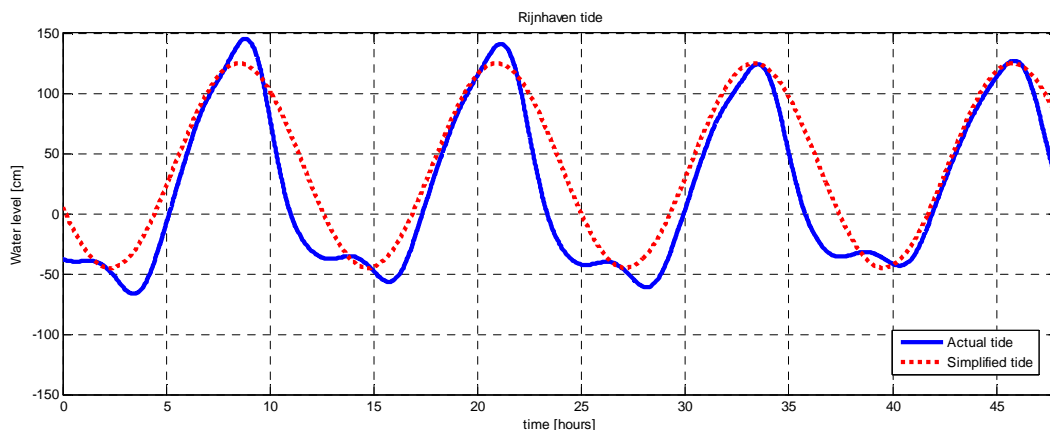


Figure 132 - Simplified tide graph

The empirically determined variables relating to the newly obtained simplified tidal motion as represented in Figure 132 (red dotted line) are presented in Table 97.

| Variable | Symbol | Value |
|-----------------------------|-----------|-------|
| Mean water level [cm] | z_0 | 40 |
| Amplitude [cm] | A | 85 |
| Rotational frequency [°/hr] | ω | 28.98 |
| Phase shift [°] | φ | 113.6 |

Table 97 - Simplified tidal constituent

The resulting motion of the simplified tidal wave is given in Equation 55. It is easily concluded that the approximation is a semi-diurnal tide with a range of 160 centimetres and a return period of 12 hours and 25 minutes, consistent with the M_2 lunar tide.

$$z(t) = 40 + 85 \cdot \cos(28.98 \cdot t + 113.6)$$

Equation 55 – Generalized tidal motion

R.2 Deriving simplified characteristics for the floating body

Because floating bodies can come in a nearly infinite variety of shapes and sizes it is difficult to determine a realistic average representation. Therefore the preferred method is to just choose a specific existing floating body and use that as a basis for the calculation. In this case the chosen floating body is a Europa II class push barge as illustrated in Figure 133.



Figure 133 - Europa II class push barge

Push barges are widely applied in the inland waterway system of the Rhine and have a certain lifespan after which they are replaced. After this lifetime the barges become redundant and are either sold as scrap metal or to countries with less sophisticated inland waterway transportation systems. A third possibility, however, would be to anchor it somewhere in the port area and have it power a Tidal Wave Energy Converter, a process that may also be suitable for barges that are still operational but temporarily out of work. The dimensions of the considered push barge are given in Table 98.

| Dimension | Symbol | Value |
|-------------------------|--------|---------------|
| Length | L | 76.5 [m] |
| Width | B | 11.4 [m] |
| Draught laden (unladen) | d | 3.5 (0.7) [m] |

Table 98 - Dimensions of a Europa II class push barge (Brolsma & Roelse, 2011)

R.3 The energy potential of the considered system

From the characteristics of the tidal motion and the considered floating body a calculation can be made regarding the energy potential of the device. Because the exact method of energy extraction is yet to be determined the extraction principle as used in the “Kiewbalg” (Ligthart, 2012) will be used where water is utilised as a medium to transfer the pressure build-up into a generator through turbines. The used methodology will be to first determine what the potential energy is that the system holds, and to subsequently determine how much of this can be harvested using the described method.

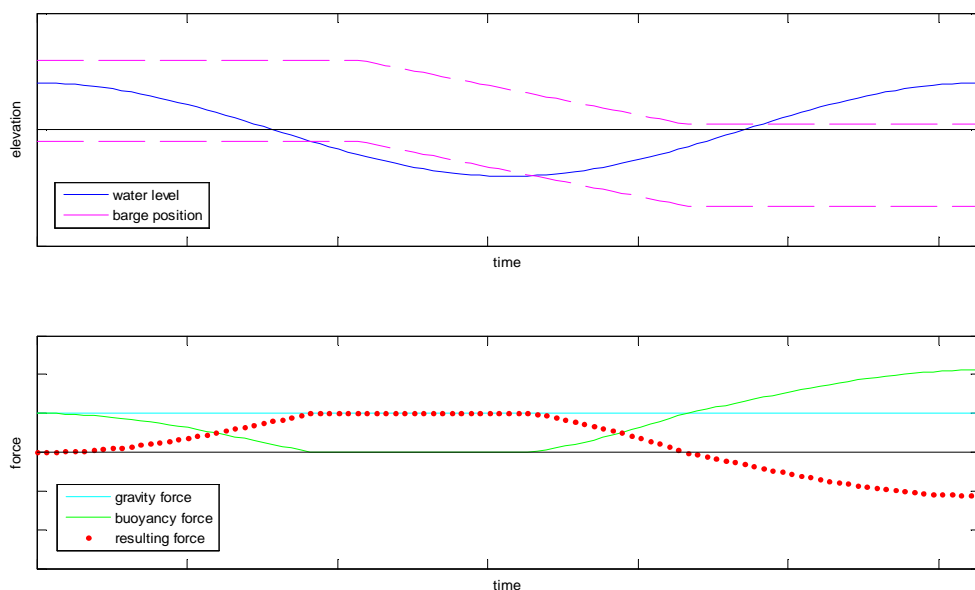


Figure 134 - Forces on the barge based on its position in the wave

Figure 134 illustrates the motion of the pontoon in the tide, where the magenta lines illustrate the top and the bottom of the barge as it moves in the tide. It can be observed that the pontoon has an optimum gravity based energy potential as long as water level is lower than the bottom of the pontoon, as the opposite buoyancy force is non-existent in that period. During the time that the pontoon is still (semi-)submerged this force will limit the revenue from the device. For the buoyancy based energy potential it holds that the energy potential is largest when the pontoon is optimally submerged. For the calculation of the potential both instances will be calculated separately as it is as of yet unknown which process is preferred. This analysis will be done at a later stage when the influence of foundation costs is also taken into account.

R.3.1 Scenario 1: Gravity based extraction with fully loaded barge

Because in the case of gravity based extraction it is important to have as much weight involved as possible the barge will be considered to be fully loaded. The scenario, which is illustrated in Figure 135, starts at high water level when the barge is at its maximum height. Here the valves will be closed meaning the barge is locked in its elevated position. As the tide moves down a pressure is built up, this will subsequently be extracted when the valves are opened again at an arbitrary point later in the tidal motion.

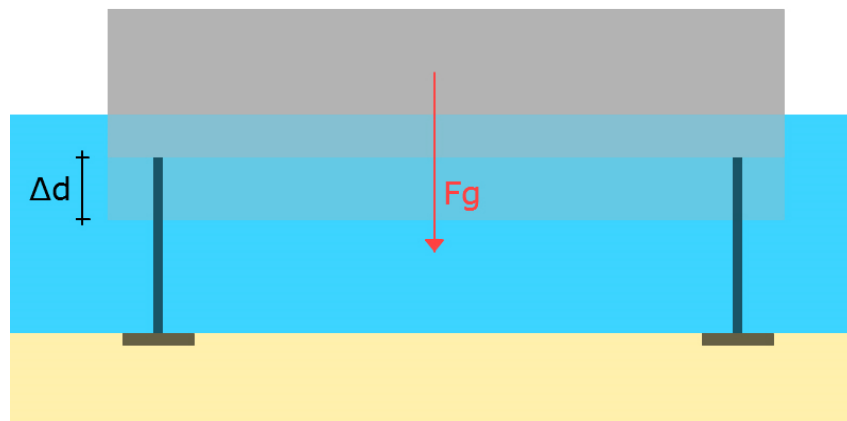


Figure 135 - Scenario 1: Gravity based extraction with fully loaded barge

The calculation in R.6 shows that under the considered circumstances an annual revenue of 1,882 [kWh] can be generated. This is a portion of 54% of the annual yearly household energy consumption in the Netherlands. Considering that the considered tidal motion is a relatively limited one in the Dutch inland waterway system, however, it is reasonable to assume that with large tidal motions this number would increase. The annual economic revenue of €147.98 has room for improvement still given that the government subsidies that are available for green energy have not been taken into account in this calculation, meaning it could easily double still. The total potential energy in the elevated system is 2,654 [kWh] per year, meaning the process efficiency of 71% is consistent with the considered turbine efficiency.

R.3.2 Scenario 2: Buoyancy based extraction with empty barge

In the case of the buoyancy based scenario the important aspect is only related to the emerging motion of the barge from the water. This motion is the same regardless of the weight of the barge and therefore the most economical solution is to leave the barge empty. This also means the barge has an added amount of freeboard that can be used without having to alter the barge in some way. The basic principle is that at the point where the water level is at its minimum, in the trough of the tidal wave, the valves are closed and the barge is locked in its position. As the tide moves upward the buoyancy forces create an under pressure in the previously mentioned water medium, at some arbitrary point the valves are opened and the outside water flows into the pressure chamber through a turbine. The scenario is illustrated in Figure 136.

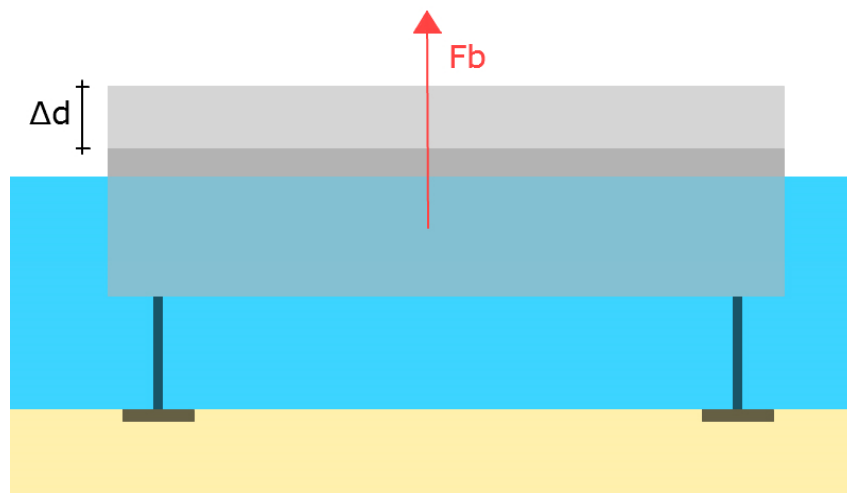


Figure 136 - Scenario 2: Buoyancy based extraction with empty barge

It can be observed from the calculations in R.6 that the results are identical to those in scenario 1. This is to be expected because the extrusion of the pontoon from the mean is identical and the process in both cases involves an equal but opposite water displacement causing the energy potential.

R.3.3 Scenario 3: Gravity based extraction with empty barge

The final situation to consider is that of the gravity based process with an empty barge. The reason this is interesting is because in the considered conditions this means that at some point the bottom of the barge will be above the water table completely taking away the influence of buoyancy on the process, as can be seen in Figure 137. The rest of the process is that same as that of scenario 1, under different boundary conditions the principle would be the same.

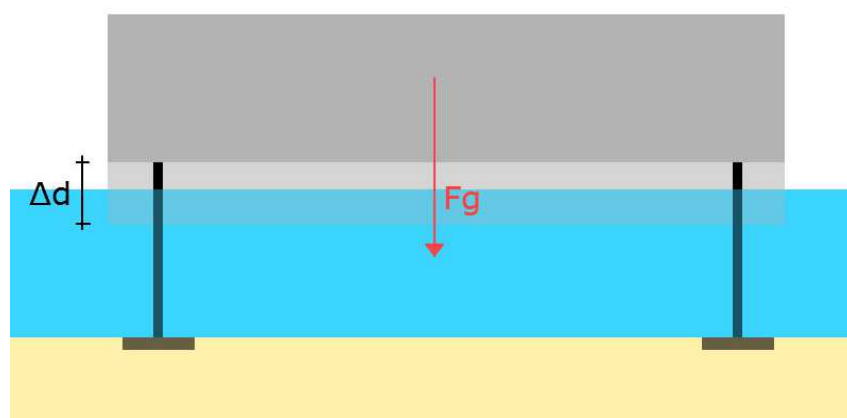


Figure 137 - Scenario 3: Gravity based extraction with empty barge

This scenario yields considerably lower results with only 1,322 kWh per year. This can be explained due to the fact that the weight is considerably lower than before and that the pressure build-up flattens out as soon as the bottom of the barge is lifted from the water surface. This phenomenon would also occur in the case of a buoyancy based combination being completely pulled under water as the build-up of buoyant forces would cease.

R.3.4 Summary

The calculations on revenue show that the differences between a device based on gravity and one based on buoyancy are not that big when the costs of structure are not taken into account. The difference becomes notable when the tidal range is larger than the draught of the barge, in which case production decreases. The same holds true for when the floating device is fully submerged, but it is deemed more economical to increase the freeboard than to increase the draught. Moreover increasing the draught is not always possible when bathymetric limitations apply. Figure 138 assumes a laden draught of 3.5 meters and an unladen draught of 0.7 meters. This is consistent with the previously determined push barge characteristics.

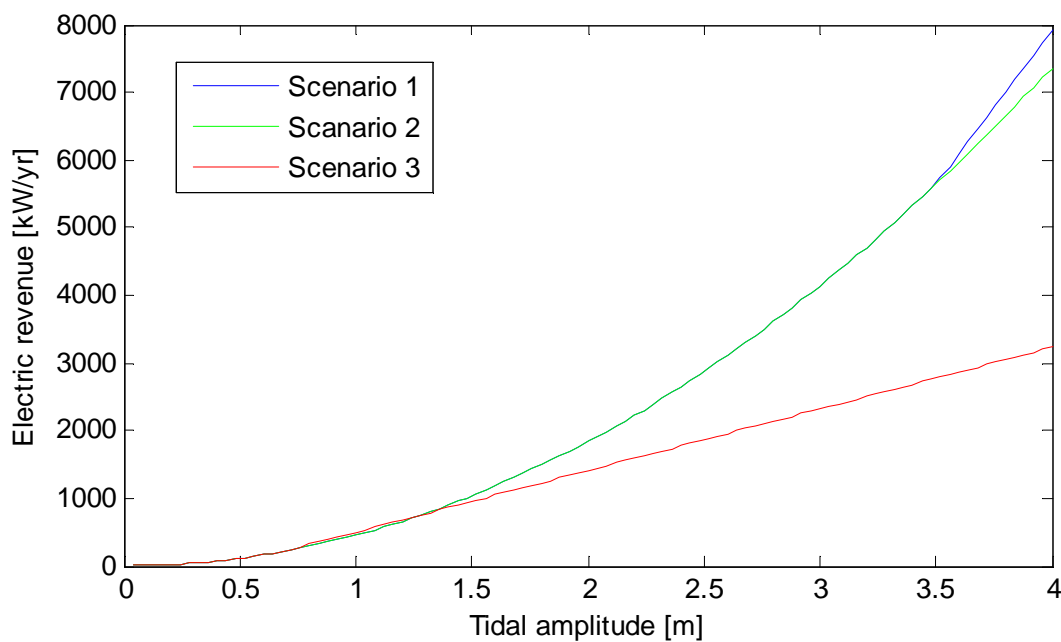


Figure 138 - Revenue profile of different scenarios in relation to tidal amplitude

The graph gives an interesting insight in the processes that occur. As analysed in the previous paragraphs the build-up of energy potential during the submerged phase is equal regardless of whether the system is based on buoyancy or gravity. During this period the increase in revenue follows a relation $P \propto d\sqrt{d}$ as deduced in R.6.4. After the barge frees itself from the water surface, when the tidal range exceeds the barge's draft, the gravity based revenue increases at a slightly more rapid pace than if it were still submerged due to the lack of buoyant forces pushing it back. As the tidal range increases it loses this advantage again and from roughly twice the draught onward the buoyancy based system is yielding better revenue again.

Table 99 gives a summary of all the information that has been acquired in the preceding paragraphs. It can easily be seen that the revenue approaches the maximum revenue as long as the barge is semi-submerged. The losses that occur here are fully accounted for by the efficiency of the turbines. When, however, the structure fully emerges or fully submerges the losses drastically increase.

| Scenario | Annual revenue [kWh] | Annual revenue [€] |
|-------------------|----------------------|--------------------|
| Scenario 1 | 1,882 | 147.98 |
| Scenario 2 | 1,882 | 147.98 |
| Scenario 3 | 1,322 | 92.59 |
| Maximum potential | 2,654 | 185.78 |

Table 99 - Summary of scenario revenues

R.4 Preliminary conclusion on feasibility

The previous chapter shows that the Tidal Wave Energy Converter is preliminary feasible to continue developing. Because this primary feasibility study only considers a small amount of involved variables it is important to determine what requirements need to be satisfied to come to a positive conclusion. The different aspects the device is judged based on are listed in Table 100.

| Requirement | Satisfied (✓/✗) |
|---|-----------------|
| Is there reason to believe the break-even point of a stand-alone device is within 10 years of operation? | ✗ |
| Is there reason to believe the break-even point of a when installed on an existing host structure is within 10 years of operation? | ✓ |
| Is there reason to believe the application range of the concept is large enough to justify development? | ✓ |
| Is there reason to believe areas with different, more favorable, boundary conditions exist and are suitable for application of the principle? | ✓ |
| Is the calculation conservative enough to say the real life solution will likely be more favorable? | ✓ |

Table 100 - Judgment table

The relatively low revenue of the device in low-tide areas mean it is implausible it will have financial feasibility if the host structure itself is a part of the development costs. It could very well be that this is different in larger tidal ranges with larger host structures, but that does not become evident from the considered situation in this preliminary feasibility study. This study does, however, show that the revenue yielded from it in relatively unfavourable conditions is promising and that it warrants further investigation to see what it does in different circumstances.

R.5 Tidal Constituents at the Parkhaven station

The tidal constituents of the considered area in the Rijnhaven are not directly available. The nearest measuring station is in the nearby Parkhaven of which data has been obtained from [Port of Rotterdam]. The mean sea water level in the area is at 22 cm +NAP. The tide is semi-diurnal as per Equation 56.

$$F = \frac{K_1 + O_1}{M_2 + S_2} = \frac{6.664 + 9.614}{77.536 + 18.373} = 0.17 < 0.25$$

Equation 56 – Tidal diurnality ratio

Table 101 shows the complete set of tidal constituents present in the Parkhaven area as provided by (Port of Rotterdam, 2014).

| Constituent | Amplitude (A) [cm] | Rotational velocity (ω) [°/hr] | Phase shift (ϕ) [°] |
|-------------|--------------------|---|----------------------------|
| SA | 7.100 | 0.041069 | 238.00 |
| SM | 2.900 | 1.015896 | 41.00 |
| Q1 | 2.852 | 13.398661 | 144.72 |
| O1 | 9.614 | 13.943036 | 202.30 |
| M1C | 1.493 | 14.492052 | 143.33 |
| P1 | 3.217 | 14.958931 | 4.06 |
| S1 | 1.007 | 15.000000 | 313.80 |
| K1 | 6.664 | 15.041069 | 12.44 |
| 3MKS2 | 1.068 | 26.870175 | 342.08 |
| 3MS2 | 2.227 | 26.952313 | 346.30 |
| OQ2 | 0.867 | 27.341696 | 28.57 |
| MNS2 | 1.944 | 27.423834 | 202.00 |
| 2ML2S2 | 1.329 | 27.496687 | 25.26 |
| NLK2 | 2.890 | 27.886071 | 42.81 |
| MU2 | 8.373 | 27.968208 | 231.23 |
| N2 | 11.797 | 28.439730 | 86.43 |
| NU2 | 5.106 | 28.512583 | 81.48 |
| MSK2 | 1.358 | 28.901967 | 326.28 |
| MPS2 | 1.230 | 28.943036 | 219.78 |
| M2 | 77.536 | 28.984104 | 113.60 |
| MSP2 | 1.250 | 29.025173 | 83.22 |
| MKS2 | 0.823 | 29.066241 | 260.06 |
| LABDA2 | 3.230 | 29.455625 | 132.91 |
| 2MN2 | 7.410 | 29.528479 | 316.25 |
| T2 | 1.453 | 29.958933 | 164.81 |
| S2 | 18.373 | 30.000000 | 174.85 |
| K2 | 5.753 | 30.082137 | 177.73 |
| MSN2 | 1.853 | 30.544375 | 21.38 |
| 2SM2 | 2.502 | 31.015896 | 50.10 |
| SKM2 | 1.263 | 31.098033 | 57.19 |
| NO3 | 0.612 | 42.382765 | 168.09 |
| 2MK3 | 1.220 | 42.927140 | 206.74 |
| 2MP3 | 0.255 | 43.009277 | 188.21 |
| SO3 | 0.741 | 43.943036 | 296.45 |

| | | | |
|--------|--------|------------|--------|
| MK3 | 1.346 | 44.025173 | 340.71 |
| SK3 | 0.610 | 45.041069 | 39.10 |
| 4MS4 | 0.630 | 55.936417 | 58.30 |
| 2MNS4 | 1.115 | 56.407938 | 269.60 |
| 3MS4 | 2.647 | 56.952313 | 284.93 |
| MN4 | 6.768 | 57.423834 | 195.42 |
| 2MLS4 | 2.388 | 57.496687 | 353.82 |
| 2MSK4 | 1.073 | 57.886071 | 28.23 |
| M4 | 17.705 | 57.968208 | 217.08 |
| 3MN4 | 2.783 | 58.512583 | 30.51 |
| MS4 | 11.278 | 58.984104 | 276.43 |
| MK4 | 3.597 | 59.066241 | 279.67 |
| 3MSN4 | 2.066 | 59.528479 | 109.63 |
| S4 | 1.075 | 60.000000 | 13.76 |
| MNO5 | 0.990 | 71.366869 | 251.12 |
| 3MK5 | 1.547 | 71.911244 | 291.24 |
| 2MP5 | 0.832 | 72.927140 | 20.32 |
| 3MO5 | 1.263 | 73.009277 | 101.75 |
| MSK5 | 0.473 | 74.025173 | 158.16 |
| 3KM5 | 0.099 | 74.107310 | 8.33 |
| 3MNS6 | 1.164 | 85.392042 | 322.85 |
| 2NM6 | 0.785 | 85.863563 | 191.89 |
| 4MS6 | 1.551 | 85.936417 | 357.30 |
| 2MN6 | 3.073 | 86.407938 | 207.28 |
| 2MNU6 | 1.480 | 86.480792 | 200.61 |
| 3MSK6 | 0.706 | 86.870175 | 74.09 |
| M6 | 5.724 | 86.952313 | 237.65 |
| MSN6 | 0.756 | 87.423834 | 265.87 |
| MKNU6 | 0.403 | 87.578825 | 280.69 |
| 2MS6 | 5.021 | 87.968208 | 294.83 |
| 2MK6 | 1.433 | 88.050346 | 301.01 |
| 3MSN6 | 1.544 | 88.513583 | 147.64 |
| 2SM6 | 0.627 | 88.984104 | 349.53 |
| MSK6 | 0.431 | 89.066241 | 352.28 |
| 2MNO7 | 0.595 | 100.350974 | 281.97 |
| M7 | 0.317 | 101.449007 | 100.38 |
| 2MSO7 | 0.602 | 101.911244 | 46.96 |
| 2(MN)8 | 0.484 | 114.847667 | 300.55 |
| 3MN8 | 1.094 | 115.392042 | 320.02 |
| M8 | 1.424 | 115.936417 | 355.76 |
| 2MSN8 | 0.938 | 116.407938 | 32.69 |
| 2MNK8 | 0.420 | 116.490075 | 29.37 |
| 3MS8 | 2.157 | 116.952313 | 43.86 |
| 3MK8 | 0.617 | 117.034450 | 45.89 |
| 2(MS)8 | 0.898 | 117.968208 | 110.97 |
| 3MSK8 | 0.484 | 118.050346 | 111.86 |
| 3MNK9 | 0.112 | 130.433111 | 169.75 |
| 4MK9 | 0.101 | 130.977486 | 221.90 |
| 3MSK9 | 0.132 | 131.993381 | 252.16 |

| | | | |
|----------|-------|------------|--------|
| 4MN10 | 0.702 | 144.376146 | 16.77 |
| M10 | 0.697 | 144.920521 | 51.96 |
| 3MSN10 | 0.789 | 145.392041 | 64.96 |
| 4MS10 | 1.260 | 145.936417 | 90.21 |
| 2(MS)N10 | 0.164 | 146.104938 | 156.40 |
| 3M2S10 | 0.748 | 146.952313 | 143.86 |
| 4MSK11 | 0.144 | 160.977486 | 334.22 |
| M12 | 0.194 | 173.904625 | 166.53 |
| 4MSN12 | 0.297 | 174.376146 | 172.63 |
| 5MS12 | 0.328 | 174.920521 | 203.26 |
| 4M2S12 | 0.268 | 175.936417 | 254.98 |

Table 101 - Tidal constituents at the Parkhaven measuring station

R.6 Calculation of feasibility study scenarios

The calculation of the revenue of the scenarios is done through Maple using the pre-determined variables as given in Table 102.

| Variable | Symbol | Value |
|------------------------|----------------|----------------------------|
| Length of the barge | L | 76.5 [m] |
| Width of the barge | B | 11.4 [m] |
| Draught of the barge | d | 3.5 [m] |
| Gravitational constant | g | 9.81 [m s ⁻²] |
| Water density | ρ_w | 1000 [kg m ⁻³] |
| Bearing surface | A | 40 [m ²] |
| Diameter of flow area | D _s | 0.025 [m] |
| Turbine efficiency | η | 0.75 [-] |
| Price of electricity | € | 0.70 [€] |

Table 102 - Pre-determined variables (Milieu Centraal, 2014)

Apart from these pre-determined variables another set of symbols will be used along the calculation process as presented in Table 103.

| Variable | Symbol | Unit |
|------------------------------------|--------------------|-----------------------------------|
| Draught in loaded situation | d _{new} | [m] |
| Force applied by gravity/buoyancy | F | [N] |
| Pressure applied on bearing medium | σ | [N m ⁻²] |
| Hydraulic head | H | [m] |
| Discharge | Q | [m ³ s ⁻¹] |
| Power | P | [W] |
| Drainage time | T _i | [hr] |
| Yearly electric revenue | R _y | [kWh yr ⁻¹] |
| Yearly economic revenue | R _{y,€} | [€] |
| Yearly potential energy supply | E _{pot,y} | [kWh yr ⁻¹] |

Table 103 - Undetermined variables

R.6.1 Scenario 1: Gravity based extraction with fully loaded barge

The situation in scenario 1 as depicted in Figure 135 can be calculated with a set of equations as described in Equation 57. This scenario revolves around a system that is elevated by the tide to a point where the bottom of the barge is still submerged.

$$\begin{aligned}
 z(t) &= 40 + 85 \cdot \cos(28.98 \cdot t + 113.6) \\
 d_{new} &= d - [\max(\eta(t)) - \min(\eta(t))] = 3.5 - 1.8 = 1.7[m] \\
 F &= \frac{1}{2} \cdot L \cdot B \cdot \rho \cdot g \cdot (d - d_{new}) = \frac{1}{2} \cdot 76.5 \cdot 11.4 \cdot 1000 \cdot 9.81 \cdot (3.5 - 1.7) = 7,700[kN] \\
 \sigma &= \frac{F}{A} = \frac{7,272}{40} = 192.5[kN \cdot m^{-2}] \\
 H &= \frac{\sigma}{\rho \cdot g} + \frac{u^2}{2 \cdot g} = \frac{192500}{1000 \cdot 9.81} = 19.62[m] \\
 Q &= \frac{1}{4} \cdot \pi \cdot D_s^2 \cdot \sqrt{2 \cdot g \cdot H} = 0.25 \cdot \pi \cdot 0.025^2 \cdot \sqrt{2 \cdot 9.81 \cdot 19.62} = 0.0096[m^3 \cdot s^{-1}] \\
 P &= \eta \cdot \rho \cdot g \cdot H \cdot Q = 0.75 \cdot 1000 \cdot 9.81 \cdot 19.62 \cdot 0.0096 = 1.390[kW] \\
 T_l &= \frac{A \cdot [\max(z(t)) - \min(z(t))]}{Q} \cdot \frac{1}{3600} = \frac{40 \cdot 1.8}{0.0096} \cdot \frac{1}{3600} = 2.08[h] \\
 R_y &= 2 \cdot T_l \cdot 365 \cdot P = 2 \cdot 2.08 \cdot 365 \cdot 1.390 = 2,114[kWh \cdot yr^{-1}] \\
 R_{y,€} &= R_y \cdot € = 2,114 \cdot 0.07 = €147.98 \\
 E_{pot,y} &= \frac{F \cdot [\max(z(t)) - \min(z(t))]}{3,600,000} \cdot 2 \cdot 365 = \frac{7,272,000 \cdot 1.8}{3,600,000} \cdot 2 \cdot 365 = 2,654[kWh \cdot yr^{-1}]
 \end{aligned}$$

Equation 57 – Estimation of TWECE revenue scenario 1

R.6.2 Scenario 2: Buoyancy based extraction with empty barge

The situation in scenario 2, as depicted in Figure 136, can be calculated with a set of equations as described in Equation 58. This scenario revolves around a system that is engorged by the tide creating buoyancy forces larger than the forces of gravity so that an upward resulting force is created.

$$\begin{aligned}
 z(t) &= 40 + 85 \cdot \cos(28.98 \cdot t + 113.6) \\
 d_{new} &= d + [\max(z(t)) - \min(z(t))] = 0.7 + 1.8 = 2.5[m] \\
 F &= \frac{1}{2} \cdot L \cdot B \cdot \rho \cdot g \cdot (d - d_{new}) = \frac{1}{2} \cdot 76.5 \cdot 11.4 \cdot 1000 \cdot 9.81 \cdot (0.7 - 2.5) = 7,700[\text{kN}] \\
 \sigma &= \frac{F}{A} = \frac{7,272}{40} = 192.5[\text{kN} \cdot \text{m}^{-2}] \\
 H &= \frac{\sigma}{\rho \cdot g} + \frac{u^2}{2 \cdot g} = \frac{192500}{1000 \cdot 9.81} = 19.62[m] \\
 Q &= \frac{1}{4} \cdot \pi \cdot D_s^2 \cdot \sqrt{2 \cdot g \cdot H} = 0.25 \cdot \pi \cdot 0.025^2 \cdot \sqrt{2 \cdot 9.81 \cdot 19.62} = 0.0096[\text{m}^3 \cdot \text{s}^{-1}] \\
 P &= \eta \cdot \rho \cdot g \cdot H \cdot Q = 0.75 \cdot 1000 \cdot 9.81 \cdot 19.62 \cdot 0.0096 = 1.390[\text{kW}] \\
 T_l &= \frac{A \cdot [\max(z(t)) - \min(z(t))]}{Q} \cdot \frac{1}{3600} = \frac{40 \cdot 1.8}{0.0096} \cdot \frac{1}{3600} = 2.08[h] \\
 R_y &= 2 \cdot T_l \cdot 365 \cdot P = 2 \cdot 2.08 \cdot 365 \cdot 1.390 = 2,114[\text{kWh} \cdot \text{yr}^{-1}] \\
 R_{y,\text{€}} &= R_y \cdot \text{€} = 2,114 \cdot 0.07 = \text{€}147.98 \\
 E_{pot,y} &= \frac{F \cdot [\max(z(t)) - \min(z(t))]}{3,600,000} \cdot 2 \cdot 365 = \frac{7,272,000 \cdot 1.8}{3,600,000} \cdot 2 \cdot 365 = 2,654[\text{kWh} \cdot \text{yr}^{-1}]
 \end{aligned}$$

Equation 58 - Estimation of TWEC revenue scenario 2

R.6.3 Scenario 3: Gravity based extraction with empty barge

The situation in scenario 3, as depicted in Figure 137, can be calculated with a set of equations as described in Equation 59. This scenario revolves around a system that is elevated by the tide to a point where the bottom of the barge is extrudes the water level. This creates two different situations for the system to be in where different properties apply. These two situations are depicted with indices in the calculation and added up to obtain the desired results.

$$z(t) = 40 + 85 \cdot \cos(28.98 \cdot t + 113.6)$$

$$d_{new} = d + [\max(z(t)) - \min(z(t))] = 0.7 + 1.8 = 2.5[m]$$

$$z < d \left\{ \begin{array}{l} F_1 = L \cdot B \cdot \rho \cdot g \cdot h = 76.5 \cdot 11.4 \cdot 1000 \cdot 9.81 \cdot 0.7 = 5,989[\text{kN}] \\ \sigma_1 = \frac{F}{A} = \frac{5,989}{40} = 149.7[\text{kN} \cdot \text{m}^{-2}] \\ \langle H_1 \rangle = \frac{1}{2} \cdot \frac{\sigma}{\rho \cdot g} + \frac{u^2}{2 \cdot g} = \frac{1}{2} \cdot \frac{149,700}{1000 \cdot 9.81} = 7.63[m] \\ Q_1 = \frac{1}{4} \cdot \pi \cdot D_s^2 \cdot \sqrt{2 \cdot g \cdot H} = 0.25 \cdot \pi \cdot 0.025^2 \cdot \sqrt{2 \cdot 9.81 \cdot 7.63} = 0.006[m^3 \cdot s^{-1}] \\ P_1 = \eta \cdot \rho \cdot g \cdot H \cdot Q = 0.75 \cdot 1000 \cdot 9.81 \cdot 7.63 \cdot 0.006 = 337[\text{kW}] \\ T_{l1} = \frac{A \cdot [\max(z(t)) - \min(z(t))]}{Q} \cdot \frac{1}{3600} = \frac{40 \cdot 0.7}{0.006} \cdot \frac{1}{3600} = 1.30[h] \end{array} \right.$$

$$z \geq d \left\{ \begin{array}{l} F_2 = L \cdot B \cdot \rho \cdot g \cdot h = 76.5 \cdot 11.4 \cdot 1000 \cdot 9.81 \cdot 0.7 = 5,989[\text{kN}] \\ \sigma_2 = \frac{F}{A} = \frac{5,989}{40} = 149.7[\text{kN} \cdot \text{m}^{-2}] \\ \langle H_2 \rangle = \frac{\sigma}{\rho \cdot g} + \frac{u^2}{2 \cdot g} = \frac{149,700}{1000 \cdot 9.81} = 15.26[m] \\ Q_2 = \frac{1}{4} \cdot \pi \cdot D_s^2 \cdot \sqrt{2 \cdot g \cdot H} = 0.25 \cdot \pi \cdot 0.025^2 \cdot \sqrt{2 \cdot 9.81 \cdot 15.26} = 0.0085[m^3 \cdot s^{-1}] \\ P_2 = \eta \cdot \rho \cdot g \cdot H \cdot Q = 0.75 \cdot 1000 \cdot 9.81 \cdot 15.26 \cdot 0.0085 = 954[\text{kW}] \\ T_{l2} = \frac{A \cdot [\max(z(t)) - \min(z(t))]}{Q} \cdot \frac{1}{3600} = \frac{40 \cdot 1.1}{0.0085} \cdot \frac{1}{3600} = 1.44[h] \end{array} \right.$$

$$R_y = 2 \cdot (T_{l1} \cdot P_1 + T_{l2} \cdot P_2) \cdot 365 = 2 \cdot (1.30 \cdot 337 + 1.44 \cdot 954) \cdot 365 = 1,322[\text{kWh} \cdot \text{yr}^{-1}]$$

$$R_{y,\text{€}} = R_y \cdot \text{€} = 1,882 \cdot 0.07 = \text{€}2.59$$

Equation 59 - Estimation of TWEC revenue scenario 3

R.6.4 Deduction of proportionality

To make a comparison between types of scenarios it is important to know what the relation is between the tidal amplitude and the expected power that can be yielded from the process. To achieve this relation the used formulas from the previous paragraphs are combined into one big relation. Assuming all variables relating to anything other than the tidal range remain constant this leaves the relation that is desired. Equation 60 gives the deduction of this relation. This proportionality relates to the power and the tidal range and does not give an indication of the amount of energy that can actually be yielded from the process as it does not include the duration of the power extraction period. It is therefore only a valid tool for determining the slope of the submerged structure's revenue graph.

$$F = L \cdot B \cdot \rho \cdot g \cdot \Delta d$$

$$\sigma = \frac{F}{A}$$

$$H = \frac{\sigma}{\rho \cdot g}$$

$$Q = \frac{1}{4} \cdot \pi \cdot D^2 \cdot \sqrt{2 \cdot g \cdot H}$$

$$P = \rho \cdot g \cdot \frac{1}{4} \cdot \pi \cdot D^2 \cdot \sqrt{2 \cdot \frac{L \cdot B \cdot \rho \cdot g \cdot \Delta d}{\rho \cdot A}} \cdot \frac{L \cdot B \cdot \rho \cdot g \cdot \Delta d}{A \cdot \rho \cdot g}$$

$$= \sqrt{\frac{2}{\rho \cdot A}} \cdot \underbrace{\frac{\rho \cdot g \cdot \frac{1}{4} \cdot \pi \cdot D^2}{A \cdot \rho \cdot g}}_{\gamma} \cdot (L \cdot B \cdot \rho \cdot g)^{1.5} \cdot \Delta d \sqrt{\Delta d}$$

$$= \gamma \cdot \Delta d \sqrt{\Delta d}$$

$$P \propto \Delta d \sqrt{\Delta d}$$

Equation 60 – Revenue proportionality deduction